Schröder, Hans Christoph

Large-scale High Head Pico Hydropower Potential Assessment

Mitteilungen. Institut für Wasser- und Umweltsystemmodellierung, Universität Stuttgart

Zur Verfügung gestellt in Kooperation mit/Provided in Cooperation with:
Universität Stuttgart

Verfügbar unter/Available at: https://hdl.handle.net/20.500.11970/106484

Vorgeschlagene Zitierweise/Suggested citation:
Schröder, Hans Christoph (2018): Large-scale High Head Pico Hydropower Potential Assessment. Stuttgart: Universität Stuttgart, Institut für Wasser- und Umweltsystemmodellierung (Mitteilungen. Institut für Wasser- und Umweltsystemmodellierung, Universität Stuttgart, 260).
http://dx.doi.org/10.18419/opus-10236.

Universität Stuttgart

Institut für Wasser- und Umweltsystemmodellierung

Mitteilungen

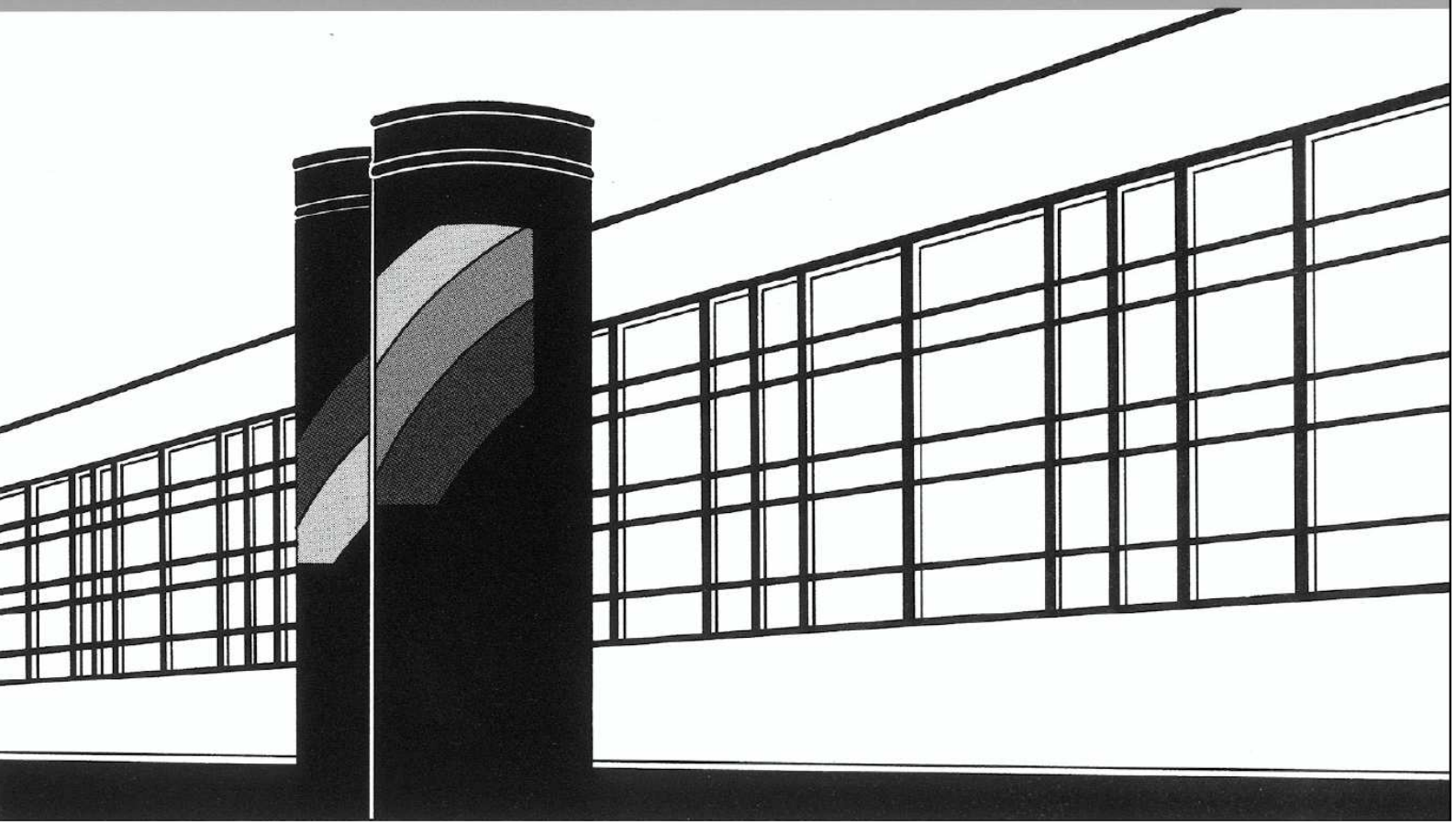

Heft 260

Hans Christoph Schröder

Large-scale High Head Pico Hydropower Potential Assessment

Large-scale High Head Pico Hydropower Potential Assessment

von der Fakultät Bau- und Umweltingenieurwissenschaften der Universität Stuttgart zur Erlangung der Würde eines Doktor-Ingenieurs (Dr.-Ing.) genehmigte Abhandlung

vorgelegt von

Hans Christoph Schröder

aus Wiesensteig

Hauptberichter: Prof. Dr.-Ing. Silke Wieprecht

Mitberichter: Prof. Dr. Volker Hochschild

Tag der mündlichen Prüfung: 27. April 2018

Institut für Wasser- und Umweltsystemmodellierung
der Universität Stuttgart
2018

Heft 260

Large-scale High Head Pico Hydropower Potential Assessment

von
Dr.-Ing.
Hans Christoph Schröder

Eigenverlag des Instituts für Wasser- und Umweltsystemmodellierung
der Universität Stuttgart

D93 Large-scale High Head Pico Hydropower Potential Assessment

Bibliografische Information der Deutschen Nationalbibliothek
Die Deutsche Nationalbibliothek verzeichnet diese Publikation in der Deutschen Nationalbibliografie; detaillierte bibliografische Daten sind im Internet über http://www.d-nb.de abrufbar

Schröder, Hans Christoph:
Large-scale High Head Pico Hydropower Potential Assessment, Universität Stuttgart. - Stuttgart: Institut für Wasser- und Umweltsystemmodellierung, 2018

(Mitteilungen Institut für Wasser- und Umweltsystemmodellierung, Universität Stuttgart: H. 260)
Zugl.: Stuttgart, Univ., Diss., 2018
ISBN 978-3-942036-64-1

NE: Institut für Wasser- und Umweltsystemmodellierung <Stuttgart>: Mitteilungen

Herausgegeben 2018 vom Eigenverlag des Instituts für Wasser- und Umweltsystem-modellierung

Druck: DCC Kästl e.K., Ostfildern

Acknowledgements

First of all, I want to thank Prof. Dr.-Ing. Silke Wieprecht, director of the Institute for Modelling Hydraulic and Environmental Systems (IWS) at the University of Stuttgart, for her willingness to supervise this thesis. It is not a matter of course to find supervision for such a topic!

Likewise I want to thank my co-supervisor Prof. Dr. Volker Hochschild, University of Tübingen, for the expertise from a geographer´s point of view.

My "port of entry" to the University of Stuttgart has been the International Doctoral Program Environment Water (ENWAT). Apart from the invaluable organizational support provided by this program, I particularly enjoyed the scientific interaction beyond the horizon of the own institute - and the Brezeln - at the "Doktorandentag" seminar. Unfortunately, while living in China it was quite a task to be able to attend it.

Without the ENWAT support it would moreover not have been possible to obtain an IPSWaT scholarship for which I am very grateful as well. This scholarship, provided by the German Ministry of Education and Science (BMBF), in fact "revitalized" my efforts to complete this work and was the single best reason to move back to Germany.

For the then following field trips I want to extend my gratitude to numerous transport providers that facilitated traveling many thousands of kilometers on the roads of Costa Rica, China, Ecuador and Sri Lanka without any incident, not to speak of several tens of thousands kilometers in the air to get there at all.

And last but not least I want to thank my colleagues at the university for the wonderful distractions from the topic, particularly during the coffee breaks!

Table of Contents

List of Figures

List of Tables

Abbreviations and Notations

ρ	Density of water, being 1 [kg/m^3]
g	Gravity constant, being 9.81 [m/s^2]
Q	Flow [m^3/s]
h	Drop (head) [m]
η	energy conversion efficiency
PHP	Pico Hydropower
MHP	Micro Hydropower
SHP	Small Hydropower
GIS	Geographical Information System
DEM	Digital Elevation Model
POI	Point Of Interest (A location marker used in GPS tracking software)
H0	Class 0, high head Pico Hydropower potential
H1	Class 1, high head Pico Hydropower potential
H2	Class 3, high head Pico Hydropower potential
H8	Class 8, high head Pico Hydropower potential
H9	Class 9, high head Pico Hydropower potential
X1	Single stream, suitable for PHP, crossing the observation track
D1	Single dry stream, crossing the observation track
ZZ	Single streamlet, crossing the observation track
R	surface runoff
P	precipitation
C	cloud captured moisture
AET	actual evapotranspiration
FIC	Forest Influence Component
FC	Forest cover [0.0 to 1.0 in steps of 0.1, i.e. 10% coverage]
MP	monthly precipitation of the least precipitation month [mm/month]
GR	groundwater recharge
ET	evapotranspiration
C_r	runoff coefficient
WB	annual total water balance
h_{max}	highest point of a watershed
h_{min}	lowest point of the watershed
wb_{dm}	water balance of the driest month
DCL	side length of DEM cell
DCS	average slope of DEM cell

List of equations and formulas

Abstract

Individual treatment as a customized engineering solution, a standard feature in the hydropower domain for all stages of project development, would be cost prohibitive for Pico hydropower (PHP) installations because of the small project size. The cost problem already appears at the very first stage of the project planning: the hydropower potential assessment. Individual site information, typically based on measured streamflow information of a particular watercourse, is therefore normally not available for PHP projects.

Due to this lack of site-related information, PHP has not been a projectable resource so far. This is particularly true for large area PHP potential information that could open a perspective to increase the size of development projects by aggregating individual PHP installations.

GIS based spatial analysis is an established tool for large-scale hydropower potential assessment. The technique is capable of producing complete hydropower potential estimates for large areas and moreover is able to replace some of the costly on-site data collection.

The present work is extending the capabilities of GIS based hydropower potential assessment into the PHP domain.

Because of the unit-size-related characteristics of PHP, the traditional feasibility-centered concept of hydropower potential is inadequate for GIS based large-scale PHP potential assessment. To overcome the need for largely unavailable high-resolution spatial data that is capable of resolving small streams suitable for PHP size units, an alternative PHP potential definition is applied:

Based on the conclusion that the hydropower site selection planning sequence is typically reversed for PHP, hydropower potential of an area is represented in relation to the specific site requirement of a “standard PHP unit”. The unit is optimized for the expected global application potential and technically represented by a range of high head turbine-generator assemblies with an electrical output capacity of one kilowatt. Cost considerations on penstock length and transmission wiring dictate the placement of all components between water intake and electrical consumer onto an area that is equal or smaller than one square kilometer.

The qualitative concept of hydropower potential permits a threshold-value-based Boolean query to evaluate the suitability of this area for a standard PHP unit. Moreover, in this concept the watercourse does not have to be tangible anymore; its existence (or absence) is a result of the threshold-value-based calculation as well.

The GIS procedure behind the large-scale PHP potential assessment, a rule-based expert system, utilizes a combination of two approaches (A) and (B). (A) is a hydraulic power calculation, based on a quantification of minimum flow, derived from hydrological parameters without the consideration of explicit watercourses, resulting in a “total baseflow per area”, and a quantification of hydraulic head, based on DEM data. (B) is a qualitative reasoning process that analyzes the absence of (adequate) flow, resulting in a set of “exclusion factors”. Both approaches followed an evolutionary process, driven by the availability and suitability of various spatial datasets that were iteratively replaced to improve the overall performance of the procedure. Both results, (A) and (B), are used qualitatively for the PHP potential assessment: (A) against the thresholds of the “standard PHP unit”-specific minimum flow and minimum head requirements and (B) against a threshold of zero. The entire analytical part of the potential assessment process is realized

as a sequence of raster calculation facilitated threshold evaluations, performed with open source GRASS GIS and based on freely accessible spatial data with global or near-global coverage.

Due to the prospective applicability of the GIS procedure for project planning of PHP installations, extensive measures are considered in the conceptualization of the GIS procedure to avoid overestimations of PHP potential that could result in an economically disadvantageous underperformance of PHP installations.

The GIS based PHP potential assessment procedure is capable of discriminating areas without high head PHP potential against areas with PHP potential and so called “favorable PHP potential”. The basic unit of the spatial output is a consequence of the underlying PHP potential definition of this work: a standardized PHP installation and the required hydraulic source, together called standard unit, are located on an area of one square kilometer (the so-called PHP unit cell).

The gradation of the output is a consequence of the verification techniques. Several large-area PHP potential field assessment methods, based on contemplative analysis techniques, are developed in this work. Field assessments were conducted in Yunnan Province/China, Costa Rica, Ecuador and Sri Lanka. The aim for all field assessments is to get a comprehensive view on the PHP potential distribution of the entire country/province.

Comparison of PHP potential results from the GIS based PHP potential assessment against the field assessment results revealed immature field assessment techniques during the first field assessments (Yunnan Province), as well as specific limitations for both methods, however also a very high overall conformity between GIS assessment and (mature) field assessment techniques for the areas of Costa Rica, Ecuador and Sri Lanka. It is therefore justified to assume a general suitability of the GIS based PHP potential assessment procedure for the global tropical and subtropical regions.

Climatic regions with recurrent freezing conditions cannot reliably sustain continuous high head PHP operation, which in turn is a prerequisite for the PHP operating conditions defined in the scope of this work. The present version of the GIS based PHP potential assessment procedure will therefore classify large parts of the global temperate as well as the entire cold region as being unsuitable for PHP application.

Zusammenfassung

Ingenieurstechnisch ausgeführte angepasste Einzellösungen gelten im Wasserkraftbereich als Standard in allen Phasen der Projektentwicklung. Für Kleinstwasserkraftanlagen wären solche Lösungen aufgrund der geringen Projektgrösse allerdings unverhältnismässig teuer. Diese Problematik offenbart sich bereits in einer sehr frühen Phase der Projektplanung bei der Ermittlung des Wasserkraftpotentials. Individuelle Standortdaten, basierend auf gemessenen Abflussprofilen eines Wasserlaufs, stehen für die Ermittlung des Wasserkraftpotentials von PHP-Projektvorhaben deshalb normalerweise nicht zur Verfügung.

Aufgrund des Mangels an Standortdaten konnte PHP bisher nicht als raumübergreifend projektierbare Ressource in Erscheinung treten. Insbesondere Informationen über grossräumiges PHP Potential könnten hier eine Perspektive für Entwicklungsprojekte, bestehend aus aggregierten PHP Einzelinstallationen unter Ausnutzung der Skaleneffekte des Gesamtprojektes, eröffnen.

Wasserkraftpotentialuntersuchungen bedienen sich heute üblicherweise der GIS-unterstützten Raumplanung als zentrales Werkzeug für Berechnung und Darstellung. Die Technik ermöglicht die Erstellung grossräumig zusammenhängender Darstellungen des Wasserkraftpotentials und ermöglicht in vielen Fällen auch die Vermeidung kostspieliger Vor-Ort-Untersuchungen.

Die vorliegende Arbeit eröffnet die Möglichkeit, die Vorteile der GIS-unterstützten Raumplanung auch im PHP Bereich zu nutzen.

Wegen der speziellen, durch die geringe Grösse der Anlagen bedingten Charakteristik der PHP Projekte bei gleichzeitigem Fehlen von Abflussdaten kleiner, PHP geeigneter Wasserläufe, ist es erforderlich, das traditionelle, machbarkeitsorientierte Wasserkraftpotentialkonzept aufzugeben und stattdessen ein spezielles PHP Potentialkonzept zu entwickeln.

Dieses basiert auf der Erkenntnis, dass die Abfolge der Planungsschritte für die Standortbestimmung im Bereich PHP typischerweise umgekehrt zur oft üblichen Abfolge im Wasserkraftbereich verläuft. Dadurch wird es möglich, PHP Potential als spezifische Standortanforderungen einer “PHP-Standardanlage” auszudrücken. Der Begriff Standardanlage bezieht sich hier auf eine marktübliche high head Turbine-Generator-Einheit mit einer elektrischen Leistung von 1kW als erwartete Optimalkonfiguration für das globale PHP Anwendungspotential. Kostenerwägungen begrenzen die maximale Länge von hydraulischer Zuleitung und elektrischer Ableitung. Daraus resultiert, dass die Gesamtfläche für sämtliche Komponenten einer “PHP-Standardanlage” (Wasserlauf bis Verbraucher) auf maximal einen Quadratkilometer begrenzt ist.

Das solchermassen gewonnene qualitative Wasserkraftpotentialkonzept ermöglicht eine rein boolesche Abfrage von Eignungskriterien für die Standard-Gesamtfläche ($1km^2$) einer PHP-Standardanlage. Dadurch wird auch der zur Standardfläche zugehörige geeignete Wasserlauf zur virtuellen Grösse; seine Existenz (oder Nichtexistenz) ist ebenso ausschliesslich das Resultat der Abfrage von Eignungskriterien.

Die der grossräumigen PHP Potentalermittlung zugrundeliegende GIS Prozedur, ein regelgestütztes Expertensystem, nutzt eine Kombination zweier Herangehensweisen (A) und (B):
(A) ist eine Berechnung des hydraulischen Potentials, basierend auf einer modellierten Quantifizierung jährlicher Minimalabflüsse ohne Berücksichtigung realer Wasserläufe als Gesamt-Basisabfluss/Flächeneinheit, sowie der Quantifizierung der Fallhöhe aus digitalen Geländemodelldaten.
(B) besteht aus einem qualitativen Evaluierungsprozess, welcher das Nichtvorhandensein

adäquater Abflussmengen analysiert, realisiert als Abfolge von Abfragen zu Ausschlusskriterien.

Beide Herangehensweisen sind durch evolutionäre Prozesse entstanden, die in erster Linie von der Optimierung durch neu verfügbare oder besser geeignete Kartendatensätze getrieben waren.

Die Ergebnisse beider Teilschritte (A) und (B) werden für die PHP Potentialermittlung qualitativ verwendet: (A) in Bezug auf Schwellenwerte die aus den minimalen hydraulischen Anforderungen der PHP Standardanlage resultieren, und (B) in Bezug auf einen Schwellenwert von Null (d. h. als Ausschlusskriterium). Die gesamte GIS Prozedur der eigentlichen Potentialanalyse ist daher als Abfolge von Rasterdatenkalkulationen zur Abfrage von Schwellenwerten realisiert. Nur nichtkommerziell verfügbare Datensätze mit globaler oder annähernd globaler Abdeckung wurden verwendet. Alle GIS Operationen sind in GRASS GIS ausgeführt.

Die Fehlervermeidung wurde im Hinblick auf die mögliche Verwendung der GIS Prozedur in der Projektplanung konzipiert. Allzu optimistische Potentialabschätzungen hätten möglicherweise zur Folge, dass installierte Anlagen nicht wirtschaftlich arbeiten können. Deshalb wurde für alle Komponenten ein konservativer Ansatz gewählt.

Die Bezugsgrösse der Ergebnisdarstellung, die sogenannte "PHP unit cell", ist als PHP-Standardanlage auf der Standard-Gesamtfläche ($1km^2$) definiert. PHP Potential findet sich also auf denjenigen ($1km^2$) Quadranten, auf denen möglich ist, mindestens eine PHP-Standardanlage nach den Leistungsanforderungen kontinuierlich zu betreiben.

Die GIS Prozedur zur PHP Potentialabschätzung ist in der Lage, Flächen ohne high head PHP Potential, Flächen mit high head PHP Potential, sowie Flächen mit herausragendem high head PHP Potential zu unterscheiden.

Eine feinere Abstufung der Ergebnisse, mit der GIS Prozedur ohne weiteres durchführbar, wäre nicht mehr mit den hierfür entwickelten Verifizierungstechniken kontrollierbar. Diese, auf kontemplativen Methoden basierenden Felduntersuchungen wurden für die Provinz Yunnan/China, Costa Rica, Ecuador and Sri Lanka durchgeführt. In allen Felduntersuchungen wurde angestrebt, einen Gesamtüberblick über die tatsächliche Verteilung des PHP Potentials der erwähnten drei Länder bzw. der erwähnten Provinz zu erhalten.

Ein Vergleich der Ergebnisse der GIS-basierenden Untersuchung mit den Felduntersuchungen zeigte sowohl die anfangs unausgereifte Verfassung der Felduntersuchungstechniken (Untersuchung Yunnan), als auch bleibende, spezifische Einschränkungen der Anwendbarkeit beider Untersuchungsverfahren, jedoch grundsätzlich eine sehr hohe Übereinstimmung der Ergebnisse in den ausgereiften Versionen der Untersuchungsverfahren (Untersuchungen Costa Rica, Ecuador and Sri Lanka). Zusammenfassend kann daher von der globalen Eignung des GIS-basierenden Untersuchungsverfahren zum PHP Potential für die tropischen und subtropischen Regionen ausgegangen werden.

Klimazonen in denen saisonaler Frost auftritt sind zwar nicht grundsätzlich ungeeignet für die Anwendung von high head PHP, jedoch ist hier kein kontinuierlicher Einsatz möglich und damit eine für diese Arbeit definierte Anwendungsvoraussetzung nicht erfüllt.

Die vorliegende Version des GIS-basierenden PHP Wasserkraftpotential-Untersuchungsverfahrens klassifiziert daher die gesamten kalten und den überwiegenden Teil der gemässigten Klimazonen als ungeeignet für die Anwendung von high head PHP.

1 Introduction

1.1 Background

Mountain areas had always been attractive to humans for the resources they provide. Forest and mineral related resources may be the most obvious of these, however water is probably the most important one (Funnell & Parish, 2001). Running water, disproportionately abundant in mountain areas compared to equally sized lowland areas (Viviroli et al., 2003) is an important resource for energy generation. In 2009, hydropower accounted for 16 percent of the world electricity production (OECD, 2012). At the same time, the living conditions in mountain areas are attributed with expressions like "remote", "harsh and risky", and "unsustainable" (Kreutzmann, 2001). Difficult economic conditions, inaccessible terrain, and low population density, all widespread in mountain areas, create an adverse environment for electricity grid extension activities (Urmee et al., 2009). As a conclusion from the aforementioned facts it is safe to assume that in mountainous areas of developing countries a good correlation between difficult access to grid electricity and prospective hydropower potential can be expected.

Lack of access to electricity is a global issue with 1.26 billion people in Africa, Asia, and South America being affected (OECD/IEA, 2012). Access to a certain minimum amount of electrical energy is one of the prerequisites to reach the U.N. Millennium Development Goals. The actuality of this situation had further been U.N.-acknowledged by declaring 2012 the ''International Year of Sustainable Energy for All''. Decentralized distributed "off-grid" electricity generation options, most of them using renewable energy technologies, are increasingly successful and are gaining recognition as an alternative to grid extension. One system typically supplies one to several households with a limited amount of electricity. This household electricity generation has become a stable factor in rural electrification in a number of developing and emerging countries in Asia, Africa and South America (Niez, 2010). For mountainous areas with hydropower potential the smallest subdivision of hydropower, so-called Pico-Hydropower (PHP), is considered to be the most cost effective option for small-scale decentralized rural electricity production (ESMAP, 2007).

1.2 Intention, Motivation, Objectives and Hypothesis

Compared to other household size off-grid electricity generation technologies like Photovoltaic "Solar Home Systems" or small fuel powered generators, the recognition of PHP is very low. This is not only true for potential users but also for dissemination entities, such as development organizations or hydropower project developers. Current publications refer to PHP as being an "invisible" or "overlooked" technology (LKYSPP, 2010).

Widespread use of PHP can only be found in a few countries or regions worldwide. Three conditions, of which at least two need to be fulfilled, seem to be prerequisite for the occurrence of significant numbers of PHP installations:

A. Indigenous knowledge of household size hydropower installations (e. g. water wheels for grain milling)
B. Affordable PHP generation equipment is available for sale in the normal operating range of potential users
C. Low availability of grid electricity

Exemplary areas are Nepal with an A-B-C situation or the Vietnam-Laos-China border region with a B-C situation.

In several other countries and regions, efforts by development assistance projects to introduce PHP as an option for rural decentralized electricity generation had gained appraisal by local project owners, however were not able to initiate a self-sustaining local market for affordable PHP generation equipment, therefore were not sustainable beyond demonstration scale (Fulford et al., 2000; Karki & Shresta, 2002; Susanto & Stamp, 2012).

To advance from demonstration scale it would be necessary to artificially create a B-C situation through a massive market introduction effort (Schröder, 2005a). This effort could resemble a conventional PHP dissemination project, however on a larger scale. The threshold for a self-sustaining market is reached when the market volume causes import or manufacture and maintenance of PHP equipment to become attractive for local entrepreneurs. Struben & Sterman (2007) describe such a market introduction process for alternative fuel vehicles that would be widely analogous for PHP technology.

Hydropower is a highly site-dependent technology. Site evaluation and energy potential assessment are integral parts of hydropower projects and have a strong influence on the project economy (ESMAP, 2007). In the case of a large-scale PHP dissemination project, conventional field-based hydropower potential assessment methods would be cost prohibitive due to the large number of possible sites and the necessity to gain an overview of their spatial distribution already at the project planning stage.

Spatial analysis facilitated by GIS (Geographical Information System) and driven by digital elevation data and streamflow information obtained from measurements is an established and cost effective method for stream-specific potential estimates for the larger sized Giga and multi-Megawatt range subdivisions of hydropower down to Small Hydropower (SHP) in the lower Megawatt range. This conventional hydropower potential is represented as hydraulic potential of individual stream segments that carry sufficient flow for the respective hydropower size class of interest (Cyr et al., 2011).

PHP equipment is typically operated on streams that cannot be directly identified on spatial data due to their small size. Flow information for small streams is usually not available. Consequently, the approach to delineate large-scale PHP potential needs to be

fundamentally different from conventional hydropower potential and moreover requires a novel, indirect approach to determine it. Along this way, four principal challenges have to be met:

First challenge: defining a standard PHP system

The field of PHP consists of a wide spectrum of technologies that have different application requirements and specific advantages and disadvantages. A large-scale PHP potential evaluation can only consider those areas of the PHP technical spectrum that have similar site requirements. To optimize the effort vs. applicability relationship in the process of developing a PHP potential evaluation method it is necessary to define a standard PHP system from the technological PHP subgroup that covers as much as possible of the worldwide PHP application potential, and at the same time has relatively uniform hydraulic requirements.

The associated installation site requirements are not only determined by the PHP technology, but moreover include economic considerations.

The expected overall result is a set of PHP system parameters that comprehensively define the minimum site requirements and are applicable both in the field as well as in a remote sensing data processing environment.

Second challenge: definition and classification of PHP potential

With a set of fixed PHP system parameters it is possible to define PHP potential on a systems per area base, thus circumventing the need for dedicated (measured) stream information such as location and flow. The limitations of this new concept need to be identified, since they have a direct influence on the possible gradation and accuracy of the PHP potential representation.

The expected overall result is a gradation of PHP potential that can be reliably delineated with a spatial data based technique and at the same time adequately resolved in a field assessment.

Third challenge: developing a GIS procedure to delineate PHP potential

Large-scale spatial data processing requires the utilization of GIS. A procedure to predict the spatial distribution of PHP potential needs to be developed. In a first stage, the PHP site requirements have to be translated into data requirements that can be represented by spatial data. The spatial data then has to be conditioned into a suitable format for GIS processing. The GIS procedure itself needs to be formulated as a sequence of GIS-specific formulas.

The expected overall result is a GIS procedure that is able to convert spatial data input into a spatial representation of PHP potential.

Fourth challenge: verifying the GIS procedure results against real data

The GIS procedure has to be verified against real PHP potential information. A large-scale field-based assessment method needs to be developed, tested, and executed in selected areas to accomplish this task.

The expected overall result is a reference dataset of spatial PHP potential that is directly usable to verify the results of the GIS procedure for the respective area.

Summarizing the four challenges leads to the formulation of the central hypothesis of this work:

The spatial distribution of PHP potential over a large area can be delineated with a procedure that is based entirely on publicly available spatial data with global or near-global coverage.

It is expected that the procedure can be applied to any part of the global land surface in order to determine the occurrence and distribution of PHP potential that fulfills the requirements for economically viable operation of a predefined PHP system.

Cost effectiveness is the key advantage of PHP over competing household size off-grid electricity generation technologies (ESMAP, 2007). To protect this advantage, and to pay tribute to the fact that PHP application typically takes place in less developed conditions, it is conditional within this work to use only royalty free data and software for the development of the evaluation method.

It is hoped that the results can contribute to establish a large-scale option for decentralized rural electrification with PHP.

1.3 Work structure

The main sections of this work consist of four chapters, numbered two to five:

Chapter 2 gives an overview of the hydropower potential assessment field. Fundamental techniques with particular emphasis on large-scale or large-area hydropower potential assessment are described; the development of hydropower potential assessment with the associated data requirements is elucidated. The state of research in large-scale or large-area hydropower potential assessment is documented in assessments at country level that were conducted in several countries for a variety of hydropower size classes.

Chapter 3 leads to the development of a PHP potential definition. To outline the scope of the underlying technology, distinctions between PHP and hydropower classes larger by unit size, particularly MHP as the next larger class, are analyzed.

Subsequently, available turbine technologies, hydraulic requirements, system components, and associated cost considerations are evaluated to find an approach to a PHP system definition that has optimal applicability prospects and at the same time is suitable for a large-scale potential assessment.

The hydraulic and topographic requirements of the resulting PHP system are defined as standards, and demarcated against out-of-scope conditions.

Chapter 4 covers the entire process of developing the PHP potential assessment method, consisting of the two main sections of “reference data collection” and “GIS based PHP potential assessment”.

The reference data collection describes all aspects of the field acquisition of PHP potential data in the four countries that were chosen as reference areas for their exemplary

distribution of PHP potential. Several acquisition methods are documented that were developed for the field acquisition of PHP potential data.

Examples of field observed PHP potential gradations are presented and field assessment related error sources are discussed.

The GIS based PHP potential assessment procedure is a rule based expert system that utilizes several spatial datasets as input to process an output map of PHP potential. The sequence of input-processing-output therefore represents the main sections of this sub-chapter.

The input section discusses each of the nine topical categories of input dataset, such as topography, runoff, and land cover. Technical parameters (data acquisition methods, spatial extent, resolution), the heritage, its function in the respective version of the procedure, the limitations, and possible alternatives are described for the respective dataset. The data processing section provides a description of the individual data processing steps that are grouped into a preparation stage, an intermediate stage, and a power calculation. The output section is represented by the last data processing step, the evaluation stage.

Each data processing step (e.g. the 'land cover exclusion component' to discriminate potentially suitable from definitely not suitable land cover classifications for PHP installations) is described by its purpose, the underlying scientific assumption, a discussion about the assets and limitations of the approach, and particularly about the individual measures to minimize the inherent errors. The description closes with a detailed formulation of the associated GIS procedure for the respective step.

Chapter 5 is devoted to the application and testing of the large-scale PHP potential assessment method. Each of the four assessment areas, Yunnan Province (China), Costa Rica, Ecuador, and Sri Lanka were subjected to a succession of field PHP potential assessment, GIS assessment, and results analysis. Initially, the validation process for the field assessment data by dry season check and the validation process of the GIS assessed PHP potential by comparison with the validated field assessment data is explained.

The documentation for each assessment area commences with a characterization of the regional natural conditions relevant to PHP potential, divided into topography, climate, and geology, followed by a documentation of the GIS assessed PHP potential and an overview of the reference data collected in the respective field-based assessment. Discrepancies between the GIS based assessment and the field-based assessment are documented as a table and individually analyzed for discrepancy causes. An overall view on the degree of conformity between the two datasets is added.

The conformity of the field assessment data with regular dry season conditions is evaluated separately and followed by a summarizing account of selected representative cell statistics for the respective assessment area.

Following an overall evaluation of the PHP potential assessment results, the next steps beyond large-scale PHP potential assessment are demonstrated in a simulated evaluation of parameters without significance for hydraulic potential, however for the application potential of PHP.

Chapter 6 presents the conclusions and outlook.

2 Hydropower potential assessment

2.1 Basics/Terminology/Definitions

Hydropower relies on the potential and kinetic energy content of surface water. Despite of the ubiquitous presence of water in the environment, only a fraction thereof permits the extraction of mechanical energy, such as hydropower generation, with reasonable effort.

To determine a possible location for hydropower installations or generally the spatial distribution of suitable water bodies for hydropower generation, a hydropower potential assessment is performed.

Conventional hydropower potential assessment methods are based on the calculation of power generated from potential energy of water, formulated as:

$$P = \rho g Q h \eta \qquad \text{E/F 2-1}$$

and simplified to a rough estimation as:

$$P = 8 Q h \qquad \text{E/F 2-2}$$

Three fundamental methods are utilized in conventional hydropower potential assessment. Following is a description of each method:

An **area potential** is the sum of the potential of its sub-areas, each contributing with its available amount of water (flow) and its geodetic height difference to a reference level. A sub-area is usually represented by a grid cell that is exposed to a single hydrological value, such as precipitation.

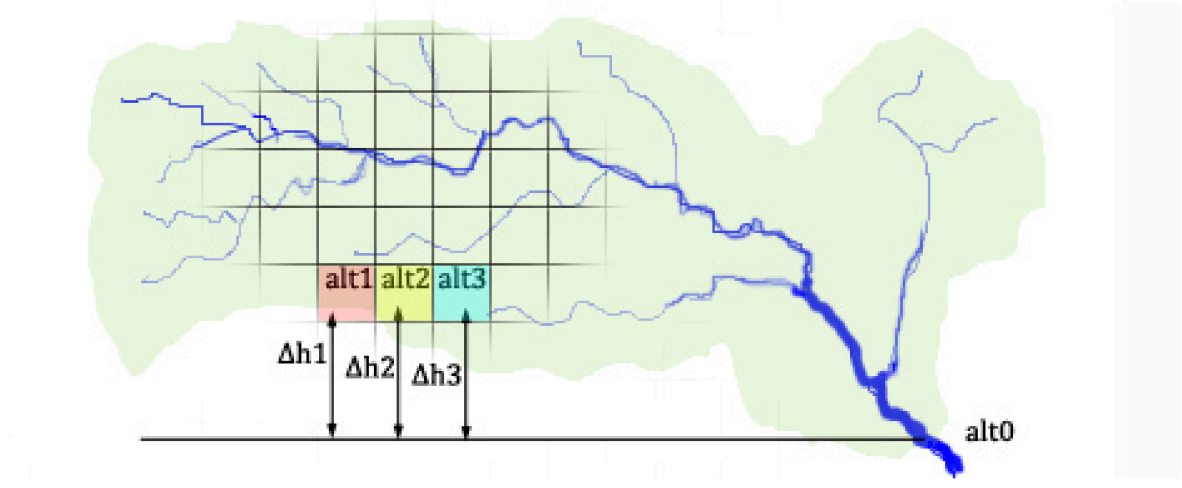

Figure 2-1: Area potential of a watershed (green), expressed as the sum of grid cell potentials that are based on the altitude difference (Δh1, 2, 3) between the grid cell altitudes (alt1, 2, 3) and the reference altitude (alt0) at the drainage point and the respective hydrological value (precipitation, runoff) of the respective grid cell (modified after Weiss & Faeh, 1990).

A **line potential** represents the theoretical upper limit of the hydropower potential of a distinct watercourse. It is derived by dividing the stream into reaches, i.e. the sections between confluences to the stream. Ideally, flow parameters, such as the mean annual discharge, are measured at each respective reach. Hydropower potential is calculated from the flow data and the altitude difference between the two ends of the reach. The total potential of a stream is obtained by summing up the potentials of the stream reaches and their respective confluences.

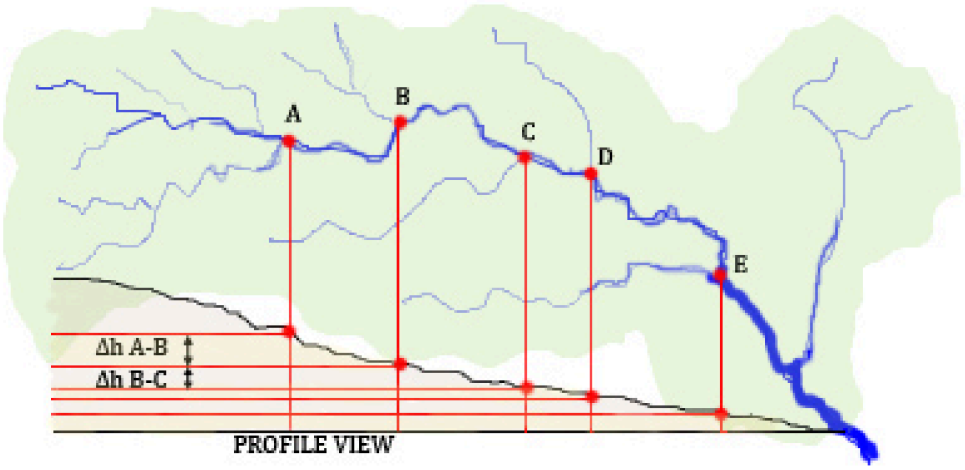

Figure 2-2: Line potential of stream sections between confluences (A-E), expressed as the sum of the hydraulic potentials calculated from the altitude difference (Δh) between two confluences (e.g. A and B), and the respective mean annual discharge, measured between the confluences. (modified after Weiss & Faeh, 1990).

The **usable potential** considers the actual annual power yield that can be expected from a stream at a certain proposed or existing location for a hydroelectric system, called hydropower site. Technical parameters, such as setup-specific hydraulic and electric conversion efficiencies, as well as information about the temporally resolved runoff conditions (monthly and yearly variations) are necessary to calculate the usable potential.

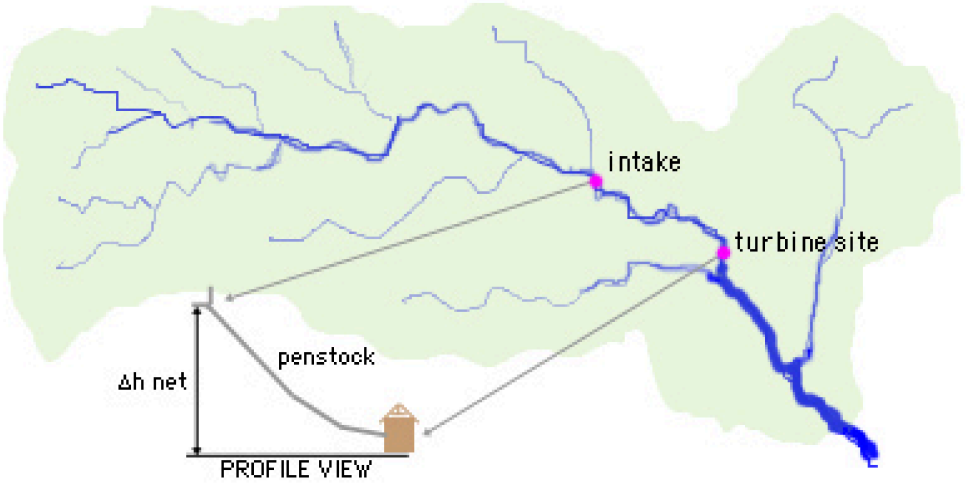

Figure 2-3: Usable potential of a stream section, expressed as a potential calculated from the altitude difference between intake and turbine site, discounted by pressure losses (Δh net), the utilizable flow, and technical efficiency factors of the proposed equipment. (modified after Weiss & Faeh, 1990).

2.2 The development of large-scale hydropower potential assessment

The available amount of water mentioned in the definition for the area potential is called surface runoff or surface flow in hydrological terms. It is a component of the water cycle.

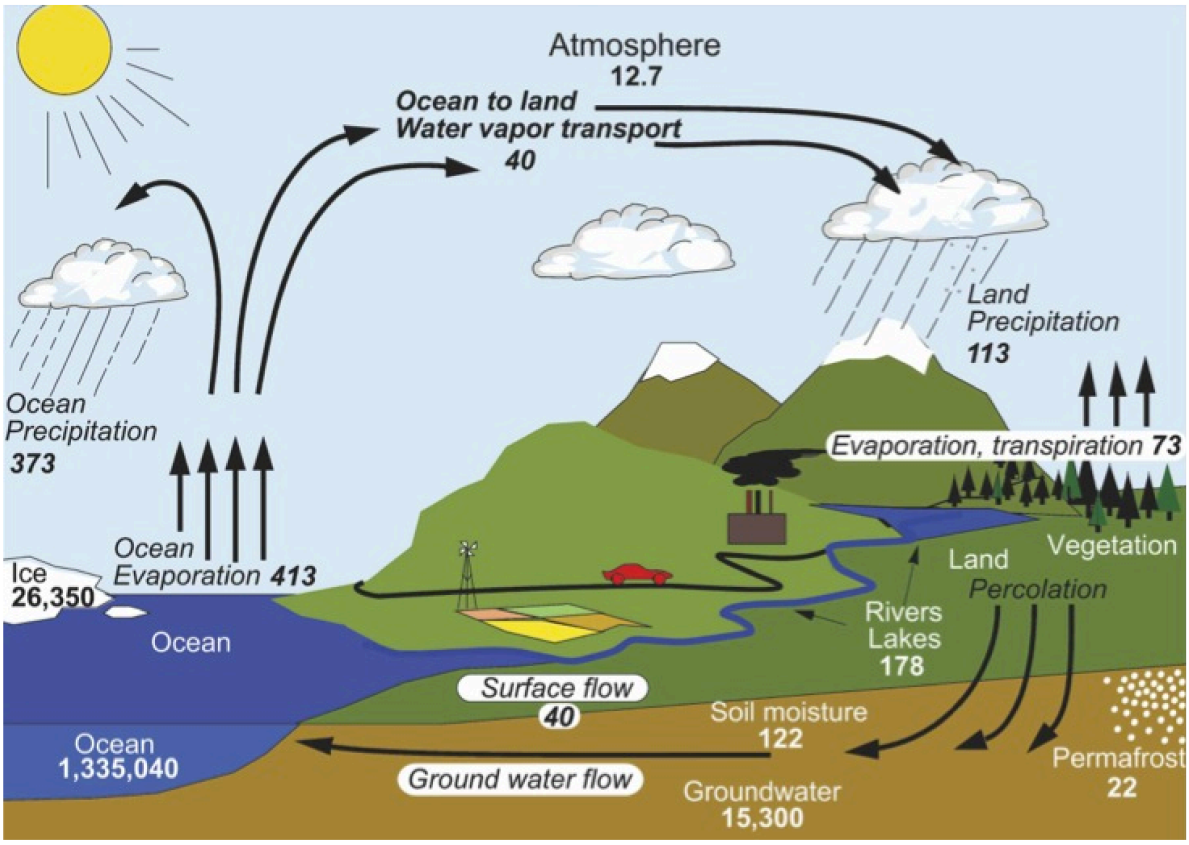

Figure 2-4: Surface flow (runoff) as a component of the global water cycle. Figures in italics are global annual exchanged quantities, the remaining figures are global static quantities. Both are expressed in units of 1000km³. Obtained by reanalysis of various terrestrial and remote sensing meteorological data (Trenberth et al., 2007).

A water balance equation describes the dynamic processes of the water cycle system. Following is a basic representation of the water balance equation, solved for surface runoff:

surface runoff = precipitation - percolation – evapotranspiration E/F 2-3

In practice, the data necessary to represent all components of a water balance are usually unavailable. The water balance is therefore further simplified and unavailable data may furthermore be substituted by proxy data. For example, information on surface runoff, in engineering terms often called streamflow, is often substituted by more readily available, but for this purpose less accurate precipitation information. This substitution causes significant changes in the resulting hydropower potential. Wittenberg & Schulte (1987) compare the results of several studies and document differences between surface runoff based area potential and precipitation based area potential:

Table 2-1: Exemplary comparison of results between surface runoff based area potential and precipitation based area potential (Wittenberg & Schulte, 1987)

Study area	**Size [1000km²]**	**Area potential, based on *precipitation* [TWh/a]**	**Area potential, based on *runoff* [TWh/a]**
Austria 1979	84	252	150
Guatemala 1976	109	326	160

Area potential hydropower assessments are able to illustrate the physical upper limit of hydropower potential based on the topographical and hydrological conditions of a region (Hildebrand & Kern, 1989). The quantification of area hydropower potential is highly influenced by the type of hydrological information used and therefore comparability of area hydropower potential between different studies, which are usually based on different types and quality of data, is very limited.

Early area potential hydropower assessments were based on topographical maps and iso-lines of runoff data from gauging stations. The problem of inaccurate runoff data caused by unevenly distributed gauging stations had first been tackled by empirical studies on the basic relationship between annual runoff, precipitation, and temperature (Langbein et al., 1949). This led to the development of numerous water balance equation models that consider the main components of the water cycle. Advances in the systematic understanding of the natural water supply and more capable computer technology enabled the development of regional regression models to derive annual streamflow information for large areas, based on gauging station flow data, precipitation, temperature, and watershed topography (Vogel et al., 1997). Further research concentrated on regional flow duration models for ungauged watersheds to estimate flow duration curves, a parameter of particular importance for the reliability of hydropower generation (Castellarin et al., 2004).

Likewise, the spatial distribution of precipitation, increasing in complexity with the extent and the altitude variation of the study area, is subject to extensive research. Two exemplary approaches to this effect are (a) an expert system that considers “many localized, facet-specific precipitation/elevation relationships rather than a single domain-wide relationship” as the core function to generate detailed precipitation maps (Daly, 1996) and (b) regional regression models to predict spatial precipitation distribution for areas with unevenly or sparsely distributed gauging stations in complex terrain (e. g. Clark & Slater, 2006). Furthermore, interpolation methods are applied to estimate the spatial distribution of streamflow from limited flow measurement data. This can be achieved for example by utilizing the correlation between measured streamflow and certain characteristics of its corresponding drainage area in an interpolation process similar to kriging (Sauquet, 2006).

Most of the fundamental research related to large-scale hydropower potential assessment, including all examples mentioned above, originates from the domains of meteorology, hydrology, and geography. Dedicated large-scale area potential hydropower assessment research is not a common practice and temporally linked to the emergence of geographical information systems (GIS). Through GIS processing, utilizing various geographic data derived from remote sensing, such as digital elevation models (DEM), a user-friendly implementation of computation intensive hydrogeographic models became possible.

The limiting factor for trans-border large-scale hydropower potential assessments is the availability of spatially consistent streamflow measurement data. Such information is usually prepared for specific purposes and commissioned by administrative bodies and is

therefore available on a national scale at best. Consequently, the maximum extent of area potential hydropower assessments, if prepared with both reasonable effort and accuracy, is normally limited to the area within a national boundary plus overlapping minor extent of near-border watersheds.

Large-scale hydropower potential assessments are published only for a number of countries. The following, seemingly random, compilation of national-scale hydropower potential assessment descriptions reflects this limitation and illustrates the diversity of approaches to this task:

United States

A series of studies conducted by the Idaho National Engineering and Environmental Laboratory for the U.S. Department of Energy assessed the hydropower potential of the entire United States with site potential distinctions ranging between „high power“ (above one MW), Small Hydropower (less than one MW) and Micro Hydropower (below 100kW). Sites between 100kW and 1MW capacity were sub-classified according to their hydraulic head. The initial study „produced an engineering estimate of the magnitude of United States water energy resources on a comprehensive scale and with delineation that was not previously possible“ (U.S. Dept. of Energy, 2004). It is based on the U.S. Geological Survey's Elevation Derivatives for National Applications (EDNA) dataset for both hydrographic and elevation information. Annual mean flow rates for synthetic stream segments were calculated from EDNA and additional climatic data with regional regression equations. The output represents the „total annual mean (hydro)power potential of the United States“ and considers the potential of every stream segment (section between two confluences) generated from the EDNA dataset. The streams were then verified against the U.S. National Hydrography Dataset and protected areas like national parks were excluded from consideration. The assessment procedure can be categorized as line potential assessment, however some of the streamflow data had been derived from area and precipitation information analog to area potential assessments. This practice is normal for GIS-based assessments that are usually hybridizing the classical hydropower assessment methods.

In a subsequent study (U.S. Dept. of Energy, 2006), the potential hydropower sites identified in the previous study were evaluated for their feasibility, considering electrical transmission, accessibility, and environmental concerns.

South Africa

Both, decentralized micro hydropower (MHP) of less than 100kW unit size and “macro”, i.e. grid-connected hydropower potential, are evaluated in a GIS-based study on the Republic of South Africa (Balance et al., 2000). The techno-economic definition of a MHP system used in this study takes into account that water storage measures are likely to be necessary in South Africa to compensate uneven flow conditions. MHP potential results are expressed as five “classes of suitability” according to the expected annual kWh yield per square kilometer. The MHP potential estimates are based on data from a simulated 72-year time series of monthly runoff at fourth order catchment level (Midgley et al., 1994) and use the mean annual flow volume per square kilometer of catchment and the gradient of one kilometer of river reach as base parameters for the power calculation. Particular attention was given to the highly variable flow conditions in South Africa. This is delineated on separate maps for a coefficient of variation and a three-month low flow index. It is noted in the study that the resolution of the underlying hydrological data is too low to directly incorporate the influence of low flow conditions into the MHP suitability map.

Austria

Several hydropower potential studies for the entire extent of Austria were prepared over time. The most recent one (Pöyry Energy GmbH, 2008) is considered to be an update of a previous study (Schiller, 1982) and covers the whole country, except the area draining into the Vltava watershed. The line potential of all main rivers in Austria and their tributaries with streamflows of more than one cubic meter per second at confluence was calculated from various flow records surveyed by a relatively dense grid of gauging locations. The study is geared towards hydropower unit sizes above 10MW. To document the present capacity and yield profile of hydropower in Austria, operators of existing units above 10MW were individually contacted to obtain yield data. SHP (below 10MW) total generation was determined indirectly as the discrepancy of documented total generation vs. documented generation of the individually surveyed LHP stations.

Switzerland

An extensive GIS-study (Weingartner et al., 2012) on the hydropower potential of Switzerland is focused on the following topics:

- total theoretical hydropower potential of Switzerland, calculated from median annual flow rates
- determination of unused hydropower potential under consideration of socioeconomic and ecological limiting factors
- development of an evaluation tool for sustainable hydropower development to be used by regulatory authorities

The water head data for the total hydropower potential generation process is based on an artificial river network generated from a 25m DEM. This network is verified against a discrete dataset of all existing water bodies of Switzerland and furthermore filtered to include only natural watercourses. Flow data is available as modeled median yearly and monthly runoff (period 1981-2000) in raster format with 500m resolution. This data layer is the result of a modeling process with subsequent optimization by data based on field measurements (Pfaundler & Zappa, 2006). The resolution of both head and flow input data available for Switzerland facilitates a line potential assessment with 50m sections that is able to delineate the hydropower potential of streams down to 250m total length. It therefore has a sufficiently high resolution to represent PHP potential. Existing hydropower units above 300kW are considered by the corresponding theoretical potential between intake and outlet of the unit and are deducted from the overall potential of the respective watercourse. The study aims primarily at SHP below 10MW.

Philippines

Micro hydropower (MHP) of less than 100kW unit size is the target of a study conducted in the Philippines (NREL, 2000). The study is a component of a larger GIS project assessing the renewable energy resources of the Philippines. It is based on remote sensing data for terrain data, topographical map data for the stream network, and gauging station data for mean annual precipitation and streamflow. Spatial consistency of the streamflow information is achieved through a model using an empirical, watershed specific runoff coefficient. Hydropower potential is then calculated over the altitude difference between the elevation of a DEM cell containing a stream with the lowest point (drainage outlet) of the upstream neighboring DEM cells. The coarse 0.9km^2 DEM resolution provided more of an overview on the spatial distribution of the MHP resources than of the exact location and power potential of MHP sites.

3 Development of a PHP potential definition

3.1 Hydropower potential and the peculiarities of PHP

Hydropower is a highly site-dependent technology. The planning process for a new hydropower installation is only initiated when a suitable site is identified. A hydropower site is a location where a proven hydraulic energy resource meets favorable conditions on physical accessibility and electricity consumption and no prohibitive competing land use. In subsequent planning steps, the technical components of the prospective installation are optimized to match the conditions of the site and the requirements of the electricity consumers. This planning sequence is necessary not only for economic considerations, but also for legal reasons. Construction of large permanent structures, as well as diversion and exploitation of significant natural water resources are subject to regulation in most, if not all countries.

Hydropower potential is an expression to indicate the spatial distribution and facilitate the localization of possible hydropower sites. It quantifies the hydraulic energy resource at a stream location and dismisses areas that meet predefined unsuitability conditions, such as a protected status, insufficient streamflow, and inaccessibility. Recently conducted spatial hydropower potential assessments often serve the purpose of identifying prospective stream sections with unexploited feasible hydropower potential. The feasibility criteria vary considerably between the individual assessment studies, however the intentions for the studies are similar: to document the additional potential of national hydroelectric power generation. The overall results are expressed as a number or list of sites with the corresponding total feasible hydraulic potential. Examples are studies on the United States (U.S. Dept. of Energy, 2006) and Germany (Anderer et al., 2010).

PHP is the smallest size classification of hydropower. Because its core technologies are shared with the larger sized classifications of hydropower, the site requirements are shared as well. The site selection process however is principally different from the larger sized hydropower applications. This is due to the following features of PHP (Maher & Smith, 2001; Green et al., 2005; Schröder, 2005; Rijssenbeek, n.d.):

- The turbine-generator unit is sold “off-the-shelf” with limited adjustment possibilities. It is designed for a narrow range of hydraulic and electric conditions that are already fixed at the time of purchase
- The turbine-generator unit is perceived by the typical buyer as an appliance. In analogy to electricity consuming applicances after plugging to the electricity source it is expected to be ready for use after plugging it to the water source
- Many typical PHP units can be relocated manually without disassembly of the core hydroelectric components
- All technologically unfamiliar components of a PHP system are integrated into the turbine-generator unit, which usually requires no user configuration. The external components, requiring configuration, are familiar (in both size and material) to typical users from normal rural household applications. The overall PHP system therefore is designed to require no special technical expertise
- The incentives to buy, install, and use the PHP system originate directly from the electricity user. No operating entity is interposed between PHP equipment and the end-user

In summary, the peculiarities of PHP lead to the following conclusion:

Compared to the the larger sized classifications of hydropower, the site selection planning sequence for PHP is typically reversed: suitable equipment is no longer adapted to the existing (identified) site, but rather a suitable site is found for the existing equipment.

Due to the small size and thus undemanding hydraulic requirements of PHP installations, the spectrum of streams that are suitable for PHP extends down to small watercourses that are normally not considered for hydropower extraction. In practice, usually either a small fraction of the available flow of a larger watercourse or an entire small stream is utilized for a PHP installation.

However, conventional hydropower potential assessments typically document the total or feasible hydraulic energy content of a particular stream or area. They have to concentrate the considerable efforts necessary to delineate a feasible hydraulic potential onto stream locations that carry a reasonable probability to become economically viable hydropower sites. These requirements inevitably exclude small streams from detailed investigation, particularly where cost intensive field measurement activities are involved.

In areas where high-resolution runoff data is readily available, cost effective yet detailed and comprehensive hydropower potential investigations can be entirely completed by GIS (see Figure 3-1). In many such cases it would be possible to integrate the documentation of PHP potential without additional effort. The fact that PHP potential results are not documented may be explained by a lack of awareness for this technology (LKYSPP, 2010).

In most high head situations however, documented hydropower potential for larger streams indicates an elevated probability to find concomitant PHP potential in the appendant tributary streams (see Figure 3-1). In other geographic circumstances, particularly in arid climates, lower stream reaches, and certain geological settings, hydropower potential may not be associated by PHP potential (see Figure 3-2).

Consequently, conventional hydropower potential results, normally based on the hydraulic potential (i.e. as Watt units), and usually purposed to delineate a line or feasible potential, have very limited value for the representation of PHP potential and in most cases cannot be directly utilized in the site selection process of a PHP installation.

Figure 3-1: Comprehensive GIS-generated hydropower potential documentation (Neckar river watershed tributaries; Southern Germany), featuring existing hydropower units (grey squares) repowering potential (orange) and additional potential (yellow) in six size classifications between 0.5-1MW (largest squares) and 8-20kW (smallest) (Reiss et al., 2011). PHP potential is not documented, however the hydraulic prerequisites for PHP potential can be assumed to be present in the appendant tributaries (blue) of the streams with documented hydropower potential. Map extent: ca. 70x130km.

Source: http://eol.jsc.nasa.gov/sseop/images/ESC/small/ISS017/ISS017-E-20975.JPG

Figure 3-2: Hydropower installation (Aswan hydroelectric facilities, Southern Egypt), indicating (exploited) hydropower potential in an area that, except for the Nile river (center, with reservoir), an exotic stream flowing through an arid area, otherwise is completely void of PHP potential due to a lack of tributary streams. Field of view: ca 13x8km.

Considering the end-user driven PHP site selection planning sequence, the indicator of suitability to support the deployment of economically feasible PHP installations on a given area, subsequently called PHP potential, would ideally be expressed as a function of the following factors:

- Distribution of suitable watercourses
- Distribution of households
- Electricity availability and pricing
- Household income level and distribution
- Land use
- Water use
- PHP equipment availability and pricing
- Local availability of technical expertise

At this point it becomes clear that the end-user-driven PHP installation process causes local socio-economic factors, such as the individual household income, to play a much greater role for PHP than for larger hydropower. With above spectrum of factors, PHP potential could even be described as a market potential. However most of these factors are neither documented as available large-scale spatial data, nor could they be standardized for large areas. Consequently, quantitative large-scale PHP potential could not be represented using this approach.

To develop a more pragmatic approach for the delineation of large-scale PHP potential, the focus is laid on the occurrence of suitable watercourses, since these are the primary prerequisite for hydropower extraction. Furthermore, other relevant parameters are integrated according to their availability as datasets with global coverage. These include factors that not necessarily affect the hydraulic potential itself, however the economic application of PHP in areas with hydraulic potential. The output of this approach will therefore describe a qualitative potential defined as a likelyhood to find suitable watercourses for economic PHP deployment in a given area.

Following this definition of large-scale PHP potential, the suitability of watercourses is inevitably linked to a certain outline or concept of a PHP system. The following section defines a standard PHP system outline for the scope of this work. General design preferences focus on:

- Established and widespread technology
- Small environmental impact
- Large application potential
- Favorable cost/performance ratio

3.2 Outline of the "standard" PHP system

3.2.1 General considerations on capacity

Any hydropower device with output ratings below 1kW can be classified as PHP. The size classification threshold between PHP and MHP is usually agreed to be 5kW (e.g. Maher & Smith, 2001). Not untypical between hydropower size classes, the distinction between PHP and MHP is not only based on technological differences (see Table 3-1). The transition zone

between PHP and MHP systems can be characterized as a mixture of features on the same system that are either typical for PHP or MHP appliances. This transition zone appears to stretch over the range of 1 to 10kW. Typical distinction features between the classifications are:

Table 3-1: Distinctive features of MHP and PHP

PHP	**MHP**
One user household connected to the system.	Multiple user households connected ("micro grid").
User-operator intervenes irregularly, e.g. at incidents of malfunction.	Designated operator ensures regular system maintenance.
Penstock pipe is made from flexible material that can be coiled. Ideally no joints are necessary in the penstock.	Penstock pipe is made from rigid material and needs to be assembled from segments.
Portable (usually plastic, metal and wooden) water intake structures with no or temporary weir structure.	Permanent (usually concrete) water intake structures, usually with weir and diversion channel.
Turbine-generator unit is exposed to the environment or shielded with a simple structure, such as an open roof.	Turbine-generator unit is protected by a permanent powerhouse structure.
Turbine-generator unit is portable for 1-2 persons or transportable by horse.	Turbine-generator unit needs motorized transportation or disassembly before manual transportation.

PHP is a typical "off-grid" technology that obviously finds the best application conditions in un-electrified mountainous areas of the wet tropics and subtropics. A minimum electricity consumption level for electrification is defined at 0.68 kWh/d (OECD/IEA, 2012). Exemplary household electricity use (either as actual consumption or average demand) for various locations in non-industrialized areas is referred to as 3.7 kWh/d for South Africa (Kusakana & Vermaak, 2013), 0.22 kWh/d for a village in Tibet, China (Engelmann & Ritter, 2003) and 2.7 kWh/d for urban Nepal (Bhandari & Stadler, 2011). These figures reflect a wide range of income situations, climatic conditions, electricity consumption scenarios, electricity sources and temporal references and therefore cannot be directly compared against each other. It is however evident from all mentioned references that a typical PHP installation capable of generating 5 kWh/d is able to supply at least one household under the targeted application conditions.

The technical prerequisites for generating 5 kWh/d would require a 200W system to generate permanently, or a 1000W system to generate for five hours per day. Economic considerations clearly favor the latter option, because:

- The life cycle cost for the generating equipment is similar for both scenarios (Smits & Bush, 2010)
- Typical daily household consumption patterns would require a costly electricity storage solution for the 200W system

- Additional electricity production capacity extends the usage options at an insignificant extra cost

In conclusion, the PHP system size for the scope of this work will be defined as "one kW electrical generation capacity".

3.2.2 General considerations on PHP technology

Hydropower turbine technology is divided into the two main subgroups of impulse and reaction type turbines. Both are available for the whole range of PHP system capacities. From a user perspective, the principal distinctive features between the two types are found in the water intake structures and the head vs. flow requirements.

This results in a distinction between low head and high head systems.

A low head PHP system is most commonly designed around an impeller turbine and consists of the following main components:

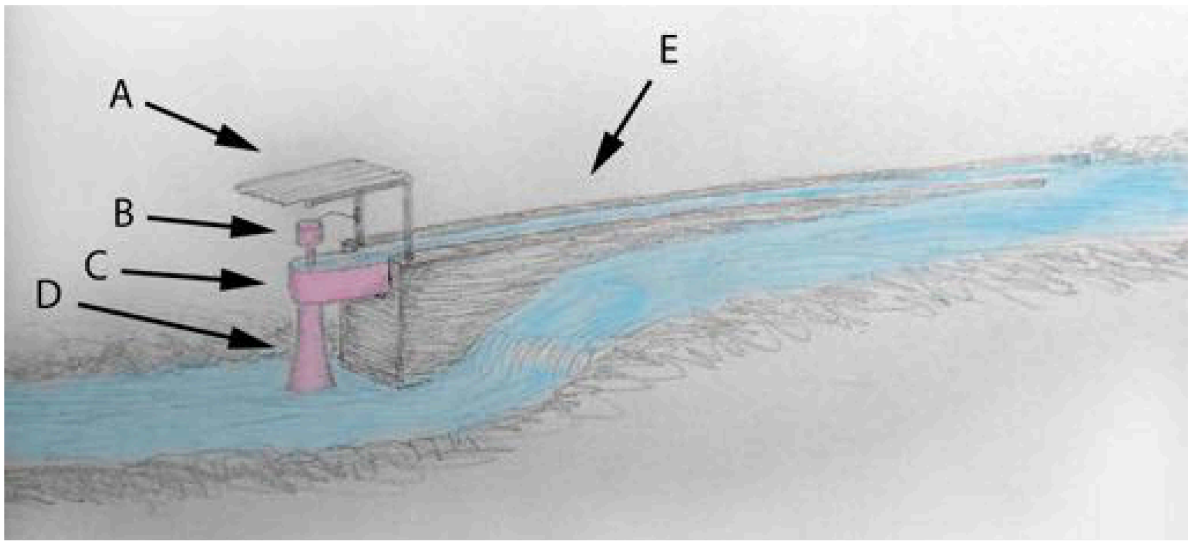

Figure 3-3: Low head PHP system components; (A) Weather-protection; the roof covers about one square meter. (B) Turbine-generator unit with controller. (C) Intake basin with swirl chamber (usually concrete or steel) to force the water in the direction required by the turbine. (D) Draft tube. (E) Diversion channel with trash rack.

Low head PHP technology is typically applied on water heads of 1-2m. The corresponding flow for a 1kW system, assuming a system efficiency factor of 0.6, is in the range of 85-170 l/sec. This quantity of water requires a solid intake structure, usually as an open flume made from concrete, wood, or steel that is not available as ready-made part, thus needs to be individually constructed on site. This construction task, additionally complicated by the need of a swirl chamber to facilitate a suitable reaction angle with the turbine impeller, requires a level of engineering-related knowledge that is normally not found in a typical PHP application environment (Schröder, 2005a).

To bypass this problem, low head PHP turbines in Laos and Vietnam are modified for "zero head" application by replacing the impeller with a larger diameter boat propeller. The turbine assembly is attached to a simple mounting structure in a stream without any water

intake or outlet structures, directly exposed to the flow of the stream (Smits & Bush, 2010). The hydraulic efficiency of this application is very low, and the electric output fluctuates with the streamflow velocity.

Source: Jiangcheng county (Yunnan Province, China) business and tourism promotion brochure.

Figure 3-4: Mass installation of zero head propeller turbines mounted on bamboo racks. China-Vietnam-Laos border region, ca. 1990.

The base model for the zero head modification resembles the presumably most common type of low head PHP turbine, a gearless generator/turbine assembly mounted on a single shaft that is submerged to about half of the total length. The following technical example is representative for a number of models from a diversity of manufacturers.

Turbine type: **Propeller** **Manufacturer:** **unspecified, probably Chinese** **Model:** **Axial ZD2.0-0.5DCT4-Z**	
Power output (Watts, at 220VAC)	500
Hydraulic head (meters)	2
Flow, rated (liters/sec)	45
The required swirl chamber and draft tube are usually manufactured locally. Most “Low Head Family Hydro” units, widespread in Vietnam and Lao PDR, are of the same type but mostly of lower quality.	

Figure 3-5: Bare turbine-generator unit with controller. Source: micro-hydro-power.com

The application potential for low head PHP is particularly sensitive to competition with grid electricity. Flat and accessible areas with abundant flowing water, therefore with good low head PHP potential, are priority areas for agriculture and human settlement. This promotes development and brings along electrification. After the establishment of grid electricity, PHP usually retreats to the role of having been a temporary solution for electricity access (Greacen, 2004; Schröder, 2007). Exemplary areas for such development are the Mekong and Red River watersheds in Southeast Asia. In the 1980s, low head PHP equipment was designed and produced in China to support the rural electrification in less developed areas of PR China, including the Chinese parts of the watersheds in Yunnan Province and Guangxi Autonomous Region (Tong, 1997). Twenty years later, low head PHP utilization had shifted away from China to less developed regions of the watersheds further downstream in Vietnam, Burma/Myanmar and Lao PDR (Smits & Bush, 2010). At present, due to advances in development with extensive and reliable availability of grid electricity, low head PHP utilization has presumably disappeared in Southwestern China. Even though it is technically possible to connect PHP to the grid (e.g. Leite et al., 2016), own experience from China and Ecuador indicates that this is unlikely to become widespread due to (a) user convenience reasons, since PHP installations are relatively maintenance and thus labor intensive, and (b) economic reasons, with investment uncertainties induced by fear of, or experience with, failure or loss of the generating equipment.

To optimize the expected PHP potential for off-grid situations, the PHP potential assessment method of this work is therefore exclusively geared towards high head PHP application.

A high head PHP system is most commonly designed around a Pelton or Turgo type impulse turbine and consists of the following main components:

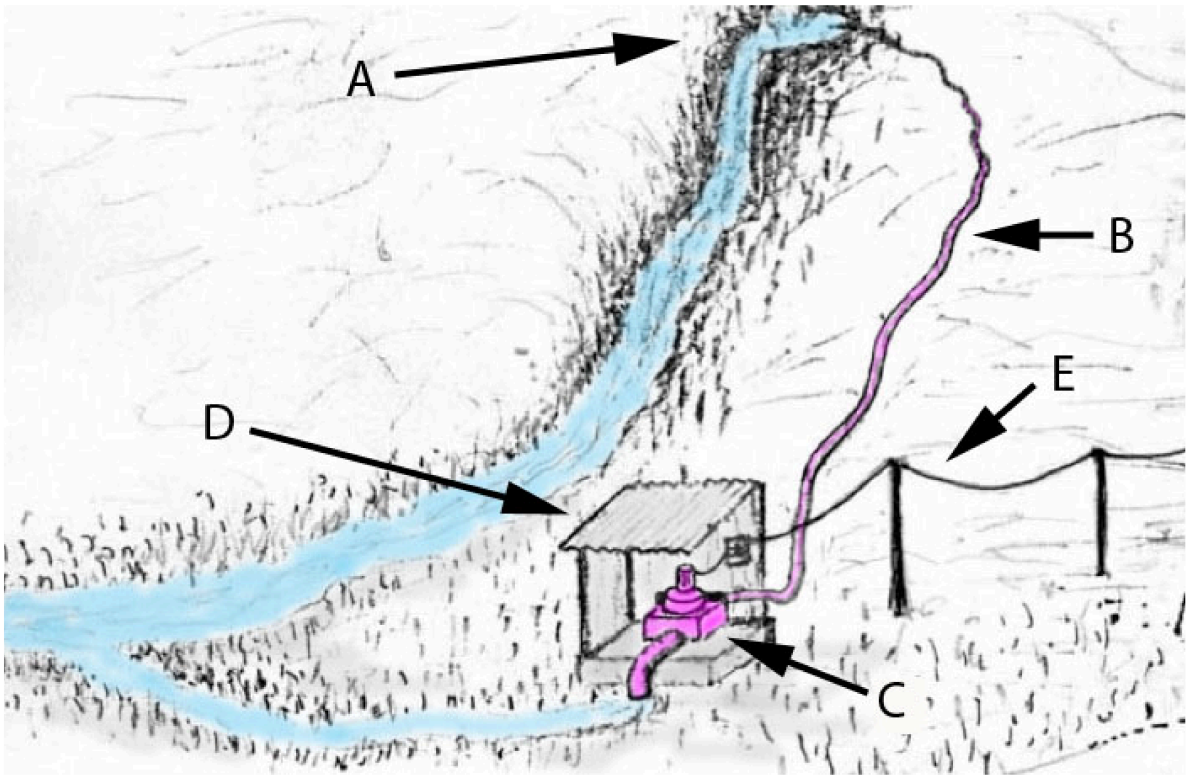

Figure 3-6: High head PHP system components; (A) intake basin (usually reinforced) to collect the water and trap debris, (B) penstock pipe (usually PE plastic) to convey the water to the turbine, (C) turbine-generator unit with controller, (D) weather-protected foundation (usually concrete). The foundation structure covers about one square meter. The runoff is either a short pipe or a channel in the turbine foundation, (E) electrical transmission wiring to the user household.

High head PHP technology is operated with water quantities of less than 10l/sec. The corresponding water heads for 1kW systems are in the range of 10 to 80 meters. Penstock pipes are usually made from one or few segments of flexible material. Such kind of pipe technology and the handling of the associated water quantities are familiar to many rural households in mountainous areas, both from a farming and drinking water supply context. The best hydraulic conditions for the application of high head PHP can be expected in areas with steep hillsides and perennial small streams. Because of the rugged terrain and low population density, such conditions are inherently unattractive for electricity grid extension (Urmee et al., 2009).

3.2.3 Technical outline

The entries of this sub-chapter outline the "standard" PHP system on the component level, illustrated by examples of existing technology. The overall requirements (see chapters 3.2.1 and 3.2.2) call for a high head system definition that is technologically as flexible as possible within the hydraulic and electrical requirements, yet consists of components that are established, cost effective, and easy to use.

Turbine-generator unit

No preference is given to a specific turbine technology, however the unit has to be operable within a range of 10 to 80 meters head, reach a "water to wire" (penstock connector to electrical connector, both on the hydroelectric unit) conversion efficiency of at least 0.6 and an electrical output capacity of 1000 to 1500W. It is confirmed by an online market investigation that various commercial PHP models can fulfill these specifications. Moreover available are do-it-yourself options for PHP units as detailed instruction handbooks (e.g. Portegijs, 2003, for a smaller system) that were prepared with the intention of promoting the local production of PHP units in developing countries.

Following are typical examples of commercially available high head PHP turbine-generator units that are within or close to the specifications of the standard PHP system.

Turbine type: **Turgo** **Manufacturer:** **Dali LIDA, Dali, PR China** **Model:** **XJ18-1.5DCT4-Z**	
Power output range (Watts, at 220VAC)	100-1500
Hydraulic head range (meters)	15-27
Flow range (liters/sec)	2-16
Mechanically solid construction that needs regular maintenance every three months. Simplified low-cost runner with relatively low efficiency.	

Figure 3-7: Dali LIDA turbine-generator unit with controller

Turbine type:	**Turgo**
Manufacturer:	**ENERGY SYSTEMS & DESIGN, Sussex, NB, Canada**
Model:	**Stream Engine**
Power output range (Watts, at 12-48VDC)	100-1000
Hydraulic head range (meters)	2-130
Flow range (liters/sec)	1-25
The unit can be equipped with DC or AC generators of various voltages. The DC versions are used for battery charging. A load controller has to be bought separately.	

microhydropower.com

Figure 3-8: ES&D turbine-generator unit with controller.

Turbine type:	**Pelton**
Manufacturer:	**Kathmandu Metal Industries, Kathmandu, Nepal**
Models:	**Peltric Set (various sizes)**
Power output range (Watts, at 220VAC)	300-120000
Hydraulic head range (meters)	5-100
Flow range (liters/sec)	10-200
The units are usually custom-made according to site specifications. Typical sizes are in the range of 1-5kW. Several hundred units are in operation, mainly in Nepal (A. M. Nakarni, pers. comm., 2004).	

dlenergy.com.np

Figure 3-9: Peltric set turbine-generator unit (MHP size) with flow adjustment valve.

Intake, foundation, trashrack and other civil works

The PHP system is operated as a "run-of-river" setup. This means that the streamflow is not interrupted by artificial structures, such as dams, and water storage is inherently impossible. Diversion channels, particularly if made from local materials, are acceptable as a measure to keep the penstock as short as possible. The same applies to weirs as a measure to locally increase water depth in shallow, fast flowing streams. In situations with abundant flow, the construction of concrete and metal structures is often not necessary for portable PHP units, however serves as an optional measure to improve the operating conditions. Concrete turbine foundations are recommended as a measure against erosion from the turbine outflow and for better turbine maintenance accessibility. The civil works are usually constructed by the owner-operator with construction materials familiar to him. In practice, this is reflected by a diversity of technical solutions (see Figure 3-10) with highly different cost, durability, and performance.

Concrete foundation with integrated runoff pipe.

Wooden foundation situated above a natural watercourse.

Wooden flume (at right) leading to a metal drum (center) that serves as intake basin. The basket is used as a debris filter.

Wire mesh as trashrack on a natural intake basin that is confined by large stones.

Concrete intake basin with diversion channel that concomitantly serves as part of a rice terrace irrigation system.

Turbine house with concrete pole for electricity transmission.

Figure 3-10: Examples for civil work structures of PHP installations at various degrees of sophistication. All examples are from Yunnan Province, China, 2007.

Penstock

Polyethylene (HDPE) at diameters between 50 and 100mm is defined as preferential penstock material for the standard PHP system (see Figure 3-11). The material is widely available, relatively simple to transport in coils, and resistant against mechanical impact, UV degradation, and corrosion. Other penstock materials are usable as well, however are less advantageous at the chosen diameter range (e. g. Maher & Smith, 2001). The definition of a preferential penstock diameter range is necessary for the delimitation of the head and flow ranges in the subsequent calculations.

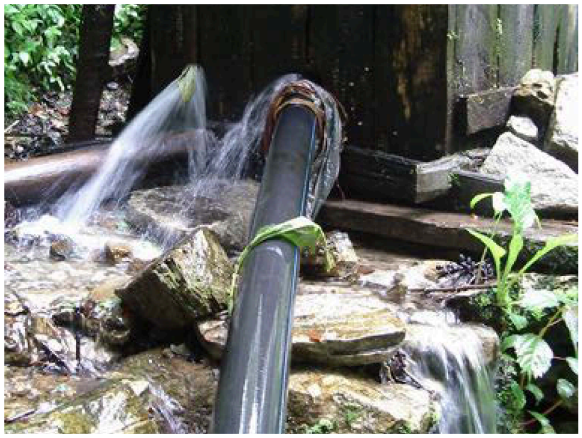

Penstock pipe (75mm PE) connected to a wooden intake basin/settling tank.

PE penstock pipe on site.

Figure 3-11: Examples for high head PHP penstock applications in Yunnan Province, China, 2007.

Electrical system and transmission

The electrical output may either be a direct current (DC) in commonly used voltages (12, 24, 36V) or alternating current (AC) at the local line voltage (110 or 220V). DC systems include a designated electricity storage device (usually a lead acid type battery) and an inverter for AC loads. AC transmission is facilitated by insulated wire of appropriate specifications (see Figure 3-12). The voltage drop caused by the required cable lengths of up to several hundred meters can be compensated by adjusting the AC output voltage at the turbine-generator controller.

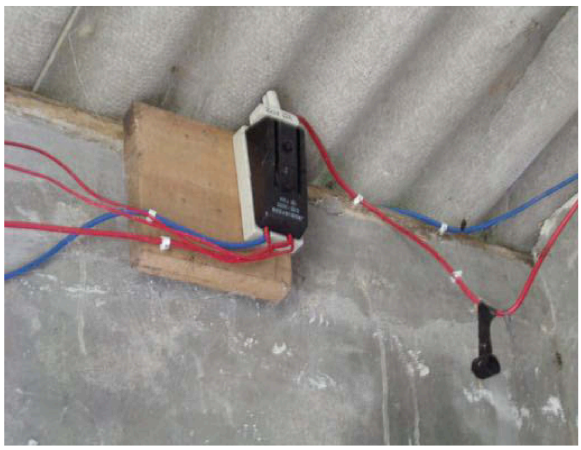

Electrical output wiring of PHP installation with main circuit breaker.

Example for an indequate generator output connection.

Figure 3-12: Examples for electrical connections of high head PHP installations in Yunnan Province, China, 2007.

3.3 Hydraulic and topographic requirements of the "standard" PHP system

General topographic requirements

An electrical generation capacity of 1kW at an overall efficiency of η=0.6 for the turbine-generator unit, as specified in the technical definition for the standard PHP system (see chapter 3.2.3) requires according to

$$P = 9.81 Q h \eta \qquad \text{E/F 3-1}$$

a hydraulic power of 1.66kW. The corresponding head vs. flow diagram is shown in Figure 3-13. Considering the technical and economical requirements on the components of the standard PHP system, both head and flow have to be limited.

The decision on the upper limit of the flow rate is predominantly influenced by the chosen penstock material (see chapter 3.2.3). In a realistic PHP application scenario that represents an average penstock slope of 13.3 degree, 100m of HDPE pipe with 75mm internal diameter at a flow rate of 10l/sec have a pressure loss equivalent of roughly six meters of head (Maher & Smith, 2001). This accounts for 26 percent of the required head and 26m of the total pipe length, however represents the largest diameter to exceed the recommended ten percent (Eisenring, 1991) of head loss. Larger penstock diameters with less pressure loss require additional effort on transport, joining, and structural support (Maher & Smith, 2001). Besides the cost of the HDPE pipe, the overall cost of the different penstock diameter choices depends on the local price of above cost factors and thus cannot be generalized. The maximum flow of 10l/sec therefore represents an artificial limit that is based on a realistic application scenario.

The upper limit of the head range is defined in the technical outline for the turbine-generator unit to be 80 meter (see chapter 3.2.3). This figure, again an artificial limit (see Figure 3-13), is influenced by the limitations of the chosen penstock material as well. Own surveys during the field investigations for this work showed that HDPE pipe of 75mm diameter, on sale in rural markets in China, Ecuador, and Sri Lanka, was found to have a wall thickness around 5mm. This wall thickness translates into a pressure rating range between 60m and 100m head equivalent, depending on the PE quality (e.g. Jain Irrigation Systems, 2016). A limitation to 80m is therefore advised to avoid exceeding the safety margins of lower quality penstock material.

Commercially available high head Pelton and Turgo PHP units in the 1kW range cover a wide range for both maximum head and flow. Some units are optimized for larger flow and therefore relatively low maximum heads, others can be operated on heads beyond 100m that may require a custom made metal penstock (see Figure 3-8 and preceding).

The lower limits for both head and flow originate from the requirement to deliver 1kW output (see chapter 3.2.1). According to

$$P = 9.81 Q h \eta \qquad \text{E/F 3-1}$$

at η=0.6, the head at maximum flow (Q=10l/sec) is 17m, which is therefore the minimal head, whereas the flow at maximum head (h=80m) is 2.1 l/sec, which represents the minimal flow (see Figure 3-13).

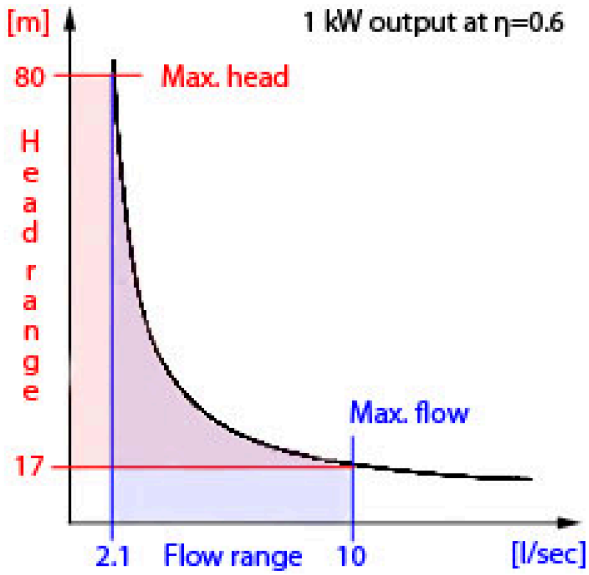

Figure 3-13: Head/flow range definition for 1kW high head PHP system at η=0.6.

The overall efficiency rating is representative for standard quality commercial equipment (e.g. Harvey et al., 1993). Simplified designs, optimized for local manufacture, often have lower efficiencies (e.g. Ho-yan, 2012). Field application conditions can further decrease the overall efficiency due to individual loss factors, such as an increasing mechanical resistance, caused by wear on moving turbine parts. Penstock friction losses and electrical transmission losses are both not quantified in the efficiency considerations. They are independent of the parameters relevant for PHP potential and therefore outside of the scope of this work, however receive some consideration in application scenarios used for definition purposes.

The topographic site requirements have to regard the location of three system components: (1) water intake, (2) turbine-generator unit, and (3) user household (see Figure 3-14). The physical distances between these components have a strong influence on the system efficiency and the overall system cost and should be kept as short as possible (Maher & Smith, 2001). However, realizing short distances between the components (1) and (2) is only possible in steep terrain, which obviously is difficult to traverse and relatively less favorable for farming and human settlement. Thus, areas with favorable natural high head PHP application conditions have a tendency for low population densities. The maximal distances between the system components are subjected to the overall concept of the PHP installation and predominantly represent a result of economic considerations over technical limitations. For the standard PHP unit, the following definitions are developed:

Distance 1-2, Figure 3-14, (straightened penstock length): Maximum 100m. The standard PHP system is conceptualized as a single user household system that is aimed to be economically competitive against grid electricity and other small-scale renewable energy sources, such as photovoltaic solar home systems. It consequently requires relatively favorable natural conditions for PHP application, which means that sufficient head and flow can be accessed with relatively short penstocks. Concomitantly, user acceptance is improved by avoiding both the excessive cost and inconvenient maintenance conditions of long penstocks. The maximal penstock length of the standard PHP system is therefore defined by practical reasons: 100m resemble two 50m coils of HDPE penstock material. Personal experience from Yunnan Province, China (Schröder, 2005b) indicates that the cost for material and transport is particularly favorable for one or two entire 50m coils of 75mm HDPE material, which is the largest diameter that is handled in coils.

Distance 2-3, Figure 3-14, (electricity transmission line to user household): Maximum 900m. This distance causes a voltage drop of 35V with exemplary low cost cable material from Nepal (Maher & Smith, 2001). Conclusions from own field experience (China, Laos, Nepal, Sri Lanka, Ecuador, Costa Rica, USA) and PHP equipment manufacturers (e.g. Lawley, 2010) indicate that (a) voltage loss of this magnitude is approaching the limit of the compensation abilities of PHP equipment voltage regulators, (b) the willingness of PHP users to invest in better transmission cables and electric connectors to reduce voltage drop is marginal, and (c) the spread of typical distances between existing PHP installations and user households implies that distances over about one kilometer are considered impractical by the users of PHP installations.

Distance 1-3, Figure 3-14, (water intake to user household): Maximum 900m. The distance is a result of the two preceding distances. It is subject to the same considerations on practicality to the PHP users as distance 2-3.

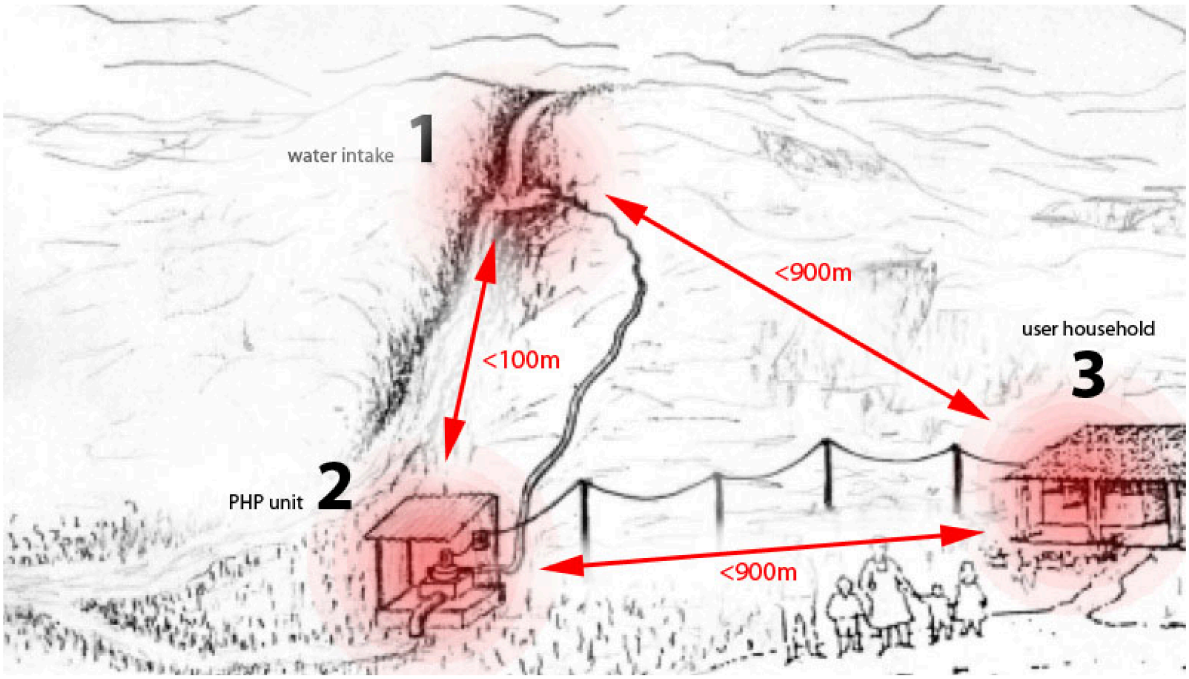

Figure 3-14: Distance limitations between PHP system components influencing the topographic site requirements of the standard PHP system.

The network of distances between the PHP system components is optimized for cost. The length of the distance-dependent component with the highest specific cost, usually the penstock, is therefore kept as short as possible. This is usually achieved at the expense of transmission means with a lower specific cost, such as diversion channels and electric lines (e.g. Harvey et al., 1993; Maher & Smith, 2001).

System area definition

A globally applicable definition for the maximal component placement area of an individual PHP system can only be based on a generalizing assumption. The distance-related technical limitations (see Figure 3-14) are considered in the following PHP system area definition:

For the scope of this work, the maximum area to place all components of an individual PHP system is defined as a one by one kilometer square that is graphically represented as a 30 by 30 arc second cell (926m side length at zero latitude, usually referred to as 900m side length due to the simplification of one arc second cells to 30m side length). It is henceforth referred to as "PHP unit cell" (see Figure 4-12).

Developing a DEM-based model of the distance relationship network of PHP system components is theoretically possible on local and regional scales where cost information for technical components and installation, requirements originating from local farming practices, and the exact location of individual households are known. A model on such a level of detail could provide accurate estimates on the main cost factors of individual prospective PHP sites. For a large-scale assessment, as for this work, the data mentioned above are either not available or insufficiently consistent over the assessment area. Exact distances between the PHP system components moreover require real stream network information.

A qualitative approach with the available data focuses on the spatially consistent, and relatively accurate, topographical data to extract terrain inclination information. Being the main influence factor for penstock length, terrain inclination influences all component distances and therefore all cost factors. As a solution, a qualitative "threshold slope for PHP potential" is deducted from a combination of empirical information and technical requirements and serves as a generalizing assumption for this work. The average slope of the corresponding DEM area is analyzed for the fulfillment of the threshold slope criterion.

Threshold slope definition

The minimal terrain inclination requirements ("worst case" application conditions concerning topography) for the standard PHP system are based on the minimal head (see Figure 3-13 and preceding definitions) and maximal penstock length (see Figure 3-14 and preceding definitions). At 17m vertical distance, which is the minimal head required to generate 1kW of electrical power, 100m of penstock length correspond to 9.5 degree average DEM slope. This value is used to define the threshold slope for PHP potential in this work.

Figure 3-15: Derivation of the threshold slope for PHP potential.

Favorable high head PHP application conditions are accompanied by either penstock length reductions or reduced flow requirements at constant penstock length to achieve the nominal output. Both require, if all other parameters are left unchanged, an increase in

hydraulic head to obtain a terrain inclination that is higher than the threshold slope for PHP potential.

The hydraulic head requirements that are associated with favorable high head PHP application conditions are justified by technical reasons. Several own random online market searches, executed between 2002 and 2016 for commercial high head PHP generation equipment operating at flows under 10l/sec (examples: see Figure 3-7 and 3-9), confirm the rough division into a lower head range operated by Turgo turbines and a higher head range operated by Pelton turbines that is found in turbine application diagrams of larger hydropower equipment manufacturers as well (e.g. Gilkes.com, 2015). For commercial PHP equipment with 1-1.5kW output capacity, the upper border of the overlap between both application ranges is defined by the upper margin of the Turgo application range and found at hydraulic heads between 25 and 30m.

Figure 3-17 is based on the data of a PHP equipment manufacturer and exemplarily depicts the application domain of the standard PHP system against the application ranges of the different turbine types.

The minimal terrain inclination requirements for favorable high head PHP application conditions are therefore based on 30m (vs. 17m for worst case conditions) of head. This is the area of the high head PHP turbine application range where, considering the limitations of 100m maximal penstock length and 10l/sec maximal flow, the largest selection of generating equipment can be expected.

The resulting average DEM slope for favorable high head PHP application conditions is 17.5 degrees (see Figure 3-16).

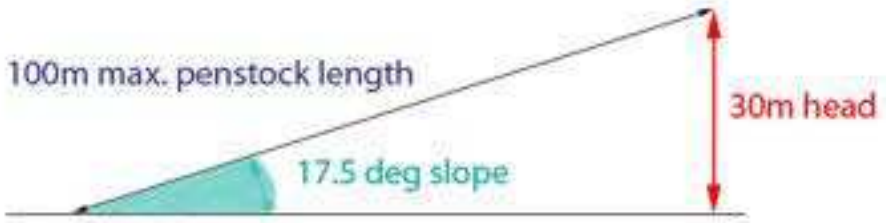

Figure 3-16: Derivation of the threshold slope for favorable PHP potential.

The threshold slope condition as a prerequisite for PHP potential is justified by an interlocked combination of economic and technical requirements arising from the specifications of the standard PHP unit. At 9.5 degree average DEM slope the threshold slope condition is not an overall exclusion condition for PHP potential, however for high head PHP potential. Therefore it defines the border between high head and low head PHP potential in the scope of this work.

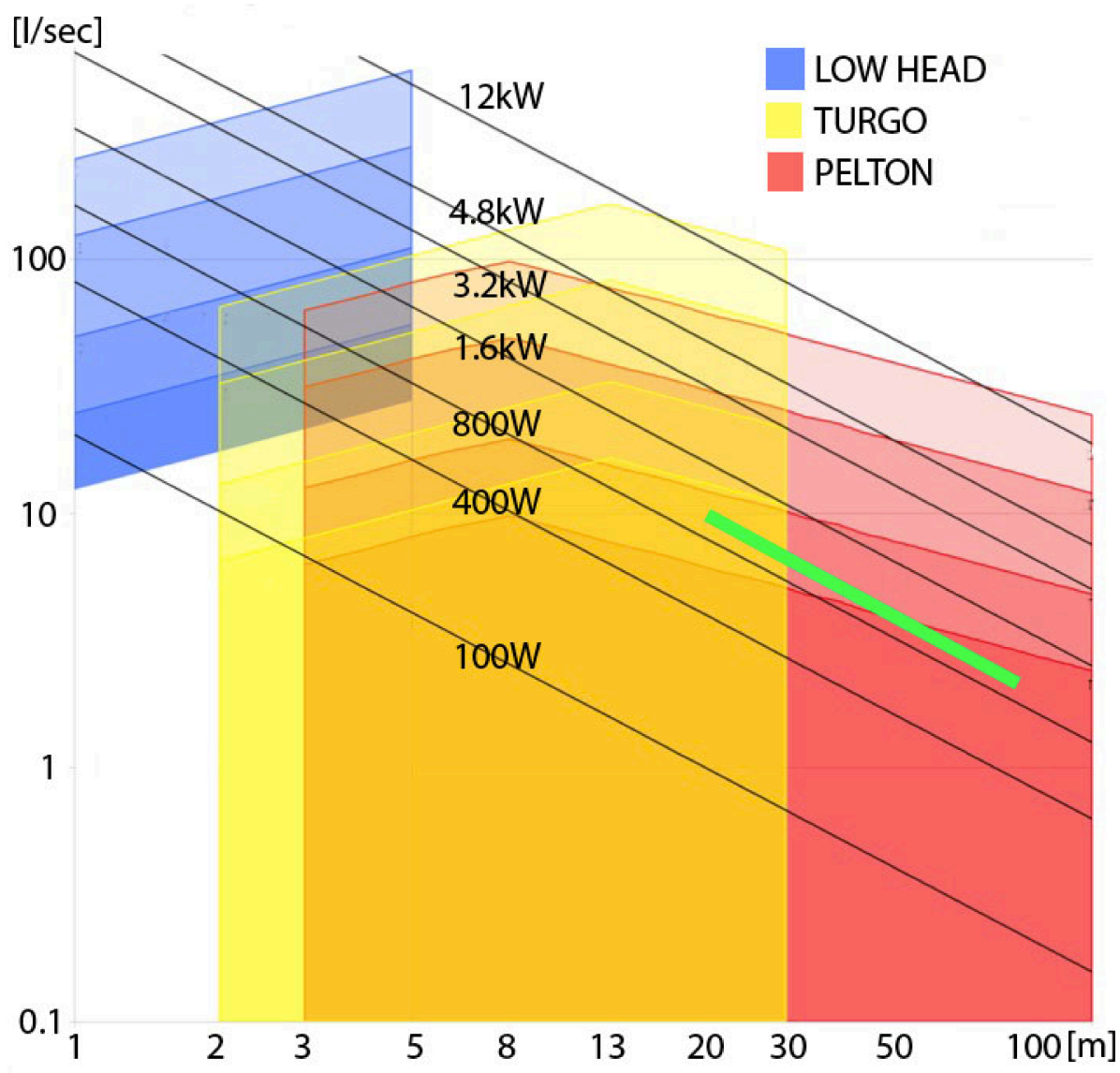

Figure 3-17: Application range diagram of different types of PHP turbines (modified after EcoInnovation, 2014). Head and flow are in logarithmic scale to facilitate a linearized output graph (black). The green bar illustrates the application domain of the standard PHP system at 1kW output.

Hydraulic conditions threshold definition

The maximal area of one square kilometer for the placement of all components of a PHP system requires the threshold size for a first order stream watershed in the GIS watershed delineation procedure to be one square kilometer as well. This ensures that at least one virtual, GIS generated, stream per PHP unit cell (1km^2) is present (see Figure 3-18). It depends on hydrological parameters whether this stream is suitable for a standard PHP system. Referring to the hydraulic requirements set out in Figure 3-13, a minimum streamflow of 2.1-10 l/sec, depending on the available head, is necessary to generate 1kW output with the standard PHP system.

According to the water balance equation of a watershed:

surface runoff = precipitation – groundwater recharge - evapotranspiration E/F 3-2

the streamflow, or surface runoff, from a watershed is a fraction of the precipitation onto the watershed area. By combining the individual loss fractions into a coefficient, it is expressed as:

*surface runoff = precipitation * runoff coefficient* E/F 3-3

To estimate streamflow from precipitation information, various approaches had been developed to determine the runoff coefficient C_r. Engineering favors deterministic methods to make C_r usable for practical applications. Chow (1962) describes numerous, mostly empirical approaches, based on geomorphologic parameters like soil type, vegetation cover classifications, and drainage area, usually with only regional validity and targeted at specific applications. Exemplary for a simplified approach is the rational method, credited to several authors of the late 19th century, and still in use for small area communal drainage tasks like sewage capacity dimensioning. The rational method uses tables of fixed runoff coefficients that are attributed to land cover classifications, and further sub-classifications according to terrain inclination, where no further data analysis is required or possible. More accurate determination methods to develop regional precipitation to runoff relationships require precipitation data with high temporal resolution. Apart from regression models, probabilistic, statistical, perturbation, and fuzzy modeling approaches are utilized (Şen & Altunkaynak, 2006). Global monthly average precipitation data is available in relatively coarse 0.25 degree resolution, translating into 27.7km cell size (GPCC Precipitation Climatology 025, Meyer-Christoffer et al., 2011). Global surface runoff data is available in even more coarse 0.5 degree resolution, which translates into 55.5km cell size (Fekete et al., 2002). Both data sets were used in preliminary versions of the GIS based PHP potential assessment procedure of this work and proved to be an obvious individual source of error due to their coarse resolution.

The surface runoff information used in the final version of the GIS based PHP potential assessment procedure of this work is obtained from the WaterWorld version 2 (2014) model, a water balance model with global extent and 1km resolution (Mulligan, 2013). Surface runoff is calculated in the WaterWorld model as

annual total water balance = (precipitation + cloud captured moisture) – actual evapotranspiration

E/F 3-4

and subsequently converted into a monthly water balance for the driest month of the year by multiplying the fractional contribution of the driest month to the yearly precipitation with the annual total water balance values. The minimal monthly precipitation value is derived from the respective GPCC Precipitation Climatology 025 data (Meyer-Christoffer et al., 2011) at monthly resolution.

The qualitative PHP potential estimate of this work does not depend on absolute flow data for particular watercourses (see chapter 3.1). It is therefore appropriate to utilize modeled water balance data to identify areas with sufficient continuous runoff that can provide the minimum flow requirements (see Figure 3-13).

According to

$$\frac{0.01 m^3/\sec * 2592000 \sec}{1000000 m^2} \approx 0.026 m \qquad \text{E/F 3-5}$$

a streamflow of 10 l/sec from a watershed of one square kilometer approximately amounts to an equivalent of 26mm monthly surface runoff. The minimal hydraulic requirements (10

l/sec) for the operation of one 1kW PHP system per square kilometer at conditions of minimal head (17m) are therefore fulfilled and a runoff threshold factor is postulated for the standard PHP system:

"A monthly runoff of 26mm in the minimum-runoff-month of the year is a prerequisite for PHP potential"

To adjust this threshold to (typically seasonal) lower flow conditions it can be lowered to an absolute minimum of 7mm if it is compensated by sufficient hydraulic head to result in a continuous electrical output of 500W at minimal runoff conditions.

The minimal hydraulic requirements for favorable high head PHP application conditions are founded on a prerequisite ability to operate more than one 1kW PHP system per square kilometer at full output capacity. The corresponding monthly surface runoff is therefore 2*26mm = 52mm, which is a representation of two suitable streams on the same square kilometer quadrant (PHP unit cell). This two-stream condition is defined in disregard of possible arrangements that operate more than one PHP system per square kilometer on the same stream, such as a cascaded installation.

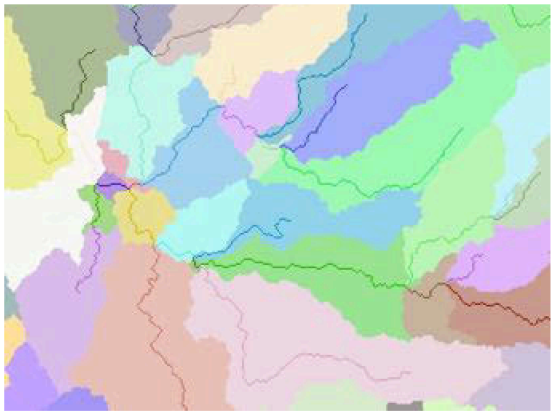

Minimal watershed generation area larger than 1km2 (threshold: 2000 cells at DEM resolution); the resolution of the generated stream network is too coarse: The minimal runoff conditions for PHP installations may be met not only by the first-order stream, but also by second-order streams of the same watershed. The minimal runoff threshold is invalid because of the mismatch between PHP unit cell and minimal watershed size.

Desired watershed size; exactly one stream with a threshold of 1000 cells (30.8m x 30.8m x1000) occurs on an area of 1km^2 or larger. The minimal runoff threshold is able to distinguish adequate from inadequate streamflow conditions for a standard PHP installation on this watershed.

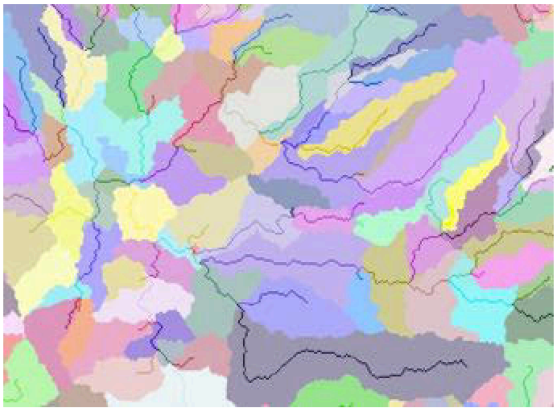

Minimal watershed area smaller than 1km² (threshold: 500 cells); Watersheds are generated that may contain first-order streams without adequate streamflow, caused by insufficient drainage area. The minimal runoff threshold is invalid because of the mismatch between PHP unit cell and minimal watershed size.

Figure 3-18: Visualization of the influence of the watershed delineation threshold. Different watershed delineation thresholds are applied onto the same area. Only the result of the 1000-cells-threshold delineation is compatible with the concept of minimal runoff threshold, because both underlying concepts (1000-cell watershed delineation and PHP unit cell) refer to an approximate area of one square kilometer.

Operability requirements definition

The main reason for the approach via the minimum-yearly-runoff month is to ensure PHP system operability over the entire year, without interruptions caused by insufficient or absent streamflow. It is moreover expected that the site conditions permit the continuous operation of the PHP system at full output (1000W for the standard system). A temporary reduction of monthly average output of the PHP system is only acceptable if it exceeds 50 percent of the output capacity (500W for the standard system).

Technically, the output of PHP systems is regulated either by adjustable turbine nozzles (needle valves or interchangeable fixed-diameter orifices) or by small reservoirs that are drained over the PHP system during the dry season on a daily base (e.g. Inversin, 1986). Because of the monthly resolution of the global precipitation data used, it is not possible to consider flow related output fluctuations within the same month.

Typical flow related “out of scope” conditions for the standard PHP system

The requirement for continuous streamflow, prerequisite for continuous operation of a PHP system, obviously reduces the global PHP application area considerably. Reasons for seasonal flow interruptions are either a falling water table, causing streams to run dry, or low temperatures, causing streams to temporarily freeze. Both conditions are considered in the suitability discrimination procedure of this work (see chapter 5) as individual thresholds for runoff and snow cover.

Another exclusion condition is karst. Unlike the previous exclusion factors karst is not affecting the continuous operability. Instead, it affects the PHP potential by altering the character of the surface flow conditions and therefore the probability to find suitable watercourses for PHP application. The runoff threshold factor becomes invalid in karst-typical conditions of rapid percolation.

The paramount cause for this phenomenon is the dissolution of carbonate and evaporate rock types that results in a network of large underground cavities. Spring formation in such karst areas takes place after an underground accumulation process that leads to fewer and larger springs at lower altitudes. Input–output analyses of karstic systems may even consider surface stream runoff to be negligible in karst areas with the entire runoff concentrated into the discharge of one or few major springs (Labat et al., 2000). The effect of karst on stream formation, when compared to otherwise identical conditions over less soluble, silicate based, rock types, is illustrated in Figure 3-19. The overall effect on PHP potential in karst conditions is caused by the relative absence of higher order streams that are otherwise the main contributors for high head PHP potential.

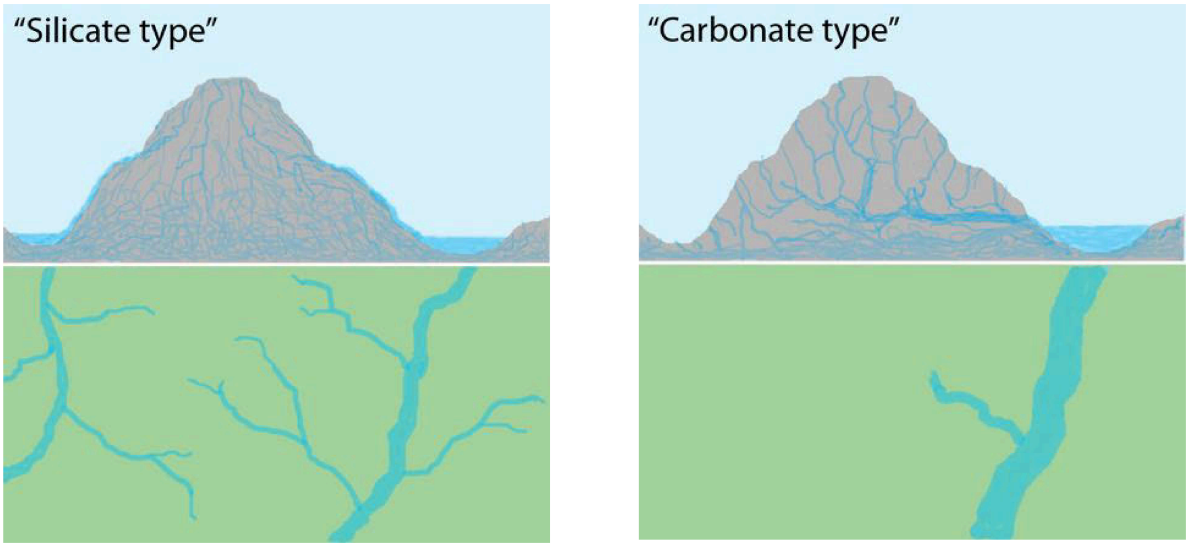

Figure 3-19: Idealized spring formation patterns to illustrate the effect of karst on PHP potential. Comparison of regular "silicate type" against karst ("carbonate type") spring formation patterns as terrain cross cut (at upper half), and the resulting stream networks (at lower half). Equal amounts of precipitation are assumed for both types.

About 20 percent of the exposed global land surface is dominated by carbonate and related evaporite (e.g. salt, gypsum) rock types, of which 50-75 percent display carbonate karst features (Ford & Williams, 2007). Due to the largely absent small perennial streams with sufficient inclination for high head PHP utilization, carbonate outcrop areas are generally classified as unsuitable for PHP application in the context of this work.

A visualization of the global impact on the exclusion factor for snow cover can be found in Figure 4-22, and for carbonate karst in Figure 4-17.

4 Development of a large-scale PHP potential assessment method

4.1 Reference data collection

PHP potential data was collected between January 2010 and March 2012 in China (Yunnan Province), Costa Rica, Ecuador and Sri Lanka. The reference data collection is lead by the following aims:

- To develop a rapid potential assessment instrumentation as a means to gain an overview on the qualitative PHP potential of large area
- To collect reference data for PHP potential classifications
- To collect reference data on small streams
- To collect reference data on land cover, land use, and water use patterns as supplementary information for the PHP potential data

To maximize data collection efficiency, the reference areas were chosen according to the following prerequisites:

- Complete transitions between an absence of high head PHP potential and favorable high head PHP potential can be expected
- The prospective areas provide suitable traffic infrastructure for overland traveling at medium speed (bus, slow train)
- The areas are familiar from previous traveling (China/Yunnan Province, Ecuador, Sri Lanka), or provide expectedly similar conditions to countries previously traveled (Costa Rica)
- Climatically suitable conditions for continuous PHP operation prevail (no freezing conditions below 3000m altitude in the entire assessment area)
- The extent of the assessment area permits the collection of spatially representative data in the given time

The respective traveling times were chosen to meet the driest conditions of the year for the most significant assessment region (e.g. for the SW of Sri Lanka). The aim was to encounter the seasonal worst-case conditions for PHP application during the field assessment.

Due to the considerable spatial extent of the reference areas, stationary potential assessment techniques, such as flow measurements, could not be utilized. Instead, data collection is performed by permanent observation of the surrounding landscape from the moving means of transport. PHP potential is concluded from the landscape features. The traveling velocity causes a trade-off between the resolution of the observed features and the spatial coverage in the given time. Actual traveling velocities varied, depending on infrastructure conditions and means of transport. Overland bus traveling was found to be the fastest practicable and most frequently used means of transport.

Three approaches on reference data collection were developed prior to the field assessments and were iteratively improved in the course of the assessments:

- Field-based assessment by direct PHP potential attribution
- Field-based potential assessment by stream frequency
- Field-based potential assessment by indicator vegetation

4.1.1 Field-based assessment by direct PHP potential attribution and the resulting general classification of PHP potential.

The overall concept of this approach is to attribute a PHP potential class to a certain area by a single observation from a distance, usually without further examinations. It is executed by continuously observing the surrounding landscape while moving along a transport route, producing a contiguous set of observation notations. Particular attention is drawn to:

- Running water in any specification
- Water use (agriculture, human settlement, storage, hydropower)
- Topography (particularly in respect to the position in an assumed watershed)
- Human settlement density and patterns
- Land use and agricultural practice

The method draws from previous own experience in PHP site assessment and field application. It relies on personal judgement that is based on criteria that are only partially penetrable. Results among different data collectors are likely to be reproducible only with substantial deviations. This seems to be generally the case with rapid assessment techniques that involve relatively complex decision taking. Nevertheless, such methods are often the only choice and thus fairly widespread in scientific fields that have to assess large physical areas for both static features, such as exploration geology (e.g. Marjoribanks, 2010) and dynamic features, such as ecosystem biology in various states of alteration (e.g. O'Shea et al., 2011). Research by Oliver & Beattie (1993) about rapid assessments of biodiversity suggests that for higher organizational levels of data (in this case: the number of occurring species) a more reliable result can be expected than for lower organizational levels of data, such as the taxonomic determination at species level. The trade-off between assessment speed and assessment detail, justified in tropical ecosystem biology by the need for quick inventories to initiate conservation measures in areas threatened by environmental destruction, is justified for large-scale field based PHP potential assessments as well. Here, the challenge is to assess a large, contiguous area in relatively short time during the seasonal minimum flow conditions. For these reasons, the results classification is kept as simple as possible, with three classes of high head PHP potential and two supplementary (sub)classes:

Table 4-1: High head PHP potential classification.

High head PHP potential	**PHP potential specification**	**Referral code**
no	"No PHP potential"	Class H0
no	"Above spring horizon"	Class H8
no	"Only low head PHP potential"	Class H9
yes	"(high head) PHP potential"	Class H1
yes	"Favorable (high head) PHP potential"	Class H2

The supplementary classes H9 and H8 are introduced to better distinguish the type of transition between presence and absence of PHP potential, e.g. the transition between H0 and H1 vs. H9 and H1. These classes are only used for the processing and verification stages. Without practical use for the representation of high head PHP potential they are merged into class H0 for the final result. The classes H0, H1 and H2 were postulated prior to the first field assessment, however were only established after they had been tested and confirmed in the field. This is to ensure that the classes are reliably distinguishable in the field, from a set of more or less characteristic features that were established during the field assessment as well.

Typical examples for PHP potential class indicator features are described and illustrated in the following sub-chapters. The features may not be exclusive for a particular PHP potential class, are not exhaustive, may not always be applicable or even be mutually exclusive. Moisture dependant features strictly refer to dry season conditions.

The exemplary images in Figure 4-1 to Figure 4-5 should be observed as still pictures associated to an impression that is actually obtained by moving through the landscape. Therefore only details of the overall impression leading to the attribution of a PHP potential class are represented in the respective single images. Vice versa, it would usually not be possible to attribute the PHP potential class of a particular landscape from a single image. A comparable task would be to recognize the genre of a motion picture from a single still picture. It is roughly estimated that a minimum of five minutes exposure to a moving landscape, the equivalent of traveling a distance of three to four kilometers, is necessary to gather sufficient information for a PHP potential attribution. The images primarily serve the purpose of documenting the occurrence of comparable conditions across the assessment regions.

Indicator features for “no PHP potential” (Class H0)

- No running water visible at adequate ground visibility conditions
- Barren ground
- Sparse or dry vegetation
- Indicator plants for dry conditions present (e.g. agavas, cacti)
- Uninhabited
- Urban conditions
- Obvious karst indicators
- Flat topography

N-Yunnan, China: Sparse vegetation with barren patches, no surface water.

NW-Costa Rica: Dry shrub vegetation, cacti, no surface water.

W-Yunnan, China: Sparse vegetation, partially dry and with barren patches, no surface water, agavas;

W-Ecuador: Barren patches on uncultivated land, no surface water, flat terrain.

Figure 4-1: Exemplary dry season landscapes associated to Class H0.

Indicator features for "only low head PHP potential" (Class H9)

- Flat or hilly areas
- Visible streams during the dry season, with apparently sufficient flow for PHP installations
- Most of the ground that is not used by agriculture is covered by vegetation (not necessarily all green)
- Obvious karst indicators
- Distributed rural population with low to moderate settlement density

N-Costa Rica: One relatively large stream, no apparent tributaries (possibly due to pseudokarst influence). Predominantly green vegetation.

E-Ecuador: Abundant water in flat areas, low hills without tributaries, green vegetation.

SW-Yunnan, China: Only streams in flat areas, low hills, green vegetation.

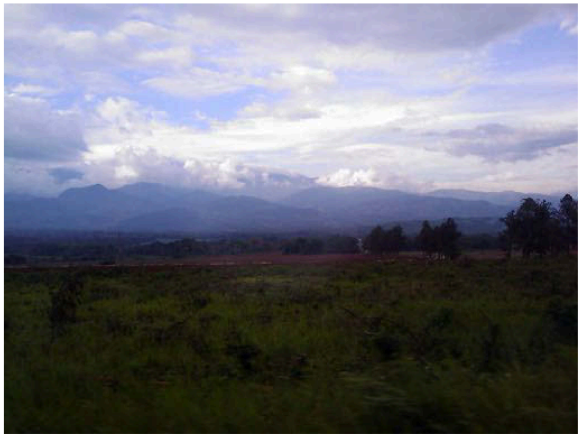

SE-Costa Rica: Numerous streams in flat terrain that originate from the mountains in the background.

Figure 4-2: Exemplary dry season landscapes associated to Class H9. Due to image scale, image size or concealing vegetation, streams are not necessarily visible in the images.

Indicator features for "above spring horizon" condition (Class H8)

- Peak regions of hilly or mountainous areas with apparent PHP potential
- No streams, or only very small streams visible during the dry season that are unsuitable for PHP installation
- Most of the ground that is not used by agriculture is covered by vegetation that is typical for the altitude
- Distributed rural population with low to moderate density

SW-Ecuador: Peak area with occasional small streams. Green vegetation.

S-Ecuador: Peak area. Very small streams contribute to mountain lakes. Green vegetation.

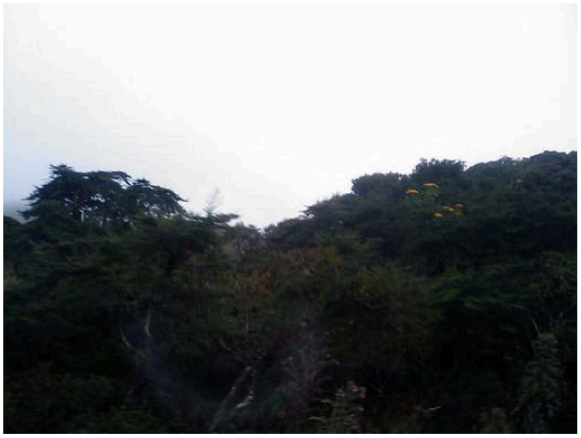

E-Costa Rica: Peak region with dense mountain forest and only very small streamlets.

S-Sri Lanka: Peak area without surface water. Streams and waterfalls in the valleys indicate a spring horizon at lower altitude. Green vegetation.

Figure 4-3: Exemplary dry season landscapes associated to Class H8. Due to image scale, image size or concealing vegetation, streams are not necessarily visible in the images.

Indicator features for "PHP potential" (Class H1)

- Hilly or mountainous areas
- Visible streams during the dry season with apparently sufficient head and flow for high head PHP installations
- Most of the ground that is not used by agriculture is covered with vegetation (not necessarily all green)
- Distributed rural population, with low to moderate settlement density

W-Yunnan, China: Hills with frequent small streams (here concealed by vegetation), green vegetation, rain at dry season.

E-Costa Rica: Frequent small streams, moderately steep topography, green vegetation.

S-Sri Lanka: Frequent small streams, moderately steep topography, green vegetation, rain at dry season.

SE-Costa Rica: Frequent small streams, moderately steep topography, green vegetation.

Figure 4-4: Exemplary dry season landscapes associated to Class H1. Due to image scale, image size or concealing vegetation, streams are not necessarily visible in the images.

Indicator features for "favorable PHP potential" (Class H2)

- Mountainous areas with steep features
- Frequent small streams that are apparently not, or not entirely used for agriculture
- Waterfalls
- Existing small-scale hydropower installations (MHP, PHP, watermills)
- Lush green dry season vegetation
- Distributed rural population, with low to moderate settlement density

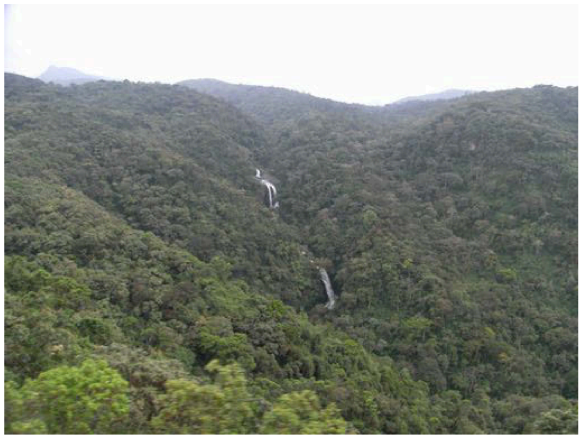

SW-Sri Lanka: Steep topography, prominent streams visible through the lush vegetation, waterfalls.

SE-Costa Rica: Hilly to steep topography, high density of small streams (concealed by the lush vegetation).

NW-Ecuador: Steep topography, frequent prominent streams visible through the lush vegetation.

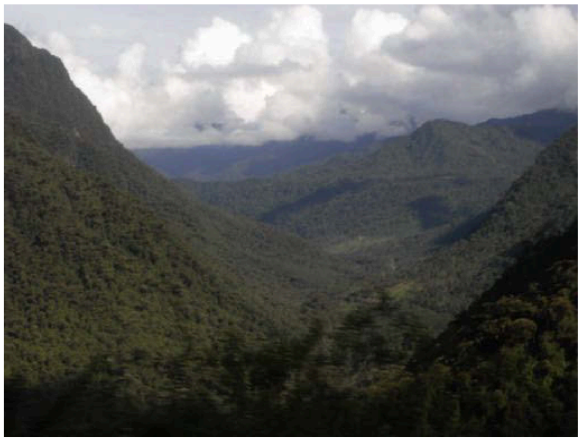

E-Ecuador: Steep topography, frequent prominent streams visible through the lush vegetation, waterfalls.

Figure 4-5: Exemplary dry season landscapes associated to Class H2. Due to image scale, image size or concealing vegetation, streams are not necessarily visible in the images.

4.1.2 Field-based potential assessment by stream frequency

Areas without perennial streams are unsuitable for PHP application. According to the definition carried out in chapter 3.3, one stream per square kilometer that permits the extraction of 1kW fulfills the threshold hydraulic conditions for PHP potential.

Concomitant to the direct attribution of PHP potential, the locations of suitable streams were recorded during the field-based assessment. “Stream location” is defined here as the intersection of a stream with the path of the observation track. “Track” is defined here as a section of road that is traveled in a single passage under continuous observation of the surrounding landscape. It is essential that all streams apparently suitable for PHP installations, coded “X1” in the results, get recorded consistently for the entire observation track. Dry streambeds “D1” and streamlets with insufficient flow “ZZ” are recorded as well and serve as complementary information. The information obtained with this method is subsequently analyzed in a GIS environment to derive a PHP potential by estimating the “stream density” of an area. It primarily serves the following purposes:

- Verification of the required stream density for the respective PHP potential class (“sufficient streams per area”). Class H1, for example, requires a density of one stream per square kilometer.
- Verification of the stream suitability (“sufficient flow in dry season conditions”).

The stream density method is limited to the assessment of visible streams that intersect with the observation track (see Figure 4-6 and Figure 4-9). It approaches objectivity in sections where the observation track follows the altitude line, provided that the streams are not hidden and there is sufficient observation time.

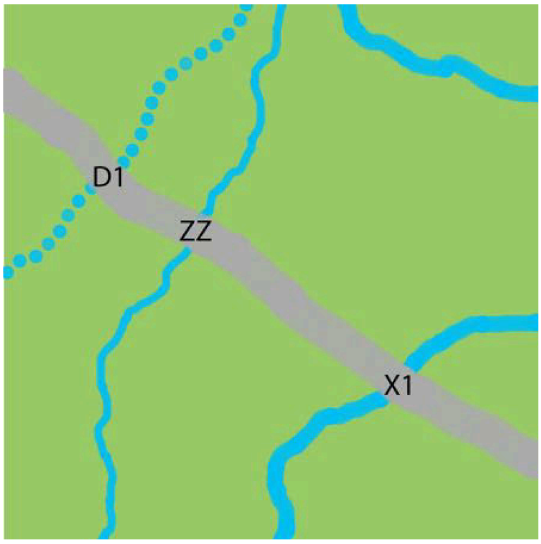

Figure 4-6: Exemplary representation of the elements of the stream density method: Observation track (grey), intersected by a suitable stream (X1 location), dry stream (D1 location), and unsuitable streamlet (ZZ location). The area shown in this example represents a stream density of 1 because only the X1 location is contributing to the stream density considerations.

4.1.3 Field-based potential assessment by indicator vegetation

The apparent diversity of vegetation types and agricultural practices of Yunnan Province/China initiated the idea to utilize plants and vegetation types as auxiliary indicators for PHP potential. Observations of the following crop cultivations:

Rubber tree (code: VR), banana (VB), rice (VRI), tea (VT), bamboo (VBA), maize (VCO), vegetables (VV), eucalyptus tree (VE), sugarcane (VSU), papaya (VP), agava (VA), fruit tree cultivation (VFR), willow tree plantation (VW), rapeseed (VRA), *Opuntia* cactus (VO), barley (VBR), tobacco (VTO), pineapple (VPI),

as well as the following forest and vegetation types:

Conifer mixed forest (VC), moist deciduous subtropical forest (VFS), unspecified forest (VF), wet tropical forest (VFT), epiphytes forest (VEP), pure conifer forest (VCC), hard leaf shrub (VHS), grassland (VG),

were recorded during the field assessments in Yunnan and Costa Rica. The selection of entries is based on recurring observations in the field.

For the tropical part of the assessment area (Costa Rica and Southern Yunnan) no apparent correlation between specific plants or vegetation types and PHP potential was found. Particularly in wet tropical areas, commonly cultivated species seem to be ubiquitous, regardless of any parameters relevant for PHP potential.

For the subtropical part of the assessment area (Central and Northern Yunnan) one apparent correlation, between agava plants and an absence of PHP potential (Class H0), was found. This correlation yields a limited practical use for field-based potential assessments in areas of Yunnan that feature starkly different PHP potential on relatively small areas (less than 10x10km) and at the same time have a fairly uniform topography. The underlying causes for the differences in vegetation and PHP potential are assumed to be small occurrences of karstified carbonate rock.

The recording of indicator vegetation is discontinued since the Ecuador assessment. It is not considered to be a sufficiently functional supplement for field-based PHP potential assessments. Nevertheless, the general appearance of vegetation (with and without regard to the species composition) remains to be an important decision factor for the direct PHP potential attribution.

4.1.4 Apparent error sources of the field-based potential assessment

The direct PHP potential attribution of the field-based potential assessment is a subjective method that is inevitably influenced by misjudgment. Many possible error sources remain obscure. In the following sub-chapters an overview of error sources is given that had either been already identified in the preparation process, became apparent during the field assessment, or had been identified from discrepancies between the results of the field assessment and the GIS-based assessment (see chapter 5.1). The error sources may not be applicable across the field-based potential assessment methods, are not exhaustive, and may not always be applicable or even be mutually exclusive. Moisture dependant features strictly refer to dry season conditions.

Overgrown, piped or otherwise concealed streams.

This error source leads to an underestimation of PHP potential. The probability to occur for this error increases with the distance to the observed streams, the traveling speed, and the density of the vegetation.

It is found that transport conditions preventing a detailed observation of the landscape features, such as traveling on stilted highways or at high speed, are usually instantly recognizable as being unsuitable for data collecting. Alternative ways to collect data for this particular area can be through a different (slower) means of transport or variations to the traveling routes.

Figure 4-7: Overgrown streams in open, heavily vegetated area (NC-Costa Rica). Actual stream widths in both cases are 0.5-1m.

Variations in visibility caused by mist, rain, vegetation, and other influences.

This error source is closely related to the preceding one and therefore aggravated by high traveling speed as well. It particularly affects areas that are perennially moist and densely vegetated with higher vegetation and thick undergrowth. The error may lead to an underestimate in areas of high PHP potential and needs to be prevented during the field assessment by abstaining from data collection at temporarily irregular, such as foggy,

conditions. Very dense vegetation can present a permanently irregular condition. In this case it is necessary to conduct at least part of the assessment in the affected areas with direct access to the watercourses.

Figure 4-8: Obscuration of terrestrial details in moist, heavily vegetated areas. Locations: E-Costa Rica (at left) and NW-Ecuador (at right).

Misinterpretation of stream suitability caused by insufficient observation time.

Streams are often directly visible for only a second or less from the moving means of transport. During the data collection it is important to anticipate approaching streams by observing the surrounding topographical profile and vegetation. This facilitates a quick evaluation when the stream is coming into sight. Errors associated to insufficient observation time may cause an over- or underestimation of PHP potential.

Misinterpretation of terrain inclination.

Reliable visual judgment of average terrain inclination, in particular when only a part of the terrain is visible, is not possible during the field assessment. The resulting error can cause a shift in the observed borders between H0, H1, and H2 potential classes. Errors associated to this situation may cause an over- or underestimation of PHP potential. The error is relatively common, however can be reliably detected and eliminated in a comparison between field assessed and GIS-calculated PHP potential estimate (e.g., see Table 5-4). This is possible because the DEM-based inclination information used in the GIS procedure is consistently more reliable than the visual judgment in the field.

Untypical runoff conditions at the time of the field assessment.

Untypical seasonal runoff conditions were monitored before the field trip was initiated. When necessary, traveling to the affected area was postponed to the following dry season. Short-term effects, such as variations in stream discharge after a single rainfall event, could not be avoided and cause a local overestimation of field assessed PHP potential. The total amount of precipitation during the month of the field assessment *cum* two preceding months was compared with the average figures for the respective calendar months *a posteriori* to ensure that the field assessment was undertaken at typical minimum flow conditions (see chapter 5.1.1).

Uncertainties in spatial representativeness of the field assessment.

While traversing an area on a fixed track, the visibility of the surrounding landscape is subject to constant changes. In a field assessment for PHP potential, a visible distance of 500m towards both sides of the track, or a distance of one kilometer towards one side is

ideally required to permit an evaluation of the critical landscape features. This is to ensure that the statement about the PHP potential is representative for the surrounding 1km² PHP unit cell. In a real-life situation however, the field assessment result has to be deducted from an overall impression that is based on the non-ideal actual visibility (see Figure 4-9) and an often sub-optimal amount of observation time. For the direct PHP potential attribution method it is roughly estimated that a horizontal offset of up to three PHP unit cells for an observed transition between PHP potential classes has to be put into consideration. This transition offset, the traveling distance necessary to realize the transition between PHP potential classes, is often influenced by visibility and represents approximately five minutes of observation time at a typical traveling speed of 50km/h.

The recording offset, i.e. the distance traveled between a recording feature and the completed GPS position recording, is caused by human reaction time and technical delays in the GPS fixing process. This offset is in the order of tens of meters and therefore normally confined to the same PHP unit cell. Although its relevance increases with the traveling speed, the overall effect on the PHP potential result can be neglected.

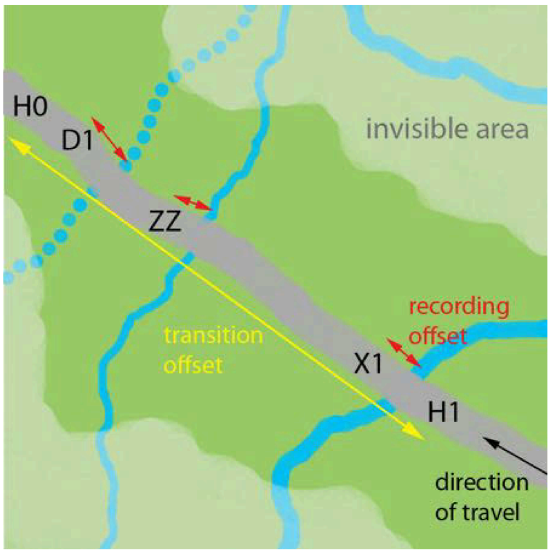

Figure 4-9: Exemplary illustration of the uncertainties in spatial representativeness of the field assessment. Areas that are invisible from the assessment track are shaded light green.

Effect classification of the apparent error sources

Visibility-related error sources lead to a moderate underestimation of PHP potential. This effect contributes to a conservative PHP potential estimate. Other, principally critical, error sources that may lead to an overestimation of PHP potential are reliably detected and eliminated in a comparison between field assessed and GIS-calculated PHP potential estimates and complemented by a dry-season validity check (see chapter 5.1). The most prominent examples are incorrect terrain inclination estimates in the field. The remainder consists of persistent error sources without a general tendency for under- or overestimation of PHP potential, such as a visual misinterpretation of the suitability of watercourses for PHP installations.

4.1.5 Technical data acquisition setup for the field assessment

Before 2010, a pocket computer (smartphone) in combination with a separate GPS device was used for data localization. Observations were recorded on paper with manually added GPS readings. Due to the slow GPS fixing and complicated setup, GPS readings at this stage

needed to be taken in stationary conditions and could only be added to major features. In a second stage (Yunnan 2010 and Costa Rica 2011) a smartphone with built-in GPS receiver and camera was used, supplemented by an external battery to enable continuous GPS operation. Locations could now be recorded by photo with GPS tag. Observations between the photo locations along the track were recorded on paper, marked with the file number of the last photo taken and manually added into the result spreadsheet. In a third stage (Ecuador 2011 and Sri Lanka 2012) the same hardware was used. The data is now entered through "OSMtracker", a dedicated POI (Points of Interest) open source logging software (Openstreetmap.org, 2010), custom configured for entering most of the recurring features (such as "stream crossing", "potential Class H1") with a single click. Short comments are also directly typed into the software. The configuration facilitates quick recording of recurring features in a format that requires only relatively straightforward conversions to become usable for GIS processing. With single-click recording it moreover becomes possible to implement the stream frequency method (see chapter 4.1.2) at minimal recording offset by recording all stream intersections of a track with their individual GPS coordinates.

4.1.6 Output format

The results of all field-based potential assessment methods are recorded in a single result matrix in GPX format. Each entry contains the following category fields:

Latitude, longitude, elevation, time and date of recording, name, comment, description.

All assessment results are contained in abbreviated form in the "description" field. This is necessary, because the GIS software can only display one field category at a time and switching between field categories is not practical for the visual GIS analysis procedure.

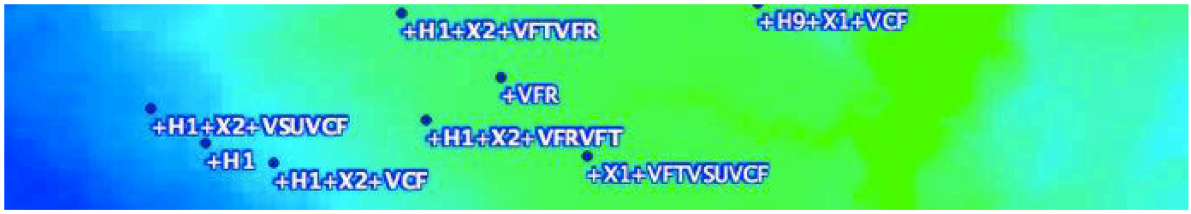

Figure 4-10: Second stage example of an assessment track section in GIS view with 'description' field active, visualized against a DEM background. The total E-W extent of the example is 3 km. The actual area is located in SE-Costa Rica. Codes "+H…" refer to PHP potential classes, codes "+X…" refer to the number of streams crossed since the last recorded location, and codes "+V…" refer to information about the vegetation. All locations (black dots) are documented by a georeferenced photo image.

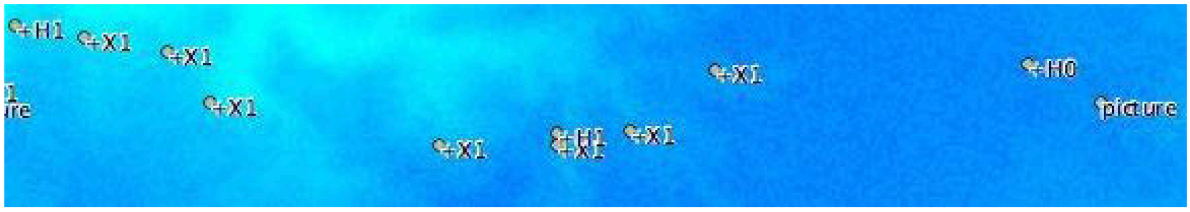

Figure 4-11: Third stage example of an assessment track section in GIS view with 'description' field active, visualized against a DEM background. The total E-W extent of the example is 7 km. The actual area is located in W-Central Ecuador. Georeferenced locations are marked by a green dot; code "+X1" refers to a single stream crossing, code "+H…" to the PHP potential in the vicinity of the location, "picture" to a commented photo reference.

4.2 GIS based PHP potential assessment procedure

A geographic information system (GIS) combines aspects of cartography with data processing and statistical analysis to serve as an application for decision support (Chrisman, 2001). In the context of this work, a GIS is developed from spatial data and software analysis routines to answer the specific question about the suitability of a given land surface area for a predefined type of PHP application. The overall GIS procedure is grouped into an input, processing, and output section.

The input data consists of spatial information of relevant parameters, in either raster or vector map format, for the delineation of PHP potential. Any hydropower potential representation, regardless of the output format, is derived from the basic hydraulic power equation, simplified here under disregard of the efficiency factor as:

$$P = 9.81 Q h \qquad \text{E/F 4-1}$$

Both head h and flow Q are considered primary parameters that contain the basic information about the theoretically available static energy of the surface water at the location.

Head is expressed as an elevation difference. This information is readily available in fine resolution as a Digital Elevation Model (DEM).

Flow in geographic terms is an expression of surface runoff per unit area. This information is either available in coarse spatial resolution as a surface runoff map or in coarse temporal resolution as a water balance modeling result (see chapter 4.2.1).

Secondary input data contains information about the main factors that affect flow: For example, seepage velocity related information is contributed from a carbonate outcrop map. Land use and vegetation cover related influences, such as flow diversion by ducting, influences in evapotranspiration by agricultural practices, and general runoff expectations specific to vegetation types, are derived from a land cover classification map. The available secondary input data permits no quantification of the respective effects on flow. The GIS procedure is therefore designed to treat the effects from secondary input data as qualitative exclusion factors only.

The processing stage of the GIS is based on raster map calculation in the GIS software environment. It contains:

A. A preparation stage to calculate auxiliary information from input map data, such as watershed boundaries and slope values
B. A series of discrimination tests for exclusion conditions, such as freezing and karst geology
C. A power calculation to evaluate the conditions associated with the DEM cell (30m grid) against the energetic requirements of a standard PHP system
D. An evaluation stage to determine the PHP potential classes for the PHP unit cell (926m grid) from the intermediate results

The output is a three-stage PHP potential classification that is attributed to a 30 arc second (926m*926m) square of land surface. It is visualized as a raster map layer in a GIS software environment.

Conventional hydropower potential assessments calculate a potential from measured head and flow data. Alternatively, knowledge of regional runoff conditions permits the

development of regional regression models that can facilitate reasonably accurate algorithmic hydropower potential calculations without comprehensive coverage of measured flow data (Cyr et al., 2011). For very small streams over very large areas, algorithmic methods relying on measured or modeled quantitative flow rates of real streams are presently not applicable due to insufficient data leading to unacceptably inaccurate results.

The GIS based PHP potential assessment procedure of the present study instead follows a heuristic approach, based on a qualitative definition of the PHP potential term, to replace the hydraulic-energy-content-based quantitative representation of potential. In this approach, a range of factors that influence the local application conditions for PHP (see chapter 3.3) are considered.

Automated analysis of specific problems through non-algorithmic methods falls into the domain of knowledge based systems. Conclusions are deducted from a computerized logical process, the inference engine, that uses the information about a specific problem that had been converted into a computer usable knowledge depository, the knowledge base (Nikolopoulos, 1997).

Inference engine and knowledge base of the GIS based PHP potential assessment procedure are integrated into a sequence of raster map calculations. In a first stage, IF…THEN conditions are utilized to compare rasterized input data against threshold values to generate intermediate results. After further calculation steps with the intermediate results, the final output is generated. This methodic approach typifies the GIS based PHP potential assessment procedure as a rule based expert system (Nikolopoulos, 1997).

The following sub-chapter describes the GIS based PHP potential assessment procedure as a sequence of input, processing, and output. Viewed from an alternative perspective, the main components of a GIS - cartography, software tooling, and decision support - are analogously represented in this tripartition.

4.2.1 Input section

General prerequisites on input data

The expected main application areas for the standard PHP system are found in sparsely populated mountainous rural regions of the tropics and subtropics. Areas with this constellation of topography, climate, and population density are often associated with a low level of development and institutional weakness (Urmee et al., 2009). Using PHP for decentralized small-scale electricity generation under these conditions typically requires low-cost solutions (Schröder, 2007). To extend the low-cost principle to the concept of large-scale PHP potential assessment, the entire GIS based PHP potential assessment procedure is designed around freely accessible input. An integral aspect of the large-scale approach of this work is the applicability of the GIS based PHP potential assessment procedure on all land areas that are suitable for the operation of the standard PHP system under the operating conditions laid out in chapter 3.3. The prerequisite for continuous operability, uninterrupted from seasonally adverse conditions, shall be particularly mentioned among the operating conditions. All spatial data used in the core parts of the GIS based assessment must therefore cover at least the entire land area between the temperate climatic zones and ideally have a global coverage.

The GIS based PHP potential assessment procedure utilizes spatial data sets that contain primary information about:

- Topography
- Precipitation
- Runoff
- Snow cover
- Land cover classifications
- Carbonate rock outcrops
- Generalized surface geology
- Water balance.

In the following sub-chapters, the respective spatial data sets are individually described and compared against possible alternative data sets.

Topography

Information about the surface relief on global scale is available as Digital Elevation Model (DEM). A DEM is either generated from remote sensing data, based on several acquisition techniques such as laser scanning, interferometry, or stereo photography, or from ground surveyed topographical data (Mukherjee et al., 2013). DEMs are available for a multitude of resolutions, data formats, access conditions, and spatial extents. Freely accessible data with global or near-global coverage is available from the following three datasets:

GTOPO30 DEM is prepared from several raster and vector topographic information sources, most with regional extent. The spatial resolution of the generated DEM is 30 arc seconds (926m). All global land surfaces except islands smaller than one square kilometer are covered (NASA LP DAAC, 1996).

SRTM (Shuttle Radar Topography Mission) DEM is prepared from radar interferometric data collected in February 2000 on a Space Shuttle Mission. SRTM data are available at a resolution of three arc seconds (90m) at near global scale (60°N to 56°S) and at one arc second (30m) for the area of the continental United States (USGS, 2006).

ASTER (Advanced Space borne Thermal Emission and Reflection Radiometer) Global Digital Elevation Model (GDEM) is a product of METI (Ministry of Economy, Trade, and Industry) of Japan and the US NASA, prepared by stereo correlation from multiband stereoscopic images retrieved by sensors onboard Terra spacecraft. The spatial resolution of the DEM product is one arc second (30m). Land surfaces between 83°N and 83°S are covered (NASA LP DAAC, 2011).

The small catchment sizes associated with the PHP potential definition of this work demand high vertical and horizontal resolutions of the DEM for the watershed analysis. ASTER was therefore chosen as the source of topographical data for this work, because of its resolution advantage compared to both SRTM and particularly GTOPO30 data sets. Furthermore, a direct comparison between ASTER and SRTM against a high resolution commercial DEM and field surveyed topographical information on an area in Northern India (Mukherjee et al., 2013) has shown that the higher vertical accuracy of ASTER compared to SRTM becomes more advantageous particularly in areas of high slope values.

The resulting dimensional relationship between DEM cell and PHP unit cell is visualized in Figure 4-12.

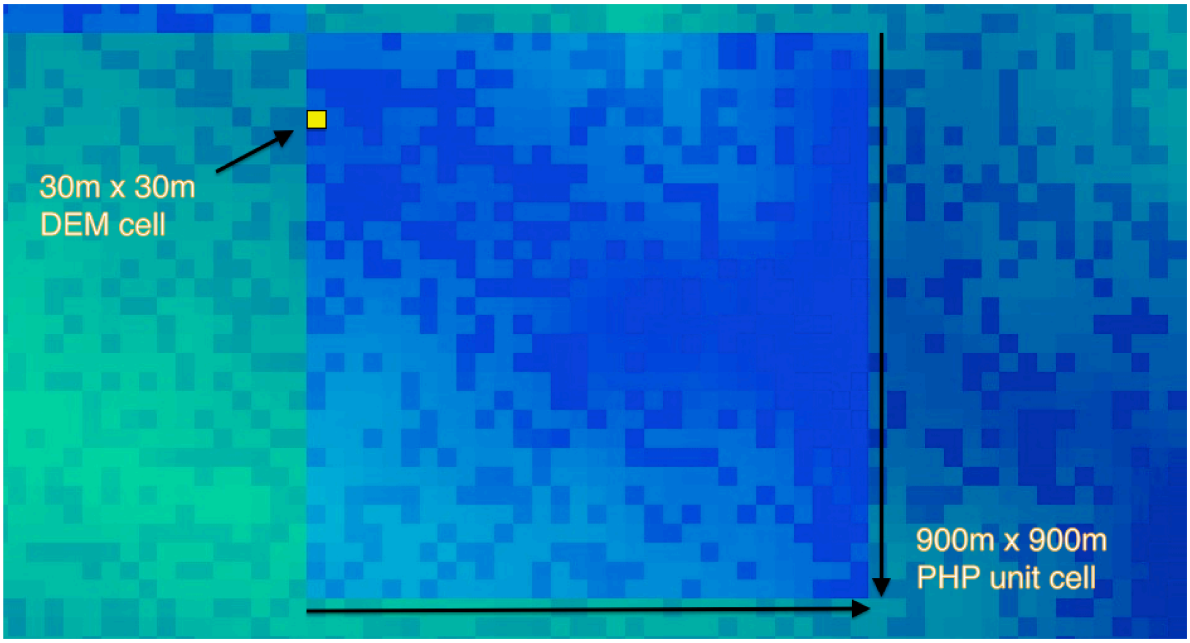

Figure 4-12: Visualization of the dimensional relationship between DEM cell and PHP unit cell.

Runoff

Global runoff data is maintained by the Global Runoff Data Center (GRDC) under the auspices of the World Meteorological Organisation (WMO). The Global Runoff Database comprises of monthly and daily river discharge data from 8962 gauging stations (BAFG, 2013). The spatial runoff data used in a preliminary version of the GIS based PHP potential assessment procedure is provided by the global composite runoff fields data set prepared and issued by CSRC-University of New Hampshire and GRDC. In this data set, observed long-term river discharge data from 861 globally distributed gauging stations is combined with a climate-driven water balance model, based on precipitation, air temperature, land cover, and soil data, to calculate a monthly runoff product with 0.5 degree (55.5km) resolution (Fekete et al., 2002).

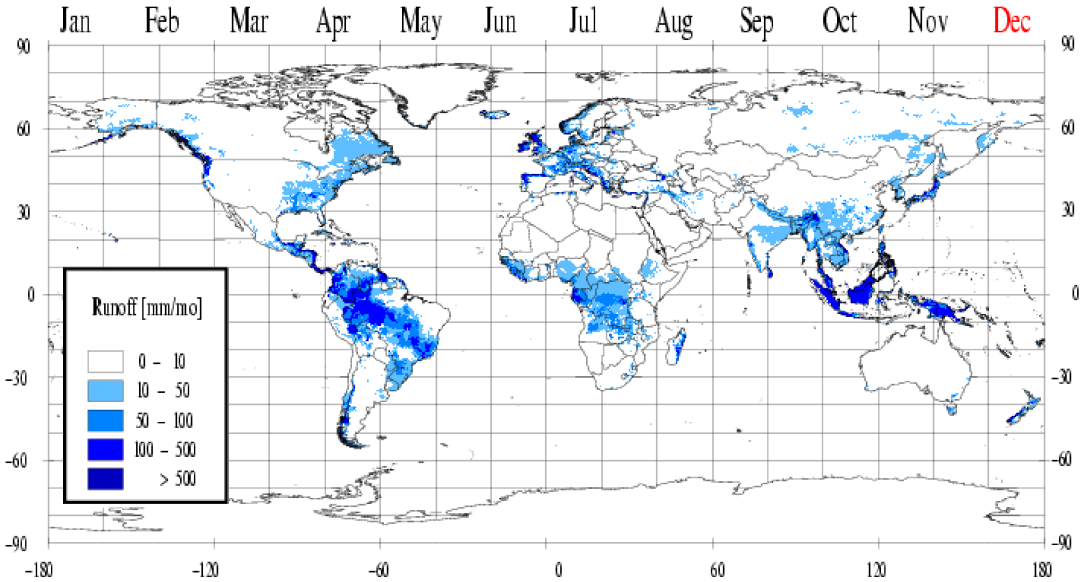

Figure 4-13: Global composite runoff fields at 0.5 degree (55.5km) resolution. Example: December runoff (Fekete et al., 2002).

Water balance

WaterWorld, a physical water balance model, can be used to calculate hydrological baselines (hydrographs) as well as hydrological scenario analyses, following changes in land use, climate, or land management (Mulligan, 2013). The water balance at the core function of this model, here solved for runoff as the decisive factor for hydropower potential, is modified to

$$surface\ runoff = \left(precipitation + cloud\ captured\ moisture\right) - actual\ evapotranspiration \quad \text{E/F 4-2}$$

Two changes in respect to commonly used water balances apply:

1. Subsurface flows are omitted
2. Cloud capturing (fog interception) is considered as a discrete contributor to the total atmospheric water input

The main reason for ignoring subsurface flows (groundwater, soil moisture) in the available versions of this model is a lack of suitable datasets with global extent (Mulligan, 2013). In the qualitative PHP potential approach of this work, the subsurface flows are assumed to be a short-term water storage that has no influence on the total runoff at one-month temporal resolution. Only the runoff at the driest month is considered for the PHP potential estimate. The influence of subsurface flows on streamflow anyhow appears to be more prominent in areas that are not considered to be prospective PHP potential areas, such as arid and karst areas.

Cloud interception (fog capturing) modeling is an important asset of the WaterWorld model, a heritage from preceding models that were developed to estimate the global extent and distribution of cloud forest (Mulligan, 2013). A common feature of the several subtypes of cloud forest is the substantial gain of throughfall water as a result of cloud interception. Gains of typically 0.5 to 1.5mm/d convert into a range of 5-35 percent increase to the associated rainfall. The gains from cloud interception are often temporally independent from rainfall incidents (see Figure 4-14) and thus represent an important contributor for dry season flow (Bruijnzeel, 2005).

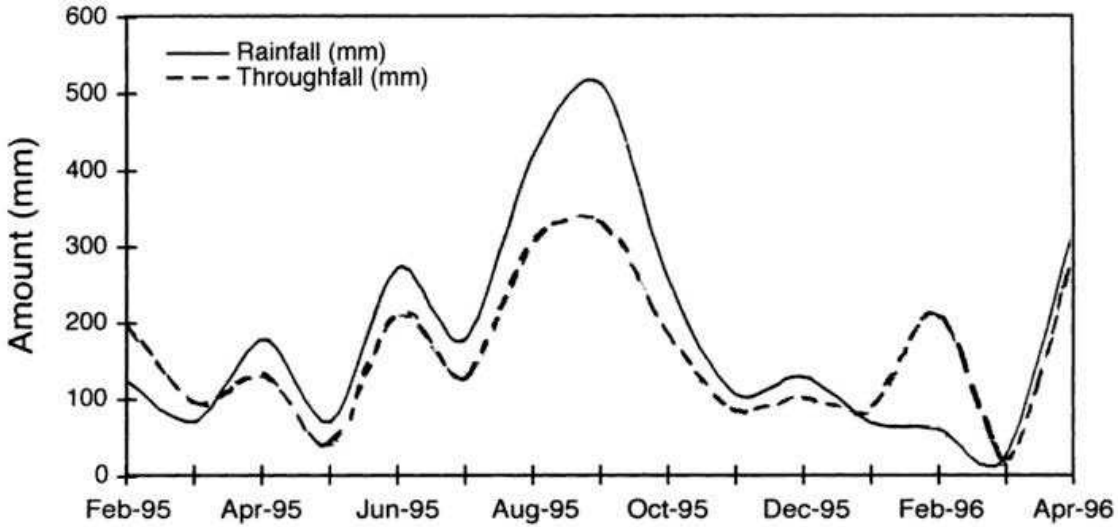

Figure 4-14: Rainfall vs. throughfall comparison for a cloud forest in Guatemala at 2200m altitude. Lower throughfall than rainfall is caused by rainfall interception from foliage and other plant matter, whereas higher throughfall than rainfall is a result of cloud capturing by the same plant matter (Bruijnzeel, 2005, after Brown et.al., 1996).

Steady runoff can particularly be expected when evapotranspiration and soil water storage are low. This is often the case in cloud forest areas as shown by a number of studies in several, mostly South American countries, compiled by Bruijnzeel (2005). The results indicate low evapotranspiration rates and near water saturated soils, particularly for the upper regions of the cloud forest range. The absolute effect on runoff generation of a particular land cover type is demonstrated by paired catchment studies that compare the runoff from two morphologically similar catchments exposed to the same climate, but with considerably different vegetation cover (Brown et al., 2005). A paired catchment study about the role of cloud forest affecting runoff in small catchments (Muñoz-Villers & McDonnell, 2013) had been conducted in Central Mexico (2100-2500m altitude, upper cloud forest zone, "silicate" geology). Annual and seasonal streamflow and runoff responses were compared between three catchments, one of 0.25 km^2 extent covered with mature cloud forest, one of 0.12 km^2 covered with 20-year old secondary cloud forest, and one of 0.1 km^2 covered with grass (cattle pasture, deforested ca. 70 years ago). The hydrological results from the study (stable flow regimes, high baseflow indices), an annual precipitation of average 3285mm, and a rugged topography are strong indicators for good PHP potential. However, on a closer look at the minimum flow conditions (see Figure 4-15) the forested catchments extrapolated to a catchment size of 1km^2 would yield flows of 28.5l/sec (mature cloud forest) and 71.3l/sec (secondary forest) respectively, confirming favorable PHP potential, whereas the deforested catchment with a minimum flow of 3.5l/sec would fail the hydraulic requirements for PHP potential. In summary, the presence of tropical montane cloud forest leads to enhanced dry season flow (Bruijnzeel, 2005). The resulting perennial streams are a key prerequisite for PHP potential.

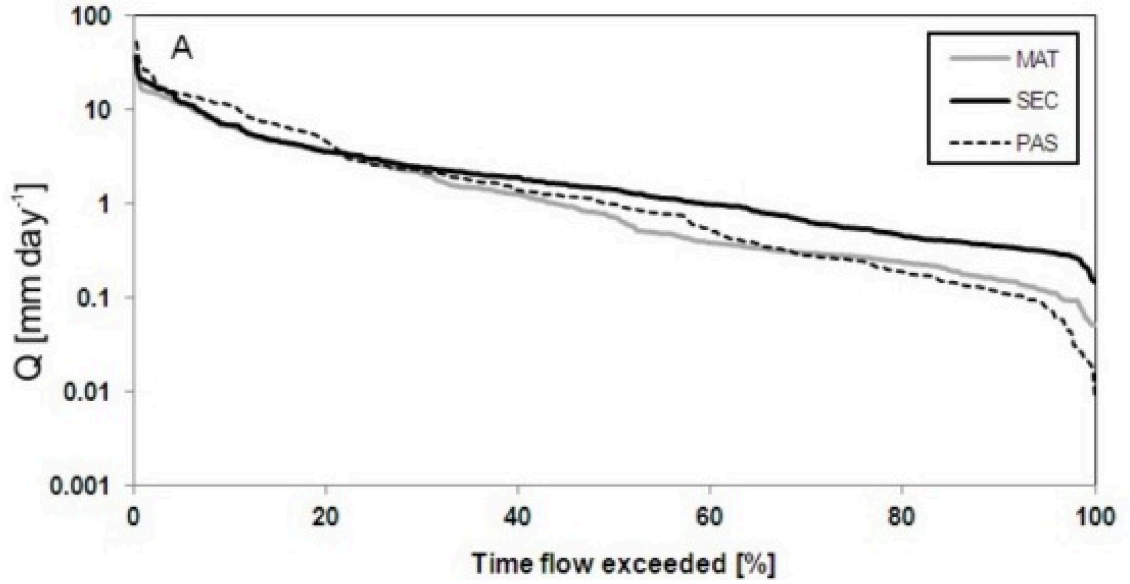

Figure 4-15: Flow duration curves (logarithmic scale) from a cloud forest paired catchment study. Note the diminished dry season flow from deforested grassland (PAS) compared to the mature cloud forest (MAT) and secondary cloud forest (SEC) (Muñoz-Villers & McDonnell, 2013).

Global cloud forest mapping approaches seek ways to reduce the data demand by using proxy factors associated with the occurrence of cloud forests, such as regionally characteristic altitude bands, specific soil related conditions, or specific hydro-climatic conditions. As an outcome of the different mapping technique used and according to the respective study-specific definition of "cloud forest" the resulting global cloud forest or cloud affected forest extent of previous studies differs considerably (Scatena et al., 2010). A preliminary version of the GIS based PHP potential assessment procedure used the cloud

forest cover results of the "DFID FRP Project ZF0216 Global cloud forests and environmental change in a hydrological context" study (Mulligan & Burke, 2005) as a regional enhancement to the GRDC runoff data. The final version of the GIS based PHP potential assessment procedure replaces the - initially separate - input datasets on runoff, precipitation, and cloud forest extent with the annual total water balance result of the WaterWorld model (Waterworld Version 2, 2014). This leads to a much higher resolution of water related input data at 30 arc seconds (926m) when compared to the previously used bilinear interpolation of 0.5 degree (55.5km) runoff data (see Figure 4-16) and brings along the integration of several additional input data sources, such as wind and cloud related data (see Table 4-2) that facilitate a more accurate physical description of the water availability.

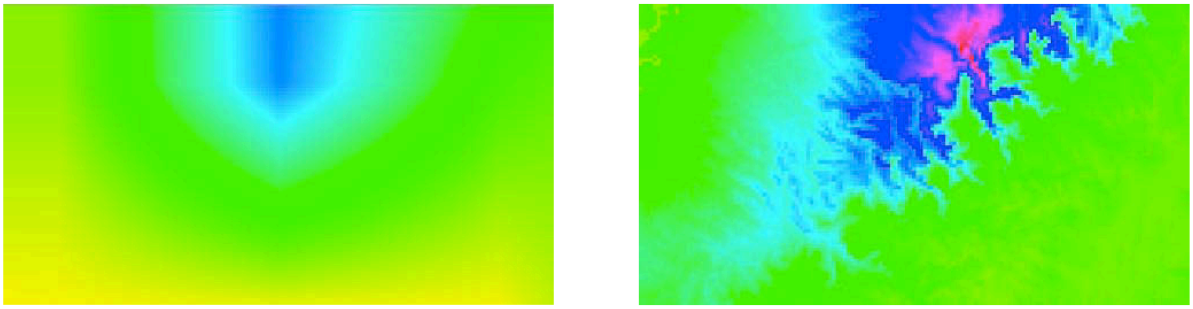

Figure 4-16: Visualization of the input data resolution difference between GRDC runoff (at left; bilinear interpolation of monthly data) and WaterWorld water balance (at right; derived from annual water budget and monthly precipitation data). Yearly runoff values range between 20mm (yellow), 100mm (blue-green), 200mm (dark blue), 300mm (purple), and 400mm (red). Approximate map extent: 120x50km; Location: N-Ecuador.

WaterWorld is remotely run via a web browser interface and generates 10x10 degree result raster maps at 926m resolution. An output format of 1x1 degree at 90m resolution is also available, however it is based on input data that had been resampled from a range of native 250m to 1km resolutions. The meteorological input data for the WaterWorld Version 2 model data is based on mean 1950-2000 climate data, whereas the land cover data originates from 2000.

The WaterWorld model consists of submodules for:

- Interaction of rainfall with wind and the resulting rainfall distribution
- Fog deposition contribution on total precipitation
- Incoming solar radiation
- Potential and actual evapotranspiration
- Water balance calculation
- Downstream cumulation (runoff)

Evapotranspiration is modeled by an energy driven approach that considers the solar radiation interception fractions caused by atmospheric water (clouds, fog) and vegetation. Leaf area, classified into three types of land cover: (1) no vegetation (bare land), (2) low vegetation (grassland), and (3) high vegetation (forest) is used as a representative factor to describe the processes of radiation interception by plants (Mulligan & Burke, 2005).

Only a very limited selection of WaterWorld modeling result maps are freely available for scientific use and thus fulfill the requirements for input data of this work. This is justified by the fact that WaterWorld uses commercial datasets as input. Freely available water balance modeling results are limited to annual scale.

Table 4-2: Input data sources for the WaterWorld model (modified after Mulligan, 2013).

Variable	**Units**	**Source**
Boundary layer wind direction (monthly)	degrees from N	Derived from BADC (2004)
Mean sea level pressure (monthly)	mbar	Derived from BADC (2004)
Elevation (SRTM 1k)	meters	Farr & Kobrick (2000)
Elevation	meters	Jarvis et al. (2008)
Mean air temperature (monthly)	°C	New et al. (2008)
Mean wind speed (monthly)	m s^{-1} / 10	New et al. (2008)
Mean relative humidity (monthly)	%	New et al. (2008)
Mean air temperature (annual)	°C	Hijmans et al. (2005)
Mean precipitation (monthly)	mm $month^{-1}$	Hijmans et al. (2005)
Total precipitation (annual)	mm $year^{-1}$	Hijmans et al. (2005)
Mean daily maximum temperature (monthly)	°C / 10	Hijmans et al. (2005)
Mean temperature (monthly)	°C / 10	Hijmans et al. (2005)
Mean daily minimum temperature (monthly)	°C / 10	Hijmans et al. (2005)
Cloud frequency (DecJanFeb)	Fraction	Mulligan (2006b)
Cloud frequency (JunJulAug)	Fraction	Mulligan (2006b)
Cloud frequency (MarAprMay)	Fraction	Mulligan (2006b)
Cloud frequency (SepOctNov)	Fraction	Mulligan (2006b)
Mean cloud frequency (annual)	Fraction	Mulligan (2006b)
Cloud frequency (monthly)	Fraction	Mulligan (2006b)
Cloud frequency 00:00-06:00 hrs	Fraction	Mulligan (2006b)
Cloud frequency 12:00-18:00 hrs	Fraction	Mulligan (2006b)
Cloud frequency 18:00-24:00 hrs	Fraction	Mulligan (2006b)
Cloud frequency 06:00-12:00 hrs	Fraction	Mulligan (2006b)
Local drainage direction	Direction	Mulligan (2006a)
Local drainage direction	Direction	Mulligan (2006a)
Cover of bare ground	Percentage	Hansen et al. (2006)
Cover of herb-covered ground	Percentage	Hansen et al. (2006)
Cover of tree-covered ground	Percentage	Hansen et al. (2006)
Daily temperature range (monthly)	°C / 10	Hansen et al. (2006)

Snow cover

Snow cover is used as a proxy for seasonal freezing conditions. Sub-zero ambient temperatures have the potential to interrupt the flow of small streams, thus preventing a continuous operation of PHP installations. The source for the snow cover data is the Moderate-resolution Imaging Spectroradiometer (MODIS) on board the Terra Satellite, scanning the reflection of the earth surface for 36 spectral bands in the visible and infrared spectrum. For the data products, reflectance signals characteristic for snow cover are algorithmically purged of interferences and presented as percent fractional area per pixel. MODIS snow cover data is available with global land coverage at a daily time step from February 2000 to present (Hall et al., 2004).

Two MODIS data products are used in this work:

MOD10CM (Hall et al., 2006b) is a monthly composite of daily snow cover data. Tiles of native 500m resolution are assembled in the MOD10CM dataset to a reprojected global map and resampled to 0.1 deg (11.1km) cell size. The information derived from this dataset is utilized to delineate the global application area of PHP against areas that are defined as unsuitable for continuous PHP operation for bearing the risk of seasonal stream freezing (see Figure 4-22).

MOD10A2 (Hall et al., 2006a) is an eight day composite of daily snow cover data. The MOD10A2 dataset consists of 1200km tiles at 500m resolution with data levels for snow cover percentage and maximum snow extent. The information derived from this dataset is utilized for PHP potential assessments in largely snow free regions that contain areas with intermittent snow cover, such as the border regions between subtropical and temperate zones and higher elevations in the subtropics.

Land cover

Global land cover data is retrieved from a number of space-borne radiometers. In combination this data covers a wide spectrum of electromagnetic radiation. Several land cover products with global extent and classification for multiple land cover types were developed since the 1990s from 1km resolution Advanced Very High Resolution Radiometer (AVHRR) data (USGS-LCI, 2012). A higher spatial resolution of 10 arc seconds (300m) became available with the GlobCover land cover product (Arino et al., 2012). Version 2.3 is used in this work. The GlobCover land cover Version 2.3 products are based on data retrieved in 2009 with the Medium Resolution Imaging Spectrometer (MERIS) on board the ENVISAT satellite.

The classification scheme of the GlobCover global land cover product is composed of 22 land cover classes defined with the United Nations (UN) Land Cover Classification System (LCCS) (Bontemps et al., 2011).

GlobCover land cover data is primarily utilized in the GIS based PHP potential assessment procedure to discriminate generally unsuitable from potentially suitable areas by land cover type. Flat areas (i.e. flooded or temporarily flooded land and most types of irrigated land), urban and artificial-surface areas, dry-type vegetation areas, and permanently water/ice covered areas are declared as being generally unsuitable for high head PHP application. The categorization of dry-type vegetation areas presumably contributes to a conservative estimate on PHP potential. Certain areas classified as bare (value code 200), such as post-harvest croplands, and certain grassland areas (value codes 140/150), such as tropical

forest converted into pasture, may actually generate sufficient runoff to fulfill the requirements for PHP application, however are declared as being generally unsuitable as well.

Table 4-3: GlobCover global land cover classes with associated value and color code (Bontemps et al., 2011) complemented by comments on suitability for high head PHP application.

Value Code	GlobCover global legend		High head PHP: application suitability
11	Post-flooding or irrigated croplands		Too flat
14	Rainfed croplands		Potentially suitable
20	Mosaic cropland (50-70%) / vegetation (grassland, shrubland, forest) (20- 50%)		Potentially suitable
30	Mosaic vegetation (grassland, shrubland, forest) (50-70%) / cropland (20- 50%)		Potentially suitable
40	Closed to open (>15%) broadleaved evergreen and/or semi-deciduous forest (>5m)		Potentially suitable
50	Closed (>40%) broadleaved deciduous forest (>5m)		Potentially suitable
60	Open (15-40%) broadleaved deciduous forest (>5m)		Potentially suitable
70	Closed (>40%) needleleaved evergreen forest (>5m)		Potentially suitable
90	Open (15-40%) needleleaved deciduous or evergreen forest (>5m)		Potentially suitable
100	Closed to open (>15%) mixed broadleaved and needle-leaved forest (>5m)		Potentially suitable
110	Mosaic forest/shrubland (50-70%) / grassland (20-50%)		Potentially suitable
120	Mosaic grassland (50-70%) / forest/shrubland (20-50%)		Potentially suitable
130	Closed to open (>15%) shrubland (<5m)		Potentially suitable
140	Closed to open (>15%) grassland		Too dry
150	Sparse (>15%) vegetation (woody vegetation, shrubs, grassland)		Too dry
160	Closed (>40%) broadleaved forest regularly flooded - fresh water		Too flat
170	Closed (>40%) broadleaved semi-deciduous and/or evergreen forest regularly flooded - saline water		Too flat
180	Closed to open (>15%) vegetation (grassland, shrubland, woody vegetation) on regularly flooded or waterlogged soil - fresh, brackish or saline water		Too flat
190	Artificial surfaces and associated areas (urban areas >50%)		Too altered
200	Bare areas		Too dry
210	Water bodies - (refers to cells (300x300m) that predominantly consist of water surface)		Too flat
220	Permanent snow and ice		Too cold

GlobCover global land cover distinguishes ten land cover types that contain forest that is not subject to seasonal inundation. They represent ten of the twelve land cover classes considered potentially suitable for high head PHP application (see Table 4-3). Because of the considerable influence of forest cover on streamflow (Bruijnzeel, 2004; Calder, 2005; Scott et al., 2005) it is justified to assume for these land cover classes that the dominant land cover related influence on PHP potential is linked to the forest cover itself.

Forest cover

Flow duration curves are usually not available for small streams of the size typically used for high head PHP installations. Flow related PHP site evaluations are usually limited to a simple dry season flow estimate to check the most critical flow condition (e.g. Maher & Smith, 2001), since recurrent flow interruptions would render most PHP installations uneconomical (Schröder, 2005a). Focus is therefore laid on the influence of forest cover on low-flow conditions.

Contrary to traditional perception, forest cover on a watershed is usually not causing an increase in runoff (Bruijnzeel, 2004; Calder, 2005). It is however one of the factors contributing to an increased water retention capacity, which in turn has a leveling effect on the flow duration curve (Muñoz-Villers & McDonnell, 2013). This would include a reduction in peak flow as well as an enhanced dry season flow. Forestation experiments however show that the (theoretically positive) effect on dry season flow is overcompensated (on non-degraded soils) by the effects from the higher evapotranspiration rates of forest cover as compared to non-forest land cover types (e.g. grassland) (Calder, 2005). A positive effect of forest cover on dry season flow can only be expected for conditions where precipitation exceeds evapotranspiration in the dry season. The role of precipitation is particularly important in areas with low seasonal temperature variation that prevents a reduction of evapotranspiration caused by seasonal temperature conditions. A compilation of 16 studies estimating annual evapotranspiration rates for forest cover varied by tree species, elevation, tree age, and mean annual precipitation, taken at locations across tropical South America, Africa, and Asia lists evapotranspiration rates between 900 and 1925mm/a with an average of 1385mm/a (Scott et al., 2005). Assuming an even distribution of the evapotranspiration over the year, which is only justifiable at conditions that are not seasonally limited by low temperatures or low water availability (and congruent with the requirements for PHP application), a minimum monthly precipitation of 1385mm/12 = 115mm would be necessary to compensate the evapotranspiration rate of forest cover. This idealized figure defines the threshold between beneficial and detrimental influence of forest cover on dry season flow in the GIS based PHP potential assessment procedure. It is integrated in a “forest influence component” that was utilized in preliminary versions of the GIS based PHP potential assessment procedure to supplement the coarse resolution global runoff information with a spatially more detailed composite from precipitation and forest cover data. The overall purpose of the component is to distinguish beneficial from detrimental influence of forest cover on dry season flow.

The forest influence component FIC is defined as:

$$FIC = FC\left((MP - 115)/115\right) \qquad \text{E/F 4-3}$$

with FC representing the forest cover in steps of 0.1 (i.e.10 percent forest coverage) and MP representing the precipitation [mm/month] of the least precipitation month.

The forest cover data used in this component is the global forest change 2000–2012 dataset (Hansen et al., 2013). It is based on Landsat 7 ETM+ images that document the spectral response of the earth surface at 30m resolution in seven visible and infrared bands. The dataset consists of three separate maps with global extent at 30m resolution: (1) year 2000 forest extent, (2) forest loss by year, and (3) forest gain by year. Forest is defined for this dataset as "all vegetation of over five meters height". Adding the forest gain data to the year 2000 forest extent and subsequently subtracting the forest loss data yields the global forest extent of 2012, which is used in the forest influence component.

In the final version of the GIS based PHP potential assessment procedure a separate consideration of forest cover is discontinued. A distinction between no, low, and high vegetation as land cover classification is integrated in the WaterWorld model and thus already considered in the WaterWorld annual water balance result.

Precipitation

Precipitation datasets that meet the criteria of global or near global coverage and free access are available from several sources:

The Tropical Rainfall Measuring Mission (TRMM), jointly operated by Japan NASDA and US NASA, is acquiring rainfall data since 1997. It initially covered the tropics and subtropics to 38 degree latitude and was later extended to 50 degree latitude. Both, active and passive microwave instruments on board the TRMM satellite measure microwave-band absorption caused by liquid water in the atmosphere. A series of precipitation estimate products, usually mergers of active and passive detection results and some of these supplemented by the results of other remote sensing precipitation estimates, are available for several spatial (at best 4.3km) and temporal resolutions (at best 3 hours) (Hrubiak, 2002). The TRMM satellite mission is already in its final stage and will be succeeded by the Global Precipitation Measurement (GPM) mission, a satellite network around a core observatory that had been launched in 2014. GPM measurements are expected to be more detailed and are capable of detecting solid water (snow, ice) and additionally cover higher latitudes (NASA, 2011).

GPCC Precipitation Climatology 025 (Meyer-Christoffer et al., 2011) and WorldClim precipitation (Hijmans et al., 2005) represent global datasets that are interpolated from ground measurement (meteorological station) data. The spatial resolutions are 0.25 deg (27.7km) for the GPCC dataset and 30 arcsec (926m) for the WorldClim dataset. Both datasets refer to a target reference period from 1950 to 2000.

A bilinear interpolation of the GPCC Precipitation Climatology 0.25 degree precipitation data for the least precipitation month was used in a preliminary version of the GIS based PHP potential assessment procedure for comparison against an empirically determined precipitation threshold factor for PHP potential. This factor was subsequently replaced by runoff data based on water availability calculations. The final version of the GIS based PHP potential assessment procedure uses the quotient of the GPCC monthly precipitation average (least precipitation month) and GPCC yearly precipitation average as a factor to convert the WaterWorld annual total water balance result (Waterworld Version 2, 2014) into a driest month water balance approximation.

The limitations of this method (e.g. if the month of least precipitation will not coincide with the driest month of the water balance result) and their implications for PHP potential assessment are explained for the following cases:

Case A: Moisture throughfall predominantly or entirely originates from cloud capturing. If this is a temporary condition, as for example in cloud forest areas during the dry season (see Figure 4-14), the condition will contribute to an underestimation of PHP potential. It is assumed that permanent conditions of case A type only occur in areas with generally no PHP potential, such as in coastal deserts.

Case B: An area has considerable seasonal differences in actual evapotranspiration. Concomitantly, peak actual evapotranspiration is not coinciding with the rainy season. This condition can occur in (seasonally) vegetated areas that are predominantly supplied by stored water, such as irrigated cultivations or ground water fed vegetation in desert areas. It is assumed that the condition will only occur in areas that are generally too dry for PHP application.

Carbonate outcrops

Due to their specific spring formation patterns (see Figure 3-19) and the resulting scarcity of small perennial streams, carbonate karst areas in the GIS based PHP potential assessment procedure are generally treated as exclusion areas for PHP potential. The data source for the karst area exclusion step of this work is the World Map of Carbonate Rock Outcrops V3.0 (Williams & Fong, 2010), which is based on a compilation of surface carbonate occurrences from various sources by Ford & Williams (1989, 2007). The map generalizes a carbonate occurrence for areas of both continuous and discontinuous surface carbonate outcrop.

Karst as an geomorphological phenomenon relevant for the formation of PHP potential can be grouped into three subgroups with different geochemical background:

Carbonate karst includes most carbonate rock formations. It occurs in all climatic zones and shows no obvious correlation to the other parameters that are relevant for the definition of PHP potential.

Pseudokarst is a disputed term attributed to a karst-like characteristic porosity of various geological backgrounds such as fractured volcanic rock, tubular lava flow forms, weathering-caused interstitial cavities, or landslide deposit forms. Unlike carbonate and evaporite karst, it is not caused by a chemical dissolution-precipitation process (Eberhard & Sharples, 2013). Like carbonate karst, it shows no obvious correlation to the other parameters that are relevant for the definition of PHP potential.

Evaporite karst (mainly gypsum and rock salt outcrop) is relatively rare as surface outcrop due to its significant water solubility and occurs mainly in arid areas. It is expected that areas with surface occurrences of water soluble minerals are generally too dry for PHP application.

In preliminary versions of the GIS based PHP potential assessment procedure the Karst Regions of the World (KROW) map is used. This dataset with worldwide coverage consists of carbonate, evaporite, and pseudokarst outcrop data from a multitude of sources, compiled and published by Hollingsworth (2009) as vector data (see Figure 4-17). The pseudokarst entries of the dataset apparently consist of an incomplete representation of potentially pseudokarst bearing geological formations that were extracted from the US Geological Survey Energy Resources Program World Geologic Maps series (e.g. Schenk et al., 1999). The World Karst Aquifer Mapping Project – WOKAM currently prepares a global map of carbonate outcrop with further distinction between continuous and discontinuous occurrence as well as information on non-exposed continuations of exposed carbonate rocks (Goldscheider & Chen, 2014). Preliminary versions of this map show a considerably higher resolution than the previously described material.

Pseudokarst

For the purpose of assessing "the undiscovered, technically recoverable oil and gas resources of the world" (Wandrey & Law, 1999), a series of geologic maps with worldwide coverage was released by the World Energy Project of the U.S. Geological Survey. Compared to the underlying geological reference data, the geology in this map series is presented in a simplified form (both spatially and stratigraphically) with additional information on geologic provinces and oil and gas field data. It has to be mentioned that the internal division and codification of the strata is inconsistent between the maps of this series. The extraction of pseudokarst information therefore requires an individual analysis procedure for each map and results in information of differing quality in between the maps. The geological data utilized to extract the pseudokarst area information for the reference areas is based on the following maps:

Table 4-4: Data sources for the extraction of pseudokarst information for the respective reference area.

Country	USGS map	Reference
Costa Rica	Map Showing Geology, Oil and Gas Fields, and Geologic Provinces of the Caribbean Region, Open-File Report 97-470-K	French & Schenk, (2004)
Ecuador	Maps Showing Geology, Oil and Gas Fields and Geologic Provinces of the South America Region, Open-File Report 97-470-D	Schenk et al., (1999)
Sri Lanka	Maps Showing Geology, Oil and Gas Fields and Geologic Provinces of South Asia, Open-File Report 97-470C	Wandrey & Law, (1999)
Yunnan Prov. , China	Maps Showing Geology, Oil and Gas Fields and Geologic Provinces of the Asia Pacific, Open-File Report 97-470F	Steinshouer et al., (1999)

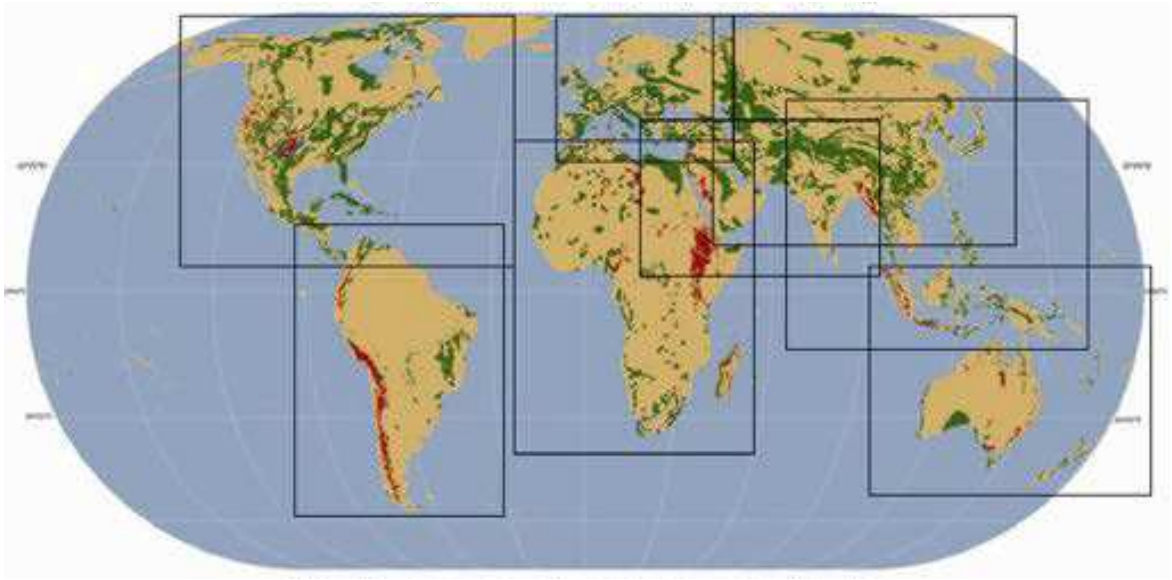

Figure 4-17: Visualization of an approximate global karst distribution with carbonate karst (green), evaporite karst (blue) and pseudokarst (red) areas (Hollingsworth, 2009)

Summary of input data sources used in the GIS based PHP potential assessment procedure

According to function and output format, the input data sources are characterized by four categories:

Main: The data is either used for the PHP potential calculation or to define exclusion factors.

Auxiliary: The data is used for correction factors or unit conversions.

Qualitative: The initial processing step of this data in the GIS based PHP potential assessment procedure yields a Boolean result.

Quantitative: The initial processing step of this data in the GIS based PHP potential assessment procedure yields a numerical result.

Table 4-5: Input data sources used in preliminary and final versions of the GIS based PHP potential assessment procedure

Dataset	Input data characterization in preliminary versions	Input data characterization in final version	Source
ASTER Global Digital Elevation Model	main, quantitative	main, quantitative	(NASA LP DAAC, 2011)
Global Forest Change 2000–2012	auxiliary, quantitative	not used	(MC Hansen et al., 2013)
DFID FRP Project ZF0216 Cloud Forest Cover	auxiliary, quantitative	not used	(Mulligan & Burke, 2005)
WaterWorld Annual Total Water Balance	not used	main, quantitative	(Waterworld Version 2, 2014)
GRDC Global Composite Runoff	main, quantitative	not used	(Fekete et al., 2002)
GPCC Precipitation Climatology 025	main, quantitative	auxiliary, quantitative	(Meyer-Christoffer et al., 2011)
World Map of Carbonate Rock Outcrops V3.0	not used	main, qualitative	(Williams & Fong, 2010)
US Geological Survey Energy Resources Program World Geologic Maps Series	not used	main, qualitative	(e. g. Schenk et al., 1999, for South America)
Karst Regions of the World (KROW)	main, qualitative	not used	(Hollingsworth, 2009)
MODIS/Terra Snow Cover Monthly Global 0.1Deg	main, qualitative	main, qualitative	(D. K. Hall et al., 2006b)
MODIS/Terra Snow Cover 8-day Global 500m	main, qualitative	main, qualitative	(D. K. Hall et al., 2006a)
GlobCover Land Cover Version 2.3	main, qualitative	main, qualitative	(Arino et al., 2012)

4.2.2 Data processing

Software prerequisites

In analogy to the prerequisites for input data (see chapter 4.2.1), all software used in the GIS based PHP potential assessment procedure is freely accessible without license cost for noncommercial use. The software is compatible with common types of operating systems and computer hardware environments.

GIS environment

GRASS GIS (Geographic Resources Analysis Support System) Version 6.4.1 is used for the map calculations in the GIS based PHP potential assessment procedure. The software was originally (1982-1995) developed by US military and other US federal institutions. Early applications focused on environmental analyses for military installation planning. Subsequently, software development shifted to the scientific community. The software consists of a core system that is maintained by a core development group and several hundred modules that contribute specific functionalities. Modules can be developed by "anyone interested" (Westervelt, 2004).

The free QGIS Version 1.6.0 'Copiapó', formerly named Quantum GIS, is used as the Graphical User Interface (GUI). File handling and invoking of most GRASS modules are handled via QGIS in the present study.

Preceding data preparation steps, such as map data reformatting and data importing, are facilitated mainly by QGIS or GRASS GIS modules. In some cases manual data format modifications require the use of an external text editing or spreadsheet software.

A: Preparation stage

The PHP potential assessment requires subcomponents that are results of individual GIS facilitated procedures based on the input data discussed in the previous chapter, however are not intermediate components of the processing stage of the PHP potential assessment (see Figure 4-31). These subcomponents, comprising the preparation stage, can therefore be seen as precursor components to the intermediate components. The preparation stage consists of the following steps: watershed delineation (A1), spring horizon (A2), minimum precipitation month (A3), steepness/slope (A4), and maximum snow extent (A5).

Step A1: watershed delineation

Purpose: The assessment area is divided into watersheds of approximately 1 km^2 (first order streams in mountainous areas) or larger (in less inclined areas) extent.

Assumption: A watershed of 1 km^2 fulfills the topographical prerequisite for the occurrence of at least one first order stream per square km, i.e. a single drainage point with a contributing area of at least 1km^2. Whether or not this stream fulfills the requirements for PHP potential, or even exists at all, will depend on other, predominantly hydrological factors that will be discussed later. Higher order stream sub-watersheds may be smaller.

Discussion: A comparison between DEM-based watershed delineation and ground surveyed watershed delineation in Canada (Cyr et al., 2011) demonstrates a significant drainage area error for DEM-generated watersheds smaller than approximately 30km² (see Figure 4-18).

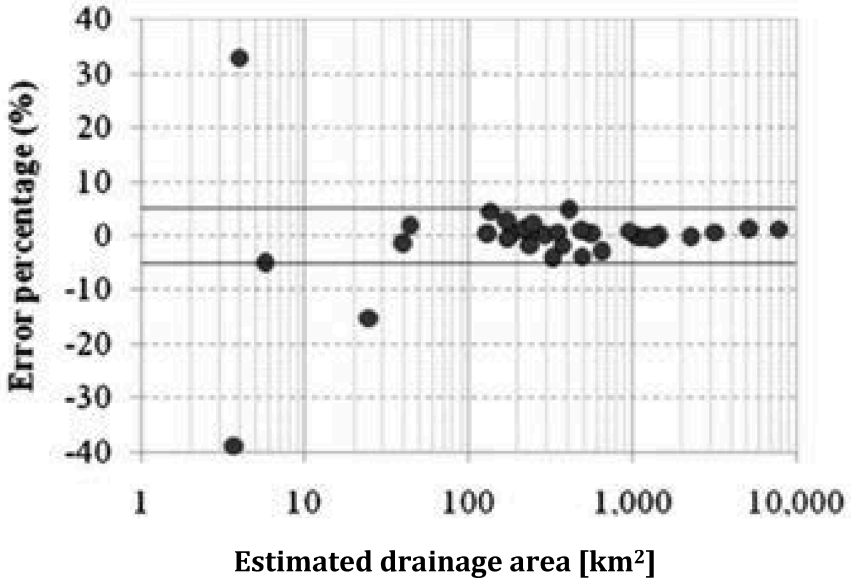

Figure 4-18: Watershed size vs. relative error for DEM-based watershed delineation (Cyr et al., 2011).

The deviation can be explained by methodical errors in the altitude measurements that furthermore depend on the utilized remote sensing technology. Radar reflection generated elevation data exhibits for example a tendency to assume the top of the vegetation (particularly tree tops) as ground level (NASA, 2005). Such errors rapidly gain significance with a reduction of both watershed size and DEM resolution. The actual effect on watershed delineation can be observed in Figure 4-19. Here, an artificial stream network generated from a 10m-resolution commercial DEM (Cartosat) is superimposed to the 30m ASTER DEM and the 90m SRTM DEM (Mukherjee et al., 2013). The inability to generate accurate watershed delineations with the available free DEM datasets is one of the reasons for prefering a primarily qualitative approach to large-scale PHP potential assessment in this work. Because of the qualitative approach, the streams and watersheds generated in step A1 of the GIS based PHP potential assessment procedure are not required to represent the actual (real) stream courses anymore. Their function is now reduced to the representation of a spatial stream density. This value only depends on topographical data and is visualized as a virtual stream network with surrounding virtual watersheds with a minimal size of 1 km² (see Figure 3-18).

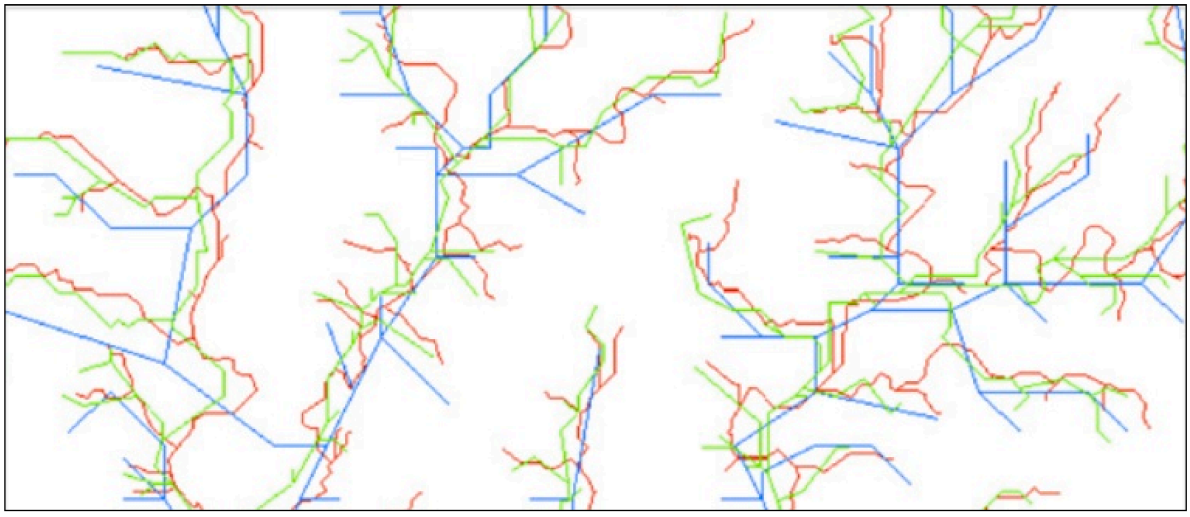

Figure 4-19: Superimposed DEM drainage networks generated from 10m Cartosat DEM (red), 30m ASTER DEM (green), and 90m SRTM DEM (blue) elevation data (after Mukherjee et al. , 2013)

GRASS procedure: The task is performed by *r.watershed*, a dedicated, raster based watershed basin analysis program. It utilizes the A^T least-cost search algorithm which, compared to other watershed analysis tools, proved to be more accurate, but more time consuming in processing (Ehlschlaeger, 2003). To obtain an approximate "one stream per square km" density for mountainous areas (see Figure 3-18), a threshold of 1000 inflowing cells for a first order stream is set. 1000 cells at the resolution of the ASTER DEM (1 arcsec; 30m) correspond to an area of 0.948 km^2.

GRASS formulation: *r.watershed elev=aster_30myunnan@ynset1 thresh=1000*

All GRASS formulations documented in this study use filenames that had been used in actual raster map calculations. The naming convention has to follow the mapname@mapset style of GRASS GIS. The name of the respective map is chosen to be as descriptive as possible.

Step A2: spring horizon (peak cutoff)

Purpose: Areas are identified that have a low probability to feature permanent streams due to convex terrain curvature and insufficient slope length, commonly described as "areas above the spring horizon", "peaks", or "ridges".

Assumption: Perennial streams only occur below a certain "spring horizon altitude", which is simplified here to be one particular watershed-specific altitude and assumed to depend on three components: (A) a relation between the maximum and minimum altitude in a watershed (B) the water balance of the driest month of the year and (C) a vertical constant minimal distance between the highest point of a watershed and the highest point where perennial streams are found in this particular watershed (see Figure 4-20). The components of the formula defining the spring horizon altitude are based on the following generalizations:

1. Springs emerge in the upper third of the vertical distance between lowest and highest point of a sub-watershed.

2. More water available for base flow formation moves the spring horizon upslope.

3. Springs that are large enough to be considered for PHP applications do not occur in peak or ridge-top areas.

The influence of karst geology on spring formation (see Figure 3-19) is not considered in step A2; the method is conceptualized for non-karst areas only.

Based on the assumptions above and further fortified by observations taken during the field assessments in Ecuador and Sri Lanka, the spring horizon altitude h_{sh} for the GIS based PHP potential assessment procedure is formulated as:

$$h_{sh} = 0.7\left(h_{\max} - h_{\min}\right) + h_{\min} + \left(\frac{wb_{dm}}{525}\right) - 50 \qquad \text{E/F 4-4}$$

with h_{max} and h_{min} being the highest and lowest point of the watershed and wb_{dm} the water balance of the driest month at the watershed location.

The term *(wb_{dm} / 525)* represents assumption (B). The maximal value of 1 represents the worldwide highest wb_{dm} calculation result of the datasets used. The respective area is located in southern Colombia.

The term *0.7(h_{max} - h_{min})+ h_{min}* represents assumption (A), and the value *50* represents assumption (C). Both are empirically derived from field observations in Ecuador and Sri Lanka.

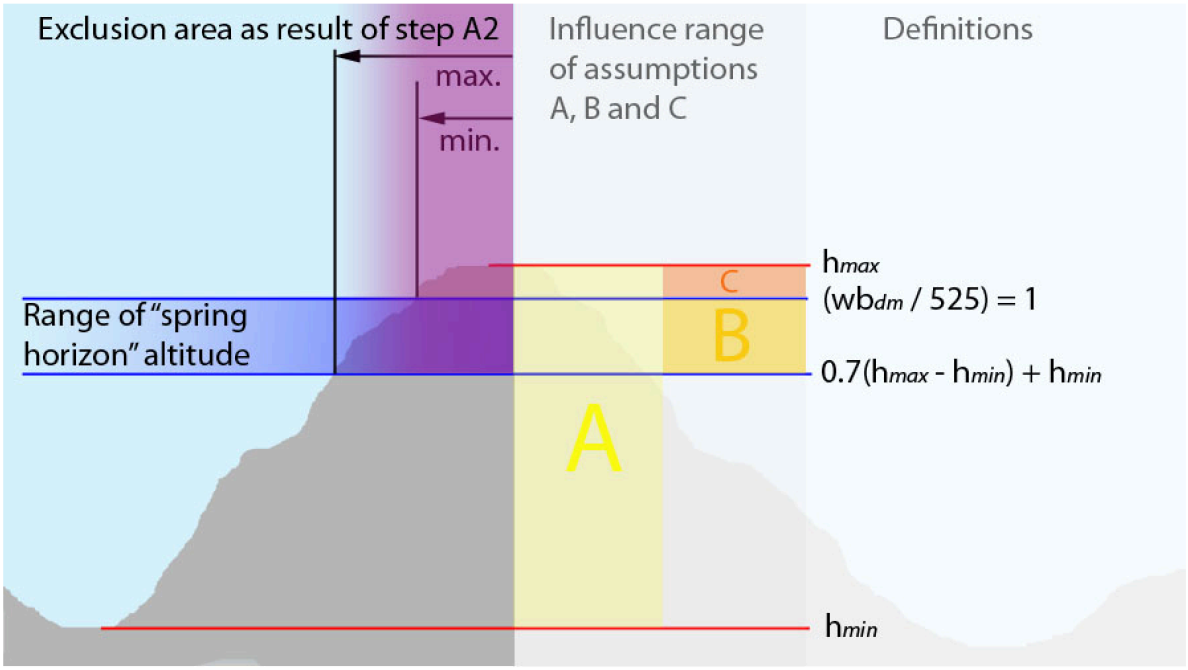

Figure 4-20: Graphical representation of the spring horizon altitude determination step.

Discussion: Spring formation on a slope is the result of a higher elevation of the hydraulic head in an aquifer compared to the land surface where the emergence takes place. The location of the aquifer itself depends on the subsurface distribution of water bearing voids and their respective size, at the emergence resulting in tubular springs (from large rock openings), fracture or fissure springs (from structural faults in consolidated rock), and seepage springs (from voids between the small particles of unconsolidated material, such as sand or soil) (Kresic, 2010). The modeling of real spring horizons requires a multitude of subsurface information parameters that are not available at large scale. Both, the method implemented as step A2 as well as the alternative method mentioned below are therefore

coarse generalizations resulting in virtual spring horizons that are entirely based on topographical and hydrological information.

Areas with convex curvature had already been identified in step A1 as a byproduct of the watershed delineation procedure. Convex areas extend from the borderlines of sub-watersheds and act as starting points for the flow accumulation routine, which yields a drainage network as result (Jenson & Domingue, 1988). A function that analyzes the terrain curvature to describe the upper regions of the area between a sub-watershed borderline and the respective drainage channel can be considered an alternative method for the DEM-based identification of areas above the spring horizon, however is not implemented here. Accuracy comparisons between different methods would be extremely complex. Obviously in the center regions of the result areas of both the step A2 procedure and the mentioned alternative method (which are in vicinity to the peak contour lines) the probability to not encounter any stream is very high, whereas towards the border regions of the result areas (i. e. the virtual spring horizon) the methodical generalizations, which furthermore vary between the alternative methods, gain influence on the result. A quantitative comparison of the A2 results to real spring horizon lines is not possible within the scope of this work. A visual comparison of field assessment data (information collected about PHP potential, stream size and/or apparent spring horizons; at random locations) with A2 results (see Figure 4-21) however indicates suitability of the A2 procedure for qualitative PHP potential assessment.

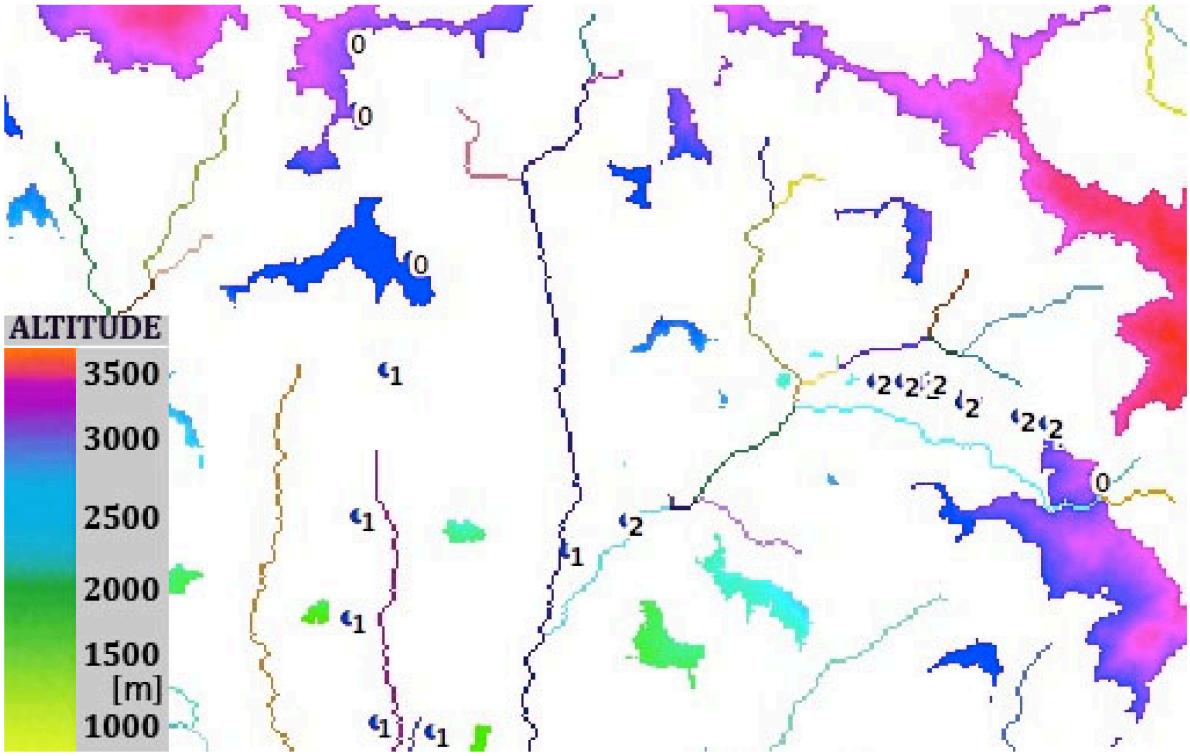

Figure 4-21: Exemplary area showing field assessed (2011) PHP potential results superimposed on step A2 delineation results.

Areas above the spring horizon delineated by step A2 are shown in solid color of the respective altitude. Field assessed H0, H1 and H2 PHP potential is shown as figures. The drainage network shown is a result of the step A1 delineation. Map extent: approx. 20km x 13km; location S-Central Costa Rica.

GRASS procedure and formulation:

Substep 1: Minimal and maximal altitudes of each watershed are determined. The watersheds are the result of the delineation in step A1.

r.statistics base=30m_watershed1000@costaricaset cover=Aster_30m_costarica@costaricaset method=max output=altmax_watershed1000

r.category map=altmax_watershed1000@costaricaset

r.mapcalc maxalta=@altmax_watershed1000

r.statistics base=30m_watershed1000@costaricaset cover=Aster_30m_costarica@costaricaset method=min output=altmin_watershed1000

r.category map=altmin_watershed1000@costaricaset

r.mapcalc minalta=@altmin_watershed1000

Substep 2: The spring horizon altitude for each watershed is determined.

r.mapcalc " springhorizonalt_wb = ((((minalta@costaricaset +(0.7(maxalta@costaricaset - minalta@costaricaset)))+((maxalta@costaricaset - minalta@costaricaset)*(waterbudgetminm900m_mm@costaricaset/525)))-50))"*

Substep 3: Areas below the spring horizon altitude are removed from the DEM.

r.mapcalc "abovespringhorizon = (if((springhorizonalt@costaricaset <Aster_30m_costarica@costaricaset), Aster_30m_costarica@costaricaset,null()))"

Step A3: minimum precipitation month

Purpose: Recurrent conditions of prolonged precipitation minima (usually referred to as dry season) are identified and represented as a dry season factor.

Assumption: A flow minimum in a small stream is the result of a precipitation minimum in the surrounding area. Both occur in the same month of the year.

Discussion: In simplified water balances runoff, or flow, is the difference between precipitation and evapotranspiration (e.g. Viviroli et al., 2003). For conditions that do not exhibit extreme climatic seasonality, precipitation is the main influence factor on runoff. Consequently the flow minimum occurs in close temporal vicinity to the precipitation minimum. Exemplary runoff vs. precipitation diagrams for this condition are found in Kadioglu & Sen, 2001 and TVA, 2014 at monthly resolution. Scenarios that disprove the assumption of co-monthly flow and precipitation minima apparently involve significant seasonal differences in evapotranspiration and precipitation. Such scenarios are easily constructed, based on the following features:

- extensive dry seasons with strong fluctuations of subsurface water levels.

- strong seasonal fluctuations in evapotranspiration rates due to low temperatures.

Both scenarios are widespread on global scale, however bear conditions that are prohibitive for PHP application according to the definition in chapter 3.3. Consequently, the validity of

the underlying assumption of this step is limited to areas that meet the prerequisites for PHP potential.

In a GIS context, the assumption is based on a comparison of the GPCC precipitation data against the water balance time series results of the WaterWorld model. The comparison shows a very good correlation of the annual patterns. Both time series however are only available as temporally detailed (7 days) but spatially coarse (10 deg) resolution if the consideration is limited to the free versions of the modeling results. The 10 degree resolution is too coarse for the GIS based PHP potential assessment procedure. Instead, monthly GPCC precipitation data at 0.25 deg resolution (see chapter 4.2.1), smoothened by bilinear interpolation, is used to determine the dry season factor.

GRASS procedure and formulation:

Substep 1: Identification of the minimum precipitation month from monthly GPCC precipitation data at 0.25 deg resolution (global area).

*r.mapcalc "precipitation_minmonth = (min(min(min(precipitation12@costaricaset,precipitation11@costaricaset,precipitation10@costaricaset),min(precipitation9@costaricaset,precipitation8@costaricaset,precipitation7@costaricaset),min(precipitation6@costaricaset,precipitation5@costaricaset,precipitation4@costaricaset)),min(precipitation3@costaricaset,precipitation2@costaricaset,precipitation*1@costaricaset)))"

Substep 2: Determining the quotient of minimum monthly to yearly precipitation at 0.25 deg resolution (global area).

r.mapcalc "gpcc_minmyrquot= ((precipitation_minmonth@costaricaset / precipitation_year@costaricaset))"

Substep 3: Bilinear interpolation at 30arcsec (926m) resolution.

r.resamp.interp input=gpcc_minmyrquot@costaricaset method=bilinear output=CRgpcc_minmyrquotbilin

Step A4: steepness (slope)

Purpose: Steepness (slope) values of the DEM cells are calculated. The result represents an average slope value for a 30x30m area.

GRASS procedure: The discrete GRASS command *r.slope.aspect* is executed. A slope value (in degree inclination from horizontal) is calculated for each raster cell of the DEM except for the outermost row of cells. The calculation is based on the elevation data of a 3x3 cell neighborhood around the respective cell (Shapiro & Waupotitsch, 2003).

GRASS formulation: *r.slope.aspect elevation= Aster_30m_costarica@costaricaset slope=YN_slope*

Step A5: maximum snow extent

Purpose: To discriminate areas with permanent or temporary snow cover from permanently snow-free areas.

Assumption: The maximal extent of the snow cover is approximated by an aggregation of two years of MODIS/Terra Snow Cover data.

Discussion: Snow cover is detected by its reflectance characteristics in the visible and near-infrared spectral regions and verified by a series of subsequent criteria tests. Obstructions by clouds are masked out with the MODIS Cloud Mask data product, another dataset from the same product series. The snow mapping algorithm used in MODIS/Terra Snow Cover data products is optimized for maximum snow detection ability and therefore has an inclination to overestimate snow cover, notably in situations that involve unclear coastlines, frozen inland water bodies, and low solar illumination in boreal summers (Riggs et al., 2006). A possible overestimation of snow extent, caused by this systematic error, would contribute to a conservative estimate of PHP potential by increasing the area not suitable for PHP application. At 0.1 deg resolution of the snow cover input data, step A5 is only capable of coarsely distinguishing suitable from unsuitable climatic zones with an uncertainty radius of approximately 50km. At this coarse resolution step A5 is utilized to delineate large, climatically unsuitable regions (see Figure 4-22) at the advantage of no further data preparation requirements. PHP potential assessments in areas with temporally and spatially incomplete snow cover necessitate the use of 500m resolution MODIS/Terra Snow Cover data (see Figure 4-25), as described in step B2. This usage is at the cost of considerably increased data preparation work.

GRASS procedure and formulation (low resolution version): Monthly snow cover duration data (MODIS/Terra Snow Cover Monthly Global 0.1Deg) of years 2012 and 2013 are aggregated (II). Before the aggregation, NULL values (represented as value 255) are converted into zero values for each respective month (I).

(I); example for December 2013 data:

r.mapcalc "sd1213 = (if((s1213@costaricaset<255),s1213@costaricaset,0))"

(II); general aggregation:

r.mapcalc "snowglobal_accd_1213 = (sd1213@costaricaset+sd213@costaricaset+sd1012@costaricaset+sd1112@costaricaset+sd112@costaricaset+sd212@costaricaset+sd312@costaricaset+sd412@costaricaset+sd512@costaricaset+sd712@costaricaset+sd612@costaricaset+sd812@costaricaset+sd912@costaricaset+snowd1212@costaricaset+sd1113@costaricaset+sd113@costaricaset+sd313@costaricaset+sd413@costaricaset+sd513@costaricaset+sd613@costaricaset+sd713@costaricaset+sd813@costaricaset+sd913@costaricaset+sd1013@costaricaset)"

GRASS procedure and formulation (high resolution version, example Yunnan Province, China): Following an external conversion and reprojection of MODIS/Terra HDF formatted data, 8-day snow cover duration data (MODIS/Terra Snow Cover MOD10A2 maximum extent 500m resolution) of December 1, 2012 to February 16, 2013, representing the core snow season of Yunnan Province, are aggregated.

r.mapcalc "YN_winter13snow500 = (((testss1_413.tif@costaricaset+s1_313@ynset1)+(s1_213@ynset1+s1_113@ynset1)+(s12_412@costaricaset+s12_312@costaricaset)+(s12_212@costaricaset+s12_112@costaricaset)+(s2_213@costaricaset+s2_113@costaricaset)))"

Coverage discrepancies, caused by the shape of the satellite swath area, have to be treated subsequently.

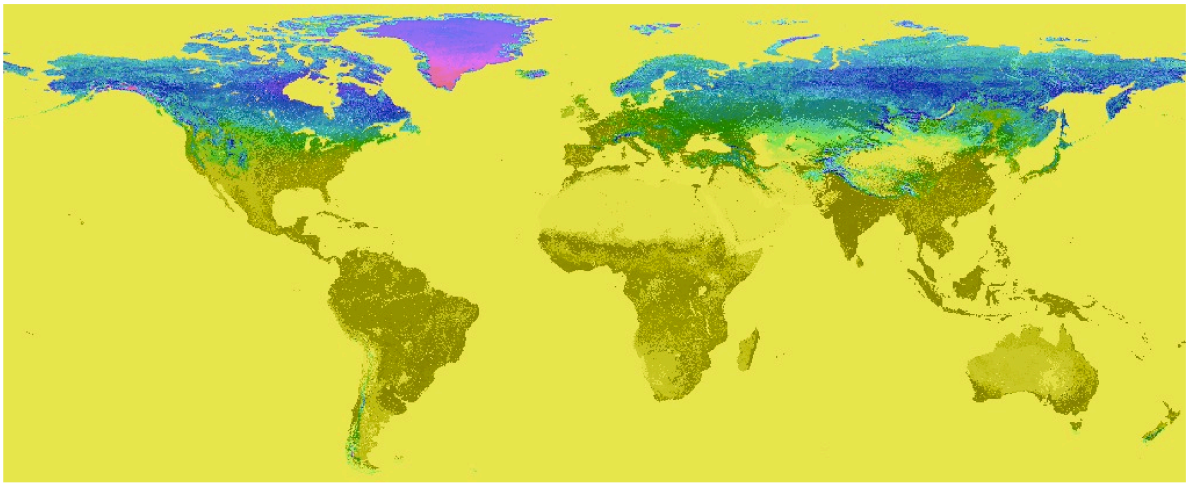

Figure 4-22: Visualization of the result of step A5 (coarse version), based on aggregated MOD10CM global-ex-Antarctica snow coverage January 2012 to December 2013, ranging from one month (bright green) to 24 months (red) of snow cover. Missing data and detection errors are both treated as zero snow cover for the respective month. Boreal latitudes show underestimates. Permanently snow free areas are colored according to their land cover in various shades of olive green. The data resolution is 0.1deg (11.1km).

B: Qualitative, intermediate (exclusion) components stage

Exclusion components define areas that are unsuitable for PHP application according to the definitions in section three. All steps of the qualitative intermediate components stage yield Boolean results (true/false), regardless of the format of the underlying input data. The components of this stage can therefore only present statements about an absence of PHP potential (see Figure 4-31).

The qualitative intermediate components stage consists of the following steps: land cover exclusion component (B1), freezing component (B2), karst component (B3), above spring horizon component (B4), insufficient slope component (B5).

Step B1: Land cover exclusion component

Purpose: To discriminate, by land cover class, areas that are generally unsuitable for PHP application from potentially suitable areas.

Assumption: Globcover land cover classes that indicate flat, dry, cold, or highly altered areas are generally unsuitable for high head PHP application.

Discussion: The definition of the Globcover land cover classes follows the UN Land Cover Classification System. Land cover classifications based on remote sensing data are the result of a compromise between the technical ability to discriminate different surface covers on one hand and useful, consistent, and reproducible land cover definitions on the other hand (Bontemps et al., 2011).

The UN Land Cover Classification System is aimed to achieve maximal flexibility to „address the potential for the classification system to describe enough classes to cope with the real world" (Di Gregorio & Jansen, 2005), while maintaining a high level of standardization through an *a priori* definition of a limited number of clearly discernible, uniquely featured

and therefore "mappable" land cover classes. The challenges for this two-way optimization process are visualized in Figure 4-23:

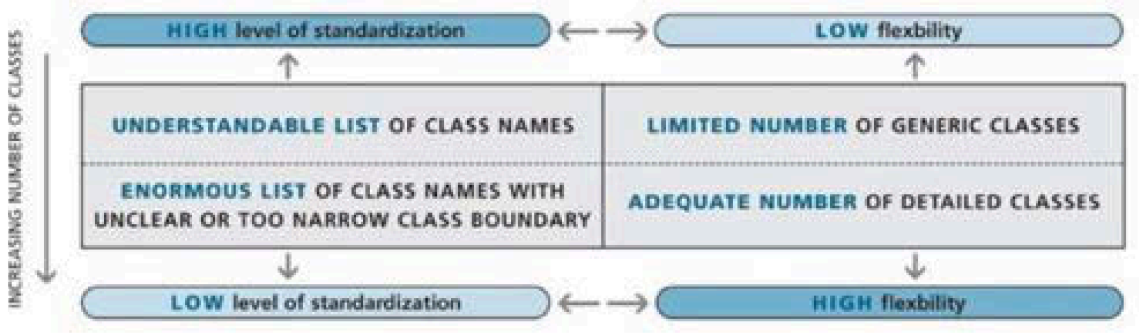

Figure 4-23: Vicious circle relationship between aims (dark blue) and problems (light blue) of *a priori* land cover classification system designs (source: Di Gregorio & Jansen, 2005).

The UN Land Cover Classification System utilizes a hierarchical set of "independent diagnostic attributes" called classifiers, of which the most basic ones are: (1) the presence of vegetation, (2) the ground condition, and (3) the cover artificiality (Di Gregorio & Jansen, 2005). The classification approach of the UN Land Cover Classification System is structurally similar to the GIS based PHP potential assessment procedure, and therefore permits a straightforward integration of the land cover related analysis results.

The global version of Globcover land cover distinguishes 22 land cover classes. All classes are individually evaluated for features that concern high head PHP application (see Table 4-3). The field assessment results clearly indicate that the suitability of a particular land area for high head PHP application could not be determined from land cover information (see chapter 4.1.3). Therefore an inverted approach, based on the identification of land cover classes that are generally unsuitable for high head PHP application, is pursued. For this purpose, the classifier-defined characteristics of the respective land cover class in respect to the basic requirements for high head PHP application – head and continuous flow - are evaluated. The following "PHP unsuitability rules" are found:

1. Land cover classes that are described as permanently or temporarily inundated cannot feature sufficient head for high head PHP application.
2. Land cover classes that are not vegetated, or feature either sparse or low vegetation (e.g. desert, shrubland, grassland), are too dry to support a sufficient density of perennial small streams.
3. Artificial surfaces (e.g. built-up areas, mine pits) are generally not a target for PHP application. Streams in these areas are often not accessible for structural (underground channeling and piping) and legal (urban water regulations) reasons.
4. Permanently ice or snow covered areas lack flowing water.

All of above unsuitability rules reflect generalizations that in real-life situations inevitably will be disproved by positive exceptions. As a whole, step B1 represents therefore a conservative estimate of areas that are unsuitable for high head PHP application by land cover criteria.

GRASS procedure and formulation: Globcover land cover classes that represent exclusion areas for high head PHP application (refers to Global Globcover legend level 1: values 13 and smaller; 150 and larger) are excluded in a single step:

r.mapcalc "YN_globc_ex14to145 = (if(((Global_globcoverV2.3@costaricaset<14)||(Global_globcoverV2.3@costaricaset>145)),Global_globcoverV2.3@costaricaset,null()))"

Step B2: Freezing component

Purpose: Areas with cold climatic conditions that may cause flow disruptions of streams with relevance for PHP potential are excluded.

Assumption: The exclusion areas are identified by temporary or permanent snow coverage.

Discussion: According to the PHP operating conditions defined in section three, continuous operability is a prerequisite for economic operation of PHP systems. Low ambient temperatures are a possible reason for seasonal flow disruptions, causing a substantial part or even the entire cross section of a stream to freeze temporarily. Ice particles developing in flowing water moreover have a clogging effect on hydropower plant intake structures. A detailed view on these phenomena would have to consider stream specific data, such as flow velocity and local temperature profiles (Prowse & Beltaos, 2002), that are neither available on global scale, nor at the resolution required for a PHP potential assessment. Consequently, for the GIS based PHP potential assessment procedure all areas that may feature temperature induced seasonal flow disruptions of small streams are excluded.

Most frost affected areas in the tropics would not have to be excluded by step B2, as they already meet the land cover exclusion criteria of step B1 for being permanently ice covered, bare, or sparsely vegetated. With increasing distance from the equator, seasonality gains influence. Sub-zero temperatures may occur more frequently and at lower altitudes. Simple altitude-latitude relationships, which in tropical latitudes are useable to approximate the minimum altitude that sustains permanent snow cover, called snowline (see Figure 4-24), will at higher latitudes only reveal the maximum snow extent of the warmest season (see Figure 4-25, slide A). This renders altitude-latitude relationships unusable for the purpose of step B2.

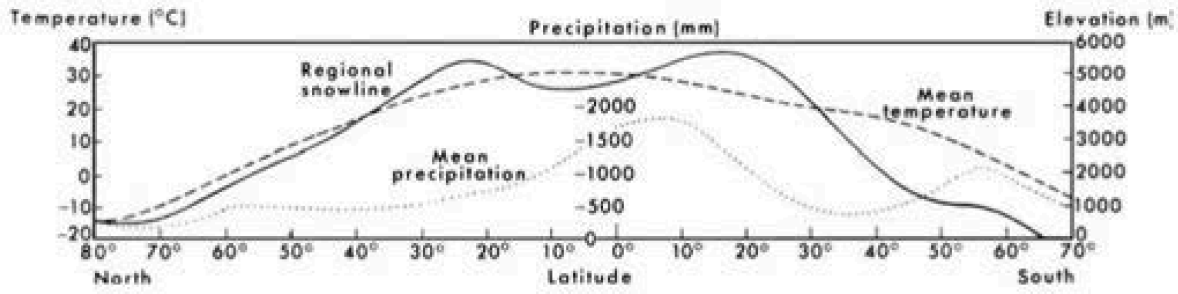

Figure 4-24: Regional snowline in dependence of altitude (elevation) and latitude. The altitude depression at the inner tropics is caused by increased precipitation and cloud coverage (Dexter et al. 2013, after Charlesworth, 1957).

Non-ephemeral snow covers are a general indicator for precipitation at climatic conditions that can sustain frozen water at the land surface (Dexter et al., 2013). During snow precipitation, ice formation in flowing water typically starts not before a snow cover had started to accumulate. Shallow and slow-flowing streams are most susceptible to freezing. The freezing process itself is controlled by several meteorological variables (Prowse & Beltaos, 2002). The maximal spatial extent of snow cover can therefore considered to be a proxy for a conservative estimate of the maximal spatial extent of ice occurring in streams. The consideration is confirmed by a comparison of GIS-assessed PHP potential, reduced by step B2 snow cover exclusion at different snow cover methods and MODIS/Terra input data resolutions (see Figure 4-25), against observed qualitative PHP potential (Schröder, unpublished, 2004-2006) for large parts of Nujiang Prefecture, NW-Yunnan Province, China. In the GIS based PHP potential assessment procedure step B2 is used for a single purpose: to exclude all areas that climatically bear the potential for directly and indirectly detrimental effects on PHP installations that are caused by ice. It is furthermore assumed that areas with climatic conditions to support stream freezing, which however did not accumulate any snow cover over the snow accumulation period (1-24 months, depending on input data resolution) and therefore are not excluded by step B2, have seasonally inadequate flow to bear PHP potential. The flow conditions are subject to scrutiny in later steps.

Using low-resolution snow cover data (e.g. 0.1 deg; see Figure 4-25, slide B) in peripheral areas of the global maximal snow extent (e.g. mountainous subtropics, lowland subtropical-temperate transition zone; see Figure 4-22) will lead to false negative PHP potential results that are directly attributable to step B2. In this case, a snow cover in the upper altitudes of a large grid cell will cause the exclusion of the entire cell, although the lower altitudes of the cell are permanently snow-free (see Figure 4-25, compare slides B and D).

Seasonal snow cover and ice formation can have a considerable effect on flow conditions of streams at adjacent lower altitudes through flow retention (Prowse & Beltaos, 2002). The magnitude of this effect is controlled by various factors that would be difficult to integrate into the GIS based PHP potential assessment procedure. The effect is therefore not addressed in the procedure, under the assumptions that:

- the effect on low flow conditions of streams at adjacent lower altitudes is relatively smaller when compared to the effect on high flow conditions.

- the generous consideration of snow extent in Step A5 and the utilization of snow extent as a proxy for actual freezing conditions of fast flowing water will create “buffer zones” around regions of assured occurrence of frozen, fast flowing streams. The buffer zones automatically fall into the unsuitability category for PHP installation, thus providing a measure to prevent false positive PHP potential assessment results.

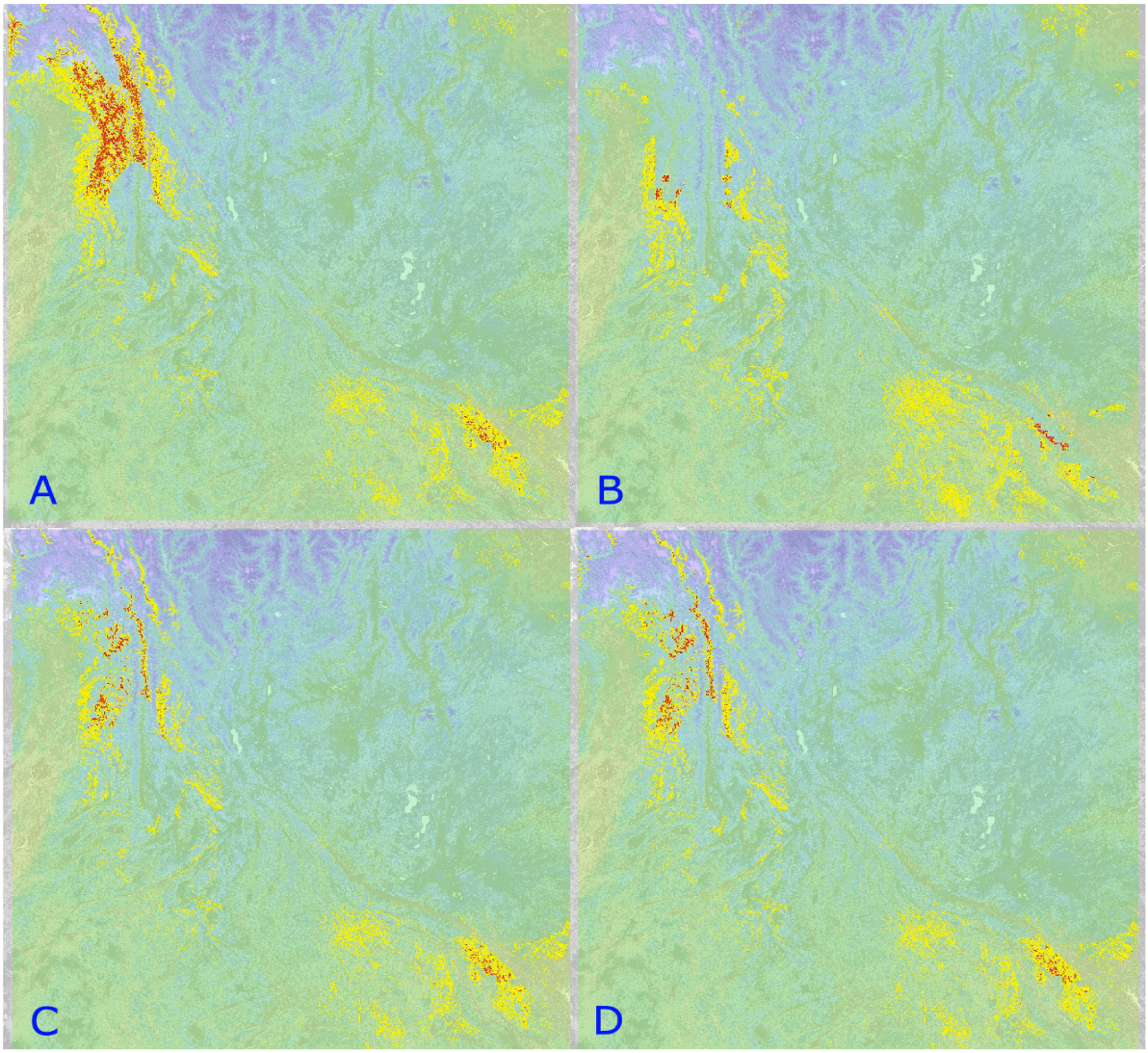

Figure 4-25: The influence of different freezing zone estimation techniques (Step A5/B2) on the GIS-assessed PHP potential (yellow: H1, red: H2 PHP potential)

A: Regional snowline approximation by altitude/latitude relationship formula. Utilized in the obsolete version of step A5/B2.
B: MODIS/Terra snow cover monthly global 0.1Deg CMG (based on MOD10CM) January 2013. Utilized to demonstrate the effects of different spatial resolution of the input data.
C: MODIS/Terra snow cover 8-day L3 global 500m grid (MOD10A2) December 1, 2012 to February 15, 2013. Utilized in the final version of step A5/B2.
D: MODIS/Terra snow cover 8-day L3 global 500m grid (MOD10A2) January 2013. Utilized to demonstrate the effects of different temporal resolution of the 500m-resolution input data.
Slide extent: 21 to 29 deg N and 95 to 105 deg E (Yunnan Province, China and adjacent areas); (890 x 890km). Nujiang Prefecture is located at the ten o'clock position of the slides.
Comparison A-C demonstrates the unsuitability of a snowline approximation for step B2. It is evident from this comparison that the snowline approximation is completely insensitive to snow cover at this latitude.
Comparison B-D demonstrates the effects of low-resolution (11.1km) snow cover data on higher resolution (1km) PHP potential estimates. Extensive false negative PHP potential estimates are directly attributable to the low resolution of the snow cover data.
Comparison C-D demonstrates the effects of the time span of 8-day high resolution (500m) snow cover data from which the maximum snow extent was compiled, on PHP potential estimates. Using a different width of the time series (December 2012 to 15 February 2013 against January 2013) for the compilation has, compared to the effect from using a coarse spatial resolution, a relatively small effect on the result.

GRASS procedure and formulation: The snow-covered area (prepared in step A5, fine resolution) is removed from the total potentially suitable area for PHP application (I). Subsequently, the land area that does not contain snow cover data (e.g. caused by different projection or swath type areal coverage) is added back to the resulting area (II).

(I)

r.mapcalc "YN_positiveDEM_wb95sw500 = (if((YN_winter13snow500@ynset1>250),null(),YN_positiveDEM_wb95@ynset1))"

(II)

r.mapcalc "YN_positiveDEM_wb95sw500m = (if((YN_winter13snow500m@ynset1==2550),(YN_positiveDEM_wb95@ynset1),YN_positiveDEM_wb95sw500@ynset1))"

Step B3: Karst component

Purpose: Areas are excluded where small streams are likely to be absent or scarce for geological reasons.

Assumption: The exclusion areas for PHP potential are identified by karst outcrops.
The term karst is used here in the geomorphological sense, not in the morphogenetic sense. In this assumption the core karst feature, regardless of its geological origin, is a presence of large underground pores and ducts that are responsible for the characteristic karst hydrology.

Discussion: Remote sensing is capable of producing relatively homogeneous data on global scale from a single data acquisition unit. In contrast to that, geological maps are a compilation of data from various sources that have to rely mostly on manual, field-based data acquisition techniques (Asch, 2003). Geological maps of larger extent moreover tend to contain a higher share of interpolated data (Marjoribanks, 2010). Both are possible explanations for the data in-homogeneity that can be obviously visible in geological data products such as the recognizable different resolutions of the respective sub-datasets of large-scale karst compilations. The resulting overall effect on PHP potential estimation is unpredictable beyond a general loss of spatial accuracy.

The aggregation of both spatially continuous and discontinuous carbonate outcrops into solid karst areas in the World Map of Carbonate Rock Outcrops V3.0 (Williams & Fong, 2010) may, regarding partially karstified areas as being fully karstified, lead to an overrepresentation of exclusion areas for PHP potential estimates. The carbonate outcrop data utilized in the GIS based PHP potential assessment procedure is therefore expected to contribute to a conservative estimate of PHP potential. The conditions are expected to improve with the availability of global carbonate maps of higher resolution that include information about the continuity of the carbonate outcrop, such as the WOKAM project (Goldscheider & Chen, 2014) currently under preparation (see Figure 4-26).

Pseudokarst is a collective and disputed term for processes other than carbonate and evaporite leaching or redeposition that altogether lead to karst-like geomorphic features (Eberhard & Sharples, 2013). Not all pseudokarst formation processes are relevant for the delineation of PHP potential. This is elucidated in the following table:

Table 4-6: Geomorphic processes causing the formation of pseudokarst (cited from: Eberhard & Sharples, 2013) and their assumed relevance for PHP potential.

Selection of geomorphic processes causing the formation of pseudokarst	**Relevance for PHP potential**
Enlargement of fractures or susceptible beds, primarily through mechanical erosion driven by wave action	not relevant
Primary voids in volcanic rocks; surficial cooling of lava flows; secondary voids in lava following decomposition of covered organisms	relevant
Meltwater caves and streams within glaciers and firn, including geothermal ablation caves on volcanoes	not relevant
Melting of ground ice	not relevant
Translocation of unconsolidated sand or clay by wind action	not relevant
Subsidence of regolith materials into cavities formed by mass movement or mechanical removal of interstitial sediment	not relevant
Toppling, sliding or rotation of rock or regolith along planes of weakness; dilation along fractures by erosional unloading or incision	relevant, if area-wide phenomenon
Rockfall or fracturing of rock masses yielding accumulations of coarse clastic deposits with interstitial cavities	relevant, if area-wide phenomenon
Progressive removal of dispersive clays and clastic particles within weakly consolidated sediment by shallow ground water movement	relevant
Solutional translocation of minerals by groundwater, deposited as concretions in caves	relevant
Human excavation (e.g. quarries, fire pits) and indirect effects of this (e.g. collapse or subsidence into underground mines)	relevant, if area-wide phenomenon

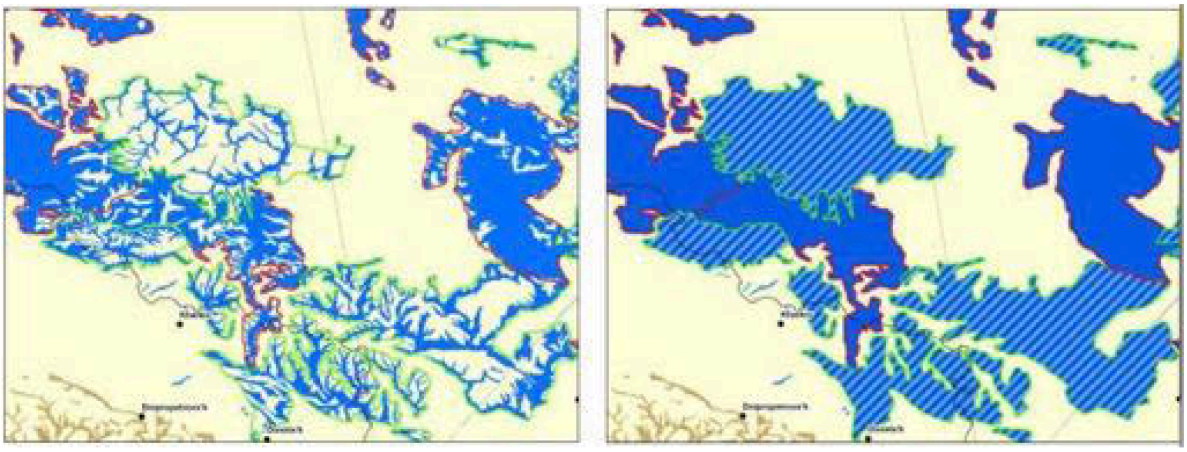

Figure 4-26: Aggregation of discontinuous carbonate outcrop occurrences into continuous (solid blue) and discontinuous (striped blue) carbonate at 65 percent cover threshold. Source: Eastern Europe section of the preliminary version of the WOKAM map (Goldscheider & Chen, 2014)

As an attempt to simplify the relationship between pseudokarst causes and PHP potential it is assumed that the pseudokarst formation mechanisms most relevant for PHP potential are associated with areas of young volcanic rock outcrop. Karst-like drainage properties in solid rock (lava tubes), both solid and unconsolidated rock (solutional and mechanical translocation), and unconsolidated pyroclastic rock (large interstitial cavities), all with possible influence on PHP potential, obviously occur in young volcanic areas. The pseudokarst potential map of the Unites States (Weary & Doctor, 2014) indicates that unconsolidated sediment, the other major geological rock class with pseudokarst potential, only occurs in drier areas of the contiguous US area. Unconsolidated sediment of non-volcanic or unspecified origin is therefore not further considered here as pseudokarst with possible influence on PHP potential. This exclusion assumption for unconsolidated sediment may not be globally valid. However it would also not be possible with realistic effort to identify sediment areas with pseudokarst potential from the coarse global-scale geological map data.

The incomplete coverage of the pseudokarst sub-dataset (Hollingsworth, 2009) of the Karst Regions of the World (KROW) map presented a preliminary “better than nothing” situation for the pseudokarst representation of the GIS based PHP potential assessment procedure.

The final stage of the GIS based PHP potential assessment procedure utilizes the World Map of Carbonate Rock Outcrops V3.0 (Williams & Fong, 2010) for the representation of carbonate karst, supplemented by a direct identification of the young volcanic rock units in the respective regional map of the U.S. Geological Survey's world energy project (e.g. Schenk et al., 1999 for South America) to represent potential pseudokarst areas.

Ecuador features both field assessed PHP potential data and documented karst and pseudokarst occurrences. The relevance and quality of the karst and pseudokarst data used in the GIS based PHP potential assessment is therefore exemplarily demonstrated here for Ecuador and adjacent areas.

The KROW dataset contains both karst and pseudokarst occurrences for Ecuador (see Figure 4-27). As primary sources for the vector data World Map of Carbonate Rock Outcrops V3.0 (Williams & Fong, 2010) was chosen to represent carbonate karst and maps showing geology, oil and gas fields and geologic provinces of the South America region, open-file report 97-470-D (Schenk et al., 1999) was chosen to represent pseudokarst.

An identification of the underlying geological units in the USGS map (Schenk et al., 1999), a simplified geological map, reveals that the pseudokarst areas in the KROW dataset represent the Mesozoic igneous unit in the USGS map. This is presumably an error, since the porosity necessary to develop karst features is most likely present in young, less altered volcanic material. Weary & Doctor (2014) mention in a North American context "no older than Miocene in age" (<23 Ma), Lysenko (1976) dates the development of the pseudokarst relief in Ecuador to the end of the Pleistocene period (0.1 Ma). The Mesozoic igneous unit thus needs to be replaced by the adjacent Cretaceous-Tertiary volcanics unit (see Figure 4-27) to represent the potential pseudokarst area for the subsequent PHP potential evaluations on Ecuador. This unit moreover includes the quaternary volcanic areas of Ecuador.

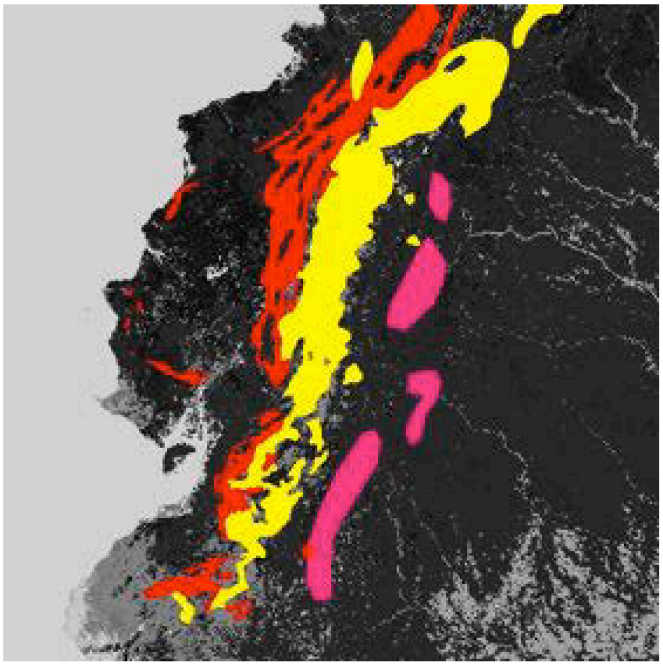

Figure 4-27: Karst extent for Ecuador and adjacent areas, based on different datasets.

The pink areas represent carbonate karst. (KROW and World Map of Carbonate Rock Outcrops datasets), the red areas represent pseudokarst at the extent of the mesozoic igneous formations (KROW dataset), the yellow areas represent pseudokarst at the extent of the Cretaceous-Tertiary igneous formations based on the USGS dataset.

Map extent: 5 deg S to 2 deg N and 75 to 82 deg W; (780 x 780km).

The carbonate karst areas of the World Map of Carbonate Rock Outcrops V3.0 dataset intersect with several mesozoic and tertiary sediment formations on the USGS map. The total extent of these sediment formations starkly exceeds the extent of the carbonate occurrences (see Figure 4-28, at left). This apparent lack of spatial relationship is not necessarily caused by error, since mapped geological formations are primarily classified by stratigraphy and lithogenesis and not by rock chemistry. In more detailed geological maps (see Figure 4-28, at right), carbonate outcrops can sometimes be directly attributed to a geological formation or sub-formation if the extent of carbonate bearing rock is limited to this formation. By comparing the carbonate data of the World Map of Carbonate Rock Outcrops V3.0 dataset with the National Geological Map of Ecuador (Longo & Baldock, 1982) it becomes evident that the southernmost of the four carbonate areas is directly attributable to the jurassic Santiago formation, composed of "limestones, shales and sandstones" (Longo & Baldock, 1982), whereas the other three areas have no analog features on the map. They overlie a number of tertiary and quaternary formations, composed of both consolidated and unconsolidated sediments without explicit mention of limestone on their map legend description.

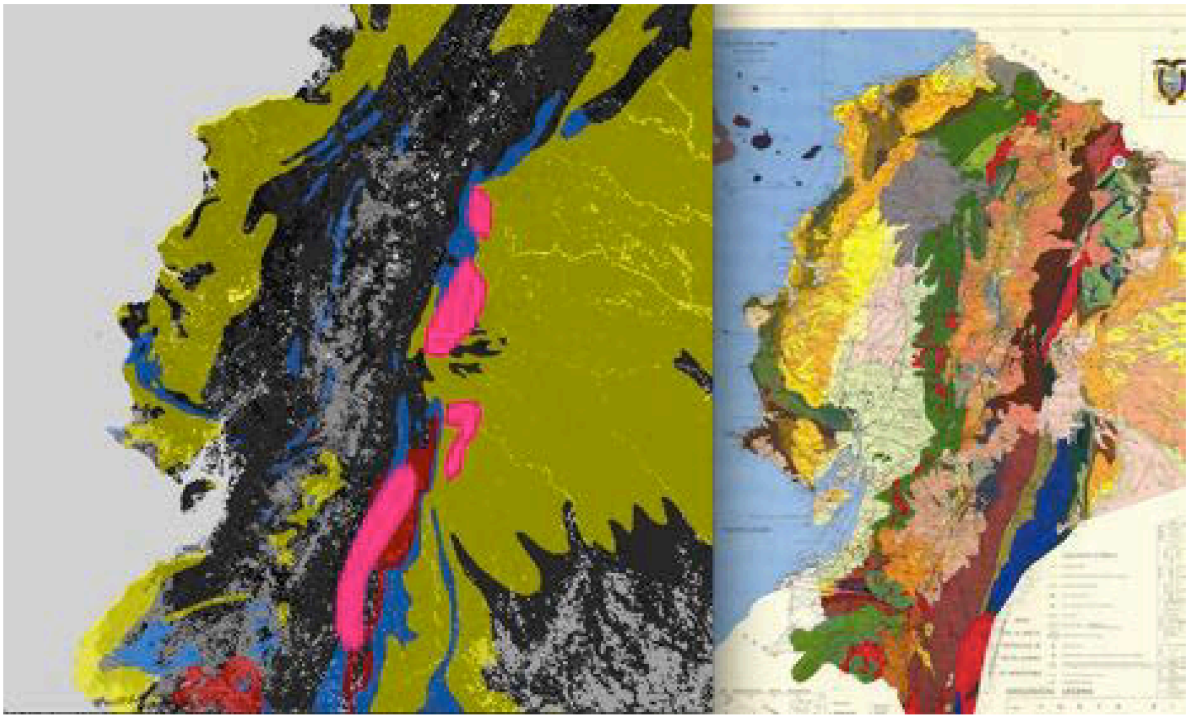

Figure 4-28: Carbonate karst extent (Williams & Fong, 2010) for Ecuador and adjacent areas (at left; pink) with underlying jurassic (red), cretaceous (blue), and tertiary (olive green) sediment formations, according to the simplified USGS geological map (Schenk et al., 1999). More detailed geological information (Longo & Baldock, 1982, at right) is not directly usable for karst identification. The dark blue area on the map at right is the Santiago formation. Extent: (map at left) 5 deg S to 2 deg N and 75 to 82 deg W (770x770km).

It can be concluded from this example that the actual extent of karstified areas within the potentially karst bearing formations is not predictable from geological maps. The purity of the carbonate minerals has a great influence on the solubility which, in conjunction with structural features, is the main driving force on karst formation in humid areas (Ford & Williams, 2007). Both of these influencing factors are not extractable from geological maps. These facts underline the necessity to utilize a dedicated carbonate karst map (see chapter 4.2.1) for the representation of carbonate karst areas.

Estimating the actual extent of pseudokarst is even more difficult, because the variety of phenomena that are summarized as pseudokarst bring an even larger spectrum of underlying formation mechanisms with them. This, and the fact that pseudokarst is not even an universally accepted term (Eberhard & Sharples, 2013), helps explaining that except for the territory of the United States, only fragmentary or highly generalized large-scale spatial data is available for pseudokarst. For example, the actual extent of pseudokarst within the Cretaceous-Tertiary igneous unit of Ecuador is locally documented by Lysenko (1976). The area surrounding the Cotopaxi volcano was investigated for pseudokarst features. Several areas that qualify as “pseudokarst hosted by unconsolidated pyroclastic material” (Lysenko, 1976) were delineated (see Figure 4-29, at left). The resulting pseudokarst fraction of the total area may seem small, however there is also mention of areas covered by pyroclastic sediments in the study. These areas may not exhibit typical karst features, but can be expected to have a karst-like drainage regime as well. Kumpulainen (1997) describes the principal drainage patterns in stratovolcanoes, such as Cotopaxi (see Figure 4-29, at right), and moreover mentions the good hydraulic conductivity of thin lava flows, characteristic for shield volcanoes, the other main volcano type. Both scenarios promote a karst-like spring formation pattern.

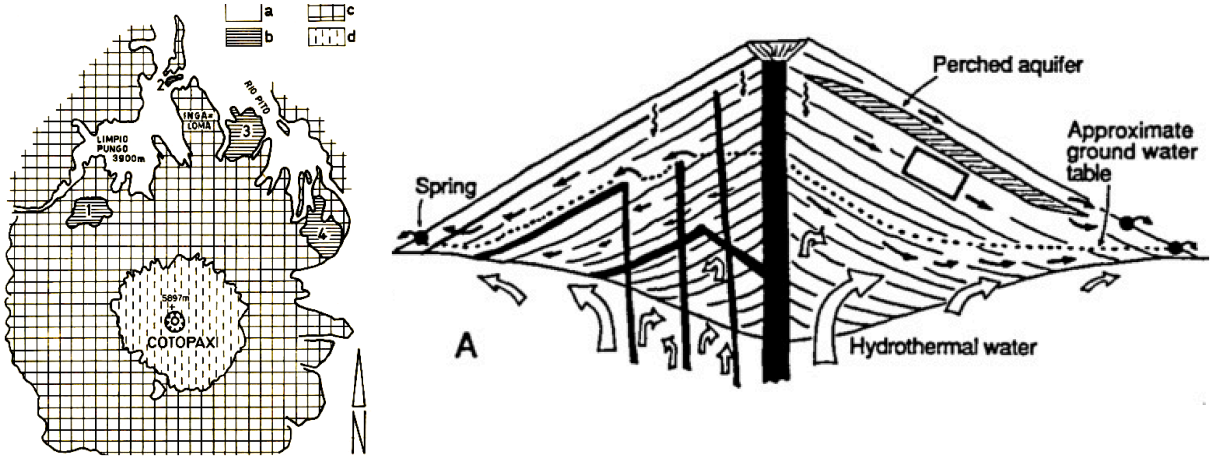

Figure 4-29: Pseudokarst and spring formation on a stratovolcano.

Left: View from above. Exposed pseudokarst areas (b; horizontal hachure), sloping volcanic material (c), glacier (d) and glacial valleys (a) on Cotopaxi volcano (Lysenko, 1976). Map extent: 15 x 20km.
Right: Cross section. Sub-surface water circulation patterns and emergences of surface water. Schematic illustration (Kumpulainen, 1997).

In summary, the identification and delineation of pseudokarst at a resolution that would be required for large-scale PHP potential estimates is not possible with the available spatial data. Nevertheless, pseudokarst needs to be considered as an important influence factor for the assessment of PHP potential and is, together with undocumented carbonate karst, the most obvious yet unproven explanation for a field-observed absence of PHP potential in areas that would be expected to exhibit PHP potential by other relevant parameters (dry month water balance, topography).

As a consequence, positive results of the GIS based PHP potential assessment procedure in areas with relevant pseudokarst according to the relevance classification of Table 4-6 are labeled as “possibly pseudokarst affected”, indicating a possible detrimental effect from the local geology on PHP potential.

For the delineation of pseudokarst areas the respective sub-dataset of the U.S. Geological Survey's world energy project geological map is used. Only tertiary (Neogene, if specified) and quaternary volcanic formations are considered.

On the other hand, carbonate karst areas based on the World Map of Carbonate Rock Outcrops V3.0 (Williams & Fong, 2010) are treated as exclusion areas for PHP application in the GIS based PHP potential assessment.

GRASS procedure and formulation:

Pseudokarst, example Ecuador:

Sub-step 1: Import of USGS geological map:

v.in.ogr -r dsn=/.../geo6ag.shp output=EC_geo6ag_vect min_area=0.0001 snap=-1

Sub-step 2: Replacement of geological abbreviation terms by numerical codes. Example: change Mv (Mesozoic volcanics) to code 82:

v.db.update map=EC_geo6ag_vect@ecuador_1 =area layer=1 column=GEO6AG_ value=82 where=GLG='Mv'

Sub-step 3: Vector to raster conversion:

v.to.rast input=EC_geo6ag_vect@ecuador_1 =area layer=1 column=GEO6AG_ output=EC_geo6ag_30m use=attr

Sub-step 4: Analysis for tertiary and quaternary volcanic rocks (code 81), representing pseudokarst:

r.mapcalc "EC_pseudokarst81 = (if((EC_geo6ag_30m@ecuador_1==81),EC_geo6ag_30m@ecuador_1,null()))"

Step B4: Above spring horizon component

Purpose: Areas with a low probability of exhibiting permanent streams due to convex terrain curvature and insufficient slope length, commonly described as "land above the spring horizon", "peaks" or "ridges" are excluded in step B4. The areas are identified and discussed in preceding step A2.

Assumption: Areas identified as located "above spring horizon altitude" exhibit no PHP potential, because the flow of the largest watercourses found in these areas is insufficient for PHP applications. These areas are excluded to avoid false positive PHP potential assessment results.

GRASS formulation:

r.mapcalc "exabovespringhorizon = (if(isnull(abovespringhorizon@costaricaset),Aster_30m_costarica@costaricaset,null()))"

Step B5: Insufficient slope component

Purpose: Areas with an average terrain inclination (slope) of less than 9.5 degree are excluded.

Assumption: Operation of the standard PHP system as defined in chapter 3.3 becomes uneconomical at an average terrain inclination of less than 9.5 degree due to excessive penstock costs.

Discussion: Slope is derived from DEM data using a 3x3 neighborhood analysis algorithm around the cell to be analyzed (Shapiro & Waupotitsch, 2003). The DEM cell resolution for analysis is 30m. Step B5 ensures that areas with insufficient slope are excluded from the subsequent power calculation step by converting these into areas with zero slope. This is not an essential measure to avoid false PHP potential estimates on DEM cell level, since the result of the power calculation in areas with insufficient slope would in any case not result in a positive PHP potential estimate. The step is rather a measure to artificially emphasize the negative influence of insufficient slope on PHP potential. The resulting moderate attenuation effect on the power calculation result contributes to a conservative estimate of the overall result after the final areal integration step.

GRASS procedure and formulation:

1. Calculation of slope
r.slope.aspect elevation=Aster_30m_costarica@costaricaset slope=CR_slope

2. Exclusion of areas with insufficient slope
r.mapcalc "CR_slopeunder95 =
(if((CR_slope@costaricaset<9.5),CR_slope@costaricaset,null()))"

C: Quantitative intermediate component ("Power calculation")

Purpose: An intermediate "potential classification value" based on the hydraulic potential is calculated at DEM cell resolution for the entire area of the PHP potential assessment.

Assumption: The parameters to calculate the hydraulic potential of a cell are represented by (1) the hydraulic head, which is derived from the average slope of the cell, and (2) the driest month water balance.

Discussion: Step C represents a hydropower potential calculation that is basically analogous to the classical area potential method (e.g. Weiss & Faeh, 1990). However, hydraulic head in step C is not represented as the altitude difference between the average cell altitude and the watershed discharge point, as in the classical method (see Figure 2-1), but rather as the absolute (maximal) altitude difference within the cell itself. The flow parameter is broken down onto cell level as well, by substituting watercourse specific data (e.g. gauged streamflow) with spatial runoff data derived from a water balance (see chapter 4.2.1). It therefore becomes spatially scalable however bears no reference to actual watercourses. Based on a hydraulic power calculation with the customized head and flow parameters, it is possible to obtain a qualitative statement for each individual cell. The statement answers the question whether (or not) the cell is able to meet certain predefined criteria for hydropower potential (or hydropower potential classifications). Hydraulic potential thus becomes an equally leveled criterion to other PHP potential criteria and can be worked with at DEM cell level. Conservative estimates on hydropower potential, not a typical feature of area potential methods (Hildebrand & Kern, 1989; Wittenberg & Schulte, 1987), are achieved in step C through a limitation of the result range. At the minimum conditions of the H1 PHP potential classification (9.5 degree average DEM slope and 26mm of monthly surface runoff; see chapter 3.3), the result of step C in "potential classification value" denomination is 1.0. The potential classification value system facilitates the direct expression of PHP potential classes in decimal value. Insufficient slope is excluded by the 9.5 degree criterion. Insufficient runoff however, when partially compensated by favorable slope conditions is permitted to cause results below 1.0. The lowest acceptable result in step C is 0.5, which is the equivalent of a slope of 17.5 degrees and 7mm of runoff (see chapter 3.3). The lower limit of the result range is therefore at 0.5. Any DEM cell with a potential classification value below 0.5 is regarded in the subsequent areal integration step as if it had zero hydraulic potential.

DEM cells with potential classification values over 2.0 (the equivalent of a hydraulic area potential of 3.33 kW/km^2) are limited to a value of 2.0. This is owed to the fact that the resolution of the GIS based PHP potential assessment procedure is limited to three high head PHP potential classes: H0, H1, and H2. Moreover, in the subsequent areal integration steps this limitation measure prevents very high hydraulic potentials in small areas from compensating insufficient hydraulic potential (or other adverse conditions) in other areas of the same PHP unit cell.

N	12.2	14.3	9.5
7.1	9.1	6.3	2.3
N	3.9	1.8	1.2
0.2	0.5	0.4	0.1

N	12.2	14.3	9.5
7.1	9.1	6.3	2.3
N	3.9	1.8	1.2
N	0.5	N	N

N	2.0	2.0	2.0
2.0	2.0	2.0	2.0
N	2.0	1.8	1.2
N	0.5	N	N

Figure 4-30: Numerical example for the processes in step C, demonstrated as raster attribute values of a 4x4 DEM cell matrix in "potential classification value" units.

Left: Result after area potential ("power") calculation. "N" are cells with NULL attribute (undefined cell value) that are excluded from further operations as a result of preceding exclusion operations.
Center: Result after area potential calculation and application of the lower limit.
Right: Result after area potential calculation and application of both the lower and upper limit. It becomes obvious at this stage that the cell values do not directly represent an area potential anymore. The result of Step C is rather the representation of an intermediate stage to the subsequent area integration step.

GRASS procedure and formulation:

Adapted from the quantitative expression for hydraulic potential

$$P = \rho g Q h \eta \qquad \text{E/F 2-1}$$

the "potential classification value", a qualitative representation of the hydraulic potential specified for the standard PHP system with a range corresponding to the PHP potential classes H0, H1, and H2 (see chapters 3.3 and 4.1) is calculated for each DEM cell with 30.8m cell length as:

$$0.23\, wb_{dm} \tan DCS \qquad \text{E/F 4-5}$$

with wb_{dm} being the water budget of the driest month and DCS being the average slope of the DEM cell.

*r.mapcalc "SL_H1H2_raw_wbh = ((((tan(SL_slopeover95@costaricaset)*30.8)*SL_waterbudgetminm900m_mm@costaricaset)/134))"*

Results lower than 0.5 and results higher than 2.0 will be treated in the subsequent range limitation steps:

Lower limitation at 0.5:

r.mapcalc "YN_H1H2wb_total_recl_ex05 = (if((YN_H1H2_raw_wb@ynset1>0.5),YN_H1H2_raw_wb@ynset1,null()))"

Upper limitation at 2.0:

r.mapcalc "YN_H1H2wb_total_reclass = (if((YN_H1H2wb_total_recl_ex05@ynset1<2),1,2))"

D: Evaluation stage

Purpose: The high head PHP potential class of a PHP unit cell (926x926m, see Figure 4-12) is calculated from the result of the preceding steps.

Assumption: The Step C results averaged over the PHP unit cell area represent the PHP potential class of the PHP unit cell.

Discussion: Following step C, DEM cells with PHP potential carry values ranging from 0.5 to 2.0. After conversion from NULL value, insufficient or absent PHP potential is expressed as a zero (0) result in this stage to facilitate a participation in the areal average calculation. Valid PHP potential of an area is expressed as the possibility to operate one (H1 potential) or two (H2 potential; see chapter 3.3) standard high head PHP systems (see chapter 3.2) on a PHP unit cell.

The final step D of the potential evaluation is entirely based on the potential classification value at DEM cell resolution (i.e. step C result). The underlying factors had been discussed and checked for plausibility in the preceding steps A-C. A comprehensive verification of the PHP potential result on PHP unit cell level is only possible through a comparison with field-assessed PHP potential data. This task is part of section 5. Additionally, a graphical plausibility check of the Step D result vs. the Step C DEM cell result pattern is performed for particularly error sensitive Step C result scenarios. The test requires the conversion of the cell values and their spatial distribution patterns into a corresponding PHP application scenario to evaluate the plausibility of the Step D results. The emphasis of the plausibility check (see Table 4-7) is put on false positive results, i.e. H1 or H2 potential results that represent impossible and unrealistic PHP application scenarios. The cases were deliberately chosen to be extreme.

GRASS procedure and formulation:

Following a change to 926x926m resolution, excluded areas (i.e. NULL values) are converted to zero values (0) to enable numerical operability of the entire contiguous area.

r.null map=YN_H1H2wb_total_reclass@ynset1 null=0

Calculation of the average value (Step D result) of the PHP unit cell:

r.resamp.stats input=YN_H1H2wb_total_reclass@ynset1 method=average output=YN_H1H2wb_total_average900m

H0 potential results (average value < 1) are separated from the other results (H1 and H2):

r.mapcalc "YN_H1andH2_wb = (if((YN_H1H2wb_total_average900m@ynset1>=1),YN_H1H2wb_total_average900m@ynset1,null()))"

H2 potential results (average value > 1.75) are separated from the other results (H1):

r.mapcalc "YN_H1andH2wb_reclass = (if((YN_H1andH2_wb@ynset1>=1.75),2,1))"

The final result of step D is visualized as a map, depicting the spatial distribution of PHP potential across the extent of the assessment area (example: Figure 5-10). PHP unit cells with H1 potential or H2 potential are marked by coloration. Areas with PHP potential that moreover may be affected by pseudokarst are distinguished by a different coloration. Areas without high head PHP potential generally remain unmarked.

Table 4-7: Test of artificial, extreme Step C result scenarios for plausibility of their Step D results, as well as their corresponding PHP application scenarios.

Step C result matrix. For visual clarity, the original 30x30 matrix of the DEM cells was reduced to a 6x6 cell matrix with integer content.	**Step D result**	**PHP application scenario**	**Plausibility of step D result**	**Expected frequency to occur in reality**
0 0 0 0 0 0 0 0 0 0 0 2 0 0 0 0 2 2 0 0 2 2 2 2 0 2 2 2 2 2 2 2 2 2 2 2	H1	Area with favorable PHP potential bordering an area with no PHP potential. The H0 area is typically an exclusion area, such as a carbonate karst outcrop.	H1 potential is plausible. The reduced potential accumulation area is compensated by increased steepness and/or high dry season flow, evident from the H2 sub-area.	not common
0 0 0 0 0 0 0 0 0 0 0 1 0 0 0 0 1 1 0 0 1 1 1 1 0 1 1 1 1 1 1 1 1 1 1 1	H0	Area with PHP potential bordering an area with no PHP potential. The H0 area is possibly an exclusion area, such as a carbonate karst outcrop or a flat area.	H0 potential is plausible. The large area without PHP potential (H0) cannot be compensated by the H1 sub-area.	common
0 2 0 2 0 2 2 0 2 0 2 0 0 2 0 2 0 2 2 0 2 0 2 0 0 2 0 2 0 2 2 0 2 0 2 0	H1	The pattern is most likely caused by extreme differences in steepness over a small area in a wet region, such as a terraced slope.	H1 potential is plausible. The reduced overall area with PHP potential is compensated by increased steepness and/or high dry season flow, evident from the H2 sub-area. The overall topography resembles a slope.	very rare
1 1 1 1 1 1 1 2 2 2 2 1 1 2 0 0 2 1 1 2 0 0 2 1 1 2 2 2 2 1 1 1 1 1 1 1	H1	The pattern represents a single peak with steep flanks and a height difference of at least 180m (in very wet areas, otherwise more); see Figure 4-20. The peak is centered on the PHP unit cell.	H1 potential is plausible. The reduced overall area with PHP potential is compensated by increased steepness and/or high dry season flow, evident from the H2 sub-area and the overall topographical setting.	very rare

Figure 4-31 summarizes the data processing (Step A-D) of the GIS based PHP potential assessment procedure as a path diagram to elucidate the step-specific interaction paths between input, processing, and output.

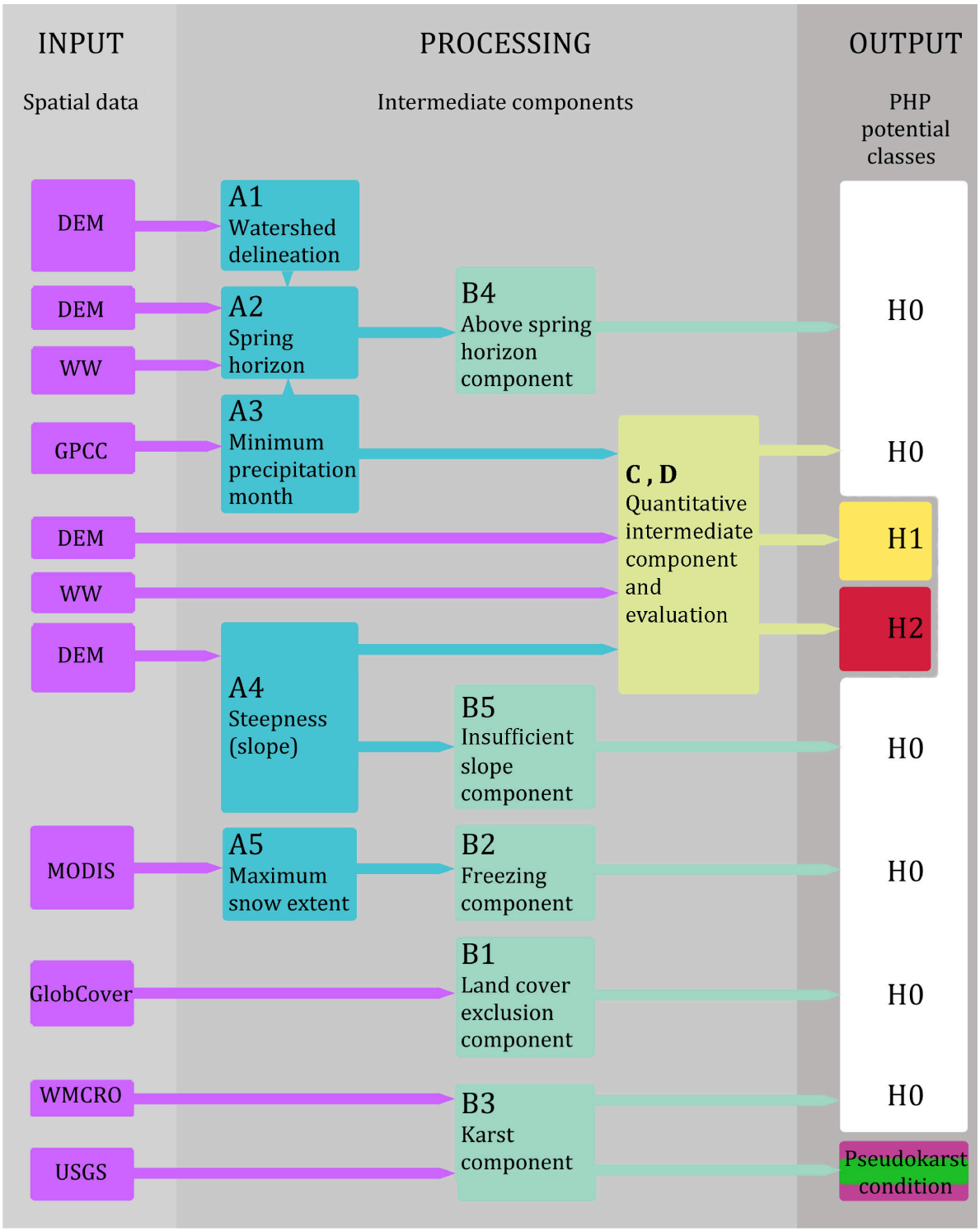

Figure 4-31: Overall view of the data processing steps in the GIS based PHP potential assessment procedure. Green and yellow arrows indicate the variances of the resulting PHP potential classes. For example, the output of exclusion components (green, steps B...) can only result in H0 potential. Input datasets (purple), documented in chapter 4.2.1, are shown in abbreviated notation.

5 Large-scale PHP potential assessment method: Application and testing

To verify the functionality of the large-scale PHP potential assessment method, GIS based PHP potential assessments were conducted in the course of this study in four geographic areas. The areas comprise Costa Rica, Ecuador, Sri Lanka, and Yunnan Province/China and include the respective adjacent areas to add up to a rectangular total extent.

The GIS procedure for all GIS based PHP potential assessments follows exactly the operational sequence outlined in Figure 4-31, based on the formulas described in chapter 4.2.2. The only permitted deviation from the operational sequence is an omission of obviously redundant steps, such as a freezing component calculation for Sri Lanka. The GIS derived PHP potential assessment results are compared against reference data obtained from field-based PHP potential assessments (see chapter 4.1) that were conducted in the respective areas between 2010 and 2012.

5.1 Reference data validation

Prior to the comparison of the two datasets, the validity of the reference data needs to be individually evaluated for each field assessment area. The purpose is to investigate possible error sources that are linked to local conditions. General uncertainties of the field-based assessment method, independent of local conditions, are outlined in chapter 4.1.

Error sources specific to the respective temporal field assessment unit, therefore dependent on local conditions, are attributable to two main fields that are documented in the subsequent subchapters:

(1) Deviations from minimum flow conditions at the time of the field assessment (dry season validity).
(2) Specific local conditions causing a misattribution of PHP potential at the field assessment (attribution validity).

5.1.1 Dry season validity of reference data

Although precipitation follows a seasonal pattern and the months of minimum precipitation are roughly predictable, the actual occurrence of the dry season for the time of the field assessment has to be verified *a posteriori* to be able to compare between typical (multi-year average) and actual (during the time of the field assessment) precipitation conditions. A field-based PHP potential assessment performed outside of the time window of minimum flow condition causes a systematic error. This error could theoretically be corrected to some extent by calibration with precipitation data from remote sensing or rain gauges. In that case, a correction factor for the respective time period would have to be introduced. However, due to the nonlinear relationship between precipitation and baseflow, correction operations are not advisable here. Instead, field-based assessment results taken at untypical dry season conditions or clearly outside of the dry season are disregarded entirely.

The following section elucidates two alternative methods to evaluate the dry season validity of reference data for the example of Costa Rica.

Temperature and precipitation are both climatic parameters with direct influence on flow conditions. Ambient temperature is directly influencing minimum flow conditions of small streams in areas where seasonal freezing conditions occur. It is moreover indirectly relevant by inducing seasonal variations in plant evapotranspiration (e.g. Brown et al., 2005; Muñoz-Villers & McDonnell, 2013). Both of these temperature related conditions are untypical for tropical areas like Costa Rica where only small seasonal temperature variations occur. Precipitation therefore remains the main influence factor for minimum flow conditions of small streams in Costa Rica. Following this argumentation leads to the assumption that minimum flow conditions of small streams coincide (a) with the least-precipitation month of the year (in the case of a distinct one-month precipitation minimum) or (b) the last month of the dry season (in the case of a distinct dry season with several consecutive months of similar low precipitation levels). This means that minimum flow conditions are approximately identifiable from multi-year average monthly precipitation data.

The average monthly precipitation diagrams illustrated in Figure 5-1 belong to localities that are representative for the main climatic distinctions in Costa Rica. All four localities were visited during the field-based assessment. The precipitation data is based on a 30-year precipitation monthly average, generated from a climate model with 926m of spatial resolution (Climate-data.org, 2014). Applying the minimum flow criteria onto the precipitation data of the four localities identifies March as the expected month of minimum flow.

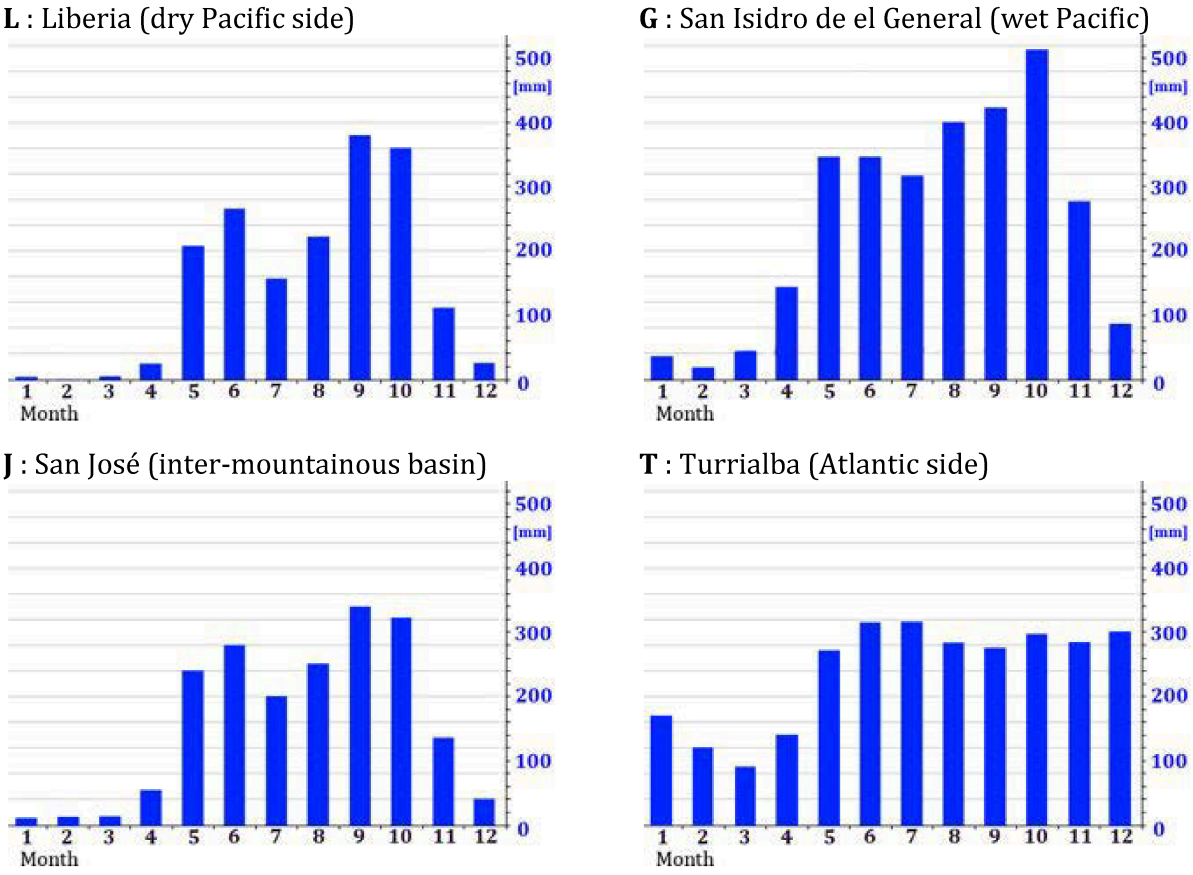

Figure 5-1: Monthly precipitation averages 1982-2012 of representative locations in Costa Rica (modified after Climate-data.org, 2014).

The actual precipitation of March 2011 and two preceding months is shown below as monthly maps of accumulated precipitation, prepared by the Tropical Rainfall Measurement Mission (TRMM) 3B43 monthly accumulated precipitation V7 reanalysis, a product based on both remote precipitation sensing (TRMM satellite) and terrestrial rain gauge data (GPCC) with original 0.25deg (27.7km) resolution (NASA GES DISC, 2014a).

January 2011

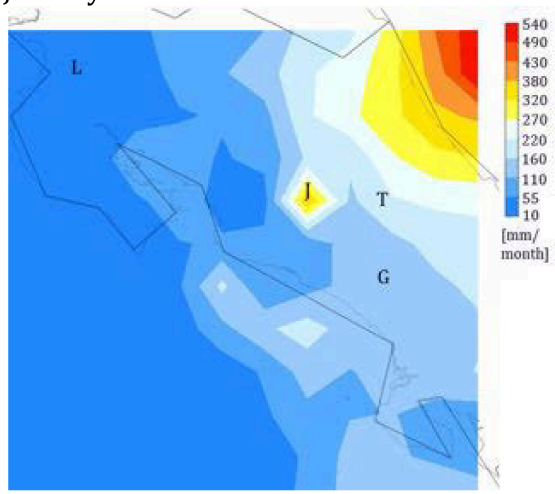

March 2011

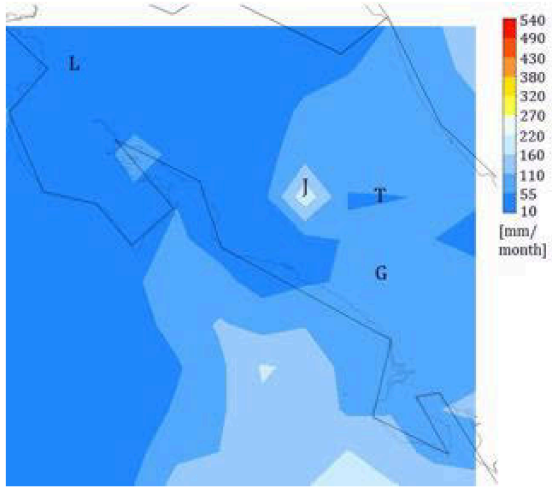

February 2011

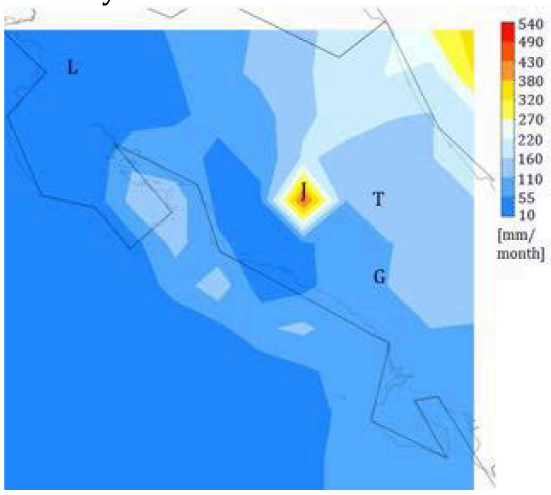

Figure 5-2: TRMM precipitation reanalysis maps of January, February and March 2011 for Costa Rica.

Visualization modified after the TRMM Online Visualization and Analysis System (TOVAS) (NASA GES DISC, 2014b).
Scaled as mm of accumulated precipitation for the respective month.
Map extent is 8 to 11 deg N and 83 to 86 deg W (330 x 330km).
Letters indicate the locations of the representative localities (see Figure 5-1) on the map.

Discrepancies between the TRMM data and the preceding Climate-data.org monthly precipitation averages data indicate deviations from the average monthly precipitation rate that are specific for the locality at the respective month of 2011.

The comparison of the two datasets reveals an obvious anomaly in the area around San José, (abbreviated "J") which, according to the TRMM data, had exceptionally high precipitation rates over the whole period from January to March 2011 with monthly amounts that would be typical for the wet season. It is suggested that the spatial extent of this anomaly coincides with the area of the "wet spot" around San José, which is prominent on all three monthly maps (see Figure 5-2). The comparison results for both the data of Liberia (L) and Turrialba (T) are inconspicuous. San Isídro de el General (G) has elevated TRMM dry season values that are still significantly lower than typical wet season values. The comparison is intended to reveal whether or not both values are within the "dry season range" for the respective locality. According to the data presented in Figure 5-1, the "dry season range" for Costa Rica is at least less than half and typically one third to one tenth of the average monthly

precipitation rate for the wet season. In conclusion from the comparison, regular dry season conditions are given for three of the four localities tested. The fourth area (San José) clearly exceeds regular dry season precipitation rates.

To overcome the shortcomings of the preceding locality based method that result in uncertainties for the areas outside the four data points, precipitation anomaly analyses are performed as spatial analysis directly from the TRMM 3B43 V7 precipitation data, which is available from January 1998 to September 2014. Figure 5-3 represents the average anomaly for the period of January to March 2011. The anomaly for the respective month is calculated as the monthly rain rate subtracted from the monthly rain rate average since 1998 and is subsequently averaged over the analysis time, here: January to March 2011 (NASA GES DISC, 2009).

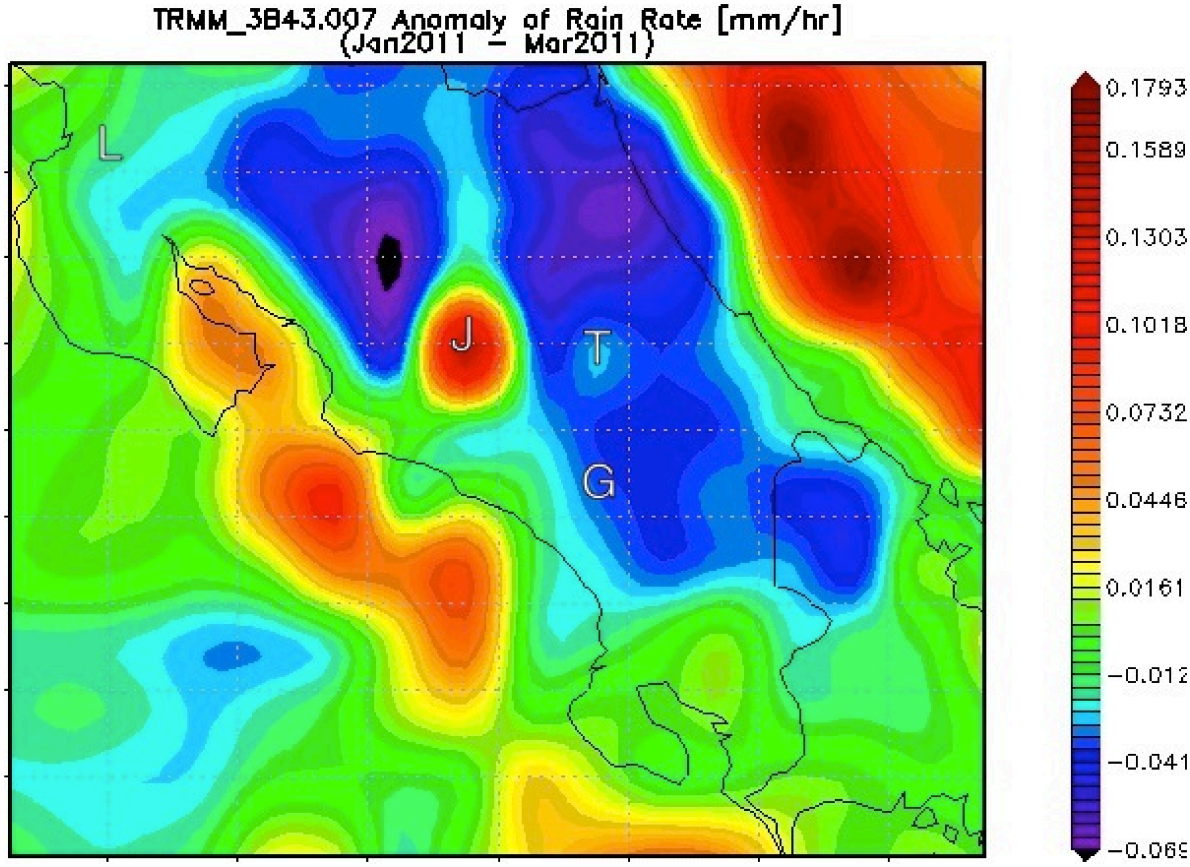

Figure 5-3: TRMM precipitation anomaly analysis January to March 2011 for Costa Rica and adjacent areas (NASA GES DISC, 2014b). Scaled as mm of average hourly precipitation deviation, for the period January to March 2011. Extent: 8 to 11 deg N and 83 to 86 deg W (330 x 330km).
The four data points of the previous method are included for comparison.

The better spatial coverage of the TRMM monthly precipitation anomaly analysis outweighs its data history disadvantage, when compared to the locality precipitation data method based on Climate-data.org material. This qualifies the TRMM monthly precipitation anomaly analysis to be the method of choice for analyzing the dry season validity of the reference data.

For the period of January to March 2011, the deviations from the 1997-2014 January to March monthly precipitation average over the land surface area of Costa Rica (see Figure 5-3) cover a range of -0.069 to 0.13 mm/h, which convert into -49.7 to 93.6 mm/month. Precipitation below average (blue to black areas) increases the probability to underestimate

the attributed PHP potential for the reference points in these areas. In effect, this would contribute to a conservative estimate of the PHP potential which is integrated into the error minimization strategy (see chapter 5.1.2). Precipitation above average in the month of a field-based assessment (yellow to red areas in Figure 5-3) can lead to an overestimate of PHP potential. A quantification of this overestimate is not possible. In the classification scale used in this study it would eventually result either in an increment step from H0 to H1 class PHP potential or H1 to H2 class PHP potential. To rule out the possibility for a PHP potential class increment step to occur, the maximum tolerable positive deviation from average precipitation would therefore be the minimum amount of runoff per km^2 necessary to fulfill the hydraulic requirements of a standard PHP system, regardless of terrain inclination. This is defined as a monthly runoff of 26mm (see chapter 3.3). Conversion into the units of the anomaly analysis (see Figure 5-3) leads to the following threshold definition:

The maximum acceptable positive deviation from the average dry season rain rate for reference data is 0.036 mm/h.

Reference data collected at irregular dry season conditions has only a potentially detrimental effect on the calibration process of the GIS based PHP potential assessment procedure if this reference data belongs to an area that fulfills all requirements for PHP potential. In other words, reference data collected at irregular dry season conditions in areas generally unsuitable for PHP application cannot detrimentally influence the calibration process. Both land areas that exceed the maximum acceptable positive deviation from the average dry season rain rate (represented as orange to red areas in Figure 5-3) are considered generally unsuitable for PHP application. Despite local dry season irregularities, the entire area of Costa Rica can therefore be considered as compliant with the dry season criteria for the period of January to March 2011.

5.1.2 PHP potential attribution validity check by comparison with reference data

Although all input steps of the GIS based PHP potential assessment procedure are individually checked for plausibility (see chapter 4.2.2) it is necessary to check the output for plausibility as well. The method of choice is a comparison of the GIS derived results with a reference obtained by dry season field-based assessment of the respective area (see chapter 4.1). The step is deliberately called comparison and not calibration, because the absolute accuracy of the reference data is inherently inconsistent. Despite correction measures, such as the dry season validation (see chapter 5.1), it is still subject to error. Adverse PHP potential attribution conditions during the field-based assessment (e.g. overgrown streams) are predictable to some extent, but nevertheless cannot be entirely avoided. For example, this may be caused by the shortened observation time on a fast moving means of transport.

These are predominantly random error sources. To minimize such errors in the field-based assessment, observation tracks were traveled twice (in either the same or opposite directions) whenever appropriate by the traveling conditions.

Generally, due to the uncertainties of both methods, discrepancies between the results of both assessment methods principally need to be analyzed, explained, and – if possible – fed back into the improvement process of the respective PHP potential assessment method.

The comparison between GIS assessed PHP potential data and reference data is conducted by visual examination of an overlay of both data sources in a GIS environment. Additional

data, such as GIS metadata or notes taken during travel on location are moreover considered. The following conformity criteria are applied:

CrA: Attributed PHP potential is conform with GIS assessed PHP potential when a PHP unit cell of the same PHP potential class is overlaying or adjacent to the reference data point (see Figure 5-4).

CrB: In areas of good overall conformity, a distance of two PHP unit cells for the occurrence of the same PHP potential class is acceptable for small (1-2 PHP unit cells), isolated areas with PHP potential. This is necessary, because the actual location of the reference point cannot be clearly defined in the direct PHP potential attribution method, as it represents the summarizing result of an "impression by transit" that refers to the surrounding landscape of a road section (see chapter 4.1 and Figure 4-9).

CrC: The stream frequency (the number of streams crossing the path of travel) exceeds five crossings on a traverse of ten PHP unit cells of GIS assessed H1 potential and ten crossings on a traverse of ten PHP unit cells of H2 potential. Again, because of the random directions of streambeds in relation to the path of travel (see Figure 4-6), this criterion cannot be applied as a strict rule. Traveling along the altitude lines will yield more stream crossings than traveling across the altitude lines. This effect can only be mediated by averaging the stream frequency over a longer stretch with the same PHP potential, which is not always available. Theoretically perfect conformity of the CrC criterion is observed when each traversed PHP unit cell with H1 potential contains one, and each PHP unit cells with H2 potential contains two or more stream crossings.

The concomitant use of both field assessment methods facilitates a plausibility check for the reference data itself. It verifies that an attributed PHP potential class is accompanied by an appropriate frequency of streams and vice versa.

Above combination of "hard" and "soft" comparison criteria, resulting in an inherent spatial uncertainty of about 1km around areas with PHP potential, and the generally qualitative approach on the definition of PHP potential (see chapter 3) leave no option for a statistical evaluation of the comparison results. Overall error minimization therefore concentrates on an approach that is based on an individual view on the effects of over- and underestimation respectively.

The targeted inclination towards a conservative estimate for both the GIS based PHP potential assessment procedure and the field assessment, already mentioned in the effect classification of the apparent error sources of the field assessment (see chapter 4.1.4), the sub-step of the GIS procedure to determine the maximum snow extent (see chapter 4.2.2 Step A5), and the dry season validity of reference data (see chapter 5.1.1) is owed to the expected application of the GIS based PHP potential assessment procedure.

The large spatial extent of the PHP potential information obtained from the GIS procedure facilitates the planning of large-scale PHP installation projects. Such, yet unprecedented, projects in their planning phase are expected to be subject to economic considerations comparable to projects in other fields of spatially distributed, indirectly evaluated resources. An exemplary analogy from an established field of expertise is the impact of mineral resources estimation for mining projects. Sinclair & Blackwell (2004), in a compilation of references, state that the majority of mining project failures is attributable to resource overestimates. An equivalent overestimation of PHP potential would result in an economically disadvantageous underperformance of PHP installations caused by insufficient hydraulic resources. Typical effects for the PHP user are periodic power losses, less than expected power output, and the need for additional construction measures for

water storage (Maher & Smith, 2001). This leads to user acceptance implications that endanger the sustainability of an installation project. Moreover, overestimates could cause avoidable project overhead cost, e.g. on planning efforts for installation areas that later prove to be unsuitable.

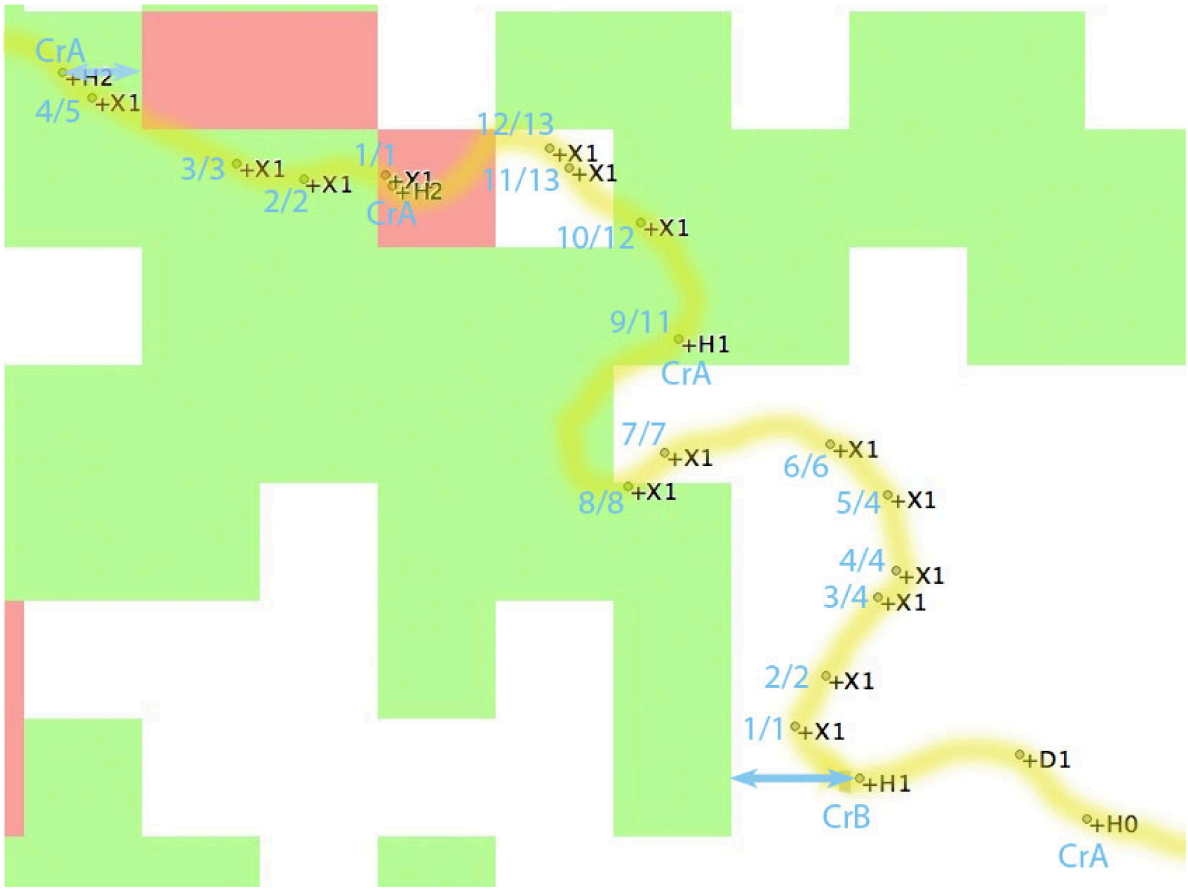

Figure 5-4: Visualization of conformity criteria between attributed PHP potential and GIS assessed PHP potential.

Each waypoint (black) on the observation track (yellow) is analyzed against the GIS assessed value of the underlying PHP unit cells (green, red, and white background raster). Conformity between GIS assessed PHP potential and reference data by the direct PHP potential attribution method is given where PHP potential classification results match:
(1) on the same PHP unit cell (CrA, no arrow),
(2) the adjacent PHP unit cell (CrA, blue arrow to indicate distance),
(3) two PHP unit cells away (CrB, blue arrow to indicate distance).
Conformity between GIS assessed PHP potential and reference data from the stream frequency method is evaluated from the number of stream crossings per traversed PHP unit cell, e.g., "5/4" indicates five stream crossings in four traversed PHP unit cells. The stream count is reset every time an area with different PHP potential classification is entered.

green: PHP unit cells with GIS assessed H1 PHP potential.
red: PHP unit cells with GIS assessed H2 PHP potential.
white: PHP unit cells without PHP potential (GIS assessed H0).
blue: conformity criterion applicable to respective waypoint (CrA and CrB) or series of waypoints (CrC).

Map extent: 10x7.5km, location: W-Central Ecuador.

On the other hand, underestimates of PHP potential may have an impact on the economies of scale of PHP installation projects, particularly when purchasing of PHP equipment is involved. In return-of-investment driven situations, resource underestimates would influence the decision on whether or not a project will be implemented at all. Own experience, gained from small-scale PHP installation projects in several Chinese provinces (Schröder, 2007) suggest that the overall effect caused by a lack of user acceptance towards PHP has a greater detrimental impact on the project implementation than the effects from a somehow incomplete market access caused by a lower utilization factor of the PHP resources would have.

The inherent disadvantage of the conservative estimate approach is therefore an unavoidable, however for PHP application less relevant reduction of control on possible underestimations of PHP potential. This is compensated by an extensive overestimation control, implemented through the control of the range of the input parameters (see chapter 4.2).

In the comparison procedure itself it is necessary to minimize effects from human error: The GIS based PHP potential assessment of each reference area was performed after the respective field-based assessment. This is to avoid any influence from GIS-produced results onto the field-based assessment in the sense of "expecting to find PHP potential in the field at the location the GIS assessment had already predicted it". In the designated sequence of operation – field-based assessment followed by GIS assessment – influence of such kind is not possible as the GIS based PHP potential assessment procedure operates on a fixed set of input data and processing algorithms.

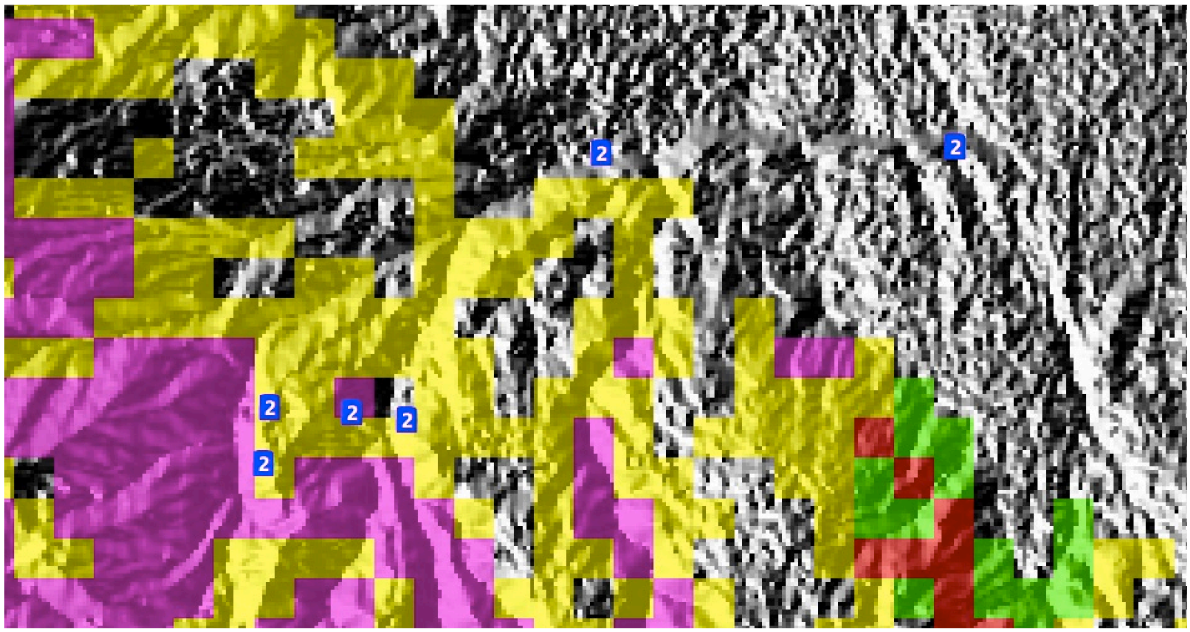

Figure 5-5: Exemplary comparison between GIS assessed data and field assessed reference data obtained by the direct PHP potential attribution method. Conformity between GIS assessed PHP potential and reference data is demonstrated by the four waypoints at lower left and deviation is demonstrated by the two waypoints at upper right.

green: PHP unit cells with H1 PHP potential (GIS assessed).
red: PHP unit cells with H2 PHP potential (GIS assessed).
yellow: H1 with possible pseudokarst influence (GIS assessed).
purple: H2 with possible pseudokarst influence (GIS assessed).
blue: Reference data point with PHP potential class H2, abbreviated as "2".
background: Shaded relief generated from DEM data.
Map extent: approx. 30x15km. Location: E-central Costa Rica, W of Guapiles.

5.2 Results of the PHP potential assessment in the reference areas

5.2.1 Assessment area: Yunnan Province, China

Yunnan Province, roughly 1.2 times the size of Germany, is bordering Burma (Myanmar) to the West, Laos and Vietnam to the South, Guizhou Province and Guangxi Autonomous Region to the East, and Tibet Autonomous Region and Sichuan Province to the North. Although subtropical and tropical by latitude, a mountainous habit with a typical altitude range of 1000-2000m and peaks up to 6700m, situated on a diverse geological background, explains the wide variety of geographical conditions.

A generalized, high head PHP-relevant topography is difficult to define for Yunnan. Most of the overall area has a suitable inclination for high head PHP application. Flat areas are small and isolated. The steepest areas occur at higher elevations in the North and Northwest of the province (Lijiang, Nujiang and Deqen Prefectures).

The climate, depending on latitude and elevation, is tropical to cold with noticeable seasonal temperature variations at the higher subtropical latitudes. Freezing occurs permanently in peak elevations of the highest mountains and seasonal snow cover, an indicator for potential ice induced flow interruptions of streams, occurs in higher elevations above 2500m in the Northwest of Yunnan. Annual total precipitation follows a general trend to higher levels towards the West and the South of Yunnan. The monsoon influences the seasonal distribution of the precipitation, causing a dry period with seasonal flow minima from December to February that coincides with the cold season.

The geology of Yunnan is highly diverse and dominated by sedimentary formations, some with metamorphic overprints. Plutonic and volcanic rock is only exposed in relatively small areas that are mainly found in the Northeast and the West. Cretaceous to recent volcanic rock types with pyroclastic sediments that may involve pseudokarst conditions with possible influence on PHP potential are only found in a single small area in the extreme west of Yunnan (Steinshouer et al., 1999). Carbonate karst occurs extensively in Yunnan and covers about one third of the total area. It is mainly concentrated in the East but also occurs in numerous areas that are distributed over the entire area of Yunnan (Williams & Fong, 2010).

PHP potential assessment results for Yunnan - documentation

The high head PHP potential of Yunnan is predominantly associated with mountainous areas in the Northwest (Nujiang Autonomous Prefecture) and South (Honghe Autonomous Prefecture and Pu'er Prefecture). The most favorable PHP potential is found in the Northwest where peak elevations in excess of 2500m occur. A large portion of the total area of Yunnan has an adequate topography to support high head PHP application. Locally inadequate dry season flow and interspersed carbonate karst areas however often contribute to a GIS calculated PHP potential result that is just below the threshold for H1 PHP potential. This means that high head PHP potential in Yunnan is noticeably more widespread than the results in Figure 5-6 would indicate, yet often at a density of less than one standard unit per 1km^2 unit cell.

Below visualization of the high head PHP potential in Yunnan concentrates on its geographic distribution in respect to topography:

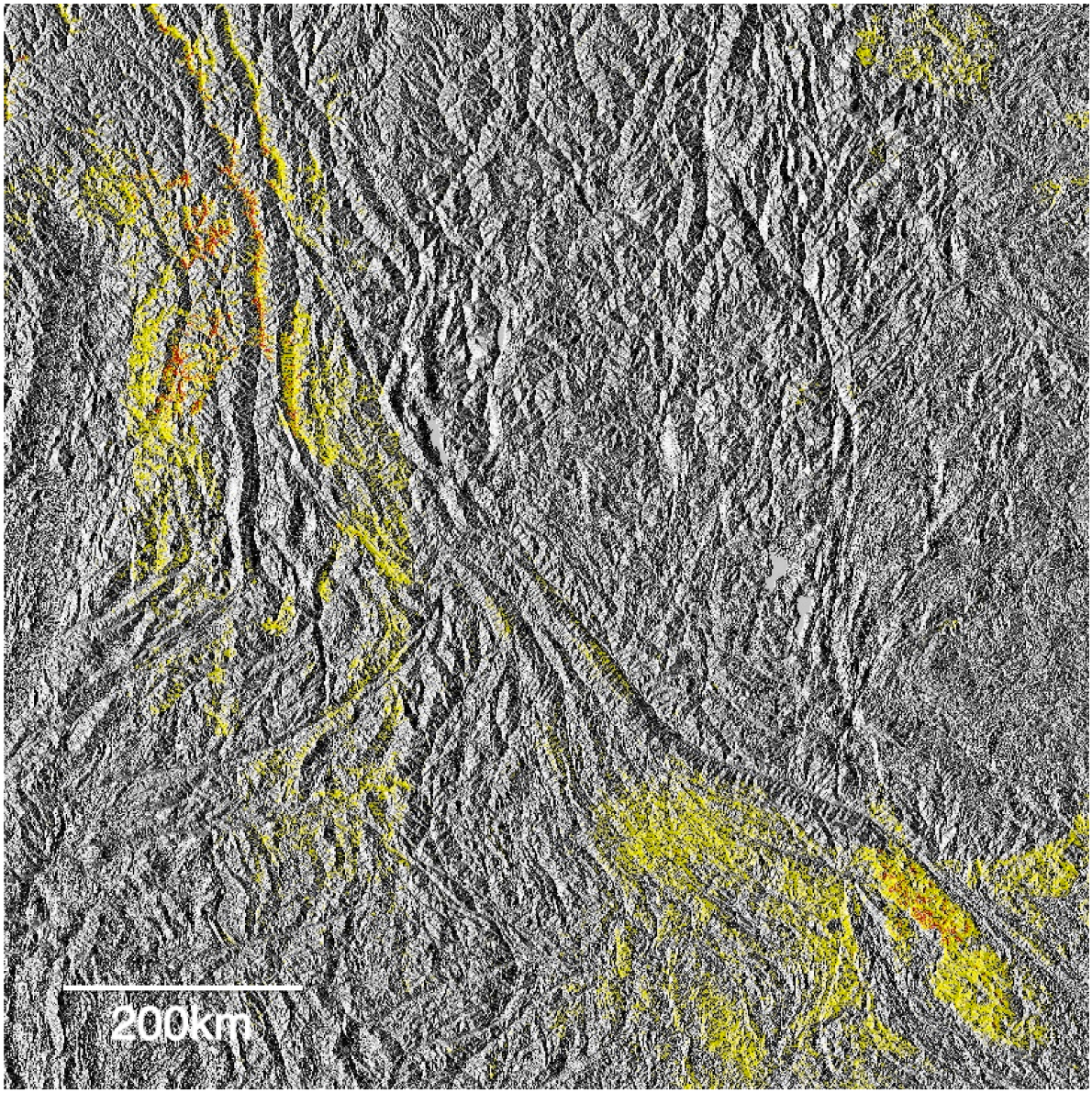

Figure 5-6: The PHP potential of Yunnan and adjacent areas against a shaded relief. Protected areas are not excluded.

PHP potential classes:
yellow: H1
red: H2
potential pseudokarst areas are too small to be resolved at this resolution.

Map extent: approx. 21 to 29 deg N and 97 to 105 deg E (890 x 890km).

Reference data was collected at 790 points along traffic routes across Yunnan. The assessment tracks were chosen according to the prerequisites (see chapter 4.1). Areas without prospective high head PHP potential were therefore not considered for the field-based investigation. This refers for example to the Southeast of Yunnan, which is largely composed of carbonate karst. Focus was laid onto the western two thirds of Yunnan, particularly on areas where transitions in relief, precipitation amount and/or geological background, all with possible influence on high head PHP potential, could be expected. A

preliminary overview about the approximate distribution of relevant areas was already present from previous consultancy work in the rural development sector of Southwestern (Lincang and Honghe Prefectures), and Northwestern (Nujiang Autonomous Prefecture) Yunnan (Schröder, 2005b). All long distance investigation routes were traveled by public bus and railway. Stream frequency recordings were only possible as aggregated stream counts between GPS recorded waypoints due to the slow waypoint recording of the GPS phototagging. For most of the field investigation in Yunnan the direct PHP potential attribution technique was therefore used (see chapter 4.1). Detailed investigations that permitted the individual localization of suitable stream crossings (a combination of both techniques) were conducted by bicycle in the areas around Lijiang City, Jinghong (Xishuangbanna Autonomous Prefecture) and Ruili (Dehong Autonomous Prefecture), as well as on foot at several other locations. Nujiang Autonomous Prefecture, a remote area in Northwestern Yunnan with extensive high head PHP potential, had been deliberately left out in the field investigations due to adequate awareness of the PHP potential situation resulting from previous work (Schröder, 2005a). Other prospective peripheral areas of Yunnan, particularly along the border with Burma/Myanmar in Lincang and Pu'er Prefectures, could not be visited due to difficult accessibility by public transport. The square outline of the investigation area extends into Burma/Myanmar, Lao PDR and Vietnam, which altogether could not be visited for organizational reasons, despite an expected high relevance for PHP potential. The Northern and Eastern margins of the investigation area, belonging to Sichuan and Guizhou Provinces respectively, are less promising for PHP potential. Several reference points are located in Sichuan Province.

Dry season validity of reference data from Yunnan

Figure 5-7 and Figure 5-8 visualize the average precipitation anomaly for January to April 2010 and November 2010 to January 2011 from TRMM 3B43 V7 precipitation data. The time periods are relevant for the two field investigations in Yunnan during March/April 2010 and December 2010/January 2011 (NASA GES DISC, 2009).

Applying the deviation criterion on the January to April 2010 rain rate anomaly map (see Figure 5-7 and chapter 5.1.1) results in deviations from regular dry season conditions for the extreme Northwest of Yunnan and the immediate area around Kunming City. Irregular conditions are colored in shades of brown. They do not overlap with reference points.

Applying the deviation criterion onto the rain rate anomaly map for the time of the Yunnan 2011 field assessment (see Figure 5-8 and chapter 5.1.1) results in deviations from regular dry season conditions for parts of the Northwest (Southern Nujiang Autonomous Prefecture), West (Northern Dehong Autonomous Prefecture), and Southwest (Lincang and Pu'er Prefectures) of Yunnan as well as the Kunming City area. All critical areas show brown coloration and are surrounded by sub-critical anomaly areas (yellow and orange) that altogether cover about a third of the total extent of the investigation area. Implications for the affected reference points are explained in Table 5-2.

In conclusion, an overall "dry season regularity" of the precipitation conditions for the reference points of the 2010 field assessment in Yunnan is given. The 2011 field assessment faces considerably elevated rain rates for approximately 30 percent of the total area. The anomalies exceed critical levels on approximately five percent of the total area. This condition is considered in the attribution validity of the respective reference data points.

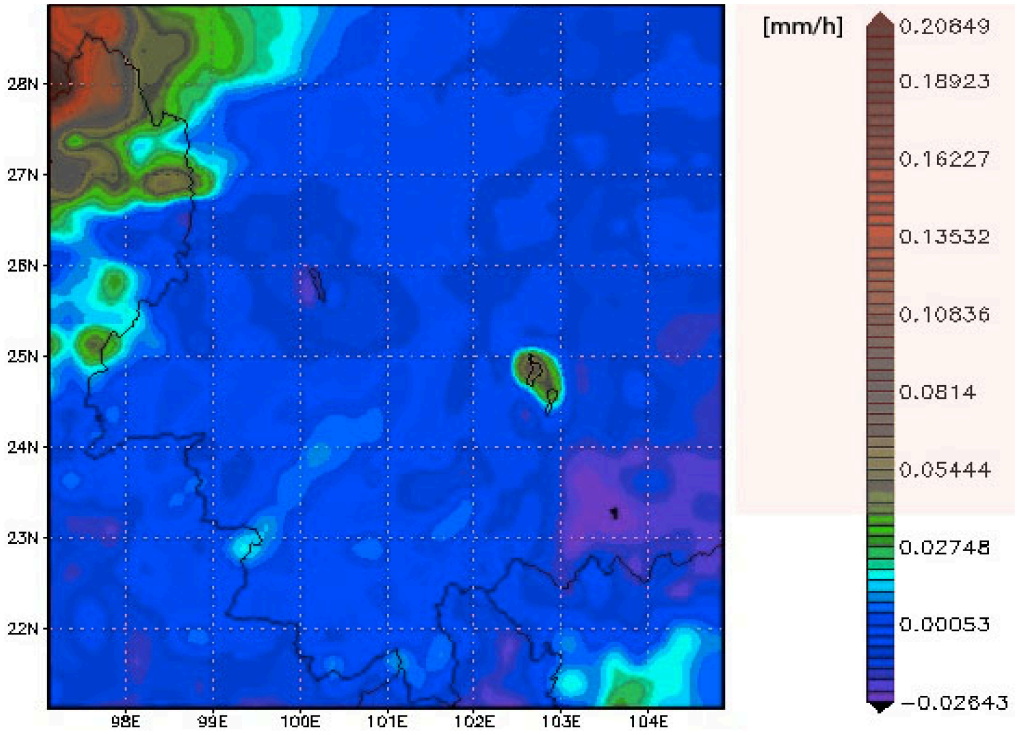

Figure 5-7: TRMM precipitation anomaly analysis for Yunnan and adjacent areas (modified after NASA GES DISC, 2014b). Scaled as mm of average hourly precipitation deviation. Period January to April 2010. The highlighted scale section (pink) corresponds to the areas where the maximum acceptable positive deviation from the average dry season rain rate for reference data is exceeded.

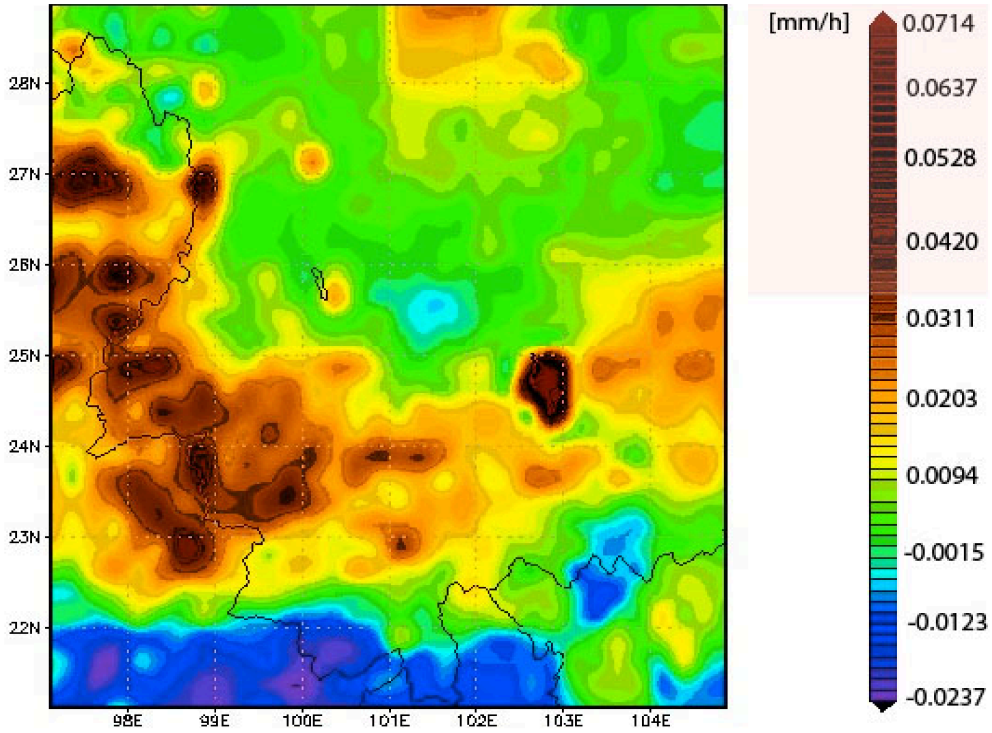

Figure 5-8: TRMM precipitation anomaly analysis for Yunnan and adjacent areas (modified after NASA GES DISC, 2014b). Scaled as mm of average hourly precipitation deviation. Period November 2010 to January 2011. The highlighted scale section (pink) corresponds to the areas where the maximum acceptable positive deviation from the average dry season rain rate for reference data is exceeded.

Attribution validity of reference data from Yunnan Province:

Discrepancies between the GIS based assessment and the two field-based assessments in Yunnan Province are documented in the following tables, separated by year. The separation is necessitated by regional differences in dry season conditions that had to be taken into account individually.

Table 5-1: Areas with discrepancies between the results of the field-based and the GIS-based PHP potential assessment in Yunnan, 2010.

Nr.	Area (center coordinates and typical local altitude)	Deviation from GIS assessment result: type and extent	Deviation attributable to:	Explanation
1	25.33N, 101.00E 2400m	False positive H1 ca. 10x10 cells affected	Field investigation (reference data)	Forested area with insufficient stream density. The overestimate is probably caused by high traveling speed.
2	25.53N, 100.52E 2000m	False positive H2 ca. 10x10 cells affected	Field investigation (reference data)	Forested area with insufficient stream density. The overestimate is probably caused by high traveling speed.
3	25.62N, 100.14E 2400m	False positive H2 ca. 12x12 cells affected	Field investigation (reference data)	Labeled as urban area and moreover as carbonate karst area.
4	25.34N, 99.24E 1900m	False positive H1 and H2 ca. 20x20 cells affected	Unclear, depends on exact karst delineation	Labeled as carbonate karst area.
5	24.82N, 98.77E 1800m	False positive H1 and H2 ca. 20x20 cells affected	Unclear, depends on exact karst delineation	Most of the area is labeled as carbonate karst area. Part of the area is too flat for H2 potential.
6	24.95N, 98.50E 2000m	False positive H2 ca. 35x35 cells affected	Field investigation (reference data)	Forested area with insufficient stream density. Part of the area is moreover too flat for H2 potential. Overestimate is probably caused by high traveling speed and rainfall during observation.
7	24.04N, 97.90E 800m	False positive H1 ca. 3x3 cells affected	Field investigation (reference data)	The area is too flat for H1 potential. Overestimate is probably caused by rainfall during observation.

Continuation of Table 5-1:

8	24.13N, 100.07E 1200m	False positive H1 and H2 ca. 20x20 cells affected	Field investigation (reference data)	The area is in vicinity of H1 areas and below H1 threshold because of insufficient stream density.
9	23.30N, 101.41E 1500m	False positive H1 ca. 20x20 cells affected	Field investigation (reference data)	The area is in vicinity of H1 areas and below H1 threshold because of insufficient stream density. Overestimate is probably caused by high traveling speed.
10	23.23N, 100.90E 1300m	False positive H1 and H2 ca. 30x20 cells affected	Unclear, depends on exact karst delineation	Labeled as carbonate karst area.
11	22.61N, 100.19E 1200m	False positive H1 ca. 10x10 cells affected	Field investigation (reference data)	The area is in vicinity of H1 areas and below H1 threshold because of insufficient stream density.
12	21.28N, 100.67E 1200m	False positive H1 ca. 10x10 cells affected	Field investigation (reference data)	The area is in vicinity of H1 areas and below H1 threshold because of insufficient stream density.
13	22.18N, 100.15E 1100m	False positive H1 and H2 ca. 20x20 cells affected	Field investigation (reference data)	The area is in vicinity of H1 areas and below H1 threshold because of insufficient stream density.

Table 5-2: Areas with discrepancies between the results of the field-based and the GIS-based PHP potential assessment in Yunnan, 2011

Nr.	Area	Deviation from GIS assessment result	Deviation attributable to:	Explanation
1	27.17N, 102.26E 1700m	False positive H1 ca. 30x30 cells affected	Field investigation (reference data)	Parts of the area are labeled as carbonate karst area and parts are too flat. Insufficient stream density.
2	23.69N, 102.00E 1000m	False positive H1 ca. 6x6 cells affected	Field investigation (reference data)	Labeled as carbonate karst area. In vicinity of H1 areas. Rainfall occurred during the field investigation.
3	23.10N, 101.10E 1500m	False positive H1 ca. 15x15 cells affected	Field investigation (reference data)	The area is in vicinity of H1 areas and of carbonate karst areas. Rainfall occurred during the field investigation approaching irregular conditions. The discrepancy is moreover caused by insufficient slope.
4	22.86N, 101.05E 900m	False positive H1 ca. 10x40 cells affected	Field investigation (reference data)	The area is in vicinity of H1 areas. Rainfall occurred during the field investigation with part of the area subject to irregular conditions. The discrepancy is moreover caused by insufficient slope.
5	22.43N, 101.55E 900m	False positive H1 ca. 7x7 cells affected	Field investigation (reference data)	The area is in vicinity of H1 areas. The discrepancy is caused by insufficient slope apparently not obvious in the field investigation.
6	22.05N, 100.80E 800m	False positive H1 ca. 3x3 cells affected	Field investigation (reference data)	Below H1 threshold, mainly because of insufficient stream density. Not obvious in the field investigation.
7	24.18N, 100.04E 1200m	False positive H1 ca. 20x20 cells affected	Field investigation (reference data)	Identical with area 8/2010. The area is in vicinity of H1 areas and below H1 threshold, because of insufficient stream density. Rainfall occurred during the field investigation.

Both field assessments, particularly the 2010 assessment, show considerable deviations from GIS calculated results, based on the final version of 2014 of the GIS based PHP potential assessment procedure. Most deviations can be traced back to an overestimation of PHP potential at the field assessments. In several cases (e.g. 8/2010, 11-13/2010) this can be explained by the still inadequate PHP potential classification definitions of the early development stages of the field assessment methods: PHP potential is undoubtedly present, and represented in the field assessment results, however it does not meet the standard of the PHP potential definitions the GIS based PHP potential assessment is based on. Other cases (e.g. 6,7,9/2010; 3-7/2011) are affected by typical methodical error sources of the early-stage field assessment methods: overestimation of water availability caused by rainy conditions at the moment of the field assessment; overestimation of average terrain inclination and overestimation of stream frequency at high traveling speed with insufficient observation time. Several overestimates of the 2011 field assessment (2,3,4,7/2011) are partially caused by abnormally wet conditions, with precipitation anomaly levels at or above the threshold for irregular dry season conditions (see Figure 5-8). Because of the camera-based slow GPS recording (see chapter 4.1.5) the spatial accuracy of most reference points in Yunnan is low.

Unclear causes for deviations (4,5,10/2010) are most probably related to the geological background. All of these deviations are overestimates of PHP potential that are located within or in close vicinity of areas that are classified as carbonate karst bearing. This indicates once more that the carbonate karst spatial data used in the GIS assessment (Williams & Fong, 2010) is a coarse representation of the extent of carbonate rock outcrop. Partial carbonate coverage tends to be labeled as full carbonate coverage. In areas of complex and small-scale distribution of potentially carbonate bearing rock, evident for large parts of Yunnan (Steinshouer et al., 1999), this may lead to an overly pessimistic PHP potential representation.

In summary, the PHP potential investigation for Yunnan is based on a comparison between data obtained from relatively unrefined and premature field assessment techniques and a more refined, yet conservative estimate from the GIS assessment. The Yunnan field investigations should therefore predominantly be regarded as a test bed for the field assessment methods. Compared to the subsequent investigations in Costa Rica, Ecuador, and Sri Lanka, which used more advanced field assessment methods, the confidence in the field assessment data from Yunnan is low. This is affecting the performance of the verification of the GIS assessed results, however not the quality of the Yunnan results of the GIS based PHP potential assessment itself, since these results are based on the latest version of the GIS assessment technique.

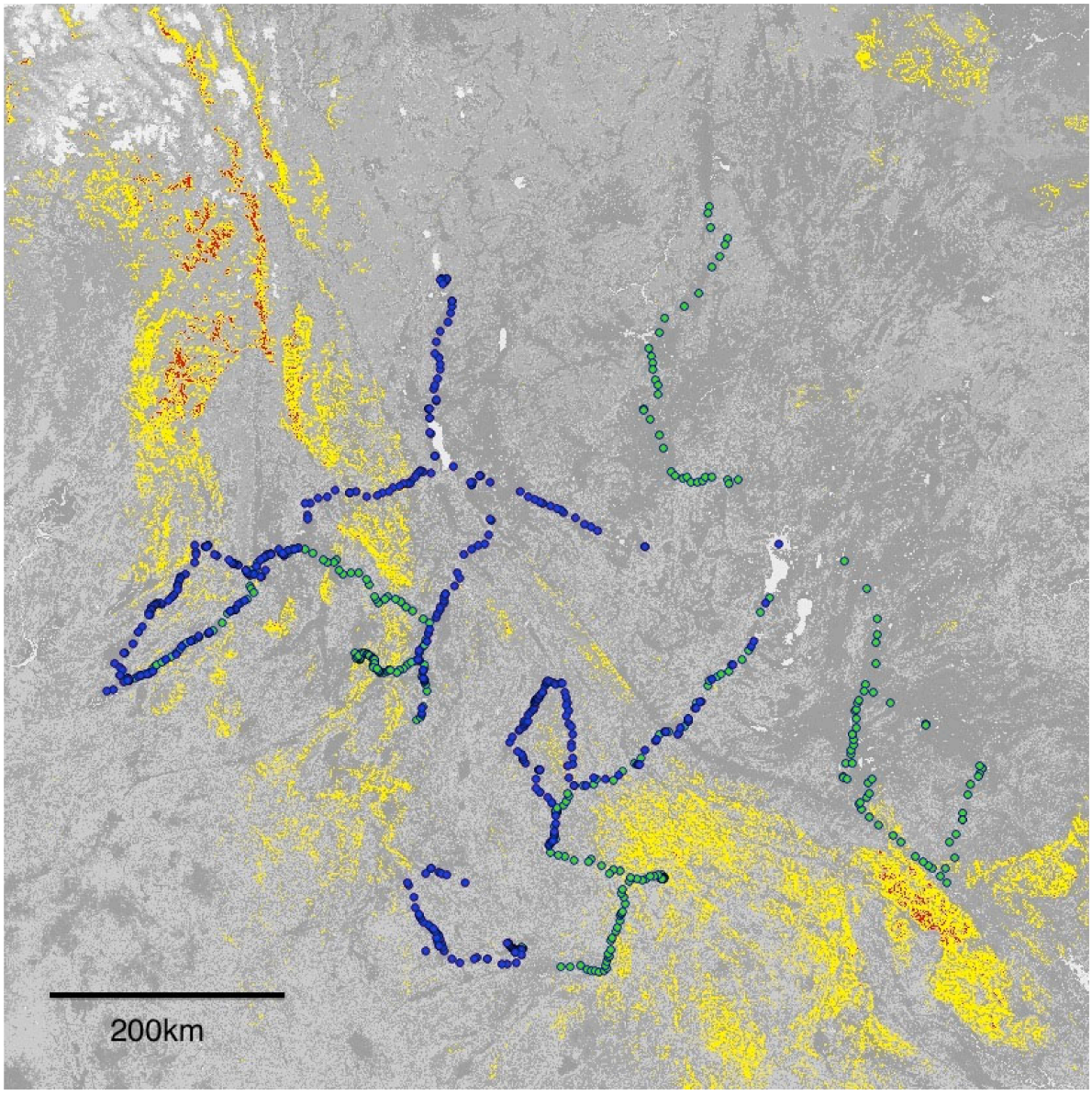

Figure 5-9: Yunnan; Location of reference points from the 2010 and 2011 field assessments; PHP potential by GIS based assessment. Protected areas are not excluded. Background: Globcover land cover map.

PHP potential classes from GIS based assessment:
yellow: H1
red: H2

PHP potential classes from reference data collection:
blue: reference data point, 2010 assessment.
green: reference data point, 2011 assessment.
Information about PHP potential classes of reference data points is not displayable at this resolution.

Map extent: approx. 21 to 29 deg N and 97 to 105 deg E (890 x 890km).

Table 5-3: Summarizing data of the PHP potential assessment results in Yunnan Province, China

Total reference points	790
Reference points with direct potential attribution	573
Reference points with stream crossing	Not resolved
Other reference points without directly usable PHP potential information	217
Excluded for irregular dry season conditions (pre-comparison)	Considered individually (see Table 5-2)
Total PHP unit cells	921600
PHP unit cells without high head PHP potential	873138
PHP unit cells with H1 high head PHP potential	46196
PHP unit cells with H1 high head PHP potential, possibly pseudokarst affected (visual estimate)	100
PHP unit cells with H2 high head PHP potential	2166
PHP unit cells with H2 high head PHP potential, possibly pseudokarst affected	0
Estimated total discrepancy area in vicinity of affected reference points (as PHP unit cells)	6000
Estimated PHP unit cells affected by discrepancies caused by the GIS method	0
Estimated PHP unit cells affected by discrepancies caused by the field assessment	4600
Estimated PHP unit cells affected by discrepancies of unclear origin	1400

5.2.2 Assessment area: Costa Rica

Costa Rica is segmented by a succession of partly overlapping mountain ranges that run along the entire country, roughly parallel to the Pacific coast. The generalized PHP relevant topography comprises of two main slope areas, one towards the Pacific and one towards the Atlantic coast and an extensive mountainous area with intermontane slopes that covers roughly the Southern third of the country (see Figure 5-10).

The climate is tropical with insignificant seasonal temperature variations and no freezing induced flow interruptions even on the highest elevations. The seasonal distribution of the precipitation differs between the Pacific and Atlantic slopes, however has a common minimum in February/March. In a generalizing view it represents the seasonal flow minimum for the entire area of the country.

The geology of Costa Rica is dominated by sedimentary and volcanic formations. Plutonic rock is exposed in the (geologically older) southern mountain range (French & Schenk, 2004). Quaternary to recent volcanic rock types with pyroclastic sediments that may involve pseudokarst conditions could have a detrimental influence for PHP potential. Such formations occur mainly in the central and northwestern mountain range (Cordillera Central) with its active volcanoes. Carbonate karst occurs in relatively small areas near the border to Panama (Williams & Fong, 2010).

PHP potential assessment results for Costa Rica - documentation

The PHP potential of Costa Rica is predominantly located in the mountainous Southeastern third of the country (Cordillera de Talamanca) and extends across the border to Panama. Most of the PHP potential in the Northern two thirds of the country is distributed over the Central and Northwestern mountain range (Cordillera Central), which is of young volcanic origin and therefore a potential pseudokarst area. The Western part of the country (Peninsula de Nicoya and adjacent area) is too dry and in parts too flat to bear PHP potential. The area North of the Cordillera Central, extending into Nicaragua, is too flat to support high head PHP potential beyond small and isolated occurrences.

Below visualization of the PHP potential in Costa Rica concentrates on its geographic distribution in respect to topography:

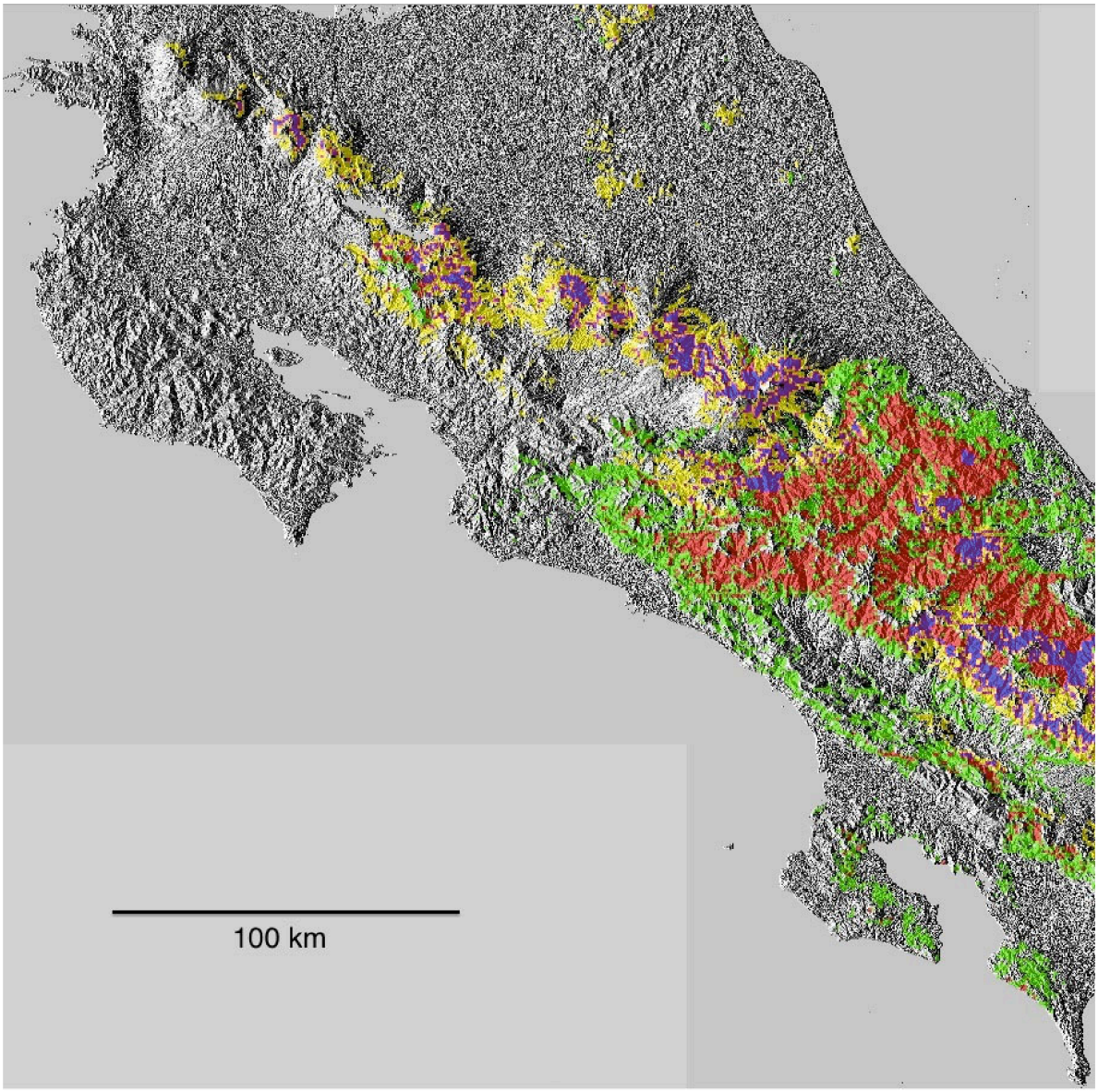

Figure 5-10: The PHP potential of Costa Rica against a shaded relief. Protected areas are not excluded. Map extent: approx. 8 to 11 deg N, and 83 to 86 deg W (330 x 330km).

PHP potential classes:
green: H1
red: H2
yellow: H1 with possible pseudokarst influence.
purple: H2 with possible pseudokarst influence.

Reference data was collected at 336 points along traffic routes across the county. The routes were chosen according to the prerequisites (see chapter 4.1). Areas where high head PHP potential could not be expected were therefore not considered for the field-based investigation. This refers, for example, to the Northeastern lowlands and the dry Northern Pacific coast. The investigative focus concentrated onto the two main cordilleras with particular emphasis on routes that traverse the mountain ranges. All long distance investigation routes were traveled by public bus. Because of the slow waypoint recording of the GPS phototagging stream frequency recordings were only possible in areas with low stream densities. For most of the field investigation in Costa Rica the direct PHP potential attribution method was therefore used (see chapter 4.1). Detailed investigations that permit

the individual localization of suitable stream crossings (a combination of both field methods) were conducted by bicycle in the road sections between La Fortuna and Arenal, Turrialba and Moravia de Chirripó, and the areas South of Monteverde and North of Upala. Most of the expected transitions between H0/H9 and H1/H2 PHP potential - important for the spatial delineation - were traversed during the field investigation. This is confirmed by the GIS assessment. A deficit in field assessment data can be attributed to the far Eastern part of the country, particularly the Northeastern slope of the Cordillera de Talamanca, where areas of carbonate outcrop coincide with natural conditions otherwise favorable for PHP application. This area is largely protected and inaccessible by road.

Attribution validity of reference data from Costa Rica:

Notable discrepancies between GIS based assessment and field assessment in Costa Rica were found in the following areas (see also Figure 5-11):

Table 5-4: Areas with discrepancies between the results of the field-based, and the GIS-based PHP potential assessment in Costa Rica.

Nr.	Area	Deviation from GIS assessment result: type and extent	Deviation attributable to	Explanation
1	W of Guapiles	False positive H2 ca. 15x15 cells affected	Field investigation (reference data)	Insufficient slope that is not obviously noticeable in a field investigation (see Figure 5-5).
2	W of La Fortuna	False positive H2 ca. 20x10 cells affected	Field investigation (reference data)	Insufficient slope that is not obviously noticeable in a field investigation.
3	S of Monteverde	False negative H0 ca. 2x10 cells affected	GIS assessment	Sharp contrast between cloud forest on higher elevations and savanna vegetation at lower elevations of a mountainous area. The streams were observed at “dry” lower elevations, however result from “wet” conditions at higher elevations. This peculiar situation cannot be resolved adequately by the GIS assessment and results here in a fringe of false negative area around a positive PHP potential area.
4	Turrialba-Siquirres	False positive (H2 vs H1/H0) ca. 4x4 cells affected	Field investigation (reference data)	Insufficient slope that is not obviously noticeable in a field investigation

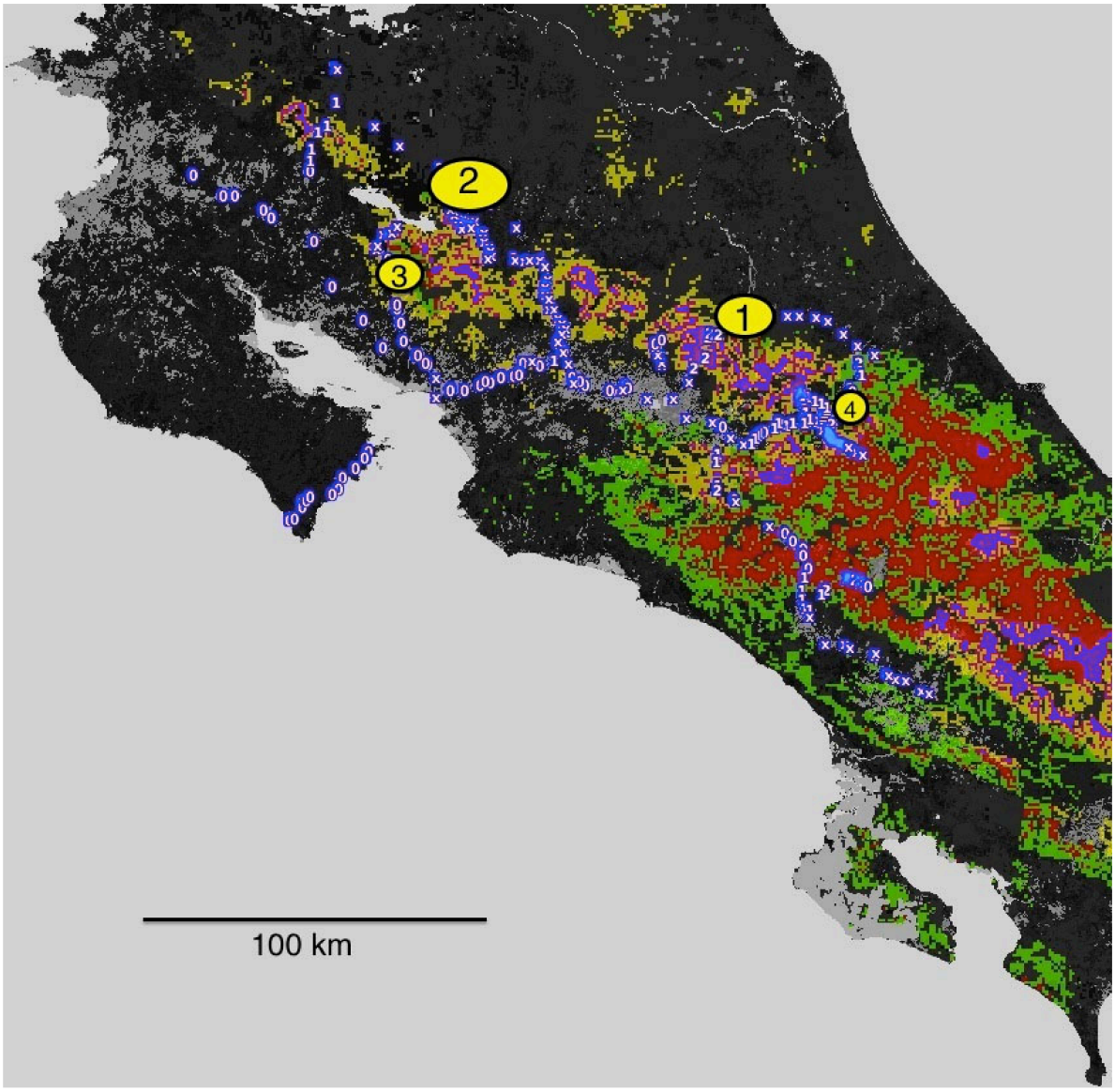

Figure 5-11: Costa Rica; PHP potential by GIS based assessment and field assessment with resulting discrepancy areas. Protected areas are not excluded. Background: Globcover land cover map.

PHP potential classes from GIS based assessment:
green: H1
red: H2
yellow: H1 with possible pseudokarst influence.
purple: H2 with possible pseudokarst influence.

PHP potential classes from reference data collection:
blue dot containing white character: reference data point with PHP potential class (0, 1, 2 representing H0, H1, H2) or stream crossing (x, representing X1).

Discrepancy areas:
yellow ovals: areas with significant PHP potential discrepancies between GIS based assessment and reference data collection, numbered 1-4.

Map extent: approx. 8 to 11 deg N and 83 to 86 deg W (330x330km).

In summary, the PHP potential investigation for Costa Rica shows a high conformity between the field assessed and the GIS assessed PHP potential results. Small, isolated discrepancy areas occur. Three out of four discrepancy areas fulfill all prerequisites for high head PHP potential, except for sufficient slope. This error can be attributed to the field assessment (see chapter 4.1.4). The single remaining discrepancy area reveals a systematic error of the GIS based PHP potential assessment procedure. The underlying cause, an inflow of water (as small streams) into a seasonally dry area, caused by regular precipitation and cloud forest cover at higher altitudes in the immediate vicinity, is assumed to be only capable of affecting small areas. It is therefore not considered to be a significant error for the overall method.

Dry season validity of reference data from Costa Rica

Applying the deviation criterion onto the rain rate anomaly map for Costa Rica (see Figure 5-3 and chapter 5.1.1) results in deviations from regular dry season conditions for the areas of San José and the eastern Península de Nicoya. The resulting doubtful reference data for both of these areas has no effect on the PHP potential analysis, because the contained reference data points do not overlap with GIS calculated PHP potential. In both areas, exclusion factors for PHP potential related to land use (for San José) and precipitation/inclination (for the Peninsula de Nicoya) apply.

In conclusion, the overall “dry season regularity” for the precipitation conditions in Costa Rica between January and March 2011 in respect to PHP potential assessment is given.

Table 5-5: Summarizing data of the PHP potential assessment results in Costa Rica

Total reference points	336
Reference points with direct potential attribution	226
Reference points with stream crossing	73
Other reference points without directly usable PHP potential information	37
Excluded for irregular dry season conditions (pre-comparison)	0
Total PHP unit cells	64405
PHP unit cells without high head PHP potential	47385
PHP unit cells with H1 high head PHP potential	6044
PHP unit cells with H1 high head PHP potential, possibly pseudokarst affected	4222
PHP unit cells with H2 high head PHP potential	4475
PHP unit cells with H2 high head PHP potential, possibly pseudokarst affected	2279
Estimated total discrepancy area in vicinity of affected reference points (as PHP unit cells)	460
Estimated PHP unit cells affected by discrepancies caused by the GIS assessment	20
Estimated PHP unit cells affected by discrepancies caused by the field assessment	440
Estimated PHP unit cells affected by discrepancies of unknown origin	0

5.2.3 Assessment area: Ecuador

Ecuador is divided by two parallel N-S trending cordilleras that include both active and inactive volcanic peaks of 3500m to 6300m elevation. In between these mountain ranges is a less precipitous highland area with typical elevations between 2000m and 3500m. To the West, the Andean highland gives way to coastal lowlands that include a coastal mountain range with elevations to 800m. The Eastern third of the county is relatively flat. It marks the westernmost extension of the Amazon basin.

The generalized high head PHP relevant topography comprises of two main slope areas, one between the Western cordillera (Cordillera Occidental) and the coast, and one between the Eastern cordillera (Cordillera Central) and the Amazon lowlands. Between the cordilleras and along the coast are extensive mountainous areas with intermontane slopes. These mountainous areas, covering about a third of the country (see Figure 5-12), are topographically prospective areas for high head PHP potential.

The climate is, depending on the elevation, warm tropical to cold with generally insignificant seasonal temperature variations due to the low latitude. Freezing occurs in peak elevations, however without seasonal ice induced flow interruptions of streams. The absolute amount of precipitation strongly differs between the regions. This, in combination with the considerable altitude differences, leads to a wide spectrum of climatic zones and vegetation types, ranging from desert to rainforest. For many areas of Ecuador, the seasonal distribution of the precipitation (in both dry and wet zones) is not very pronounced. PHP relevant areas that are subject to strong precipitation seasonality are mainly located in the Northwest of Ecuador where seasonal flow minima can be expected in November and December.

The geology of Ecuador is dominated by sedimentary and volcanic formations. Plutonic rock is only exposed at the Eastern rim of the central mountain range system. Cretaceous to recent volcanic rock types with pyroclastic sediments that may involve pseudokarst conditions could have a detrimental influence for PHP potential. These formations (see Figure 4-27) comprise most of the intermontane highland area and of the eastern cordillera (Schenk et al., 1999). Carbonate karst occurs in the lowland areas of Northern and Central Ecuador, immediately East of the cordilleras, and moreover extends into the mountain range in Southern Ecuador (Williams & Fong, 2010).

PHP potential assessment results for Ecuador - documentation

The high head PHP potential of Ecuador is predominantly associated with the transition zones between the main topographical units of Ecuador: the coastal lowland, Andean highland and Amazon lowland. In the Western transition zone, which is roughly identical with the Western slope of the Cordillera Occidental, the PHP potential is strongly influenced by the N-S gradient of the annual precipitation caused by the warm equatorial ocean current in the North and the cold Humboldt current in the South coast of Ecuador. The Eastern transition zone (Eastern slope of the Cordillera Central) has a precipitation maximum in the Central part that causes exceptional PHP potential in the more inclined parts of that area and even noticeable potential in relatively flat foothill areas. The generally prospective high head PHP potential of the Eastern transition zone is only interrupted by several occurrences of carbonate karst in its Southern half and a section of potentially pseudokarst bearing young volcanic rock in the North. The Central and South coast areas (Manabí, Los Ríos and Guayas provinces) are too flat (Rio Guayas basin) or too dry (Cordillera de Colonche) to support high head PHP potential. The Amazon lowlands (Sucumbíos, Orellana and Pastáza provinces) lack suitable topography for high head PHP potential. Except for the far North, the highland area between the two main cordilleras has relatively poor and scattered high

head PHP potential. Depending on the location this can be attributed to land use (urban areas), insufficient precipitation, or flat topography. Moreover, most of this area is of young volcanic origin. The isolated occurrences of PHP potential are therefore under possible pseudokarst influence.

Below visualization of the high head PHP potential in Ecuador concentrates on its geographic distribution in respect to topography:

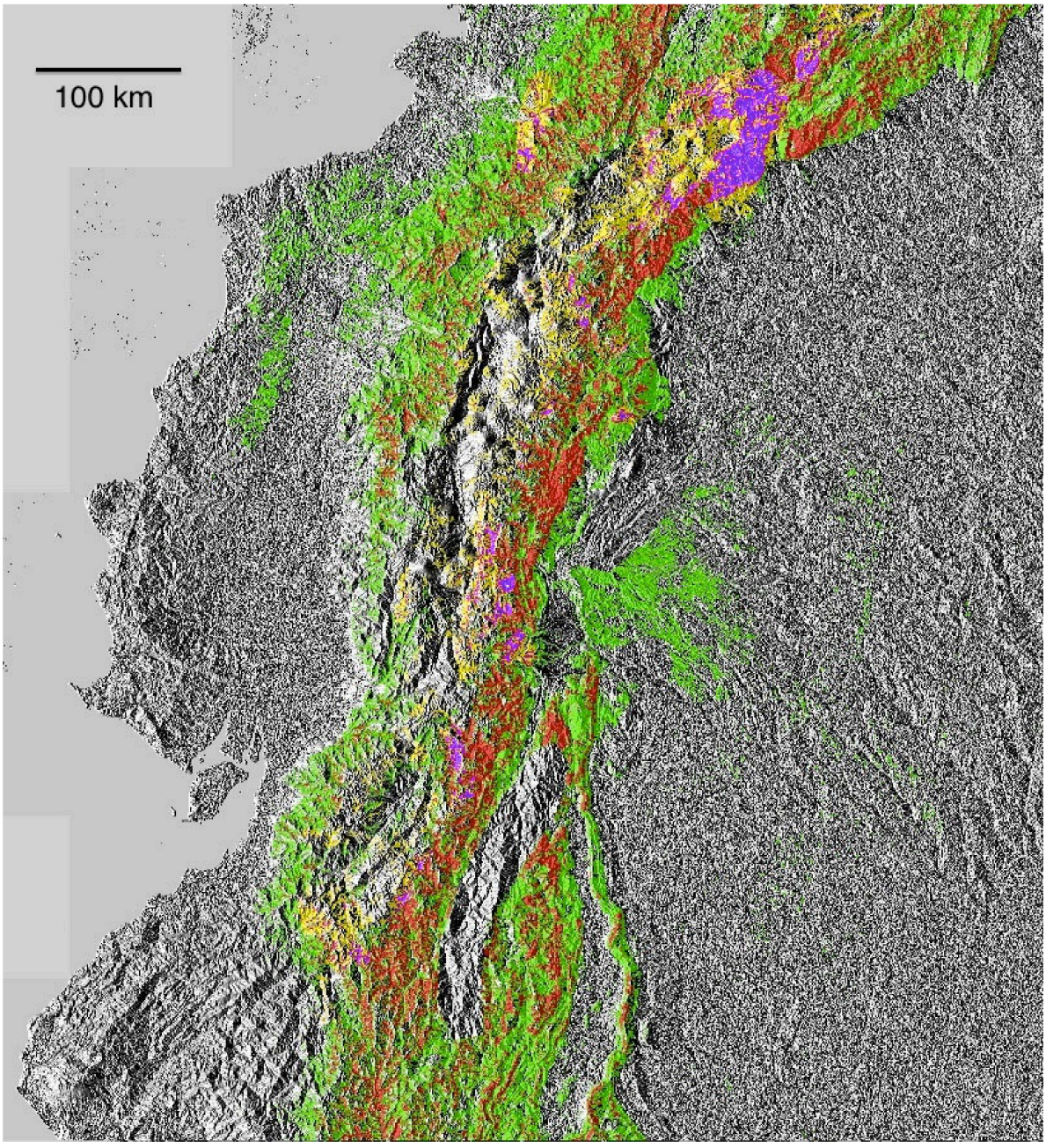

Figure 5-12: The PHP potential of Ecuador and adjacent areas against a shaded relief. Protected areas are not excluded. Map extent: approx. 5 deg S to 2 deg N, and 75 to 82 deg W (780 x 780km).

PHP potential classes:
green: H1
red: H2
yellow: H1 with possible pseudokarst influence.
purple: H2 with possible pseudokarst influence.

Reference data was collected at 1065 points along traffic routes across the county. The routes were chosen according to the prerequisites set forth in chapter 4.1 . Areas where high head PHP potential could not be expected were therefore not considered for the field investigation. This refers, for example, to the Amazon lowlands and the dry Southern coast. Focus was put onto the two main cordilleras with particular emphasis on routes that traverse these mountain ranges. All long distance investigation routes were traveled by public bus. Stream frequency recordings were taken on all routes and, particularly at apparent transition points between PHP potential classes, supplemented by direct PHP potential attribution. Detailed investigations, permitting a more thorough evaluation of the individual stream suitability, were conducted by bicycle in the road section between Baños and Puyo (Tungurahua/Napo provinces) and on foot in the García Moreno area, Imbabura Province. Most of the expected transitions between H0/H9 and H1/H2 PHP potential - important for the spatial delineation - were traversed during the field investigation. This is confirmed by the GIS assessment. A deficit in field assessment data can be attributed to the far North and the far South of the country, here particularly the area between Loja and Machála. Both areas could not be visited for time constraints.

Dry season validity of reference data from Ecuador

The map in Figure 5-13 visualizes the average precipitation anomaly for October to December 2011 from TRMM 3B43 V7 precipitation data, the time period relevant for the field investigation in Ecuador, conducted November to December 2011 (NASA GES DISC, 2009).

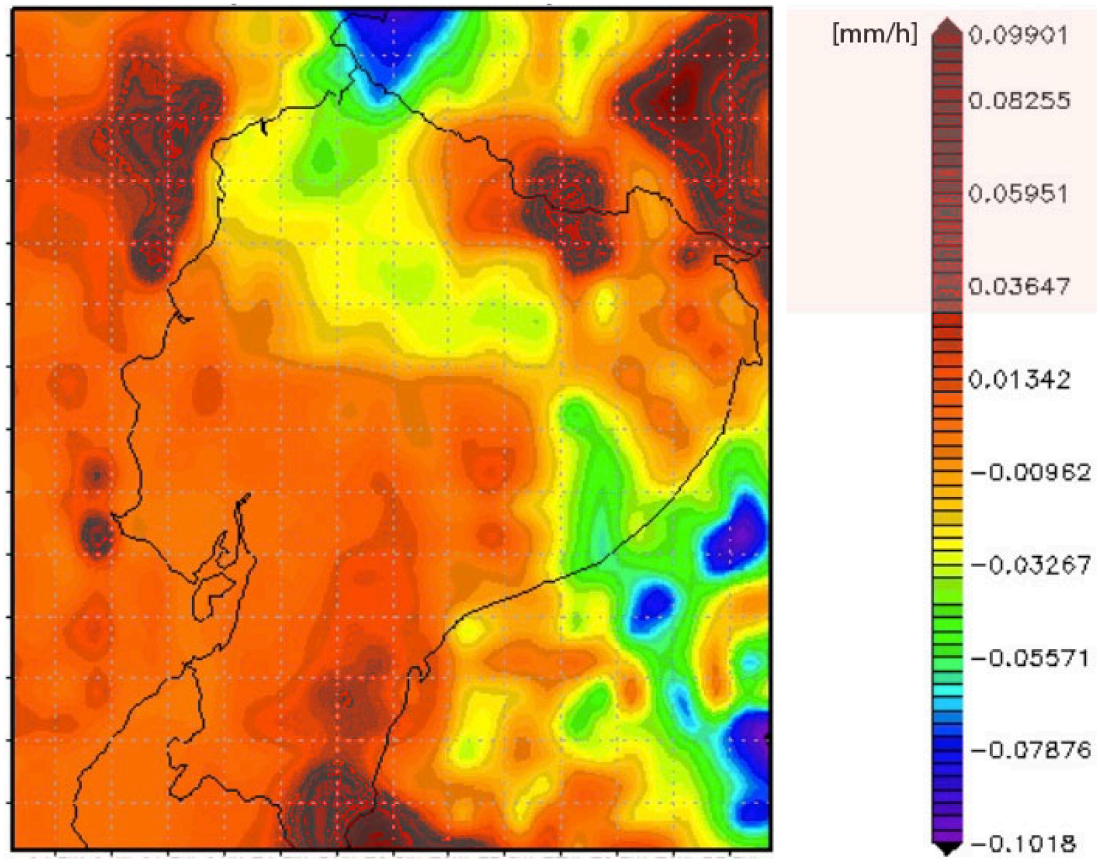

Figure 5-13: TRMM precipitation anomaly analysis for Ecuador, October to December 2011 (modified after NASA GES DISC, 2014b). Scaled as mm of average hourly precipitation deviation (average for the period October to December 2011). Map extent: 5 deg S to 2 deg N and 75 to 82 deg W (780 x 780km).

Applying the deviation criterion onto the rain rate anomaly map for Ecuador (see Figure 5-13 and chapter 5.1.1) results in deviations from regular dry season conditions for the southernmost extension of the Andean highland area (Zamóra Chinchípe province and extending across the border to Peru), as well as the Western part of Sucumbíos province in the Northeast of Ecuador extending into Colombia (dark brown to black color). Both areas were not visited and contain therefore no reference points.

In conclusion, there is an overall "dry season regularity" in respect to PHP potential assessment for the precipitation conditions in Ecuador between October and December 2011. Elevated, yet still regular, precipitation rates apply for the Southernmost reference points (Azuay and Moróna Santiago provinces).

Attribution validity of reference data from Ecuador:

Notable discrepancies between the results of GIS-based assessment and field assessment were found in the following areas of Ecuador (see also Figure 5-14):

Table 5-6: Areas with discrepancies between the results of the field-based and the GIS-based PHP potential assessment in Ecuador.

Nr.	Area	Deviation from GIS assessment result (type)	Deviation attributable to:	Explanation
1	0.33S, 78.21W 4000m alt. Cayambe Coca Reserve	False positive H1. Ca. 7x7 cells affected.	Field investigation (reference data)	High altitude grassland (Paramo vegetation). Locally too few suitable streams, despite frequent very small streams. The area is possibly affected by pseudokarst.
2	0.95S, 78.85W 3400m alt. Zumbahua-Pujilí	False positive H1. Ca. 3x3 cells affected.	Field investigation (reference data)	High altitude grassland (Paramo vegetation). Locally too few streams. The area is possibly affected by pseudokarst.
3	1.10S, 77.80W 500m alt. S of Tena, at Rio Napo	False negative H9. Ca. 5x5 cells affected.	Field investigation (reference data)	Relatively flat area with dense vegetation. The only just adequate inclination is augmented by very high precipitation to qualify for H1 PHP potential.
4	1.50S, 78.05W 1000m alt. Shell-Puyo	False positive H2. Ca. 3x3 cells affected.	Field investigation (reference data)	Relatively flat area with dense vegetation and locally high stream frequency. The only just adequate inclination is augmented by very high precipitation to qualify for H1 PHP potential.
5	1.40S, 78.43W 1900m alt. W of Baños	False negative H0. 1 cell affected.	Unclear	Very steep area in direct vicinity to an active volcano. Pyroclastic material with high probability of supporting pseudokarst conditions is prevalent. Dense vegetation.

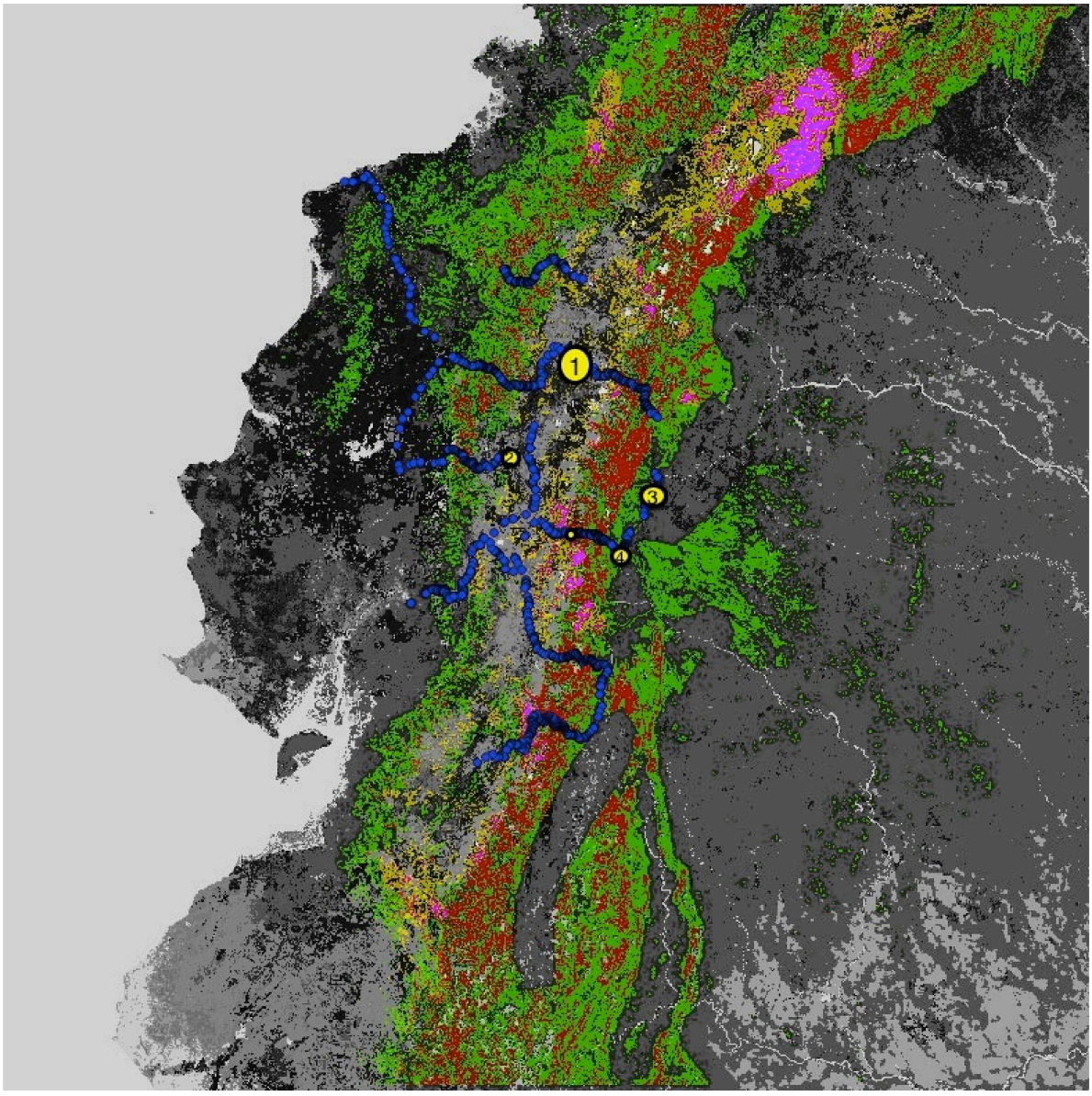

Figure 5-14: Ecuador; PHP potential by GIS based assessment and field assessment with resulting discrepancy areas. Protected areas are not excluded. Background: Globcover land cover map.

PHP potential classes from GIS based assessment:
green: H1
red: H2
yellow: H1 with possible pseudokarst influence.
purple: H2 with possible pseudokarst influence.

PHP potential classes from reference data collection (field assessment):
blue: data point location (data content cannot be displayed at this resolution).

Discrepancy areas:
yellow ovals: areas with significant PHP potential discrepancies between GIS based assessment and field assessment, numbered 1-5.

Map extent: approx. 5 deg S to 2 deg N, and 75 to 82 deg W (780 x 780km).

In summary, the PHP potential investigation for Ecuador shows a high conformity between the field-assessed and the GIS-assessed PHP potential results. Small and isolated discrepancy areas occur. Two out of five discrepancy areas fulfill all prerequisites for high head PHP potential, except for sufficient slope. This error can be attributed to the field assessment (see chapter 4.1.4). The remaining three discrepancy areas are associated with recent volcanism, which classifies them as possibly pseudokarst-affected areas. Two out of the three areas are at high altitude, with insufficient precipitation to support PHP potential. The false positive result of the field assessment is provoked by numerous very small streams that are quite prominent because of the low vegetation at this altitude. The fifth discrepancy area is very small, yet difficult to characterize. The immediate vicinity to an active volcanic crater causes extreme conditions on steepness, drainage and vegetation cover that prevent a reliable PHP potential attribution.

Table 5-7: Summarizing data of the PHP potential assessment results in Ecuador.

Total reference points	1065
Reference points with direct attribution of PHP potential	218
Reference points with stream crossing	708
Other reference points without directly usable PHP potential information	139
Excluded for irregular dry season conditions (pre-comparison)	0
Total PHP unit cells	536214
PHP unit cells without high head PHP potential	409905
PHP unit cells with H1 high head PHP potential	75531
PHP unit cells with H1 high head PHP potential, possibly pseudokarst affected	13690
PHP unit cells with H2 high head PHP potential	30874
PHP unit cells with H2 high head PHP potential, possibly pseudokarst affected	6214
Estimated total discrepancy area in vicinity of affected reference points (as PHP unit cells)	96
Estimated PHP unit cells affected by discrepancies caused by the GIS method	0
Estimated PHP unit cells affected by discrepancies caused by the field assessment	95
Estimated PHP unit cells affected by discrepancies of unknown origin	1

5.2.4 Assessment area: Sri Lanka

Sri Lanka is a drop-shaped island with extensive lowland areas that cover the entire coastal region and the Northern half of the island. The Southern half has a central highland area with elevations to 2500m.

The generalized high head PHP relevant topography is limited to the central highland area and the surrounding transition zone to the lowland area. These areas altogether cover about one fourth of the country (see Figure 5-15).

The climate**,** depending on the elevation, is warm tropical to temperate with, due to the low latitude, generally insignificant seasonal temperature variations. Freezing only occurs as a rare phenomenon at peak elevations and has no significance for streamflow. The absolute amount of precipitation greatly differs between the regions. The highest yearly precipitation levels, sustaining tropical rainforest and rain-fed cropland, are found in the mountainous areas of Southwestern Sri Lanka that are exposed to the Southwest monsoon. Here, the seasonal flow minima can be expected in January and February. The drier North and East of the country, typically with savanna vegetation and irrigated cropland, is exposed to the Northeast monsoon, with precipitation maxima from November to March and expected seasonal flow minima in May and June. The prospective PHP-relevant areas are mainly exposed to the Southwest monsoon. The field investigation was therefore conducted during the dry season of Southwestern Sri Lanka.

The geology of Sri Lanka is dominated by Precambrian formations with various metamorphic overprints. Sedimentary rock, of which some is exhibiting carbonate karst features (Williams & Fong, 2010), is only exposed at Northern and Eastern coastal and lowland areas. Pyroclastic sediments, as possible hosts for pseudokarst conditions, are absent (Wandrey & Law, 1999).

PHP potential assessment results for Sri Lanka – documentation

The area with the most extensive PHP potential of Sri Lanka roughly matches the extent of the central highland area. In addition, the Southwestern foothills of the central highland area (Sabaragamuwa Province) feature somewhat less extensive PHP potential that nearly reaches the coast at the Southernmost tip of Sri Lanka. The Eastern and Northern foothills of the central highland area show limited PHP potential. The remaining three quarters of the island of Sri Lanka are either too flat or too dry to qualify for PHP potential. Additional factors for the absence of PHP potential include karst and land use (urban area), however are confined to relatively small areas along the West coast.

Below visualization of the PHP potential in Sri Lanka concentrates on its geographic distribution in respect to topography:

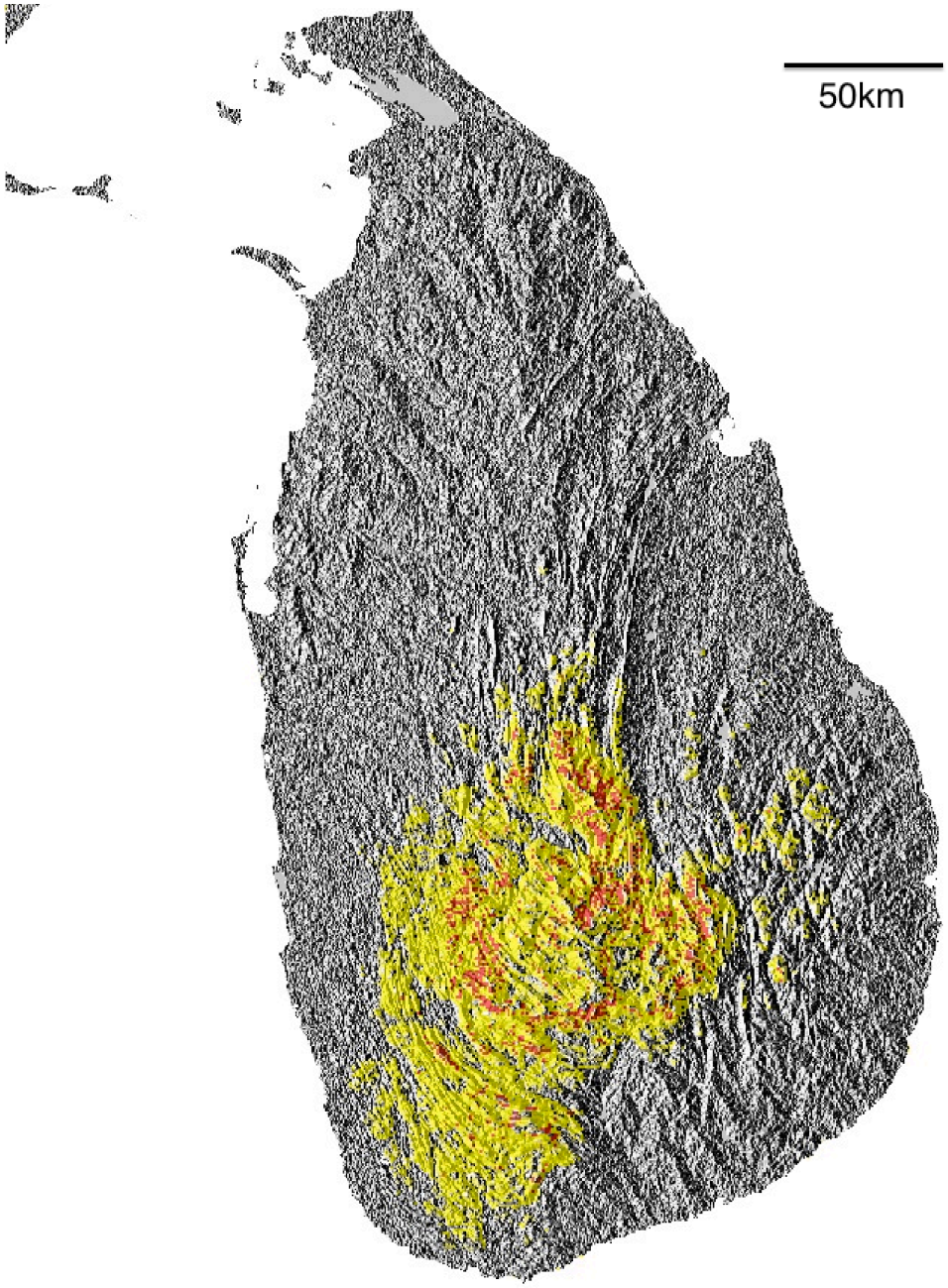

Figure 5-15: The PHP potential of Sri Lanka against a shaded relief. Protected areas are not excluded.
PHP potential classes from GIS based assessment:
yellow: H1
red: H2
Map extent: approx. 5 to 10 deg N, and 79 to 83 deg E (440 x 550km).

Reference data was collected at 768 points along traffic routes across the country. The routes were chosen according to the prerequisites (see chapter 4.1). Areas where high head PHP potential could not be expected were therefore not considered for the field investigation. This refers to all coastal areas and the entire Northern half of Sri Lanka. Focus was put on the Southwest-monsoon-affected section of the Central highland, with particular emphasis on routes that connect highland and lowland areas. Long-distance investigation routes were traveled by public bus or train. Stream frequency recordings were taken on all routes and supplemented by direct PHP potential attribution, particularly at apparent

transition points between PHP potential classes. Detailed investigations that permit a more thorough evaluation of the individual stream suitability were conducted on foot in the areas around Haputale and Ella (Uva Province), Nuwara Eliya (Central Province), and by bicycle in the Ratnapura area (Sabaragamuwa Province). Important for the spatial delineation, most of the expected transitions between H0/H9 and H1/H2 PHP potential were traversed during the field investigation. This is confirmed by the GIS assessment. Additional reference data would be advantageous from the area east of Matale (Central Province), marking the Northeastern border of the area with PHP potential, and the region Southwest of Ratnapura (Sabaragamuwa Province), the Southernmost extension of the area with PHP potential. Both areas largely have protected status and could not be visited for time restrictions. Moreover, the Northeastern border of the area with PHP potential would not have been in the dry season at the time of the field assessment.

Dry season validity of reference data from Sri Lanka

The map in Figure 5-16 visualizes the average precipitation anomaly from TRMM 3B43 V7 precipitation data for December 2011 to February 2012, the time period relevant for the field investigation in Sri Lanka in February 2012 (NASA GES DISC, 2009).

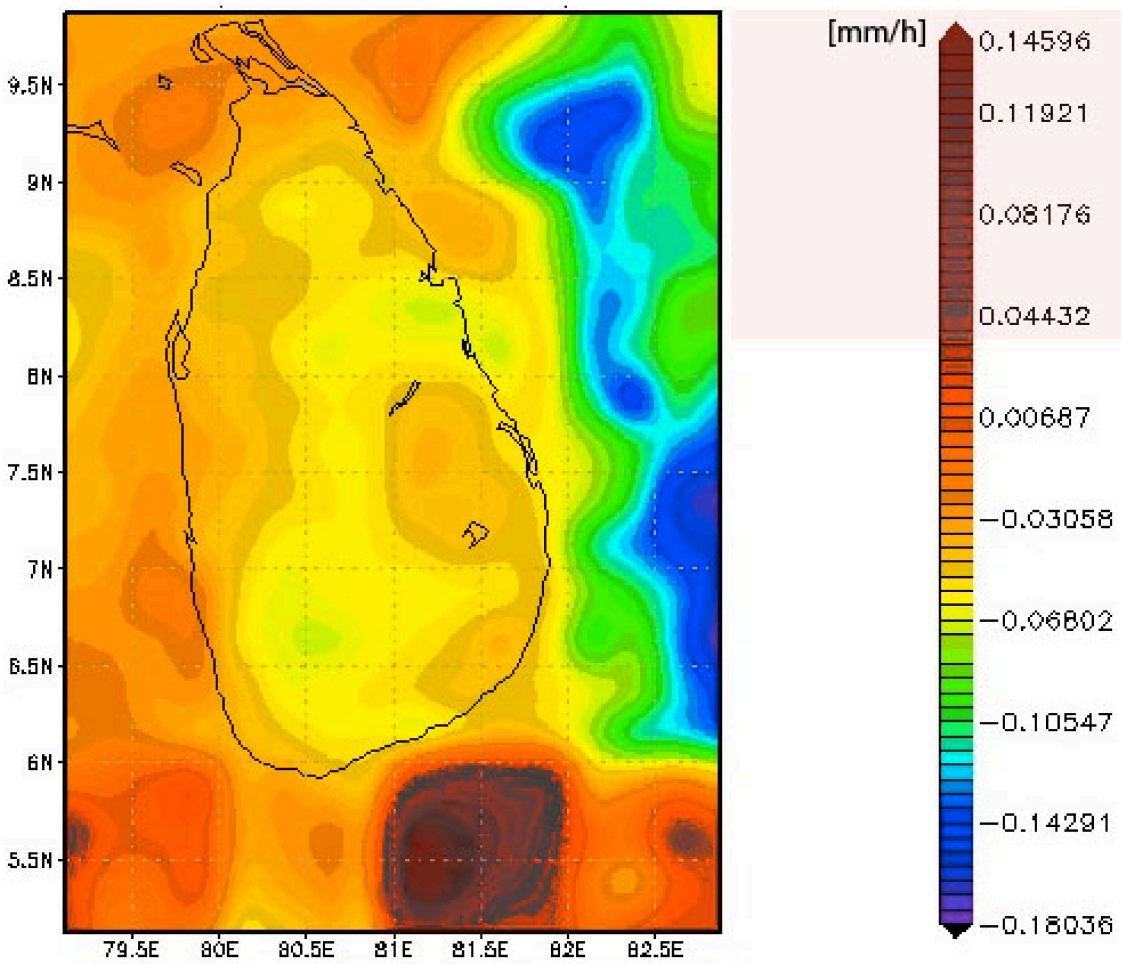

Figure 5-16: TRMM precipitation anomaly analysis for Sri Lanka, December 2011 to February 2012 (modified after NASA GES DISC, 2014b).

Scale: mm of average hourly precipitation deviation for the period December 2011 to February 2012.
Map extent: 5 to 10 deg N, 79 to 83 deg E (440 x 550km).

The weather conditions in Sri Lanka were generally drier than normal during the time of the field investigation and the two preceding months. Applying the deviation criterion on the rain rate anomaly map for Sri Lanka (see Figure 5-16 and chapter 5.1.1) results in an overall "dry season regularity" in respect to PHP potential assessment for the precipitation conditions in Sri Lanka between December 2011 and February 2012. There are hints of PHP potential underestimation from the GIS assessment results of Southeastern Sri Lanka (see Table 5-8, discrepancy area No. 3). This is acceptable under the overall conservative-estimate-approach of this study, however partially counteracted by the fact that the visit to this area, which is under the influence of the Northeastern monsoon, did not take place during the typical dry season months.

Attribution validity of reference data from Sri Lanka:

Notable discrepancies between GIS based assessment and field assessment in Sri Lanka were found in the following areas (see also Figure 5-17):

Table 5-8: Areas with discrepancies between the results of the field-based and the GIS-based PHP potential assessment in Sri Lanka.

Nr.	Area	Deviation from GIS assessment result (type)	Deviation attributable to:	Explanation
1	7.33N, 80.63E 440m alt.	False positive H1; ca. 5x5 cells affected.	Field investigation (reference data)	Insufficient inclination, not obviously noticeable in a field investigation.
2	7.35N, 80.95E 100m alt.	False positive H1; ca. 4x4 cells affected.	Field investigation (reference data)	Locally too few suitable streams.
3	7.11N, 81.05E 380m alt.	False negative H0; ca. 3x3 cells affected.	GIS assessment	Locally too few suitable streams (two out of three streams dry); Possibly caused by drier than normal conditions (-0.05mm/h; see Figure 5-16)
4	6.79N, 81.10E 220m alt.	False positive H1 ca. 4x4 cells affected (N of reference point).	Field investigation (reference data)	Locally too few suitable streams and insufficient inclination.
5	6.95N, 81.03E 790m alt.	False positive H2 vs. H1; ca. 2x2 cells affected.	Field investigation (reference data)	Probably insufficient streams for H2 potential.
6	6.93N, 80.98E 1200m alt	False positive H2 vs. H1; ca. 4x4 cells affected.	Field investigation (reference data)	Locally too few suitable streams. Proximity to peak area.
7	6.70N, 80.92E 1000m alt.	False positive H2 vs. H1; ca. 4x5 cells affected.	Field investigation (reference data)	Barely sufficient streams for H2 potential. Proximity to peak areas may not be evident from ground perspective.

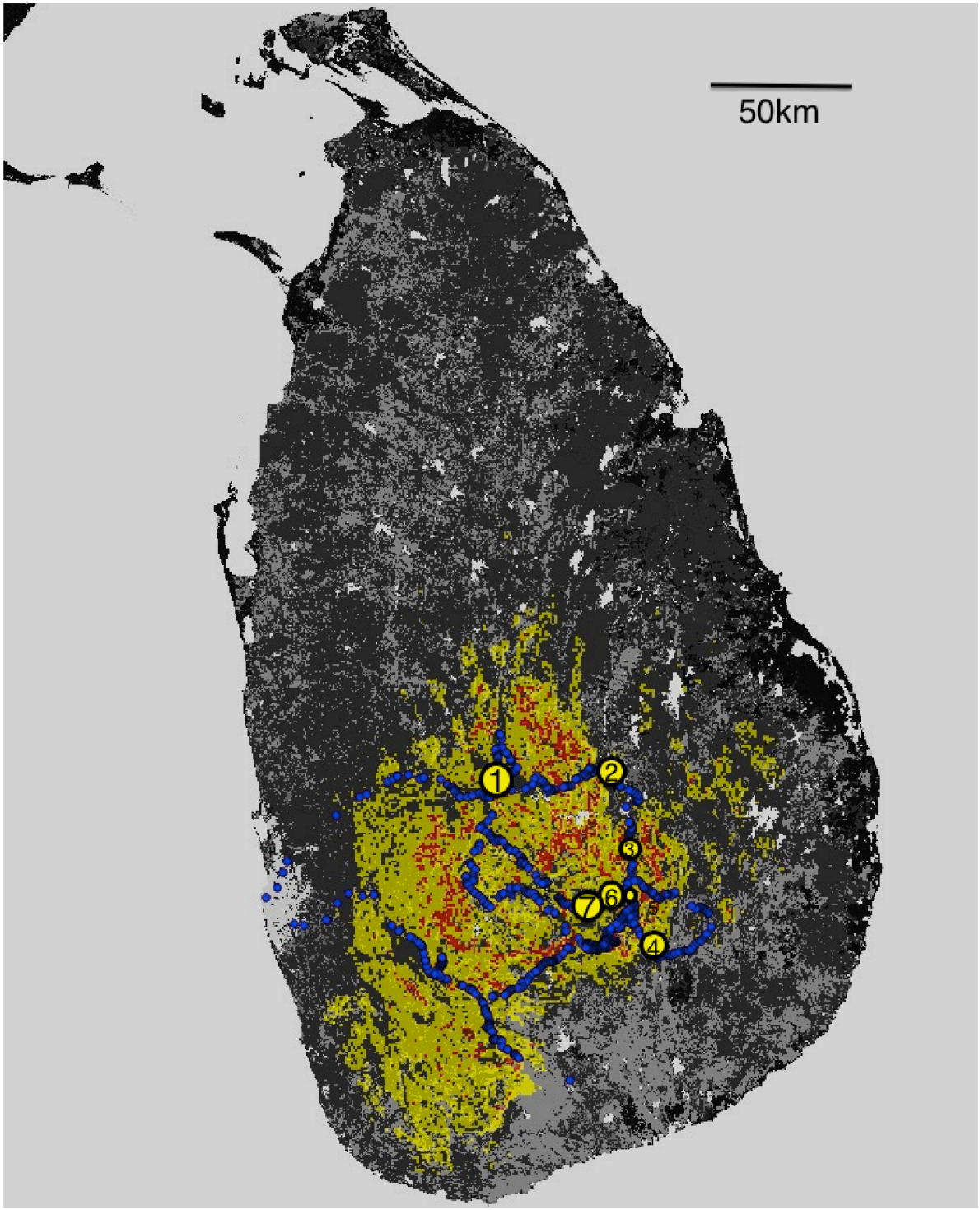

Figure 5-17: Sri Lanka; PHP potential by GIS based assessment and reference data collection with resulting discrepancy areas. Protected areas are not excluded. Background: Globcover land cover. Map extent: approx. 5 to 10 deg N and 79 to 83 deg E (440 x 550km).
PHP potential classes from GIS based assessment:
yellow: H1;
red: H2
PHP potential classes from reference data collection:
blue: data point location (data content cannot be displayed at this resolution).
Discrepancy areas:
yellow circles: areas with significant PHP potential discrepancies, between GIS based assessment and reference data collection, numbered 1-7.

In summary, the PHP potential investigation for Sri Lanka shows a high conformity between the field-assessed, and the GIS-assessed PHP potential results. Areas with differing results (discrepancy areas) are small and isolated. The effect from the underlying error cause of one of the seven discrepancy areas on the integrity of the GIS based assessment remains unclear. Here, H1 PHP potential was determined in the GIS assessment, however the field observation revealed that two out of three streams were dry and therefore unsuitable, despite of the fact that the investigation in this area may not even have been in the driest season due to a possible influence of the Northeast monsoon. The other six discrepancy areas result from false positive field assessment results that originate from overestimates of either terrain inclination or stream frequency. Both parameters are difficult to be quantified accurately in a contemplative field assessment. The slope related errors are easily revealed by a subsequent GIS assessment and the stream frequency related errors corrected by a GIS analysis of the field assessment data.

Table 5-9: Summarizing data of the PHP potential assessment results in Sri Lanka.

Total reference points	793
Reference points with direct potential attribution	123
Reference points with stream crossing	624
Other reference points without directly usable PHP potential information	46
Excluded for irregular dry season conditions (pre-comparison)	0
Total PHP unit cells	79266
PHP unit cells without high head PHP potential	66757
PHP unit cells with H1 high head PHP potential	11076
PHP unit cells with H1 high head PHP potential, possibly pseudokarst affected	0
PHP unit cells with H2 high head PHP potential	1433
PHP unit cells with H2 high head PHP potential, possibly pseudokarst affected	0
Estimated total discrepancy area in vicinity of affected reference points (as PHP unit cells)	104
Estimated PHP unit cells affected by discrepancies caused by the GIS method	9
Estimated PHP unit cells affected by discrepancies caused by the field assessment	95
Estimated PHP unit cells affected by discrepancies of unknown origin	0

5.2.5 Overall evaluation of the PHP potential assessment results

Field assessments were conducted in Yunnan Province/China, Costa Rica, Ecuador, and Sri Lanka. In all four assessment areas, the aim was to gain a comprehensive overview on the PHP potential distribution of the entire country or province. To ensure that the focus of the

traveling itinerary is laid on putative transition zones between prospective areas and areas of expected absence of PHP potential, advance planning of the traveling routes is required. Even with the focus on transition zones it is still necessary to sacrifice extensive detailed field evaluations due to time constraints. Most field assessment data was acquired by techniques based on continuous, standardized observation for PHP potential indicators along long distance transport routes. To preserve the spatial integrity of the assessment areas, their protection status was ignored. Several field assessment methods needed to be developed and tested and were continuously improved during the field assessments. Consequently, the reliability of the field assessment results improved over the first two (Yunnan), and to some extent, third assessment (Costa Rica) and was considered stable for the assessments in Ecuador and Sri Lanka. The reliability checking procedure for the GIS based potential assessment was therefore first conducted with the data from Ecuador and Sri Lanka. Reliability checking is a manual on-screen procedure to compare the results of the GIS based potential assessment with the information collected in the field for the same locality. Despite of being performed within a GIS environment, the procedure can neither be automated nor statistically evaluated, because the respective field assessment data units (waypoints) may contain very different information such as PHP potential, a stream crossing, or information about the geological situation and moreover may be spatially offset. The actual purpose of the reliability check however is consistent: to confirm that the PHP potential results of the GIS based PHP potential assessment agree with the real situation on location.

Analyzing the results reveals an improvement process and remaining shortcomings of the field assessment methods as well as remaining minor shortcomings of the GIS based potential assessment procedure. The overall conformity between GIS and field assessment for the areas of Costa Rica, Ecuador, and Sri Lanka is very high. It is therefore justified to assume a general suitability of the GIS based PHP potential assessment procedure for large-scale PHP potential assessments in the global tropical and subtropical regions.

5.2.6 Next steps beyond large-scale PHP potential assessment

The peculiar features of PHP in the hydropower spectrum, predominantly caused by the end-user driven installation and operation, require the consideration of further factors, unrelated to hydraulic potential, for the evaluation of quantitative PHP potential (see chapter 3.1). Figure 5-18 exemplifies the first stages of this evaluation process, which after further stages is expected to gradually approach the representation of a PHP market potential. The purpose of this demonstration is to emphasize that application level PHP potential, likewise true for any hydropower potential, is considerably smaller than the underlying hydraulic potential, however the underlying reasons for the reduction may be considerably different for PHP, compared to the other hydropower classifications. The example uses a result matrix from the GIS based potential assessment procedure as a starting point and therefore points towards a possible direction of continued research on high head PHP potential assessment.

Further specification stages that theoretically could provide information on the installation cost of individual PHP systems would require the exact position of the stream network (see chapter 3.3) and could therefore not be based on the present version results of the GIS based PHP potential assessment procedure.

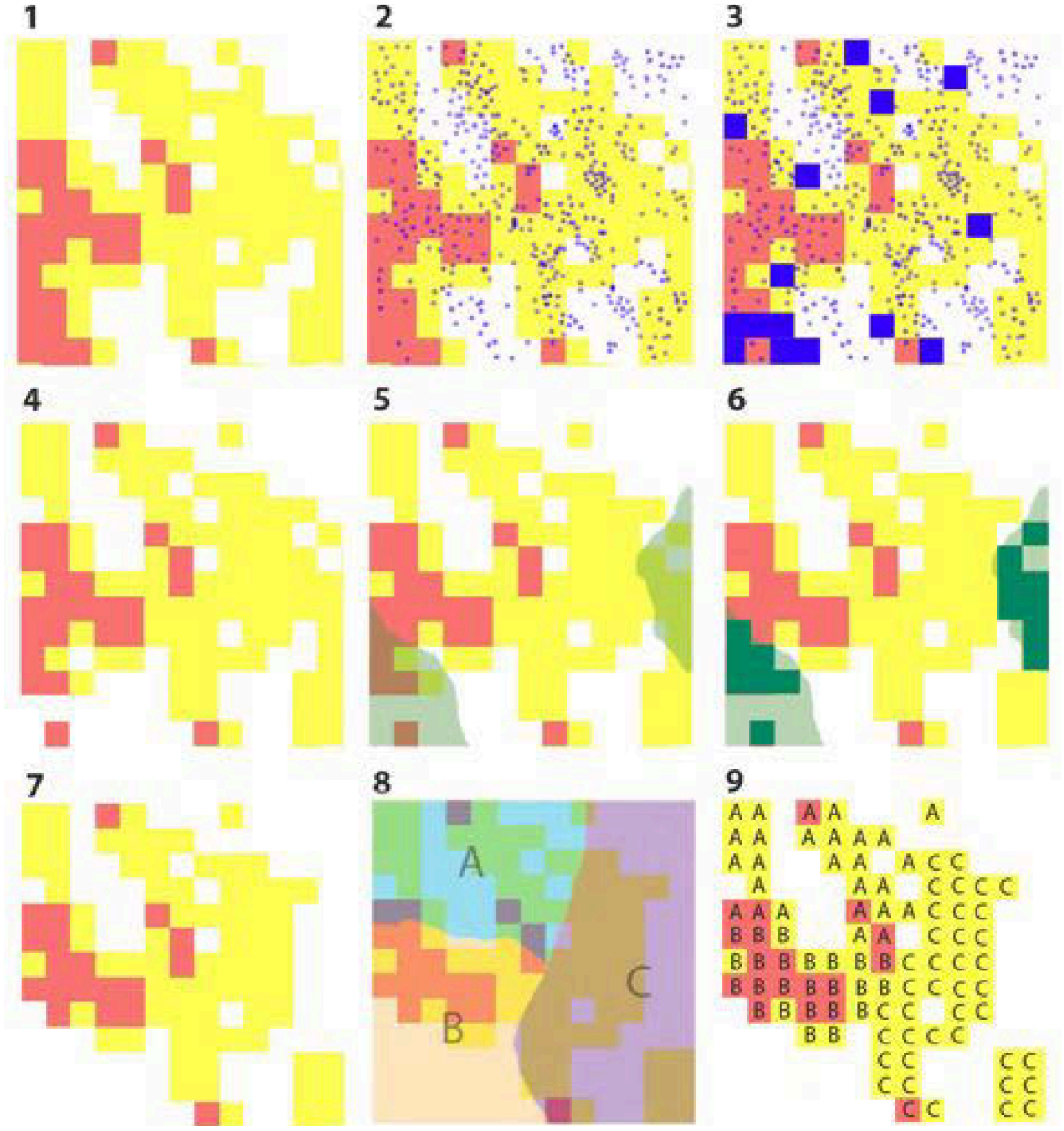

Figure 5-18: Demonstration of the first stages of an iterative approach towards a delineation of PHP market potential considering datasets unrelated to hydraulic potential, however to PHP market potential. Area size 13x13km; ficticious data.

yellow: PHP unit cells with H1 potential
red: PHP unit cells with H2 potential
The starting point (1) represents the large-scale high head PHP potential distribution obtained from the GIS based PHP potential assessment procedure.
(2) Household locations overlay. Blue dots each represent one household (e.g. from census data).
(3) Blue: PHP unit cells affected by step 2: (hydraulic) PHP potential, however no potential user household present on the respective PHP unit cells.
(4) Resulting PHP potential distribution after step 3.
(5) Green: protected areas overlay.
(6) Dark green: PHP unit cells with PHP potential within a protected area.
(7) Resulting PHP potential distribution after step 6 including preceding steps.
(8) Colored areas marked A, B, and C: administrative units with different electrification rates.
(9) Resulting PHP potential distribution after step 8. The distribution itself is not affected, however for each PHP unit cell the electrification rate of the respective administrative unit is considered as a reduction factor A, B, or C.

6 Conclusions and outlook

Because of the small project size, individual treatment as a customized engineering solution, a standard feature of all stages of project development in the hydropower domain, would be cost prohibitive for PHP installations. The cost problem already appears at the very first stage of the project planning: the hydropower potential assessment.

Individual site information, typically based on measured streamflow information of a particular watercourse, is therefore normally not available for PHP projects.

With a lack of site-related information, PHP has so far not been a projectable resource. This is particularly true for large-scale PHP potential information that could open a perspective to increase the size of development projects by aggregating individual PHP installations.

Attempts to assess hydropower potential on a large scale, typically for an entire country, have a long history, starting with cartographic techniques using manually retrieved topographic and streamflow data. Since the advent of remote sensing technology and broadly available computer processing capacity, GIS based spatial analysis had become an established tool for large-scale hydropower potential assessment. The technique is capable of producing complete hydropower potential estimates for large areas, as well as replacing some of the costly on-site data collection of conventional assessments.

The present work is extending the capabilities of GIS based hydropower potential assessment into the PHP domain. Because of the special, unit-size-related characteristics of PHP that would require largely unavailable high-resolution spatial data to resolve small streams that are only suitable for PHP size units, the traditional concept of hydropower potential is inadequate for GIS based large-scale PHP potential assessment. A new PHP potential definition was developed, based on the conclusion that the hydropower site selection planning sequence is typically reversed for PHP projects: no longer the hydropower installation is adapted to an established (identified, and confirmed by measurement) hydraulic site, but rather a suitable hydraulic site is identified for the established (off-the-shelf) PHP equipment. Consequently, PHP potential needs to be represented in relation to the specific site requirement of a “standard PHP unit” which needs to be defined as well.

With the new PHP potential definition it is possible to circumvent the problem of unavailable, high-resolution streamflow data because PHP potential does not have to be accounted as Watt (per site) anymore. This would be the traditional, quantitative concept, based on the usable hydraulic energy content of a particular stream. Instead, it can be accounted as “number of sites with predefined capacity” per area. This qualitative concept permits a threshold-value-based Boolean query to evaluate the suitability of an area for a standard PHP unit. Moreover, the watercourse does not have to be tangible anymore in this concept; its existence (or absence) is a result of the threshold-value-based calculation as well.

The standard PHP unit defined for this work is optimized for the expected application potential, according to four main criteria: (1) hydraulic requirements, (2) flexibility, (3) simplicity and (4) economy. Technically, the resulting unit is represented by a range of high head turbine technologies that are directly connected to a generator with an electrical output capacity of one kilowatt. Cost considerations on penstock length and transmission wiring dictate the placement of all components between water intake and electrical consumer onto an area equal or smaller than one square kilometer, simplified as 30x30 arc

seconds (926x926m). The associated hydraulic site requirements are defined as minimal 17m of hydraulic head for a maximal penstock length of 100m, resulting in a minimal average slope of 9.5 degree. The minimal flow requirements cover a range between 2.1l/sec and 10l/sec depending on the available hydraulic head. These are the hydraulic power related threshold factors for the site evaluation. Summarizing the technical and hydraulic requirements, PHP potential is defined as one PHP unit being able to operate continuously at 1kW electrical output (i.e. the standard PHP unit) on a one square kilometer space. This definition is represented in the "PHP unit cell", introduced here as the spatial unit of PHP potential. Areas with high precipitation and steep topography can support more than one standard PHP unit per square kilometer either as cascaded installation on the same stream or located at several streams in the vicinity. Such situations are defined as "favorable PHP potential (H2)" as opposed to "PHP potential (H1)" if they can support at least two standard PHP units on two different streams per square kilometer.

The two primary parameters that contain the basic information about the theoretically available static energy of the surface water at the location are (1) the hydraulic head and (2) the flow. Hydraulic head, in geographic terms, is represented as an elevation difference. It is readily available in fine resolution as a Digital Elevation Model (DEM). The other parameter, flow, cannot be determined directly from spatial data, since there is no comprehensive large-scale flow data available for streams that exhibit the typical flow rates of single-digit liters per second. The concept of large-scale PHP potential assessment is therefore inevitably centered on a substitution of flow data by secondary information that can be utilized to establish a proxy for the required information. Two approaches (A) and (B) are used in combination. (A) is a power calculation based on a quantification of minimum flow derived from hydrological parameters without the consideration of explicit watercourses resulting in a "total baseflow per area" and a quantification of hydraulic head based on DEM data. (B) is a qualitative reasoning process analyzing the absence of (adequate) flow and resulting in a set of "exclusion factors". Both approaches follow an evolutionary process, considering various datasets that are iteratively replaced to improve the overall performance. A final version of the minimum flow calculation in (A) utilizes the combination of a water balance modeling result that itself is based on various meteorological data, topography and land cover, as well as a precipitation dataset to determine the month of minimum flow. The final version for (B), the qualitative sub-process, considers the average inclination, an artificial spring horizon, snow cover, land cover, and karst geology as exclusion factors and moreover pseudokarst geology (which can only be represented indirectly) as an alert factor. Not all individual exclusion factors are relevant or sensitive for any given area. Both results, (A) and (B), are used qualitatively for the PHP potential assessment: (A) against the thresholds of the standard PHP unit-specific minimum flow and minimum head requirements and (B) against a threshold of zero. In doing so, the entire potential assessment process is realized as a sequence of threshold evaluations.

A geographic information system (GIS) is able to perform the threshold evaluations for a specified area, therefore is principally able to verify - if both adequate input data is used and adequate processing is initialized - the central hypothesis of this work:

The spatial distribution of PHP potential over a large area can be represented with a procedure that is entirely based on publicly available spatial data of global or near-global coverage.

Adequacy of the input data is indicated by satisfactory PHP potential assessment procedure performance with the concept outlined above. In addition, the input data carries the requirements of being "publicly available" and of "global or near-global coverage". These

additional requirements are an adaptation to the expected main application areas for high head PHP: sparsely populated mountainous rural regions of the tropics and subtropics. No other prerequisites are imposed on the input data. Consequently, the input data originates from various sources and retrieval techniques. The majority of the utilized datasets are remote sensing reanalysis products, such as the snow cover and topographical data. Other data, such as the geological and partially the precipitation data, are derived from terrestrial data acquisition. The variety of input sources prevents an error calculation on the GIS results that is based on input data error margins. Instead, each threshold evaluation is scrutinized to contain a large tolerance to underestimates and ideally no tolerance for overestimates.

The overestimation protection is realized in the processing stage. Several mechanisms are used: For the exclusion factor threshold evaluations, the protection is integrated into the "zero threshold" condition, here explained at the example of the freezing factor threshold evaluation (snow cover exclusion component): Areas with seasonal snow cover indicate that sub-zero ambient temperatures occur, a prerequisite for the interruption of streamflow in small watercourses due to freezing. A frozen stream would violate the prerequisite for permanent operability of the PHP installation and therefore lead to a "no PHP potential" classification. The correlation between snow cover and frozen streams however is often not valid; other environmental factors prevail that keep the flowing water in liquid state. Modeling a globally valid threshold factor scenario for seasonal freezing of small streams is not possible with the available data. As a contribution to the overestimation protection measures it is therefore defined for the GIS based PHP potential assessment procedure that generally all temporarily snow covered areas are considered to be void of PHP potential. The definition of "temporary snow cover" exemplarily reveals another adverse phenomenon that is shared by several of the input datasets: the utilization of the readily available dataset for the maximal monthly snow extent, which has a good temporal and spatial coverage, however coarse resolution (11km), would be individually responsible for a considerable extent of false negative PHP potential areas, entirely caused by its low resolution (see also Figure 4-25). The weekly high-resolution (500m) data version, on the other hand, when based on data that extends over one or several cold seasons, is extremely labor intensive to be manually compiled into a comprehensive maximal snow extent mapset. This effort is not practicable for large-area PHP potential assessments, therefore a compromise solution based on high-resolution data with temporally incomplete cold season coverage had to be found.

The other main building block of the processing stage, the "power calculation threshold evaluation", consists of two parts that are executed consecutively: The first part is the power calculation, an area hydropower potential that is calculated individually for each DEM cell from terrain inclination and driest month water balance data. The result of this part of the procedure states how many standard PHP units could be operated on a one square kilometer area (i.e. the superimposed PHP unit cell) if the conditions on this particular DEM cell would be representative across the entire PHP unit cell. All results from this calculation with a value greater than 2.0, representing H2 PHP potential, are limited to a value of 2.0. This overestimation protection measure, in combination with a disregard of results below 0.5 (which indicate insufficient PHP potential) becomes effective in the second part, a two-step threshold evaluation with threshold values of 1 and 2, representing three grades of high head PHP potential: no potential (H0), high head PHP potential (H1), and favorable high head PHP potential (H2). The overall overestimation protection effect of the power calculation threshold evaluation is (a) an attenuation of the influence from small areas with good conditions (steep, wet) onto surrounding, less advantageous, areas that belong to the same PHP unit cell, (b) the prevention of DEM cells with insufficient PHP

potential (below 0.5) from further contributing to PHP potential, and (c) the classification of final results that fall between two classes into the respective lower class.

The overall result of the GIS based PHP potential assessment procedure, obtained at this point and referred to as “large-scale PHP potential”, is obviously a purely qualitative representation of PHP potential. It is able to answer the question whether one, two, or no standard PHP units can be operated on a particular square kilometer area and is therefore not a representation of the total hydraulic potential, but rather narrowed down to a specific, application driven potential, reduced by all known or presumed conditions that are detrimental to the installation of PHP and at the same time integratable into the GIS procedure. Possible underestimates, despite being deviations from the representation of the actual hydraulic potential, act therefore as a protection measure against unsuccessful PHP operation and should consequently not be considered as wasted potential.

Nevertheless, the presented large-scale PHP potential is a representation of the hydraulic potential, albeit in indirect notation as number of PHP installations of fixed capacity. Consequently it is not required to consider further factors, such as population density and electrification that are highly PHP application relevant as well, however do not affect the hydraulic potential. The consideration of such further factors will ultimaterly result in an representation of a quantitative or market PHP potential.

The presented approach to represent a hydropower potential is exclusively compatible with the PHP domain of the hydropower spectrum. Here, the electromechanical PHP unit is typically purchased by an individual user household and a suitable hydraulic source is subsequently identified within limited distance to the household residence.

It inevitably remains to explain why there are only three grades of (high head) PHP potential results: A finer gradation, extended by more classifications of favorable PHP potential, such as H3 or H4, would not present an obstacle for a GIS based potential assessment, however would be indistinguishable by the large-area field assessment methods developed for this work. The resolution of the results is therefore limited by the verification techniques.

Climatic regions with recurrent freezing conditions cannot sustain continuous PHP operation, which in turn is a prerequisite in the PHP operating conditions defined for the scope of this work. The present, unmodified version of the GIS based PHP potential assessment procedure therefore classifies large parts of the global temperate regions as being unsuitable for PHP application. To extend the method towards PHP potential assessment for discontinuous PHP operation in temperate zones, modifications would be necessary on the GIS side because of a different dry season discrimination step. All other threshold factors and exclusion factors retain their global validity.

Outlook:

From a rural electrification point of view, PHP had seen better conditions some decades ago - its technology already considered mature, however not yet facing the strong competition from affordable and user friendly decentralized renewable electricity generation options (particularly Photovoltaics based) and the ever advancing grid electrification. The present PHP market potential could thus be seen as a "relic potential" in analogy to ecological relic habitats. In this light it becomes justifiable to disregard low head PHP potential evaluations on large scale, since it can be expected that low head PHP application is particularly uncompetitive to grid electricity.

With a growing world population and the limited-resources-driven need to consider all available clean energy options, it however appears unlikely that the PHP market will completely disappear, despite the technological advances in other energy generation fields. To identify this PHP market potential it is necessary to evaluate PHP against the different competing energy generation options. So far, the GIS based PHP potential assessment procedure of this work is merely able to answer the question where (and where not) high head PHP is an option in this evaluation process. For the market evaluation process itself, a new branch of the GIS based PHP potential assessment procedure, which is able to evaluate quantitative (market) potential, would have to be established. This outlook will therefore consider the large-scale PHP potential path, a direct continuation of the method of this work, as well as the PHP market potential path, which represents a more detailed evaluation method on smaller scale.

Large-scale PHP potential

The modularity of the GIS based PHP potential assessment procedure of this work is designed to incorporate improvements through the addition and replacement of input data. The presented procedure can therefore be considered as a functional, yet easily upgradable "1.0" version. Integration of new data sets either result in improvements of input data quality, such as the DEM resolution and accuracy improvements facilitated by the new TanDEM-X satellite data based reanalysis products, or as feature related functional improvements, like the consideration of high resolution precipitation data instead of runoff proxy data. Climate change related data, affecting water availability, would mostly fall into the first category.

A more extensive verification by field assessments (both over spatial and temporal extent) and more refined field assessment techniques would generally improve the integrity of the results and moreover extend the capabilities of the GIS based PHP potential assessment procedure: New PHP potential classifications can be displayed and a more detailed reasoning process for the absence of PHP potential can be realized. The influence of the local geological conditions on PHP potential could be much better understood if the possibility of geological analysis would be given during field assessments, complemented by more detailed geological map material.

In the long run, modeled flow data and finally hydropower potential data with sufficiently high resolution to directly represent PHP potential will become available for more and more countries and regions. This would reduce the large-scale PHP potential branch of the GIS based PHP potential assessment procedure to a discrimination tool for various adverse PHP installation conditions.

PHP market potential

For practical applications, the results of the GIS based PHP potential assessment procedure are combined with information on population (household) distribution, electricity grid extent, information on electricity cost and regulations, the outline of protected zones, either as generally protected areas, such as national parks, or zones with special regulations on surface water use, as well as other, yet unspecified data that may not be essential but has the capability to improve the overall assessment quality. The result of such a PHP user potential assessment still focuses on the application potential of PHP, however could moreover be regarded as a market study for PHP for a particular region. It is expected that the additional information required for a PHP market potential assessment is suitable for integration into the GIS based PHP potential assessment procedure, thus retaining the principal ability for GIS based large-scale assessments. The temporal validity of the data required for a PHP market potential assessment will inevitably play a more important role

compared to the temporally uncritical data used for the large-scale PHP potential of this work, and therefore requires extensive additions of functionality into the GIS procedure.

Even though it is obvious that technological advances in remote sensing and data analysis constantly improve the diversity and accuracy of spatial data, and therefore the quality of GIS based hydropower potential assessment procedures, it remains doubtful whether a PHP market potential can ever be represented with global validity, since many socio-economic factors, essential for its representation, are unlikely to be suitable for standardization on global scale. Realistically seen, it is equally unlikely to find any practical application for a PHP market potential evaluation on global scale, since the largest application scale imaginable would coincide with the spatial extent of technical development cooperation projects, which rarely exceed country level.

Nevertheless, detailed evaluations on country to continental level are a prolific field for further research, illuminating the complex of rural electrification with decentralized renewable energy technologies by analyzing interrelations between household income, electricity usage profiles and human factors, such as the willingness and ability to invest time and manual labor for electricity generation. This research is able to continuously draw benefit from more advanced spatial data, permitting the development of new assessment techniques under concomitant consideration of electricity generation technology advances and furthermore able to generate new options, like the direct interaction between the spatial data (e.g. weather data) and the electricity generating hardware.

Changes in water availability will predictably be a constant topic for further research on PHP potential. The insights gained in the preparation of this work clearly indicate that the impacts of climate change will be substantial.

References

Anderer, P., Dumont, U., Heimerl, S., & Ruprecht, A. (2010). Das Wasserkraftpotenzial in Deutschland. *Wasserwirtschaft*, *100*(9), 12–16.

Arino, O., Ramos Perez, J. J., Kalogirou, V., Bontemps, S., Defourny, P., & Van Bogaert, E. (2012). *Global Land Cover Map for 2009 (GlobCover 2009)*. European Space Agency (ESA) & Université catholique de Louvain (UCL). doi:10.1594/pangaea.787668

Asch, K. (2003). Digital map databases : No more hiding places for inconsistent geologists! *GEOLOGIJA*, *46*(2), 329–332.

BADC. (2004). Global Mean Sea-Level Pressure dataset. Retrieved from http://badc.nerc.ac.uk/browse/badc/ukmo-gmslp

BAFG. (2013). Bundesanstalt für Gewässerkunde: Global Runoff Data Base. Retrieved from http://www.bafg.de/GRDC/EN/01_GRDC/13_dtbse/database_node.html

Ballance, A., Stephenson, D., Chapman, R. A., & Muller, J. (2000). A geographic information systems analysis of hydro power potential in South Africa. *Journal of Hydroinformatics*, *1996*, 247–254.

Bhandari, R., & Stadler, I. (2011). Electrification using solar photovoltaic systems in Nepal. *Applied Energy*, *88*(2), 458–465. doi:10.1016/j.apenergy.2009.11.029

Bontemps, S., Defourny, P., Van Bogaert, E., Arino, O., Kalogirou, V., & Ramos Perez, J. J. (2011). *GLOBCOVER 2009 Products description and validation* (p. 53). Université catholique de Louvain (UCL) & European Space Agency (esa). doi:10013/epic.39884.d016

Brown, A. E., Zhang, L., McMahon, T. A., Western, A. W., & Vertessy, R. A. (2005). A review of paired catchment studies for determining changes in water yield resulting from alterations in vegetation. *Journal of Hydrology*, *310*(1-4), 28–61. doi:10.1016/j.jhydrol.2004.12.010

Bruijnzeel, L. A. (2004). *Hydrological functions of tropical forests: not seeing the soil for the trees? Agriculture, Ecosystems & Environment* (Vol. 104, pp. 185–228). doi:10.1016/j.agee.2004.01.015

Bruijnzeel, L. A. (2005). Tropical montane cloud forest: a unique hydrological case. In M. Bonell & L. A. Bruijnzeel (Eds.), *Forests, water and people in the humid Tropics* (digital edition, pp. 462–483). Cambridge: Cambridge University Press.

Calder, I. (2005). *Blue Revolution: Integrated Land and Water Resources Management* (second Ed., p. 353). London: Earthscan.

Castellarin, A., Galeati, G., Brandimarte, L., Montanari, A., & Brath, A. (2004). Regional flow-duration curves: reliability for ungauged basins. *Advances in Water Resources*, *27*(10), 953–965. doi:10.1016/j.advwatres.2004.08.005

Charlesworth, J. K. (1957). *The Quaternary Era. 1 (1957)*. London, United Kingdom: Edward Arnold.

Chow, V. Te. (1962). *Hydrologic Determination of Waterway areas for the Design of Drainage Structures in Small Drainage Basins*. Urbana-Champaign: University of Illinois, Engineering Experimental Station Bulletin No. 462.

Chrisman, N. (2001). *Exploring Geographical Information Systems* (second Ed., p. 12). New York: Wiley.

Clark, M., & Slater, A. (2006). Probabilistic Quantitative Precipitation Estimation in Complex Terrain. *Journal of Hydrometeorology*, *7*(February), 3–22.

Climate-data.org. (2014). Climate graph. Retrieved from http://de.climate-data.org

Cyr, J.-F., Landry, M., & Gagnon, Y. (2011). Methodology for the large-scale assessment of small hydroelectric potential: Application to the Province of New Brunswick (Canada). *Renewable Energy*, *36*(11), 2940–2950. doi:10.1016/j.renene.2011.04.003

Daly, C. (1996). Overview of the PRISM Model. Retrieved from http://www.prism.oregonstate.edu/docs/overview.html

Dexter, L., Birkeland, K., & Price, L. W. (2013). Snow, Ice, Avalanches and Glaciers. In L. W. P. Martin Price, Alton Byers, Donald Friend, Thomas Kohler (Ed.), *Mountain Geography:*

Physical and Human Dimensions (pp. 85–126). Berkeley, USA: University of California Press.

Di Gregorio, A., & Jansen, L. (2005). *Land Cover Classification System. Classification Concepts And User Manual. Software Version 2* (Vol. 8). Rome, Italy: Food & Agriculture Organization of the United Nations.

Eberhard, R., & Sharples, C. (2013). Appropriate terminology for karst-like phenomena : the problem with "pseudokarst." *International Journal of Speleology*, *42*(May), 109–113.

EcoInnovation. (2014). *PowerSpout Technical Specifications*. New Plymouth, New Zealand.

Ehlschlaeger, C. (2003). GRASS GIS manual: r.watershed. Retrieved from http://grass.osgeo.org/grass65/manuals/r.watershed.html#references

Eisenring, M. (1991). *Micro Pelton Turbines* (MHPG serie.). St. Gallen, Switzerland: SKAT Publications.

Engelmann, P., & Ritter, R. (2003). *Kleinwasserkraftförderung in Tibet : Samye-Kurze Geschichte einer Dorfentwicklung* (pp. 1–9). Lhasa: GTZ German Technical Cooperation.

Esmap Technical Paper 121/07, T. W. B. G. (2007). *Technical and Economic Assessment of Off-grid , Mini-grid and Grid Electrification Technologies*. Washington, D.C., USA: World Bank Energy Sector Management Assistance Program (ESMAP).

Farr, T., & Kobrick, M. (2000). Shuttle Radar Topography Mission produces a wealth of data. *Eos, Transactions of the American Geophysical Union*, *81*, 583–585.

Fekete, B., Vörösmarty, C., & Grabs, W. (2002). *Global composite runoff fields on observed river discharge and simulated water balances*. Koblenz: Water System Analysis Group,University of New Hampshire, and Global Runoff Data Centre, German Federal Institute of Hydrology (BfG).

Ford, D., & Williams, P. W. (1989). *Karst Hydrogeology and Geomorphology*. London: Unwin Hyman.

Ford, D., & Williams, P. W. (2007). *Karst Hydrogeology and Geomorphology* (pp. 4–5). West Sussex, England: John Wiley & Sons Ltd,. doi:10.1002/9781118684986

French, C. D., & Schenk, C. J. (2004). *Map Showing Geology, Oil and Gas Fields, and Geologic Provinces of the Caribbean Region, open-file report 97-470-K*. Denver, Colorado USA: U. S. Geological Survey.

Fulford, D. J., Mosley, P., & Gill, A. (2000). Field Report - Recommendations on the use of Micro-Hydro Power in Rural Development. *Journal of International Development*, *12*, 975–983.

Funnell, D., & Parish, R. (2001). *Mountain Environments and Communities*. London: Routledge.

Gilkes.com. (2015). Main turbine range chart. Retrieved from http://www.gilkes.com/user_uploads/main-range_chart.jpg

Goldscheider, N., & Chen, Z. (2014). The World Karst Aquifer Mapping Project – WOKAM. Presentation Karst Without Boundaries, June 2014, Karlsruhe, Germany: Karlsruhe Institute of Technology, Institute of Applied Geosciences, Division of Hydrogeology.

Greacen, C. E. (2004). *The Marginalization of "Small is Beautiful": Micro-hydroelectricity, Common Property, and the Politics of Rural Electricity Provision in Thailand*. Doctoral thesis, University of California, Berkeley.

Green, J., Fuentes, M., Rai, K., & Taylor, S. (2005). *Stimulating the Picohydropower Market for Low-Income Households in Ecuador*. Washington, D.C., USA: Energy Sector Management Assistance Program (ESMAP), The International Bank for Reconstruction and Development/The World Bank.

Hall, D., Cherry, S., Reeves, K., Lee, R., Carroll, G., Sommers, G., & Verdin, K. (2004). *Water Energy Resources of the United States with Emphasis on Low Head / Low Power Resources*. Idaho Falls: Cat. No. DOE/ID-11111. Idaho National Engineering and Environmental Laboratory.

Hall, D. K., Salomonson, V. V., & Riggs, G. A. (2004). MODIS/Terra Snow Cover 5-Min L2 Swath 500m, Version 5 - Online Documentation. Retrieved from

http://nsidc.org/data/docs/daac/modis_v5/mod10_l2_modis_terra_snow_cover_5min_swath.gd.html

Hall, D. K., Salomonson, V. V., & Riggs, G. A. (2006a). *MODIS/Terra Snow Cover 8-Day L3 Global 500m Grid, Version 5, Dec.2012-Feb15,2013*. Boulder, Colorado USA: U. S. National Snow and Ice Data Center. doi:http://neo.sci.gsfc.nasa.gov/view.php?datasetId=MOD10C1_M_SNOW

Hall, D. K., Salomonson, V. V., & Riggs, G. A. (2006b). *MODIS/Terra Snow Cover Monthly Global 0.1Deg CMG. V005 Jan2012-Jan2014*. Boulder, Colorado USA: U. S. National Snow and Ice Data Center. doi:http://neo.sci.gsfc.nasa.gov/view.php?datasetId=MOD10C1_M_SNOW

Hall, D., Reeves, K., Lee, R., Carroll, G., & Sommers, G. (2006). *Feasibility Assessment of the Water Energy Resources of the United States for New Low Power and Small Hydro Classes of Hydroelectric Plants Energy Efficiency and Renewable Energy Wind and Hydropower Technologies*. Idaho Falls: Idaho National Engineering and Environmental Laboratory, DOE-ID-11263.

Hansen, M., DeFries, R., Townshend, J., Carroll, M., Dimiceli, C., & Sohlberg, R. (2006). *Vegetation Continuous Fields MOD44B, 2001 Percent Tree Cover, Collection 4*. College Park, Maryland, USA.

Hansen, M., Potapov, P., Moore, R., Hancher, M., Turubanova, S., Tyukavina, A., … Townshend, J. (2013). High-resolution global maps of 21st-century forest cover change. *Science (New York, N.Y.)*, *342*(6160), 850–3. doi:10.1126/science.1244693

Harvey, A., Brown, A., Hettiarachi, P., & Inversin, A. R. (1993). *Micro-Hydro Design Manual: A Guide to Small-Scale Water Power Schemes*. London, United Kingdom: Intermediate Technology Publications.

Hijmans, R. J., Cameron, S. E., Parra, J. L., Jones, P. G., & Jarvis, A. (2005). Very high resolution interpolated climate surfaces for global land areas. *International Journal of Climatology*, *25*(15), 1965–1978. doi:10.1002/joc.1276

Hildebrand, H., & Kern, K. (1989). Ermittlung des Wasserkraftpotentials für große Regionen am Beispiel von Baden-Württemberg. *Wasserwirtschaft*, *79*(11), 562–567.

Ho-yan, B. P. (2012). *Design of a Low Head Pico Hydro Turbine for Rural Electrification in Cameroon*. Master thesis, University of Guelph.

Hollingsworth, E. (2009). *Karst Regions of the World (KROW)-Populating Global Karst Datasets and Generating Maps to Advance the Understanding of Karst Occurrence and Protection of Karst Species and Habitats Worldwide*. Fayetteville AR, USA: University of Arkansas.

Hrubiak, P. (2002). Tropical Rainfall Measuring Mission (TRMM) Documentation. Retrieved from http://disc.sci.gsfc.nasa.gov/precipitation/documentation/guide/TRMM_dataset.gd.shtml

Inversin, A. R. (1986). *Micro-Hydropower Sourcebook: A Practical Guide to Design and Implementation in Developing Countries*. Washington, D.C., USA: NRECA International Foundation.

Jain Irrigation Systems. (2016). HDPE Pipes - Jain High Density Polyethylene Pipes - Features and Specifications. Retrieved from http://www.jains.com/Pipefittings/hdpe pipe.htm

Jarvis, A., Reuter, H., Nelson, A., & Guevara, E. (2008). Hole-filled SRTM for the Globe Version 4, from the CGIAR-CSI SRTM 90m database.

Jenson, S. K., & Domingue, J. O. (1988). Extracting Topographic Structure from Digital Elevation Data for Geographic Information System Analysis, *54*(11), 1593–1600.

Kadioglu, M., & Sen, Z. (2001). Monthly precipitation-runoff polygons and mean runoff coefficients. *Hydrological Sciences Journal*, *46*(February), 3–11.

Karki, A., & Shresta, B. (2002). Micro-hydro power in Nepal access to electricity for isolated rural population in the hills and mountains.pdf. *International Energy Journal: Special Issue*, *3*(2), 89–97.

Kresic, N. (2010). Chapter 2 - Types and classifications of springs. In N. Kresic & Z. Stevanovic (Eds.), *Groundwater Hydrology of Springs* (pp. 31–85). Boston: Butterworth-Heinemann. doi:http://dx.doi.org/10.1016/B978-1-85617-502-9.00002-5

Kreutzmann, H. (2001). Development Indicators for Mountain Regions. *Mountain Research and Development*, *21*(2), 132–139. doi:10.1659/0276-4741(2001)021[0132:DIFMR]2.0.CO;2

Kumpulainen, R. A. (1997). Subsurface sediments tell about the hydrology of a volcano. *GFF*, *119*(2), 135–139. doi:10.1080/11035899709546469

Kusakana, K., & Vermaak, H. J. (2013). Hydrokinetic power generation for rural electricity supply: Case of South Africa. *Renewable Energy*, *55*, 467–473. doi:10.1016/j.renene.2012.12.051

Labat, D., Ababou, R., & Mangin, a. (2000). Rainfall–runoff relations for karstic springs. Part I: convolution and spectral analyses. *Journal of Hydrology*, *238*(3-4), 123–148. doi:10.1016/S0022-1694(00)00321-8

Langbein, W., & "Others." (1949). *Annual Runoff in the United States*. Washington DC: Geological Survey Circular 52, U.S. Department of the Interior.

Lawley, M. (2010). Comments to: Tehan, E; The Design , Installation and Operation of a Community Mini-Grid: Remote Implementation of Renewable Energy; Thesis, University of New South Wales, Sydney, Australia. *EcoInnovation Ltd., New Plymouth, New Zealand*.

Leite, V., Couto, J., Ferreira, Â., & Batista, J. (2016). A practical approach for grid-connected pico-hydro systems using conventional photovoltaic inverters. Leuven, Belgium: 2016 IEEE International Energy Conference (ENERGYCON). doi:10.1109/ENERGYCON.2016.7513911

LKYSPP. (2010, August). The Power of Pico-Hydro. *Asian Trends Monitoring Bulletin 5, Lew Kuan Yew School of Public Policy, National University of Singapore*, 11–17.

Longo, R., & Baldock, J. (1982). National Geological Map of the Republic of Ecuador (including Galápagos Province). Quito, Ecuador: Dirección General de Geológia y Minas (DGGM).

Lysenko, V. (1976). Der Pseudokarst des Vulkans Cotopaxi in Ecuador. *Die Höhle*, *27*(1), 32–37.

Maher, P., & Smith, N. (2001). *Pico Hydro For Village Power. A Practical Manual for Schemes up to 5 kW in Hilly Areas*. Nottingham, UK: Nottingham Trent University, Micro Hydro Research Group, Department of Electrical and Electronic Engineering.

Marjoribanks, R. (2010). *Geological Methods in Mineral Exploration and Mining*. Berlin, Heidelberg: Springer. doi:10.1007/978-3-540-74375-0

Meyer-Christoffer, A., Becker, A., Finger, P., Rudolf, B., Schneider, U., & Ziese, M. (2011). GPCC Climatology Version 2011 at 0.25°: Monthly Land-Surface Precipitation Climatology for Every Month and the Total Year from Rain-Gauges built on GTS-based and Historic Data. Offenbach, Germany: Global Precipitation Climatology Centre (GPCC, http://gpcc.dwd.de/) at Deutscher Wetterdienst. doi:http://dx.doi.org/10.5676/DWD_GPCC/CLIM_M_V2011_025

Midgley, D. C., Pitman, W. V, & Middleton, B. J. (1994). *Surface Water Resources of South Africa, 1990* (p. Volumes 1 to 6. Report Numbers 298/1.1/94 to 298/6). Pretoria, South Africa: Water Research Commission.

Mukherjee, S., Joshi, P. K., Mukherjee, S., Ghosh, A., Garg, R. D., & Mukhopadhyay, A. (2013). Evaluation of vertical accuracy of open source Digital Elevation Model (DEM). *International Journal of Applied Earth Observation and Geoinformation*, *21*, 205–217. doi:10.1016/j.jag.2012.09.004

Mulligan, M. (n.d.-a). 3 Hourly Near Global Point based Rainfall Time Series (1998–2007) Based on the TRMM 3B42 Product. Version 1.0. Retrieved from http://www.ambiotek.com/trmmtimeseries

Mulligan, M. (n.d.-b). MODIS MOD35 Pan-tropical Cloud Climatology. Version 1.

Mulligan, M. (2013). WaterWorld: a self-parameterising, physically-based model for application in data-poor but problem-rich environments globally. *Hydrology Research*, *44*(5), 748–769.

Mulligan, M., & Burke, S. (2005). *DFID FRP Project ZF0216 Global cloud forests and environmental change in a hydrological context* (pp. 1–74). London, United Kingdom: UK Department for International Development (DFID).

Muñoz-Villers, L. E., & McDonnell, J. J. (2013). Land use change effects on runoff generation in a humid tropical montane cloud forest region. *Hydrology and Earth System Sciences*, *17*(9), 3543–3560. doi:10.5194/hess-17-3543-2013

NASA. (2005). Shuttle Radar Topography Mission - FAQ - SRTM Radar Penetration. Retrieved from http://www2.jpl.nasa.gov/srtm/faq.html

NASA. (2011). The Global Precipitation Measurement (GPM) mission overview. Retrieved from http://pmm.nasa.gov/node/243

NASA GES DISC. (2009). Giovanni Operation Technical Summary: Anomaly. Greenbelt, Maryland, USA: NASA Goddard Earth Sciences Data and Information Services Center.

NASA GES DISC. (2014a). Readme for TRMM Product 3B43 (V7). Retrieved from http://disc.sci.gsfc.nasa.gov/precipitation/documentation/TRMM_README/TRMM_3B43_readme.shtml

NASA GES DISC. (2014b). TRMM Online Visualization and Analysis System (TOVAS). Retrieved from http://gdata1.sci.gsfc.nasa.gov/daac-bin/G3/gui.cgi?instance_id=TRMM_Monthly

NASA LP DAAC. (1996). GTOPO30 (Global 30 Arc-Second Elevation Data Set). Sioux Falls, South Dakota, USA: EROS Data Center (EDC) Distributed Active Archive Center (DAAC).

NASA LP DAAC. (2011). ASTER GDEM. Sioux Falls, South Dakota, USA: USGS/Earth Resources Observation and Science (EROS) Center.

New, M., Lister, D., Hulme, M., & Makin, I. (2003). A high-resolution data set of surface climate over global land areas. *Climate Research*, (21), 1–25.

Niez, A. (2010). *Comparative study on Rural Electrification policies in emerging economies. Keys to successful policies; Information paper, IEA*. Paris: International Energy Agency.

Nikolopoulos, C. (1997). *Expert Systems: Introduction to First and Second Generation and Hybrid Knowledge Based Systems* (first Ed.). New York, NY: Marcel Dekker, Inc.

NREL. (2000). *Assessment of Micro-hydro Resources in the Philippines*. Task 7Ba Report Philippine Renewable Energy Project, The National Renewable Energy Laboratory Under Contract with the US Agency for International Development.

O'Shea, B., Alonso, L., & Larsen, T. (Eds). (2011). *A Rapid Biological Assessment of the Kwamalasamutu region, Southwestern Suriname. RAP Bulletin of Biological Assessment 63.* Arlington, VA., USA: Conservation International.

OECD. (2012). *OECD-factbook 2011-2012*. (O. P. Organisation for Economic Co-operation and Development (2012): Economic, Environmental and Social Statistics, Ed.). Paris: Organisation for Economic Co-operation and Development (OECD).

OECD/IEA. (2012). *World Energy Outlook 2012; Chapter 18: Measuring progress towards energy for all.* (pp. 529–548). Paris: Organisation for Economic Co-operation and Development (OECD/IEA).

Oliver, I., & Beattie, A. J. (1993). A Possible Method for the Rapid Assessment of Biodiversity. *Conservation Biology*, *7*(3), 562–568. doi:10.1046/j.1523-1739.1993.07030562.x

Openstreetmap.org. (2010). Maps of traffic routes. Retrieved from http://wiki.openstreetmap.org/wiki/OSMtracker_(Windows_Mobile)

Pfaundler, M., & Zappa, M. (2006). *Die mittleren Abflüsse über die ganze Schweiz. Ein optimierter Datensatz im 500×500 m Raster* (pp. 1–15). Bern, Switzerland: Bundesamt für Umwelt BAFU.

Portegijs, J. (2003). The Firefly Micro Hydro System. *printed version published in 1995*. Retrieved from http://microhydropower.net/mhp_group/portegijs/firefly_bm/ffbm_index.html

Pöyry Energy GmbH, E. (2008). *Wasserkraftpotentialstudie Österreich*. Vienna, Austria: Verband der Elektrizitätsunternehmen Österreichs VEÖ.

Price, M. F., Byers, A. C., Friend, D. A., Kohler, T., & Price, L. W. (2013). *Mountain Geography: Physical and Human Dimensions*. (M. F. Price, Ed.). Berkeley, USA: University of California Press.

Prowse, T. D., & Beltaos, S. (2002). Climatic control of river-ice hydrology: a review. *Hydrological Processes*, *16*(4), 805–822. doi:10.1002/hyp.369

Reiss, J., Dußling, U., & Heimerl, S. (2011). *Potenziale der Wasserkraft im Neckar-Einzugsgebiet. Zusammenfassung der Potenzialstudie für das Neckar-einzugsgebiet ohne Bundeswasserstrasse Neckar*. Stuttgart, Germany: Ministerium für Umwelt, Naturschutz und Verkehr Baden-Württemberg.

Riggs, G. A., Hall, D. K., & Salomonson, V. V. (2006). *MODIS Snow Products User Guide to Collection 5* (Vol. 6, pp. 1–80). Boulder, Colorado USA: National Snow and Ice Data Center.

Rijssenbeek, W. (n.d.). *Pico Hydro Systems in Vietnam*. RR energy Consulting, Netherlands.

Sauquet, E. (2006). Mapping mean annual river discharges: Geostatistical developments for incorporating river network dependencies. *Journal of Hydrology*, *331*(1-2), 300–314. doi:10.1016/j.jhydrol.2006.05.018

Scatena, F. N., Bruijnzeel, L. A., Bubb, P., & Das, S. (2010). Setting the stage. In L. A. Bruijnzeel, F. N. Scatena, & L. S. Hamilton (Eds.), *Tropical Montane Cloud Forests: Science for Conservation and Management* (pp. 3–13). Cambridge, United Kingdom: Cambridge University Press.

Schenk, C. J., Viger, R. J., & Anderson, C. P. (1999). *Maps showing Geology, Oil and Gas Fields and Geologic Provinces of the South America Region, open-file report 97-470-D*. Denver, Colorado, USA: U. S. Geological Survey.

Schiller, G. (1982). *Die Wasserkraftnutzung in Österreich - Wasserkraftpotential Stand 1982*. Vienna, Austria.

Schröder, C. (2005a). *A New Strategy to solve the Dissemination Problem in PHP / MHP Proliferation. Summary of activities in Qinghai, Gansu and Yunnan, January to September 2005*. Beijing: Renewable Energy in Rural Areas Project, GTZ German Technical Cooperation.

Schröder, C. (2005b). *Support Program for Pico and Micro Hydropower for Application in China, Particularly Yunnan Province*. Beijing: Renewable Energy in Rural Areas Project, GTZ German Technical Cooperation.

Schröder, C. (2007). *Final evaluation of the PHP installations in Yunnan and Qinghai*. Beijing: Renewable Energy in Rural Areas Project, GTZ German Technical Cooperation.

Scott, D. F., Bruijnzeel, L. A., & Mackensen, J. (2005). The hydrological and soil impacts of forestation in the tropics. In M. Bonell & L. Bruijnzeel (Eds.), *Forests, water and people in the humid Tropics Book II* (digital ed., pp. 622–649). Cambridge, United Kingdom: Cambridge University Press.

Şen, Z., & Altunkaynak, A. (2006). A comparative fuzzy logic approach to runoff coefficient and runoff estimation. *Hydrological Processes*, *20*(9), 1993–2009. doi:10.1002/hyp.5992

Shapiro, M., & Waupotitsch, O. (2003). GRASS GIS manual: r.slope.aspect. Retrieved from http://grass.osgeo.org/grass65/manuals/r.slope.aspect.html

Sinclair, A., & Blackwell, G. (2004). *Applied Mineral Inventory Estimation* (pp. 14–16). Cambridge, United Kingdom: Cambridge University Press.

Smits, M., & Bush, S. R. (2010). A light left in the dark: The practice and politics of pico-hydropower in the Lao PDR. *Energy Policy*, *38*(1), 116–127. doi:10.1016/j.enpol.2009.08.058

Steinshouer, D. W., Qiang, J., McCabe, P. J., & Ryder, R. T. (1999). *Maps showing Geology, Oil and Gas Fields, and Geologic Provinces of the Asia Pacific, Open- File Report 97-470F*. Denver, Colorado, USA: U.S. Geological Survey.

Struben, J., & Sterman, J. (2007). Transition Challenges for Alternative Fuel Vehicle and Transportation Systems. *SSRN Electronic Journal*, 1–47. doi:10.2139/ssrn.881800

Susanto, J., & Stamp, S. (2012). Local installation methods for low head pico-hydropower in the Lao PDR. *Renewable Energy*, *44*, 439–447. doi:10.1016/j.renene.2012.01.089

Tong, J. (1997). *Small Hydro Power: China's practice* (second Ed., pp. 78, 126). Hangzhou, China: HIC Publications.

Trenberth, K. E., Smith, L., Qian, T., Dai, A., & Fasullo, J. (2007). Estimates of the Global Water Budget and Its Annual Cycle Using Observational and Model Data. *Journal of Hydrometeorology*, *8*(4), 758–769. doi:10.1175/JHM600.1

TVA. (2014). Valley Rainfall, Average monthly rainfall/runoff comparison 1887-2007. *Tennessee Valley Authority Homepage*. Retrieved from http://www.tva.gov/river/flood/rainfall.htm

Urmee, T., Harries, D., & Schlapfer, A. (2009). Issues related to rural electrification using renewable energy in developing countries of Asia and Pacific. *Renewable Energy*, *34*(2), 354–357. doi:10.1016/j.renene.2008.05.004

USGS. (2006). Shuttle Radar Topography Mission, 3 Arc Second filled version. College Park, Maryland, USA: Global Land Cover Facility, University of Maryland.

USGS-LCI. (2012). Land cover data. *USGS Land Cover Institute (LCI)*. Retrieved from http://landcover.usgs.gov/landcoverdata.php

Viviroli, D., Weingartner, R., & Messerli, B. (2003). Assessing the Hydrological Significance of the World's Mountains. *Mountain Research and Development*, *23*(1), 32–40. doi:10.1659/0276-4741(2003)023[0032:ATHSOT]2.0.CO;2

Vogel, R., Bell, C., & Fennessey, N. (1997). Climate, streamflow and water supply in the northeastern United States. *Journal of Hydrology*, *198*, 42–68.

Wandrey, C., & Law, B. (1999). *Maps showing Geology, Oil and Gas Fields and Geologic Provinces of South Asia, Open-File Report 97-470C*. Denver, Colorado USA: U. S. Geological Survey.

Waterworld_Version_2. (2014). Model results from the Waterworld system (non commercial-use). Retrieved from http://www.policysupport.org/waterworld

Weary, D. J., & Doctor, D. H. (2014). *Karst in the United States : A Digital Map Compilation and Database*. Denver, Colorado, USA: U. S. Geological Survey.

Weingartner, R., Hemund, C., & Schröder, U. (2012). *Erhebung des Kleinwasserkraftpotentials der Schweiz; Ermittlung des theoretischen Potentials und Methodik zu dessen ganzheitlicher Beurteilung*. Bern, Switzerland: Eidgenössisches Departement für Umwelt, Verkehr, Energie und Kommunikation UVEK, Bundesamt für Energie BFE.

Weiss, H. W., & Faeh, A. (1990). Methods for evaluating hydro potential. In *Hydrology in Mountainous Regions I - Hydrological Measurements; the Water Cycle* (Vol. 1, pp. 793–800). Lausanne, Switzerland: IAHS Publication No. 193.

Westervelt, J. (2004). GRASS Roots. In *Proceedings of the FOSS/GRASS Users Conference* (pp. 1–10). Bangkok, Thailand.

Williams, P. W., & Fong, V. T. (2010). World Map of Carbonate Rock Outcrops v3.0. Auckland, New Zealand: University of Auckland School of Environment.

Wittenberg, H., & Schulte, B. (1987). Zur realistischen Schätzung von Wasserkraftpotentialen. *Wasserwirtschaft*, *77*(12), 659–662.

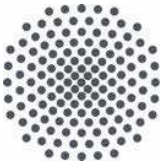

Institut für Wasser- und Umweltsystemmodellierung
Universität Stuttgart

Pfaffenwaldring 61
70569 Stuttgart (Vaihingen)
Telefon (0711) 685 - 64717/64749/64752/64679
Telefax (0711) 685 - 67020 o. 64746 o. 64681
E-Mail: iws@iws.uni-stuttgart.de
http://www.iws.uni-stuttgart.de

Verzeichnis der Mitteilungshefte

1 Röhnisch, Arthur: *Die Bemühungen um eine Wasserbauliche Versuchsanstalt an der Technischen Hochschule Stuttgart*, und
Fattah Abouleid, Abdel: *Beitrag zur Berechnung einer in lockeren Sand gerammten, zweifach verankerten Spundwand*, 1963

2 Marotz, Günter: *Beitrag zur Frage der Standfestigkeit von dichten Asphaltbelägen im Großwasserbau*, 1964

3 Gurr, Siegfried: *Beitrag zur Berechnung zusammengesetzter ebener Flächentrag-werke unter besonderer Berücksichtigung ebener Stauwände, mit Hilfe von Rand-wert- und Lastwertmatrizen*, 1965

4 Plica, Peter: *Ein Beitrag zur Anwendung von Schalenkonstruktionen im Stahlwasserbau*, und
Petrikat, Kurt: *Möglichkeiten und Grenzen des wasserbaulichen Versuchswesens*, 1966

5 Plate, Erich: *Beitrag zur Bestimmung der Windgeschwindigkeitsverteilung in der durch eine Wand gestörten bodennahen Luftschicht*, und
Röhnisch, Arthur; Marotz, Günter: *Neue Baustoffe und Bauausführungen für den Schutz der Böschungen und der Sohle von Kanälen, Flüssen und Häfen; Gestehungskosten und jeweilige Vorteile*, sowie
Unny, T.E.: *Schwingungsuntersuchungen am Kegelstrahlschieber*, 1967

6 Seiler, Erich: *Die Ermittlung des Anlagenwertes der bundeseigenen Binnenschiffahrtsstraßen und Talsperren und des Anteils der Binnenschiffahrt an diesem Wert*, 1967

7 *Sonderheft anläßlich des 65. Geburtstages von Prof. Arthur Röhnisch mit Beiträgen von* Benk, Dieter; Breitling, J.; Gurr, Siegfried; Haberhauer, Robert; Honekamp, Hermann; Kuz, Klaus Dieter; Marotz, Günter; Mayer-Vorfelder, Hans-Jörg; Miller, Rudolf; Plate, Erich J.; Radomski, Helge; Schwarz, Helmut; Vollmer, Ernst; Wildenhahn, Eberhard; 1967

8 Jumikis, Alfred: *Beitrag zur experimentellen Untersuchung des Wassernachschubs in einem gefrierenden Boden und die Beurteilung der Ergebnisse*, 1968

9 Marotz, Günter: *Technische Grundlagen einer Wasserspeicherung im natürlichen Untergrund*, 1968

10 Radomski, Helge: *Untersuchungen über den Einfluß der Querschnittsform wellenförmiger Spundwände auf die statischen und rammtechnischen Eigenschaften*, 1968

11 Schwarz, Helmut: *Die Grenztragfähigkeit des Baugrundes bei Einwirkung vertikal gezogener Ankerplatten als zweidimensionales Bruchproblem*, 1969

12 Erbel, Klaus: *Ein Beitrag zur Untersuchung der Metamorphose von Mittelgebirgsschneedecken unter besonderer Berücksichtigung eines Verfahrens zur Bestimmung der thermischen Schneequalität*, 1969

13 Westhaus, Karl-Heinz: *Der Strukturwandel in der Binnenschiffahrt und sein Einfluß auf den Ausbau der Binnenschiffskanäle*, 1969

14 Mayer-Vorfelder, Hans-Jörg: *Ein Beitrag zur Berechnung des Erdwiderstandes unter Ansatz der logarithmischen Spirale als Gleitflächenfunktion*, 1970

15 Schulz, Manfred: *Berechnung des räumlichen Erddruckes auf die Wandung kreiszylindrischer Körper*, 1970

16 Mobasseri, Manoutschehr: *Die Rippenstützmauer. Konstruktion und Grenzen ihrer Standsicherheit*, 1970

17 Benk, Dieter: *Ein Beitrag zum Betrieb und zur Bemessung von Hochwasserrückhaltebecken*, 1970

18 Gàl, Attila: *Bestimmung der mitschwingenden Wassermasse bei überströmten Fischbauchklappen mit kreiszylindrischem Staublech*, 1971, vergriffen

19 Kuz, Klaus Dieter: *Ein Beitrag zur Frage des Einsetzens von Kavitationserscheinungen in einer Düsenströmung bei Berücksichtigung der im Wasser gelösten Gase*, 1971, vergriffen

20 Schaak, Hartmut: *Verteilleitungen von Wasserkraftanlagen*, 1971

21 *Sonderheft zur Eröffnung der neuen Versuchsanstalt des Instituts für Wasserbau der Universität Stuttgart mit Beiträgen von* Brombach, Hansjörg; Dirksen, Wolfram; Gàl, Attila; Gerlach, Reinhard; Giesecke, Jürgen; Holthoff, Franz-Josef; Kuz, Klaus Dieter; Marotz, Günter; Minor, Hans-Erwin; Petrikat, Kurt; Röhnisch, Arthur; Rueff, Helge; Schwarz, Helmut; Vollmer, Ernst; Wildenhahn, Eberhard; 1972

22 Wang, Chung-su: *Ein Beitrag zur Berechnung der Schwingungen an Kegelstrahlschiebern*, 1972

23 Mayer-Vorfelder, Hans-Jörg: *Erdwiderstandsbeiwerte nach dem Ohde-Variationsverfahren*, 1972

24 Minor, Hans-Erwin: *Beitrag zur Bestimmung der Schwingungsanfachungsfunktionen überströmter Stauklappen*, 1972, vergriffen

25 Brombach, Hansjörg: *Untersuchung strömungsmechanischer Elemente (Fluidik) und die Möglichkeit der Anwendung von Wirbelkammerelementen im Wasserbau*, 1972, vergriffen

26 Wildenhahn, Eberhard: *Beitrag zur Berechnung von Horizontalfilterbrunnen*, 1972

27 Steinlein, Helmut: *Die Eliminierung der Schwebstoffe aus Flußwasser zum Zweck der unterirdischen Wasserspeicherung, gezeigt am Beispiel der Iller*, 1972

28 Holthoff, Franz Josef: *Die Überwindung großer Hubhöhen in der Binnenschiffahrt durch Schwimmerhebewerke*, 1973

29 Röder, Karl: *Einwirkungen aus Baugrundbewegungen auf trog- und kastenförmige Konstruktionen des Wasser- und Tunnelbaues*, 1973

30 Kretschmer, Heinz: *Die Bemessung von Bogenstaumauern in Abhängigkeit von der Talform*, 1973

31 Honekamp, Hermann: *Beitrag zur Berechnung der Montage von Unterwasserpipelines*, 1973

32 Giesecke, Jürgen: *Die Wirbelkammertriode als neuartiges Steuerorgan im Wasserbau*, und Brombach, Hansjörg: *Entwicklung, Bauformen, Wirkungsweise und Steuereigenschaften von Wirbelkammerverstärkern*, 1974

33 Rueff, Helge: *Untersuchung der schwingungserregenden Kräfte an zwei hintereinander angeordneten Tiefschützen unter besonderer Berücksichtigung von Kavitation*, 1974

34 Röhnisch, Arthur: *Einpreßversuche mit Zementmörtel für Spannbeton - Vergleich der Ergebnisse von Modellversuchen mit Ausführungen in Hüllwellrohren*, 1975

35 *Sonderheft anläßlich des 65. Geburtstages von Prof. Dr.-Ing. Kurt Petrikat mit Beiträgen von*: Brombach, Hansjörg; Erbel, Klaus; Flinspach, Dieter; Fischer jr., Richard; Gàl, Attila; Gerlach, Reinhard; Giesecke, Jürgen; Haberhauer, Robert; Hafner Edzard; Hausenblas, Bernhard; Horlacher, Hans-Burkhard; Hutarew, Andreas; Knoll, Manfred; Krummet, Ralph; Marotz, Günter; Merkle, Theodor; Miller, Christoph; Minor, Hans-Erwin; Neumayer, Hans; Rao, Syamala; Rath, Paul; Rueff, Helge; Ruppert, Jürgen; Schwarz, Wolfgang; Topal-Gökceli, Mehmet; Vollmer, Ernst; Wang, Chung-su; Weber, Hans-Georg; 1975

36 Berger, Jochum: *Beitrag zur Berechnung des Spannungszustandes in rotationssymmetrisch belasteten Kugelschalen veränderlicher Wandstärke unter Gas- und Flüssigkeitsdruck durch Integration schwach singulärer Differentialgleichungen*, 1975

37 Dirksen, Wolfram: *Berechnung instationärer Abflußvorgänge in gestauten Gerinnen mittels Differenzenverfahren und die Anwendung auf Hochwasserrückhaltebecken*, 1976

38 Horlacher, Hans-Burkhard: *Berechnung instationärer Temperatur- und Wärmespannungsfelder in langen mehrschichtigen Hohlzylindern*, 1976

39 Hafner, Edzard: *Untersuchung der hydrodynamischen Kräfte auf Baukörper im Tiefwasserbereich des Meeres*, 1977, ISBN 3-921694-39-6

40 Ruppert, Jürgen: *Über den Axialwirbelkammerverstärker für den Einsatz im Wasserbau*, 1977, ISBN 3-921694-40-X

41 Hutarew, Andreas: *Beitrag zur Beeinflußbarkeit des Sauerstoffgehalts in Fließgewässern an Abstürzen und Wehren*, 1977, ISBN 3-921694-41-8, *vergriffen*

42 Miller, Christoph: *Ein Beitrag zur Bestimmung der schwingungserregenden Kräfte an unterströmten Wehren*, 1977, ISBN 3-921694-42-6

43 Schwarz, Wolfgang: *Druckstoßberechnung unter Berücksichtigung der Radial- und Längsverschiebungen der Rohrwandung*, 1978, ISBN 3-921694-43-4

44 Kinzelbach, Wolfgang: *Numerische Untersuchungen über den optimalen Einsatz variabler Kühlsysteme einer Kraftwerkskette am Beispiel Oberrhein*, 1978, ISBN 3-921694-44-2

45 Barczewski, Baldur: *Neue Meßmethoden für Wasser-Luftgemische und deren Anwendung auf zweiphasige Auftriebsstrahlen*, 1979, ISBN 3-921694-45-0

46 Neumayer, Hans: *Untersuchung der Strömungsvorgänge in radialen Wirbelkammerverstärkern*, 1979, ISBN 3-921694-46-9

47 Elalfy, Youssef-Elhassan: *Untersuchung der Strömungsvorgänge in Wirbelkammerdioden und -drosseln*, 1979, ISBN 3-921694-47-7

48 Brombach, Hansjörg: *Automatisierung der Bewirtschaftung von Wasserspeichern*, 1981, ISBN 3-921694-48-5

49 Geldner, Peter: *Deterministische und stochastische Methoden zur Bestimmung der Selbstdichtung von Gewässern*, 1981, ISBN 3-921694-49-3, *vergriffen*

50 Mehlhorn, Hans: *Temperaturveränderungen im Grundwasser durch Brauchwassereinleitungen*, 1982, ISBN 3-921694-50-7, *vergriffen*

51 Hafner, Edzard: *Rohrleitungen und Behälter im Meer*, 1983, ISBN 3-921694-51-5

52 Rinnert, Bernd: *Hydrodynamische Dispersion in porösen Medien: Einfluß von Dichteunterschieden auf die Vertikalvermischung in horizontaler Strömung*, 1983, ISBN 3-921694-52-3, *vergriffen*

53 Lindner, Wulf: *Steuerung von Grundwasserentnahmen unter Einhaltung ökologischer Kriterien*, 1983, ISBN 3-921694-53-1, *vergriffen*

54 Herr, Michael; Herzer, Jörg; Kinzelbach, Wolfgang; Kobus, Helmut; Rinnert, Bernd: *Methoden zur rechnerischen Erfassung und hydraulischen Sanierung von Grundwasserkontaminationen*, 1983, ISBN 3-921694-54-X

55 Schmitt, Paul: *Wege zur Automatisierung der Niederschlagsermittlung*, 1984, ISBN 3-921694-55-8, *vergriffen*

56 Müller, Peter: *Transport und selektive Sedimentation von Schwebstoffen bei gestautem Abfluß*, 1985, ISBN 3-921694-56-6

57 El-Qawasmeh, Fuad: *Möglichkeiten und Grenzen der Tropfbewässerung unter besonderer Berücksichtigung der Verstopfungsanfälligkeit der Tropfelemente*, 1985, ISBN 3-921694-57-4, *vergriffen*

58 Kirchenbaur, Klaus: *Mikroprozessorgesteuerte Erfassung instationärer Druckfelder am Beispiel seegangsbelasteter Baukörper*, 1985, ISBN 3-921694-58-2

59 Kobus, Helmut (Hrsg.): *Modellierung des großräumigen Wärme- und Schadstofftransports im Grundwasser*, Tätigkeitsbericht 1984/85 (DFG-Forschergruppe an den Universitäten Hohenheim, Karlsruhe und Stuttgart), 1985, ISBN 3-921694-59-0, *vergriffen*

60 Spitz, Karlheinz: *Dispersion in porösen Medien: Einfluß von Inhomogenitäten und Dichteunterschieden*, 1985, ISBN 3-921694-60-4, *vergriffen*

61 Kobus, Helmut: *An Introduction to Air-Water Flows in Hydraulics*, 1985, ISBN 3-921694-61-2

62 Kaleris, Vassilios: *Erfassung des Austausches von Oberflächen- und Grundwasser in horizontalebenen Grundwassermodellen*, 1986, ISBN 3-921694-62-0

63 Herr, Michael: *Grundlagen der hydraulischen Sanierung verunreinigter Porengrundwasserleiter*, 1987, ISBN 3-921694-63-9

64 Marx, Walter: *Berechnung von Temperatur und Spannung in Massenbeton infolge Hydratation*, 1987, ISBN 3-921694-64-7

65 Koschitzky, Hans-Peter: *Dimensionierungskonzept für Sohlbelüfter in Schußrinnen zur Vermeidung von Kavitationsschäden*, 1987, ISBN 3-921694-65-5

66 Kobus, Helmut (Hrsg.): *Modellierung des großräumigen Wärme- und Schadstofftransports im Grundwasser*, Tätigkeitsbericht 1986/87 (DFG-Forschergruppe an den Universitäten Hohenheim, Karlsruhe und Stuttgart) 1987, ISBN 3-921694-66-3

67 Söll, Thomas: *Berechnungsverfahren zur Abschätzung anthropogener Temperaturanomalien im Grundwasser*, 1988, ISBN 3-921694-67-1

68 Dittrich, Andreas; Westrich, Bernd: *Bodenseeufererosion, Bestandsaufnahme und Bewertung*, 1988, ISBN 3-921694-68-X, *vergriffen*

69 Huwe, Bernd; van der Ploeg, Rienk R.: *Modelle zur Simulation des Stickstoffhaushaltes von Standorten mit unterschiedlicher landwirtschaftlicher Nutzung*, 1988, ISBN 3-921694-69-8, *vergriffen*

70 Stephan, Karl: *Integration elliptischer Funktionen*, 1988, ISBN 3-921694-70-1

71 Kobus, Helmut; Zilliox, Lothaire (Hrsg.): *Nitratbelastung des Grundwassers, Auswirkungen der Landwirtschaft auf die Grundwasser- und Rohwasserbeschaffenheit und Maßnahmen zum Schutz des Grundwassers*. Vorträge des deutsch-französischen Kolloquiums am 6. Oktober 1988, Universitäten Stuttgart und Louis Pasteur Strasbourg (Vorträge in deutsch oder französisch, Kurzfassungen zweisprachig), 1988, ISBN 3-921694-71-X

72 Soyeaux, Renald: *Unterströmung von Stauanlagen auf klüftigem Untergrund unter Berücksichtigung laminarer und turbulenter Fließzustände*,1991, ISBN 3-921694-72-8

73 Kohane, Roberto: *Berechnungsmethoden für Hochwasserabfluß in Fließgewässern mit überströmten Vorländern*, 1991, ISBN 3-921694-73-6

74 Hassinger, Reinhard: *Beitrag zur Hydraulik und Bemessung von Blocksteinrampen in flexibler Bauweise*, 1991, ISBN 3-921694-74-4, *vergriffen*

75 Schäfer, Gerhard: *Einfluß von Schichtenstrukturen und lokalen Einlagerungen auf die Längsdispersion in Porengrundwasserleitern*, 1991, ISBN 3-921694-75-2

76 Giesecke, Jürgen: *Vorträge, Wasserwirtschaft in stark besiedelten Regionen; Umweltforschung mit Schwerpunkt Wasserwirtschaft*, 1991, ISBN 3-921694-76-0

77 Huwe, Bernd: *Deterministische und stochastische Ansätze zur Modellierung des Stickstoffhaushalts landwirtschaftlich genutzter Flächen auf unterschiedlichem Skalenniveau*, 1992, ISBN 3-921694-77-9, *vergriffen*

78 Rommel, Michael: *Verwendung von Kluftdaten zur realitätsnahen Generierung von Kluftnetzen mit anschließender laminar-turbulenter Strömungsberechnung*, 1993, ISBN 3-92 1694-78-7

79 Marschall, Paul: *Die Ermittlung lokaler Stofffrachten im Grundwasser mit Hilfe von Einbohrloch-Meßverfahren*, 1993, ISBN 3-921694-79-5, *vergriffen*

80 Ptak, Thomas: *Stofftransport in heterogenen Porenaquiferen: Felduntersuchungen und stochastische Modellierung*, 1993, ISBN 3-921694-80-9, *vergriffen*

81 Haakh, Frieder: *Transientes Strömungsverhalten in Wirbelkammern,* 1993, ISBN 3-921694-81-7

82 Kobus, Helmut; Cirpka, Olaf; Barczewski, Baldur; Koschitzky, Hans-Peter: *Versuchseinrichtung zur Grundwasser und Altlastensanierung VEGAS, Konzeption und Programmrahmen*, 1993, ISBN 3-921694-82-5

83 Zang, Weidong: *Optimaler Echtzeit-Betrieb eines Speichers mit aktueller Abflußregenerierung*, 1994, ISBN 3-921694-83-3, *vergriffen*

84 Franke, Hans-Jörg: *Stochastische Modellierung eines flächenhaften Stoffeintrages und Transports in Grundwasser am Beispiel der Pflanzenschutzmittelproblematik*, 1995, ISBN 3-921694-84-1

85 Lang, Ulrich: *Simulation regionaler Strömungs- und Transportvorgänge in Karstaquiferen mit Hilfe des Doppelkontinuum-Ansatzes: Methodenentwicklung und Parameteridentifikation*, 1995, ISBN 3-921694-85-X, *vergriffen*

86 Helmig, Rainer: *Einführung in die Numerischen Methoden der Hydromechanik*, 1996, ISBN 3-921694-86-8, *vergriffen*

87 Cirpka, Olaf: *CONTRACT: A Numerical Tool for Contaminant Transport and Chemical Transformations - Theory and Program Documentation -*, 1996, ISBN 3-921694-87-6

88 Haberlandt, Uwe: *Stochastische Synthese und Regionalisierung des Niederschlages für Schmutzfrachtberechnungen*, 1996, ISBN 3-921694-88-4

89 Croisé, Jean: *Extraktion von flüchtigen Chemikalien aus natürlichen Lockergesteinen mittels erzwungener Luftströmung*, 1996, ISBN 3-921694-89-2, *vergriffen*

90 Jorde, Klaus: *Ökologisch begründete, dynamische Mindestwasserregelungen bei Ausleitungskraftwerken*, 1997, ISBN 3-921694-90-6, *vergriffen*

91 Helmig, Rainer: *Gekoppelte Strömungs- und Transportprozesse im Untergrund - Ein Beitrag zur Hydrosystemmodellierung-*, 1998, ISBN 3-921694-91-4, *vergriffen*

92 Emmert, Martin: *Numerische Modellierung nichtisothermer Gas-Wasser Systeme in porösen Medien,* 1997, ISBN 3-921694-92-2

93 Kern, Ulrich: *Transport von Schweb- und Schadstoffen in staugeregelten Fließgewässern am Beispiel des Neckars*, 1997, ISBN 3-921694-93-0, *vergriffen*

94 Förster, Georg: *Druckstoßdämpfung durch große Luftblasen in Hochpunkten von Rohrleitungen 1997*, ISBN 3-921694-94-9

95 Cirpka, Olaf: *Numerische Methoden zur Simulation des reaktiven Mehrkomponententransports im Grundwasser*, 1997, ISBN 3-921694-95-7, *vergriffen*

96 Färber, Arne: *Wärmetransport in der ungesättigten Bodenzone: Entwicklung einer thermischen In-situ-Sanierungstechnologie*, 1997, ISBN 3-921694-96-5

97 Betz, Christoph: *Wasserdampfdestillation von Schadstoffen im porösen Medium: Entwicklung einer thermischen In-situ-Sanierungstechnologie*, 1998, SBN 3-921694-97-3

98 Xu, Yichun: *Numerical Modeling of Suspended Sediment Transport in Rivers*, 1998, ISBN 3-921694-98-1, *vergriffen*

99 Wüst, Wolfgang: *Geochemische Untersuchungen zur Sanierung CKW-kontaminierter Aquifere mit Fe(0)-Reaktionswänden,* 2000, ISBN 3-933761-02-2

100 Sheta, Hussam: *Simulation von Mehrphasenvorgängen in porösen Medien unter Einbeziehung von Hysterese-Effekten*, 2000, ISBN 3-933761-03-4

101 Ayros, Edwin: *Regionalisierung extremer Abflüsse auf der Grundlage statistischer Verfahren*, 2000, ISBN 3-933761-04-2, *vergriffen*

102 Huber, Ralf: *Compositional Multiphase Flow and Transport in Heterogeneous Porous Media*, 2000, ISBN 3-933761-05-0

103 Braun, Christopherus: *Ein Upscaling-Verfahren für Mehrphasenströmungen in porösen Medien*, 2000, ISBN 3-933761-06-9

104 Hofmann, Bernd: *Entwicklung eines rechnergestützten Managementsystems zur Beurteilung von Grundwasserschadensfällen*, 2000, ISBN 3-933761-07-7

105 Class, Holger: *Theorie und numerische Modellierung nichtisothermer Mehrphasenprozesse in NAPL-kontaminierten porösen Medien,* 2001, ISBN 3-933761-08-5

106 Schmidt, Reinhard: *Wasserdampf- und Heißluftinjektion zur thermischen Sanierung kontaminierter Standorte*, 2001, ISBN 3-933761-09-3

107 Josef, Reinhold:, *Schadstoffextraktion mit hydraulischen Sanierungsverfahren unter Anwendung von grenzflächenaktiven Stoffen*, 2001, ISBN 3-933761-10-7

108 Schneider, Matthias: *Habitat- und Abflussmodellierung für Fließgewässer mit unscharfen Berechnungsansätzen*, 2001, ISBN 3-933761-11-5

109 Rathgeb, Andreas: *Hydrodynamische Bemessungsgrundlagen für Lockerdeckwerke an überströmbaren Erddämmen*, 2001, ISBN 3-933761-12-3

110 Lang, Stefan: *Parallele numerische Simulation instätionärer Probleme mit adaptiven Methoden auf unstrukturierten Gittern*, 2001, ISBN 3-933761-13-1

111 Appt, Jochen; Stumpp Simone: *Die Bodensee-Messkampagne 2001, IWS/CWR Lake Constance Measurement Program 2001*, 2002, ISBN 3-933761-14-X

112 Heimerl, Stephan: *Systematische Beurteilung von Wasserkraftprojekten,* 2002, ISBN 3-933761-15-8, *vergriffen*

113 Iqbal, Amin: *On the Management and Salinity Control of Drip Irrigation,* 2002, ISBN 3-933761-16-6

114 Silberhorn-Hemminger, Annette: *Modellierung von Kluftaquifersystemen: Geostatistische Analyse und deterministisch-stochastische Kluftgenerierung,* 2002, ISBN 3-933761-17-4

115 Winkler, Angela: *Prozesse des Wärme- und Stofftransports bei der In-situ-Sanierung mit festen Wärmequellen,* 2003, ISBN 3-933761-18-2

116 Marx, Walter: *Wasserkraft, Bewässerung, Umwelt - Planungs- und Bewertungsschwerpunkte der Wasserbewirtschaftung,* 2003, ISBN 3-933761-19-0

117 Hinkelmann, Reinhard: *Efficient Numerical Methods and Information-Processing Techniques in Environment Water,* 2003, ISBN 3-933761-20-4

118 Samaniego-Eguiguren, Luis Eduardo: *Hydrological Consequences of Land Use / Land Cover and Climatic Changes in Mesoscale Catchments*, 2003, ISBN 3-933761-21-2

119 Neunhäuserer, Lina: *Diskretisierungsansätze zur Modellierung von Strömungs- und Transportprozessen in geklüftet-porösen Medien*, 2003, ISBN 3-933761-22-0

120 Paul, Maren: *Simulation of Two-Phase Flow in Heterogeneous Poros Media with Adaptive Methods*, 2003, ISBN 3-933761-23-9

121 Ehret, Uwe: *Rainfall and Flood Nowcasting in Small Catchments using Weather Radar*, 2003, ISBN 3-933761-24-7

122 Haag, Ingo: *Der Sauerstoffhaushalt staugeregelter Flüsse am Beispiel des Neckars - Analysen, Experimente, Simulationen -,* 2003, ISBN 3-933761-25-5

123 Appt, Jochen: *Analysis of Basin-Scale Internal Waves in Upper Lake Constance,* 2003, ISBN 3-933761-26-3

124 Hrsg.: Schrenk, Volker; Batereau, Katrin; Barczewski, Baldur; Weber, Karolin und Koschitzky, Hans-Peter: *Symposium Ressource Fläche und VEGAS - Statuskolloquium 2003, 30. September und 1. Oktober 2003,* 2003, ISBN 3-933761-27-1

125 Omar Khalil Ouda: *Optimisation of Agricultural Water Use: A Decision Support System for the Gaza Strip,* 2003, ISBN 3-933761-28-0

126 Batereau, Katrin: *Sensorbasierte Bodenluftmessung zur Vor-Ort-Erkundung von Schadensherden im Untergrund*, 2004, ISBN 3-933761-29-8

127 Witt, Oliver: *Erosionsstabilität von Gewässersedimenten mit Auswirkung auf den Stofftransport bei Hochwasser am Beispiel ausgewählter Stauhaltungen des Oberrheins*, 2004, ISBN 3-933761-30-1

128 Jakobs, Hartmut: *Simulation nicht-isothermer Gas-Wasser-Prozesse in komplexen Kluft-Matrix-Systemen*, 2004, ISBN 3-933761-31-X

129 Li, Chen-Chien: *Deterministisch-stochastisches Berechnungskonzept zur Beurteilung der Auswirkungen erosiver Hochwasserereignisse in Flussstauhaltungen,* 2004, ISBN 3-933761-32-8

130 Reichenberger, Volker; Helmig, Rainer; Jakobs, Hartmut; Bastian, Peter; Niessner, Jennifer: *Complex Gas-Water Processes in Discrete Fracture-Matrix Systems: Up-scaling, Mass-Conservative Discretization and Efficient Multilevel Solution,* 2004, ISBN 3-933761-33-6

131 Hrsg.: Barczewski, Baldur; Koschitzky, Hans-Peter; Weber, Karolin; Wege, Ralf: *VEGAS - Statuskolloquium 2004,* Tagungsband zur Veranstaltung am 05. Oktober 2004 an der Universität Stuttgart, Campus Stuttgart-Vaihingen, 2004, ISBN 3-933761-34-4

132 Asie, Kemal Jabir: *Finite Volume Models for Multiphase Multicomponent Flow through Porous Media*. 2005, ISBN 3-933761-35-2

133 Jacoub, George: *Development of a 2-D Numerical Module for Particulate Contaminant Transport in Flood Retention Reservoirs and Impounded Rivers,* 2004, ISBN 3-933761-36-0

134 Nowak, Wolfgang: *Geostatistical Methods for the Identification of Flow and Transport Parameters in the Subsurface,* 2005, ISBN 3-933761-37-9

135 Süß, Mia: *Analysis of the influence of structures and boundaries on flow and transport processes in fractured porous media*, 2005, ISBN 3-933761-38-7

136 Jose, Surabhin Chackiath: *Experimental Investigations on Longitudinal Dispersive Mixing in Heterogeneous Aquifers,* 2005, ISBN: 3-933761-39-5

137 Filiz, Fulya: *Linking Large-Scale Meteorological Conditions to Floods in Mesoscale Catchments,* 2005, ISBN 3-933761-40-9

138 Qin, Minghao: *Wirklichkeitsnahe und recheneffiziente Ermittlung von Temperatur und Spannungen bei großen RCC-Staumauern*, 2005, ISBN 3-933761-41-7

139 Kobayashi, Kenichiro: *Optimization Methods for Multiphase Systems in the Subsurface - Application to Methane Migration in Coal Mining Areas*, 2005, ISBN 3-933761-42-5

140 Rahman, Md. Arifur: *Experimental Investigations on Transverse Dispersive Mixing in Heterogeneous Porous Media,* 2005, ISBN 3-933761-43-3

141 Schrenk, Volker: *Ökobilanzen zur Bewertung von Altlastensanierungsmaßnahmen,* 2005, ISBN 3-933761-44-1

142 Hundecha, Hirpa Yeshewatesfa: *Regionalization of Parameters of a Conceptual Rainfall-Runoff Model*, 2005, ISBN: 3-933761-45-X

143 Wege, Ralf: *Untersuchungs- und Überwachungsmethoden für die Beurteilung natürlicher Selbstreinigungsprozesse im Grundwasser,* 2005, ISBN 3-933761-46-8

144 Breiting, Thomas: *Techniken und Methoden der Hydroinformatik - Modellierung von komplexen Hydrosystemen im Untergrund*, 2006, ISBN 3-933761-47-6

145 Hrsg.: Braun, Jürgen; Koschitzky, Hans-Peter; Müller, Martin: *Ressource Untergrund: 10 Jahre VEGAS: Forschung und Technologieentwicklung zum Schutz von Grundwasser und Boden,* Tagungsband zur Veranstaltung am 28. und 29. September 2005 an der Universität Stuttgart, Campus Stuttgart-Vaihingen, 2005, ISBN 3-933761-48-4

146 Rojanschi, Vlad: *Abflusskonzentration in mesoskaligen Einzugsgebieten unter Berücksichtigung des Sickerraumes,* 2006, ISBN 3-933761-49-2

147 Winkler, Nina Simone: *Optimierung der Steuerung von Hochwasserrückhaltebeckensystemen,* 2006, ISBN 3-933761-50-6

148 Wolf, Jens: *Räumlich differenzierte Modellierung der Grundwasserströmung alluvialer Aquifere für mesoskalige Einzugsgebiete*, 2006, ISBN: 3-933761-51-4

149 Kohler, Beate: *Externe Effekte der Laufwasserkraftnutzung*, 2006, ISBN 3-933761-52-2

150 Hrsg.: Braun, Jürgen; Koschitzky, Hans-Peter; Stuhrmann, Matthias: *VEGAS-Statuskolloquium 2006,* Tagungsband zur Veranstaltung am 28. September 2006 an der Universität Stuttgart, Campus Stuttgart-Vaihingen, 2006, ISBN 3-933761-53-0

151 Niessner, Jennifer: *Multi-Scale Modeling of Multi-Phase - Multi-Component Processes in Heterogeneous Porous Media*, 2006, ISBN 3-933761-54-9

152 Fischer, Markus: *Beanspruchung eingeerdeter Rohrleitungen infolge Austrocknung bindiger Böden,* 2006, ISBN 3-933761-55-7

153 Schneck, Alexander: *Optimierung der Grundwasserbewirtschaftung unter Berücksichtigung der Belange der Wasserversorgung, der Landwirtschaft und des Naturschutzes*, 2006, ISBN 3-933761-56-5

154 Das, Tapash: *The Impact of Spatial Variability of Precipitation on the Predictive Uncertainty of Hydrological Models,* 2006, ISBN 3-33761-57-3

155 Bielinski, Andreas: *Numerical Simulation of CO_2 sequestration in geological formations*, 2007, ISBN 3-933761-58-1

156 Mödinger, Jens: *Entwicklung eines Bewertungs- und Entscheidungsunterstützungssystems für eine nachhaltige regionale Grundwasserbewirtschaftung*, 2006, ISBN 3-933761-60-3

157 Manthey, Sabine: *Two-phase flow processes with dynamic effects in porous media - parameter estimation and simulation,* 2007, ISBN 3-933761-61-1

158 Pozos Estrada, Oscar: *Investigation on the Effects of Entrained Air in Pipelines,* 2007, ISBN 3-933761-62-X

159 Ochs, Steffen Oliver: *Steam injection into saturated porous media – process analysis including experimental and numerical investigations*, 2007, ISBN 3-933761-63-8

160 Marx, Andreas: *Einsatz gekoppelter Modelle und Wetterradar zur Abschätzung von Niederschlagsintensitäten und zur Abflussvorhersage, 2007,* ISBN 3-933761-64-6

161 Hartmann, Gabriele Maria: *Investigation of Evapotranspiration Concepts in Hydrological Modelling for Climate Change Impact Assessment*, 2007, ISBN 3-933761-65-4

162 Kebede Gurmessa, Tesfaye: *Numerical Investigation on Flow and Transport Characteristics to Improve Long-Term Simulation of Reservoir Sedimentation*, 2007, ISBN 3-933761-66-2

163 Trifković, Aleksandar: *Multi-objective and Risk-based Modelling Methodology for Planning, Design and Operation of Water Supply Systems*, 2007, ISBN 3-933761-67-0

164 Götzinger, Jens: *Distributed Conceptual Hydrological Modelling - Simulation of Climate, Land Use Change Impact and Uncertainty Analysis*, 2007, ISBN 3-933761-68-9

165 Hrsg.: Braun, Jürgen; Koschitzky, Hans-Peter; Stuhrmann, Matthias: *VEGAS – Kolloquium 2007,* Tagungsband zur Veranstaltung am 26. September 2007 an der Universität Stuttgart, Campus Stuttgart-Vaihingen, 2007, ISBN 3-933761-69-7

166 Freeman, Beau: *Modernization Criteria Assessment for Water Resources Planning; Klamath Irrigation Project, U.S.*, 2008, ISBN 3-933761-70-0

167 Dreher, Thomas: *Selektive Sedimentation von Feinstschwebstoffen in Wechselwirkung mit wandnahen turbulenten Strömungsbedingungen*, 2008, ISBN 3-933761-71-9

168 Yang, Wei: *Discrete-Continuous Downscaling Model for Generating Daily Precipitation Time Series*, 2008, ISBN 3-933761-72-7

169 Kopecki, Ianina: *Calculational Approach to FST-Hemispheres for Multiparametrical Benthos Habitat Modelling,* 2008*,* ISBN 3-933761-73-5

170 Brommundt, Jürgen: *Stochastische Generierung räumlich zusammenhängender Niederschlagszeitreihen*, 2008, ISBN 3-933761-74-3

171 Papafotiou, *Alexandros: Numerical Investigations of the Role of Hysteresis in Heterogeneous Two-Phase Flow Systems*, 2008, ISBN 3-933761-75-1

172 He, Yi: *Application of a Non-Parametric Classification Scheme to Catchment Hydrology*, 2008, ISBN 978-3-933761-76-7

173 Wagner, Sven: *Water Balance in a Poorly Gauged Basin in West Africa Using Atmospheric Modelling and Remote Sensing Information*, 2008, ISBN 978-3-933761-77-4

174 Hrsg.: Braun, Jürgen; Koschitzky, Hans-Peter; Stuhrmann, Matthias; Schrenk, Volker: *VEGAS-Kolloquium 2008 Ressource Fläche III*, Tagungsband zur Veranstaltung am 01. Oktober 2008 an der Universität Stuttgart, Campus Stuttgart-Vaihingen, 2008, ISBN 978-3-933761-78-1

175 Patil, Sachin: *Regionalization of an Event Based Nash Cascade Model for Flood Predictions in Ungauged Basins*, 2008, ISBN 978-3-933761-79-8

176 Assteerawatt, Anongnart: *Flow and Transport Modelling of Fractured Aquifers based on a Geostatistical Approach,* 2008, ISBN 978-3-933761-80-4

177 Karnahl, Joachim Alexander: *2D numerische Modellierung von multifraktionalem Schwebstoff- und Schadstofftransport in Flüssen*, 2008, ISBN 978-3-933761-81-1

178 Hiester, Uwe: *Technologieentwicklung zur In-situ-Sanierung der ungesättigten Bodenzone mit festen Wärmequellen,* 2009, ISBN 978-3-933761-82-8

179 Laux, Patrick: *Statistical Modeling of Precipitation for Agricultural Planning in the Volta Basin of West Africa,* 2009, ISBN 978-3-933761-83-5

180 Ehsan, Saqib: *Evaluation of Life Safety Risks Related to Severe Flooding,* 2009, ISBN 978-3-933761-84-2

181 Prohaska, Sandra: *Development and Application of a 1D Multi-Strip Fine Sediment Transport Model for Regulated Rivers,* 2009, ISBN 978-3-933761-85-9

182 Kopp, Andreas: *Evaluation of CO_2 Injection Processes in Geological Formations for Site Screening,* 2009, ISBN 978-3-933761-86-6

183 Ebigbo, Anozie: *Modelling of biofilm growth and its influence on CO_2 and water (two-phase) flow in porous media,* 2009, ISBN 978-3-933761-87-3

184 Freiboth, Sandra: *A phenomenological model for the numerical simulation of multiphase multicomponent processes considering structural alterations of porous media*, 2009, ISBN 978-3-933761-88-0

185 Zöllner, Frank: *Implementierung und Anwendung netzfreier Methoden im Konstruktiven Wasserbau und in der Hydromechanik*, 2009, ISBN 978-3-933761-89-7

186 Vasin, Milos: *Influence of the soil structure and property contrast on flow and transport in the unsaturated zone*, 2010, ISBN 978-3-933761-90-3

187 Li, Jing: *Application of Copulas as a New Geostatistical Tool*, 2010, ISBN 978-3-933761-91-0

188 AghaKouchak, Amir: *Simulation of Remotely Sensed Rainfall Fields Using Copulas*, 2010, ISBN 978-3-933761-92-7

189 Thapa, Pawan Kumar: *Physically-based spatially distributed rainfall runoff modelling for soil erosion estimation*, 2010, ISBN 978-3-933761-93-4

190 Wurms, Sven: *Numerische Modellierung der Sedimentationsprozesse in Retentionsanlagen zur Steuerung von Stoffströmen bei extremen Hochwasserabflussereignissen*, 2011, ISBN 978-3-933761-94-1

191 Merkel, Uwe: *Unsicherheitsanalyse hydraulischer Einwirkungen auf Hochwasserschutzdeiche und Steigerung der Leistungsfähigkeit durch adaptive Strömungsmodellierung*, 2011, ISBN 978-3-933761-95-8

192 Fritz, Jochen: *A Decoupled Model for Compositional Non-Isothermal Multiphase Flow in Porous Media and Multiphysics Approaches for Two-Phase Flow*, 2010, ISBN 978-3-933761-96-5

193 Weber, Karolin (Hrsg.): *12. Treffen junger WissenschaftlerInnen an Wasserbauinstituten*, 2010, ISBN 978-3-933761-97-2

194 Bliefernicht, Jan-Geert: *Probability Forecasts of Daily Areal Precipitation for Small River Basins,* 2011, ISBN 978-3-933761-98-9

195 Hrsg.: Koschitzky, Hans-Peter; Braun, Jürgen: *VEGAS-Kolloquium 2010 In-situ-Sanierung - Stand und Entwicklung Nano und ISCO -,* Tagungsband zur Veranstaltung am 07. Oktober 2010 an der Universität Stuttgart, Campus Stuttgart-Vaihingen*,* 2010*,* ISBN 978-3-933761-99-6

196 Gafurov, Abror: *Water Balance Modeling Using Remote Sensing Information - Focus on Central Asia,* 2010, ISBN 978-3-942036-00-9

197 Mackenberg, Sylvia: *Die Quellstärke in der Sickerwasserprognose: Möglichkeiten und Grenzen von Labor- und Freilanduntersuchungen,* 2010, ISBN 978-3-942036-01-6

198 Singh, Shailesh Kumar: *Robust Parameter Estimation in Gauged and Ungauged Basins,* 2010, ISBN 978-3-942036-02-3

199 Doğan, Mehmet Onur: *Coupling of porous media flow with pipe flow,* 2011, ISBN 978-3-942036-03-0

200 Liu, Min: *Study of Topographic Effects on Hydrological Patterns and the Implication on Hydrological Modeling and Data Interpolation,* 2011, ISBN 978-3-942036-04-7

201 Geleta, Habtamu Itefa: *Watershed Sediment Yield Modeling for Data Scarce Areas,* 2011, ISBN 978-3-942036-05-4

202 Franke, Jörg: *Einfluss der Überwachung auf die Versagenswahrscheinlichkeit von Staustufen,* 2011, ISBN 978-3-942036-06-1

203 Bakimchandra, Oinam: *Integrated Fuzzy-GIS approach for assessing regional soil erosion risks,* 2011, ISBN 978-3-942036-07-8

204 Alam, Muhammad Mahboob: *Statistical Downscaling of Extremes of Precipitation in Mesoscale Catchments from Different RCMs and Their Effects on Local Hydrology,* 2011, ISBN 978-3-942036-08-5

205 Hrsg.: Koschitzky, Hans-Peter; Braun, Jürgen: *VEGAS-Kolloquium 2011 Flache Geothermie - Perspektiven und Risiken,* Tagungsband zur Veranstaltung am 06. Oktober 2011 an der Universität Stuttgart, Campus Stuttgart-Vaihingen*,* 2011*,* ISBN 978-3-933761-09-2

206 Haslauer, Claus: *Analysis of Real-World Spatial Dependence of Subsurface Hydraulic Properties Using Copulas with a Focus on Solute Transport Behaviour,* 2011, ISBN 978-3-942036-10-8

207 Dung, Nguyen Viet: *Multi-objective automatic calibration of hydrodynamic models – development of the concept and an application in the Mekong Delta,* 2011, ISBN 978-3-942036-11-5

208 Hung, Nguyen Nghia: *Sediment dynamics in the floodplain of the Mekong Delta, Vietnam,* 2011, ISBN 978-3-942036-12-2

209 Kuhlmann, Anna: *Influence of soil structure and root water uptake on flow in the unsaturated zone,* 2012, ISBN 978-3-942036-13-9

210 Tuhtan, Jeffrey Andrew: *Including the Second Law Inequality in Aquatic Ecodynamics: A Modeling Approach for Alpine Rivers Impacted by Hydropeaking,* 2012, ISBN 978-3-942036-14-6

211 Tolossa, Habtamu: *Sediment Transport Computation Using a Data-Driven Adaptive Neuro-Fuzzy Modelling Approach,* 2012, ISBN 978-3-942036-15-3

212 Tatomir, Alexandru-Bodgan: *From Discrete to Continuum Concepts of Flow in Fractured Porous Media,* 2012, ISBN 978-3-942036-16-0

213 Erbertseder, Karin: *A Multi-Scale Model for Describing Cancer-Therapeutic Transport in the Human Lung,* 2012, ISBN 978-3-942036-17-7

214 Noack, Markus: *Modelling Approach for Interstitial Sediment Dynamics and Reproduction of Gravel Spawning Fish,* 2012, ISBN 978-3-942036-18-4

215 De Boer, Cjestmir Volkert: *Transport of Nano Sized Zero Valent Iron Colloids during Injection into the Subsurface*, 2012, ISBN 978-3-942036-19-1

216 Pfaff, Thomas: *Processing and Analysis of Weather Radar Data for Use in Hydrology*, 2013, ISBN 978-3-942036-20-7

217 Lebrenz, Hans-Henning: *Addressing the Input Uncertainty for Hydrological Modeling by a New Geostatistical Method*, 2013, ISBN 978-3-942036-21-4

218 Darcis, Melanie Yvonne: *Coupling Models of Different Complexity for the Simulation of CO_2 Storage in Deep Saline Aquifers*, 2013, ISBN 978-3-942036-22-1

219 Beck, Ferdinand: *Generation of Spatially Correlated Synthetic Rainfall Time Series in High Temporal Resolution - A Data Driven Approach*, 2013, ISBN 978-3-942036-23-8

220 Guthke, Philipp: *Non-multi-Gaussian spatial structures: Process-driven natural genesis, manifestation, modeling approaches, and influences on dependent processes*, 2013, ISBN 978-3-942036-24-5

221 Walter, Lena: *Uncertainty studies and risk assessment for CO_2 storage in geological formations*, 2013, ISBN 978-3-942036-25-2

222 Wolff, Markus: *Multi-scale modeling of two-phase flow in porous media including capillary pressure effects,* 2013, ISBN 978-3-942036-26-9

223 Mosthaf, Klaus Roland: *Modeling and analysis of coupled porous-medium and free flow with application to evaporation processes,* 2014, ISBN 978-3-942036-27-6

224 Leube, Philipp Christoph: *Methods for Physically-Based Model Reduction in Time: Analysis, Comparison of Methods and Application*, 2013, ISBN 978-3-942036-28-3

225 Rodríguez Fernández, Jhan Ignacio: *High Order Interactions among environmental variables: Diagnostics and initial steps towards modeling*, 2013, ISBN 978-3-942036-29-0

226 Eder, Maria Magdalena: *Climate Sensitivity of a Large Lake*, 2013, ISBN 978-3-942036-30-6

227 Greiner, Philipp: *Alkoholinjektion zur In-situ-Sanierung von CKW Schadensherden in Grundwasserleitern: Charakterisierung der relevanten Prozesse auf unterschiedlichen Skalen*, 2014, ISBN 978-3-942036-31-3

228 Lauser, Andreas: *Theory and Numerical Applications of Compositional Multi-Phase Flow in Porous Media*, 2014, ISBN 978-3-942036-32-0

229 Enzenhöfer, Rainer: *Risk Quantification and Management in Water Production and Supply Systems*, 2014, ISBN 978-3-942036-33-7

230 Faigle, Benjamin: *Adaptive modelling of compositional multi-phase flow with capillary pressure*, 2014, ISBN 978-3-942036-34-4

231 Oladyshkin, Sergey: *Efficient modeling of environmental systems in the face of complexity and uncertainty*, 2014, ISBN 978-3-942036-35-1

232 Sugimoto, Takayuki: *Copula based Stochastic Analysis of Discharge Time Series*, 2014, ISBN 978-3-942036-36-8

233 Koch, Jonas: *Simulation, Identification and Characterization of Contaminant Source Architectures in the Subsurface*, 2014, ISBN 978-3-942036-37-5

234 Zhang, Jin: *Investigations on Urban River Regulation and Ecological Rehabilitation Measures, Case of Shenzhen in China*, 2014, ISBN 978-3-942036-38-2

235 Siebel, Rüdiger: *Experimentelle Untersuchungen zur hydrodynamischen Belastung und Standsicherheit von Deckwerken an überströmbaren Erddämmen,* 2014, ISBN 978-3-942036-39-9

236 Baber, Katherina: *Coupling free flow and flow in porous media in biological and technical applications: From a simple to a complex interface description,* 2014, ISBN 978-3-942036-40-5

237 Nuske, Klaus Philipp: *Beyond Local Equilibrium — Relaxing local equilibrium assumptions in multiphase flow in porous media,* 2014, ISBN 978-3-942036-41-2

238 Geiges, Andreas: *Efficient concepts for optimal experimental design in nonlinear environmental systems*, 2014, ISBN 978-3-942036-42-9

239 Schwenck, Nicolas: *An XFEM-Based Model for Fluid Flow in Fractured Porous Media*, 2014, ISBN 978-3-942036-43-6

240 Chamorro Chávez, Alejandro: *Stochastic and hydrological modelling for climate change prediction in the Lima region, Peru*, 2015, ISBN 978-3-942036-44-3

241 Yulizar: *Investigation of Changes in Hydro-Meteorological Time Series Using a Depth-Based Approach*, 2015, ISBN 978-3-942036-45-0

242 Kretschmer, Nicole: *Impacts of the existing water allocation scheme on the Limarí watershed – Chile, an integrative approach*, 2015, ISBN 978-3-942036-46-7

243 Kramer, Matthias: *Luftbedarf von Freistrahlturbinen im Gegendruckbetrieb*, 2015, ISBN 978-3-942036-47-4

244 Hommel, Johannes: *Modeling biogeochemical and mass transport processes in the subsurface: Investigation of microbially induced calcite precipitation*, 2016, ISBN 978-3-942036-48-1

245 Germer, Kai: *Wasserinfiltration in die ungesättigte Zone eines makroporösen Hanges und deren Einfluss auf die Hangstabilität*, 2016, ISBN 978-3-942036-49-8

246 Hörning, Sebastian: *Process-oriented modeling of spatial random fields using copulas*, 2016, ISBN 978-3-942036-50-4

247 Jambhekar, Vishal: *Numerical modeling and analysis of evaporative salinization in a coupled free-flow porous-media system,* 2016, ISBN 978-3-942036-51-1

248 Huang, Yingchun: *Study on the spatial and temporal transferability of conceptual hydrological models*, 2016, ISBN 978-3-942036-52-8

249 Kleinknecht, Simon Matthias: *Migration and retention of a heavy NAPL vapor and remediation of the unsaturated zone*, 2016, ISBN 978-3-942036-53-5

250 Kwakye, Stephen Oppong: *Study on the effects of climate change on the hydrology of the West African sub-region*, 2016, ISBN 978-3-942036-54-2

251 Kissinger, Alexander: *Basin-Scale Site Screening and Investigation of Possible Impacts of CO_2 Storage on Subsurface Hydrosystems*, 2016, ISBN 978-3-942036-55-9

252 Müller, Thomas: *Generation of a Realistic Temporal Structure of Synthetic Precipitation Time Series for Sewer Applications*, 2017, ISBN 978-3-942036-56-6

253 Grüninger, Christoph: *Numerical Coupling of Navier-Stokes and Darcy Flow for Soil-Water Evaporation*, 2017, ISBN 978-3-942036-57-3

254 Suroso: *Asymmetric Dependence Based Spatial Copula Models: Empirical Investigations and Consequences on Precipitation Fields*, 2017, ISBN 978-3-942036-58-0

255 Müller, Thomas; Mosthaf, Tobias; Gunzenhauser, Sarah; Seidel, Jochen; Bárdossy, András: *Grundlagenbericht Niederschlags-Simulator (NiedSim3)*, 2017, ISBN 978-3-942036-59-7

256 Mosthaf, Tobias: *New Concepts for Regionalizing Temporal Distributions of Precipitation and for its Application in Spatial Rainfall Simulation,* 2017, ISBN 978-3-942036-60-3

257 Fenrich, Eva Katrin: *Entwicklung eines ökologisch-ökonomischen Vernetzungsmodells für Wasserkraftanlagen und Mehrzweckspeicher,* 2018, ISBN 978-3-942036-61-0

258 Schmidt, Holger: *Microbial stabilization of lotic fine sediments*, 2018, ISBN 978-3-942036-62-7

259 Fetzer, Thomas: *Coupled Free and Porous-Medium Flow Processes Affected by Turbulence and Roughness – Models, Concepts and Analysis*, 2018, ISBN 978-3-942036-63-4

260 Schröder, Hans Christoph: *Large-scale High Head Pico Hydropower Potential Assessment*, 2018, ISBN 978-3-942036-64-1

Die Mitteilungshefte ab der Nr. 134 (Jg. 2005) stehen als pdf-Datei über die Homepage des Instituts: www.iws.uni-stuttgart.de zur Verfügung.